

OXYFLUORO COMPOUNDS OF BROMINE

OXYFLUORO COMPOUNDS OF BROMINE

by

PAUL HENRY SPEKKENS (B.Sc.)

A Thesis

Submitted to the Faculty of Graduate Studies

in Partial Fulfilment of the Requirements

for the Degree

Doctor of Philosophy

McMaster University

August 1977

DOCTOR OF PHILOSOPHY (1977)
Department of Chemistry

MCMASTER UNIVERSITY
Hamilton, Ontario

TITLE: Oxyfluoro Compounds of Bromine

AUTHOR: PAUL HENRY SPEKKENS, B.Sc. (University of Ottawa)

SUPERVISOR: Professor R. J. Gillespie

NUMBER OF PAGES: xiii, 218

ABSTRACT

A number of new oxyfluoro compounds of Br (V) have been prepared and isolated; their structures and some of their reactions have been investigated by ^{19}F nmr and Raman spectroscopy. The previously reported oxyfluoride BrO_2F has been characterized for the first time, and the preparation and characterization of the previously unknown BrOF_3 is described. Reaction of these oxyfluorides with the Lewis acids BF_3 and AsF_5 has been shown to produce the new cations BrO_2^+ and BrOF_2^+ . The anions BrO_2F_2^- and BrOF_4^- have also been prepared for the first time by several methods. These new cations and anions have been characterized by Raman and ^{19}F nmr spectroscopy. Similar results have been simultaneously reported by other groups, working independently.

Two selenium (IV) anions SeO_2F^- and $\text{SeO}_2\text{F}_2^{2-}$, which are isoelectronic with BrO_2F and BrO_2F_2^- , respectively, have been investigated. The Raman spectrum of the SeO_2F^- anion has been reassigned and evidence for the formation of the $\text{SeO}_2\text{F}_2^{2-}$ anion is presented for the first time.

The ^{19}F nmr spectrum of the bromine (VII) oxyfluoride BrO_3F has been recorded and interpreted. The Raman spectra of solid and liquid BrO_3F have been obtained and used to support the previously reported assignments of the fundamental bending modes of this molecule. A number of reactions involving the bromine (VII) species BrF_6^+ , BrO_4^- and BrO_3F are described. These reactions were carried out in an unsuccessful attempt to prepare the unknown oxyfluorides BrO_2F_3 and BrOF_5 .

ACKNOWLEDGEMENTS

The author wishes to thank his research director, Professor R. J. Gillespie, for suggesting an interesting topic and for providing guidance and encouragement of this work.

Thanks are also due to Drs. J. P. Krasznai and G. J. Schrobilgen whose encouragement and experimental assistance were invaluable.

The author wishes to thank the technical staff of McMaster University for their maintenance of the Raman and N.M.R. facilities. Much appreciation is also extended to Mrs. Edith Denham who typed this thesis and to Dr. R. Burns who proof-read the manuscript.

Financial assistance from the Research Council of Canada, which provided a scholarship from 1972-1977 is gratefully acknowledged.

Finally, the author wishes to thank Fran, his wife, for her patience, understanding and support.

TABLE OF CONTENTS

	<u>Page</u>
CHAPTER I	
<u>INTRODUCTION</u>	1
A. General	1
B. Bromine Fluorides	1
C. Bromine Oxides	3
D. Halogen Oxyfluorides: Their Existence, Amphoteric Behaviour and Structures	6
E. The Unusual Nature of Br (VII) Compounds	11
F. Purpose of the Present Work	14
CHAPTER II	
<u>EXPERIMENTAL</u>	15
A. Vacuum Techniques and Sample Handling	15
B. Instrumentation	17
(i) Laser Raman Spectroscopy	17
(ii) Nuclear Magnetic Resonance Spectroscopy	19
C. Preparation and Purification of Starting Materials	20
(i) Gases	20
(a) Fluorine	20
(b) Inert Atmospheres	20
(ii) Solvents	21
(a) HF	21
(b) SO ₂ ClF and SO ₂ F ₂	21
(c) Acetonitrile	21

(iii) Lewis Acids	21
(iv) Other Reagents	22
(a) Metal Fluorides	22
(b) BrF_5 and IF_5	22
(c) KBrO_3 and KBrO_4	22
(d) SeO_2 and SO_2	23
(e) Iodine Oxides and Oxyfluoro Species	23
(f) KrF_2	23
(g) KBrF_6	23
(h) CsSO_2F	24
(i) $\text{KrF}^+\text{AsF}_6^-$ and $\text{BrF}_6^+\text{AsF}_6^-$	24

CHAPTER III

<u>PREPARATION AND CHARACTERIZATION OF KBrO_2F_2 AND KBrOF_4</u>	25
A. Introduction	25
B. Preparation and Properties of KBrO_2F_2 and KBrOF_4	25
C. Characterization of KBrO_2F_2 and KBrOF_4 by Raman Spectroscopy	28
D. ^{19}F N.M.R. Spectrum of KBrOF_4	41
E. The Reaction of KBrO_3 and BrF_5	42
F. Experimental Section	47
(i) Preparation of KBrOF_4 and KBrO_2F_2 by the Reaction of KBrO_3 and KBrF_6	47
(ii) Hydrolysis of KBrF_6	48
(iii) Reactions of KBrOF_4 and KBrO_3 , and KBrF_6 and KBrO_2F_2	48
(iv) Reaction of KBrO_3 with BrF_5	49

CHAPTER IV

THE PREPARATION AND THE CHEMICAL AND SPECTROSCOPIC PROPERTIES

<u>OF BrO_2F AND BrOF_3</u>	50
A. Introduction	50
B. Preparation and Properties of BrO_2F	51
C. Characterization of BrO_2F by Raman and ^{19}F N.M.R. Spectroscopy	53
(i) Raman Spectroscopy	53
(ii) ^{19}F N.M.R. Spectroscopy	59
D. The Reaction of BrO_2F with KF	60
E. Preparation and Properties of BrOF_3	60
F. Characterization of BrOF_3 by Raman and ^{19}F N.M.R. Spectroscopy	63
(i) Raman Spectroscopy	63
(ii) ^{19}F N.M.R. Spectroscopy	71
G. Reaction of BrF_5 with H_2O and Iodine Oxyfluoro Species	72
(i) Hydrolysis of BrF_5	72
(ii) Reaction of BrF_5 with Iodine Oxides and Oxyfluorides	73
(iii) Reaction of BrF_5 with $\text{IO}_2\text{SO}_3\text{F}$	76
H. Reaction of BrO_2F with KrF_2	77
I. Experimental Section	78
(i) Preparation of BrO_2F	78
(ii) Decomposition of BrO_2F in HF	78
(iii) Preparation of BrO_2F Samples for Raman and ^{19}F N.M.R. Spectroscopy	79
(iv) Reaction of BrO_2F with KF	79

	<u>Page</u>
(v) Preparation and Properties of BrOF_3	79
(vi) Reaction of BrOF_3 and KHF_2	81
(vii) Preparation of N.M.R. and Raman Samples of BrOF_3	81
(viii) Hydrolysis of BrF_5	82
(ix) Reaction of I(V) Oxides and Oxyfluorides with BrF_5	83
(a) IO_2F	83
(b) I_2O_5	84
(c) IOF_3	84
(x) Reaction of IO_2F_3 and BrF_5	84
(xi) Reaction of $\text{IO}_2\text{SO}_3\text{F}$ and BrF_5	85
(xii) Reaction of BrO_2F and KrF_2	85

CHAPTER V

PREPARATION AND CHARACTERIZATION OF THE CATIONS BrO_2^+ AND BrOF_2^+

A. Introduction	86
B. Preparation and Properties of the BrO_2^+ Salts.	87
C. Characterization of $\text{BrO}_2^+\text{BF}_4^-$ and $\text{BrO}_2^+\text{AsF}_6^-$ by Raman and ^{19}F N.M.R. Spectroscopy	88
(i) Raman Spectroscopy	88
(ii) ^{19}F N.M.R. Spectroscopy	100
(iii) Discussion	103
D. Preparation and Properties of the BrOF_2^+ Salts	104
E. Characterization of the BrOF_2^+ Salts by Raman and ^{19}F N.M.R. Spectroscopy	107

	Page
(i) Raman Spectroscopy	107
(ii) ^{19}F N.M.R. Spectroscopy	124
F. Experimental Section	128
(i) Preparation of BrO_2^+ Salts	128
(a) $\text{BrO}_2^+ \text{AsF}_6^-$	128
(b) $\text{BrO}_2^+ \text{BF}_4^-$	129
(ii) Preparation of BrOF_2^+ Salts	130
(a) $\text{BrOF}_2^+ \text{AsF}_6^-$	130
(b) $\text{BrOF}_2^+ \text{BF}_4^-$	131
(c) $\text{BrOF}_2^+ \text{SbF}_6^-$	132
(d) Reaction of $\text{IOF}_2^+ \text{SbF}_6^-$ with BrF_5	133

CHAPTER VI

A REINVESTIGATION OF THE VIBRATIONAL SPECTRUM OF SeO_2F^- AND THE PREPARATION AND RAMAN SPECTRUM OF $\text{SeO}_2\text{F}_2^{2-}$

	134
A. Introduction	134
B. Vibrational Spectrum of the SeO_2F^- Ion	135
C. Purity of the KSeO_2F Samples	141
D. Preparation and Raman Spectrum of $\text{K}_2\text{SeO}_2\text{F}_2$	143
E. Attempted Preparation of the $\text{SO}_2\text{F}_2^{2-}$ Ion	146
F. Experimental Section	147
(i) KSeO_2F	147
(ii) $\text{K}_2\text{SeO}_2\text{F}_2$	148
(iii) Attempted Preparation of $\text{SO}_2\text{F}_2^{2-}$	149

CHAPTER VII

CHARACTERIZATION OF BrO_3F BY ^{19}F N.M.R. SPECTROSCOPY, AND SOMEATTEMPTED PREPARATIONS OF Br (VII) OXYFLUORO SPECIES 150

A.	Introduction	150
B.	Raman and ^{19}F N.M.R. Spectra of BrO_3F	152
	(i) Raman Spectroscopy	152
	(ii) ^{19}F N.M.R. Spectroscopy	157
	(iii) Reaction of BrO_3F with SbF_5 and AsF_5	162
C.	Reactions Involving KBrO_4	164
	(i) Solution in Hydrofluoric Acid	164
	(ii) Reactions with some Fluorinating Agents	166
	(a) AsF_5	166
	(b) BrF_5	168
	(c) KrF_2	170
D.	Reactions Involving $\text{BrF}_6^+ \text{AsF}_6^-$	174
	(i) Hydrolysis	174
	(ii) KBrO_4	176
	(iii) BrO_3F	179
E.	Miscellaneous Reactions	180
	(i) Attempted Preparation of BrOF_5	180
	(ii) Reaction of BrO_3F and KrF^+	181
F.	Discussion	182
G.	Experimental Section	184
	(i) BrO_3F	184
	(ii) Reactions of KBrO_4	185
	(a) KBrO_4 and AsF_5	185
	(b) KBrO_4 and BrF_5	186

	<u>Page</u>
(c) KBrO_4 and KrF_2	187
(iii) Reactions of $\text{BrF}_6^+ \text{AsF}_6^-$	187
(a) Hydrolysis	187
(b) $\text{BrF}_6^+ \text{AsF}_6^-$ and KBrO_4	188
(c) $\text{BrF}_6^+ \text{AsF}_6^-$ and BrO_3F	188
(iv) Reactions of BrO_3F with KrF_2 and $\text{KrF}^+ \text{AsF}_6^-$	189
(v) BrF_5 , F_2 and O_2 at High Temperature and Pressure	190

CHAPTER VIII

<u>CONCLUSIONS</u>	191
A. Introduction	191
B. Comparison of the Oxyfluorides of Bromine with those of Chlorine and Iodine	191
C. Future Directions for Research	195
(i) Br^+ (V)	195
(ii) Br (VII)	197
D. The Relation of Reactivity to Geometry in Oxyfluoro Compounds	198
E. Known and Unknown Oxyfluoro Compounds of the Halogens	204
 REFERENCES	 208

LIST OF TABLES

<u>Table</u>	<u>Page</u>
1.1 Oxyfluoro Species of Cl (V), Br (V) and I (V)	8
1.2 Structures of the Oxyfluoro Compounds of Cl (V)	10
3.1 Raman Frequencies of BrO_2F_2^- and Some Related Molecules	30
3.2 Raman Frequencies of BrOF_4^- and Some Related Molecules	36
4.1 Raman Spectra of BrO_2F , ClO_2F and SeO_2F^-	56
4.2 Raman Spectra of BrOF_3	67
5.1 Raman Frequencies of BrO_2^+ Salts and Some Related Molecules	92
5.2 Comparison of BrO_2^+ Stretching Frequencies to Some Related Molecules	97
5.3 Chemical Shifts and Coupling Constants for $\text{BrO}_2^+\text{BF}_4^-$ Dissolved in HF	101
5.4 Vibrational Frequencies for BrOF_2^+ Salts and Some Related Molecules	111
5.5 Vibrational Frequencies of $\text{BrOF}_2^+\text{Sb}_n\text{F}_{5n+1}^-$ and Some Related $\text{Sb}_n\text{F}_{5n+1}^+$ Systems	120
6.1 Fundamental Frequencies of SeO_2F^- and Some Related Molecules	137
6.2 Raman Spectrum of $\text{SeO}_2\text{F}_2^{2-}$ and Some Related Ions	145
7.1 Vibrational Frequencies of BrO_3F	156

LIST OF FIGURES

<u>Figure</u>		<u>Page</u>
3.1	Raman spectrum of solid KBrO_2F_2 at 25°C	29
3.2	Raman spectrum of solid KBrOF_4 at 25°C	34
3.3	Raman spectrum of solid KBrOF_4 at -196°C	35
4.1	Raman spectrum of solid BrO_2F at -75°C	54
4.2	Raman spectrum of liquid BrO_2F at -9°C	55
4.3	Raman spectrum of solid BrOF_3 at -196°C	64
4.4	Raman spectrum of liquid BrOF_3 at 0°C	65
4.5	Raman spectrum of a solution of BrOF_3 in HF at -78°C	66
5.1	Raman spectrum of solid $\text{BrO}_2^+\text{BF}_4^-$ at -196°C	90
5.2	Raman spectrum of solid $\text{BrO}_2^+\text{AsF}_6^-$ at -196°C	91
5.3	Raman spectrum of solid $\text{BrOF}_2^+\text{AsF}_6^-$ at -196°C	108
5.4	Raman spectrum of solid $\text{BrOF}_2^+\text{BF}_4^-$ at -196°C	109
5.5	Raman spectrum of a solution of $\text{BrOF}_2^+\text{BF}_4^-$ in HF at -72°C	110
5.6	Raman spectrum of $\text{BrOF}_2^+\text{Sb}_n\text{F}_{5n+1}^-$ at -95°C	119
6.1	Raman spectrum of KSeO_2F	136
7.1	Raman spectrum of liquid BrO_3F at -72°C	154
7.2	Raman spectrum of solid BrO_3F at -196°C	155

CHAPTER I

INTRODUCTION

A. General

The discovery of the element bromine is credited to Balard in 1826¹ and the relation of bromine to the previously discovered halogens chlorine and iodine was recognised from the very first. The rather unpleasant smell of elemental bromine is responsible for its name, which is derived from the Greek word "bromos" meaning stench.

As is the case with all the common halogens, bromine occurs naturally in the -I oxidation state. Although the largest source of bromine is the sea ($\sim 0.0065\%$ bromide), some isolated bodies of water (such as the Dead Sea) and natural brines from wells and springs are considerably more concentrated (up to 0.6% bromide). Commercially, bromine is recovered from these sources by oxidation of Br^- to Br_2 using chlorine, followed by removal of the Br_2 from the solution using a current of air or steam.

Although bromine only occurs naturally in the -I oxidation state, it nevertheless has a rather extensive chemistry in a number of positive oxidation states.

B. Bromine Fluorides

The preparation and properties of the halogen fluorides have been described at length in a number of excellent articles^{1,2,3,4} and will

not be discussed in detail. For a halogen X, the fluorides XF , XF_3 , XF_5 and XF_7 might be expected. For iodine, all four fluorides have been reported whereas for chlorine and bromine, the highest fluoride XF_7 has not yet been shown to exist.

Bromine monofluoride can be prepared by the reaction of AgF with Br_2 .



The BrF produced cannot be isolated however, since it disproportionates to Br_2 and BrF_3 .²



BrF_3 can be prepared by the direct reaction of the elements. Liquid BrF_3 is considerably self-ionized,



as shown by its high specific conductance.³ Due to its high dielectric constant ($\epsilon = 106.8$ at $25^\circ C$),⁵ it is an excellent ionizing solvent. It is also a powerful fluorinating agent and will convert many oxides or chlorides into the corresponding fluorides.

BrF_5 is the highest fluoride of bromine which has been definitely shown to exist. It can be prepared by the reaction of BrF_3 with excess fluorine at high temperature. Like BrF_3 , BrF_5 is a powerful fluorinating agent. It is, however, a much poorer ionizing solvent than the trifluoride and consequently has not been as extensively used as a

reaction medium.

Although the preparation of BrF_7 by a high temperature reaction between BrF_5 and F_2 has been reported,⁶ the evidence for the existence of this fluoride is rather tenuous. Gillespie and Schrobilgen⁷ have shown that a displacement reaction between $\text{BrF}_6^+ \text{AsF}_6^-$ and NOF fails to produce BrF_7 even at -78°C . In view of the apparent instability of BrF_7 at this low temperature, the reported preparation of this fluoride at temperatures over 250°C must be regarded with some skepticism.

C. Bromine Oxides

Whereas the fluorides of bromine are well defined and have been extensively studied, the oxides of bromine are much more poorly understood. A number of compounds have been reported and they have been on the whole rather poorly characterized. Many of the early reports relied on analysis as the only technique of identification of the products. Most of the oxides of bromine are prepared by the action of ozone on bromine under different conditions, or by the decomposition or disproportionation of another oxide. The literature prior to 1961 has been reviewed by Schmeisser and Brändle⁸ and more recent work has been summarized by Brisdon.⁹

The lowest oxide Br_2O has been the most thoroughly characterized. This oxide is best prepared by allowing the oxide Br_2O_4 (Form A) to decompose under vacuum.¹⁰ Br_2O is brown-black in colour and melts at $-17.5 \pm 0.5^\circ\text{C}$. Decomposition to Br_2 and O_2 occurs slowly at temperatures above -40°C .⁸ The infrared spectrum of Br_2O ¹¹ indicates that it has a bent structure

with oxygen as the central atom.

Br_2O_4 (Form A) is a yellow solid at low temperature which decomposes into the elements when warmed rapidly to 0°C . It was first prepared by Schwarz and Schmeisser¹⁰ by passing a mixture of bromine and oxygen through a glow discharge. It is more conveniently prepared by the reaction of Br_2 and O_3 at -50°C using CFCI_3 as a solvent.⁸ The yellow product of these reactions was generally formulated as " BrO_2 " until Pascal and Potier¹² showed, on the basis of Raman spectroscopy, that the structure was actually Br_2O_4 in which two BrO_2 units are linked by a Br-Br bond.

As was mentioned above, the controlled decomposition of Br_2O_4 (A) ultimately leads to the formation of Br_2O . Pascal et al¹³ were able to isolate another relatively stable, gold coloured material from the decomposition of Br_2O_4 (A). This material is formed before Br_2O is produced. Analysis and vibrational spectroscopy led these workers to conclude that the gold material was Br_2O_3 , and that the molecule contained a Br-O-Br bridge. By comparison of the Raman spectrum with that of the B form of Br_2O_4 (see below) they concluded that the structure was probably $\text{O}=\text{Br}-\text{O}-\text{Br}=\text{O}$ and not $\text{O}_2\text{Br}-\text{O}-\text{Br}$.¹⁴

The oxidation of Br_2O_3 with O_3 at low temperature produces a second isomer of Br_2O_4 , designated Br_2O_4 (B).¹⁴ This isomer has a bright red colour and is slowly converted to Br_2O_4 (A) at low temperature. On the basis of Raman spectroscopy, the structure $\text{O}_2\text{Br}-\text{O}-\text{Br}=\text{O}$ was assigned to Br_2O_4 (B).

Three higher oxides of bromine have also been reported. These

are $(\text{Br}_2\text{O}_5)_n$, $(\text{Br}_3\text{O}_8)_n$, and $(\text{BrO}_3)_n$. They were first produced by the direct reaction of ozone with bromine at room temperature. Lewis and his coworkers^{15,16} studied this reaction and found that an oxide of composition $(\text{Br}_3\text{O}_8)_n$ was obtained. Pflugmacher and his coworkers¹⁷ repeated the reaction using a greater excess of ozone and found that a compound of composition $(\text{BrO}_3)_n$ was formed. Arvia et al¹⁸ reinvestigated the reaction and found that the products obtained depended upon the material that the reaction vessels were made of. When Pyrex vessels were used a product of composition $(\text{Br}_2\text{O}_5)_n$ was formed, whereas using a quartz vessel, $(\text{Br}_3\text{O}_8)_n$ was obtained. These workers found no evidence for an oxide of composition $(\text{BrO}_3)_n$. More recently, Pascal et al¹⁹ have reinvestigated the reaction of ozone with bromine at temperatures between -100°C and $+4^\circ\text{C}$ in a Pyrex vessel. They found that in addition to Br_2O_4 , an oxide of composition Br_2O_5 is formed at temperatures between -28°C and $+4^\circ\text{C}$. On the basis of Raman spectroscopy they suggested that this oxide is polymerized in a manner analogous to I_2O_5 . The latter has been shown to consist of O_2IOIO_2 molecules linked in the crystal by rather strong oxygen bridges.²⁰

The bromine oxide radicals BrO , BrO_2 , and BrO_3 have been observed as short-lived species in aqueous solution.⁹ All three are produced by the pulse radiolysis of BrO_3^- in aqueous solution and can be detected by their absorptions in the ultra-violet region. All three decay rapidly in aqueous solution to mixtures of the BrO^- , BrO_2^- , and BrO_3^- anions. The BrO radical has also been extensively studied in the gas phase by various spectroscopic techniques. These three short-lived radicals

should perhaps be considered separately from the chemically isolable, more long-lived oxides described earlier. They have been included in this discussion only for completeness.

Thus the oxides of bromine are rather poorly understood. The existence of several lower oxides has been clearly demonstrated by the recent work of Pascal and his collaborators. However, the chemistry of the lower oxides of bromine has not yet by any means been fully explored and it is possible that other oxides may yet be prepared. The higher oxides are even more poorly characterized in that no detailed structural information is available for them, and the conditions leading to their formation have not been established. Moreover, the oxides of bromine are considerably less stable than their chlorine or iodine analogues. None of the oxides of bromine are stable at room temperature, although $(\text{Br}_2\text{O}_5)_n$, $(\text{Br}_3\text{O}_8)_n$, and $(\text{BrO}_3)_n$ can be kept at room temperature in the presence of ozone. The reasons for the instability of these compounds are not clear.

D. Halogen Oxyfluorides: Their Existence, Amphoteric Behaviour and Structures.

The oxyfluorides of the halogens Cl and I have been extensively studied. The oxyfluoro species of Cl have been recently reviewed by Christie and Schack.²¹ Although no recent review articles are available on the oxyfluorides of iodine, work reported prior to 1961 has been summarized by Schmeisser and Brändle.⁸ Many of the known halogen oxyfluorides have been shown to exhibit amphoteric behaviour. Thus an oxyfluoride XO_nF_m can react with a Lewis acid to produce the cation $\text{XO}_n\text{F}_{m-1}^+$

and with a fluoride ion donor to give the anion $XO_nF_{m+1}^-$. Listed in Table 1.1 are the possible oxyfluorides of Cl, Br, and I, where the central atom is in the +V or +VII oxidation state along with the related singly charged cations and anions derived from these oxyfluorides. The entries in square brackets have not yet been prepared.

At the outset of this work, all the oxyfluoro species of Cl(V) and I(V) listed in Table 1.1 had been characterized. For Br(V), on the other hand, only the preparation of $BrO_2F^{22,23}$ had been reported. Unsuccessful attempts to prepare $BrOF_3^{24}$ and adducts of BrO_2F with the Lewis acids BF_3 , AsF_5 and SbF_5^8 had also been mentioned in the literature. The relative lack of information about the oxyfluorides of Br(V) is rather surprising in view of the existence and stability of BrF_5 and BrO_3^- .

Considerably fewer of the oxyfluoro species of the halogens in the +VII oxidation state listed in Table 1.1 have been characterized. Attempts to prepare several such species ($ClO_3F_2^-$,²¹ ClO_3^+ ,²¹ $IO_2F_2^+$,^{25,26} and IOF_4^+ ^{27,28}) by fairly obvious and straightforward methods have failed. In some other cases however, e.g. $BrOF_5$, BrO_2F_3 , $BrO_2F_2^+$, and $BrO_2F_4^-$, no extensive systematic attempts at their preparation appear to have been made, although attempted preparations of $BrOF_5$ and $BrO_2F_2^+$ have been briefly reported (see Chapter VII). There appears to be no obvious reason why such species could not be prepared. A few of the possible species listed in Table 1.1 can, however, be anticipated to be of rather low stability. Thus $ClOF_6^-$ and $BrOF_6^-$ seem unlikely because of the apparent reluctance of Cl and Br to achieve a coordination number greater than six.

Table 1.1
Oxyfluoro Species of Cl(V), Br(V), and I(V)

Oxidation State of Central Atom	Cations	Neutral Molecules	Anions
V	ClO_2^+ (29, 30) ^a	ClO_2F (31, 32, 33)	ClO_2F_2^- (34, 35)
	ClOF_2^+ (36, 37, 38)	ClOF_3 (39, 40, 41)	ClOF_4^- (42, 43)
	BrO_2^+ (*, 44)	BrO_2F (*, 22, 23)	BrO_2F_2^- (*, 45, 46)
	BrOF_2^+ (*, 47)	BrOF_3 (*, 48)	BrOF_4^- (*, 49)
	IO_2^+ (50, 51)	IO_2F (50, 51, 52)	IO_2F_2^- (53, 54, 55)
	IOF_2^+ (51)	IOF_3 (51, 52, 56)	IOF_4^- (57, 58)
VII	$[\text{ClO}_3]^+$ ^b	ClO_3F (21, 59, 60,) (61, 62)	$[\text{ClO}_3\text{F}_2]^-$
	ClO_2F_2^+ (63, 64)	ClO_2F_3 (65, 66, 67)	$[\text{ClO}_2\text{F}_4]^-$
	$[\text{ClOF}_4]^+$	$[\text{ClOF}_5]^c$	$[\text{ClOF}_6]^-$
	$[\text{BrO}_3]^+$	BrO_3F (62, 68)	$[\text{BrO}_3\text{F}_2]^-$
	$[\text{BrO}_2\text{F}_2]^+$ ^c	$[\text{BrO}_2\text{F}_3]$	$[\text{BrO}_2\text{F}_4]^-$
	$[\text{BrOF}_4]^+$	$[\text{BrOF}_5]$	$[\text{BrOF}_6]^-$
	$[\text{IO}_3]^+$	IO_3F (69)	$[\text{IO}_3\text{F}_2]^-$
	$[\text{IO}_2\text{F}_2]^+$	IO_2F_3 (70, 71, 72,) (73)	IO_2F_4^- (25, 26, 27)
	$[\text{IOF}_4]^+$	IOF_5 (75, 76, 77)	$[\text{IOF}_6]^-$

* This work

a The references given do not constitute a complete survey of the literature, but refer to selected preparations and spectroscopic or structural evidence for the compounds.

b Compounds in square brackets have not yet been prepared (see Text)

c Reports of the preparations of these compounds are incorrect. For BrO_2F_2^+ , see Chapter VII; for ClOF_5 , see Reference 21.

It would, nevertheless, be important to attempt their preparation should it prove possible to prepare the parent molecules ClOF_5 and BrOF_5 , which are also unknown at the present time. Some reasons for the apparent non-existence of some of the species listed in Table 1.1 are discussed further in Chapter VIII.

The shapes of all the known oxyfluorides of the halogens have been successfully rationalized on the basis of the Valence Shell Electron Pair Repulsion Theory ⁷⁸(VSEPR). This theory states that the geometry of a molecule AX_mE_n is determined by the repulsions between the pairs of bonding electrons linking A to the ligands X and the non-bonding electron pairs E on the valence shell of the central atom A. Multiple bonds between A and X behave (to a first approximation) like a single pair of electrons, and do not change the overall arrangement of the ligands (although they will affect the angles between the ligands). The sum of the number of bonding sets of electrons (m) and non-bonding pairs of electrons (n) is the criterion which determines the structure of the molecule. Thus for $(m+n) = 2, 3, 4, 5$, and 6, linear, triangular, tetrahedral, trigonal bipyramidal, and octahedral arrangements of electron pairs, respectively, will be produced. Consideration of the numbers and types of repulsions between the various electron pairs allows one to predict which positions will be occupied by ligands and which will be taken up by non-bonding pairs.

Table 1.2 shows the structures of the Cl(V) oxyfluorides (and the singly charged anions and cations derived from them) and how these conform

TABLE 1.2

Structures of the Oxyfluoro Compounds of Cl (V)

Structure	Number of bonds (m)	Number of lone pairs (n)	m + n	Arrangement of e ⁻ pairs	Geometry of molecule
	2	1	3	trigonal	angular
	3	1	4	tetrahedral	trigonal pyramid
	4	1	5	trigonal bipyramid	disphenoid
	3	1	4	tetrahedral	trigonal pyramid
	4	1	5	trigonal bipyramid	disphenoid
	5	1	6	octahedral	square pyramid

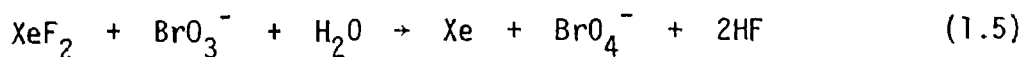
to the predictions of the VSEPR theory.

E. The Unusual Nature of Br (VII) Compounds

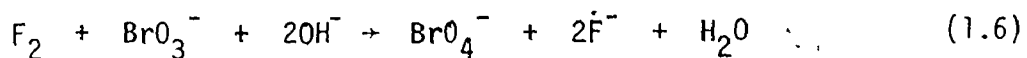
Compounds containing the halogens chlorine and iodine in the +VII oxidation state were synthesized more than a century ago. Perchlorate salts were prepared by von Stadion in 1816 by the oxidation of chlorates with sulphuric acid.⁷⁹ In 1833, Ammermüller and Magnus prepared trisodium paraperiodate $\text{Na}_3\text{H}_2\text{I}_6\text{O}_6$ by the oxidation of sodium iodate with chlorine.⁸⁰ Numerous attempts to prepare perbromate salts failed however, and several theoretical arguments have been proposed to explain the non-existence of this ion. These have been recently reviewed by Appelman.⁸¹ Perbromates were finally successfully prepared in 1968. The first synthesis resulted from a hot-atom process, the β decay of radioactive ^{83}Se incorporated into a selenate ⁸² (equation (1.4)). The



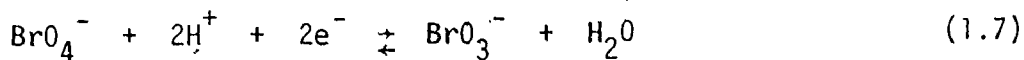
^{83}Br containing product co-precipitated with RbClO_4 and this was taken as evidence that it was present in the form of BrO_4^- . The first macro-scale preparation of perbromates was performed by means of an electrolytic oxidation of a neutral LiBrO_3 solution. The yield of this reaction was rather poor however ($\sim 1\%$).⁸² A much more efficient procedure⁸² employed an aqueous solution of XeF_2 (which forms a powerfully oxidizing solution, $E^\circ = 2.64\text{V}$ which has a half life of about 30 minutes at 25°C ⁸³) to oxidize BrO_3^- . The perbromate yield from this reaction (equation (1.5)) was



about 10%. Precipitation of the perbromate as RbBrO_4 led to the first isolation of a perbromate salt. The most convenient preparation of perbromates is by the oxidation of bromate with molecular fluorine in alkaline solution (equation (1.6)). This reaction produces BrO_4^- in 20% yield.^{84,85}



The numerous unsuccessful attempts to prepare the perbromate ion and its long-time status as a "non-existent" species are thus rather surprising, particularly in view of its considerable stability.⁸⁴ Pure KBrO_4 is stable up to about 275°C at which temperature it decomposes smoothly to KBrO_3 and oxygen. Aqueous solutions of perbromic acid are stable up to a concentration of 6 M. At higher concentrations, decomposition to Br_2 and O_2 takes place. In dilute solution at room temperature, perbromates are rather sluggish oxidizing agents. Even I^- is only very slowly oxidized by perbromate in dilute acid. At higher temperatures and concentrations, however, perbromic acid becomes a vigorous oxidizing agent. The electrode potential for the half-reaction (1.7) has been determined⁸⁶ to be 1.74V. Thus perbromate is a much more powerful



oxidant than perchlorate ($E^\circ = 1.23\text{V}$) and more powerful than periodate ($E^\circ = 1.64\text{V}$); this trend is similar to the one observed in group VI.⁸¹

Although, in view of the potential of 1.74V, a number of oxidizing agents should be capable of converting BrO_3^- to BrO_4^- no evidence for this oxidation has been obtained.^{81,87} For instance, ozone ($E^\circ = 2.07\text{V}$ ⁸⁸) and peroxydisulphate ($E^\circ = 2.01\text{V}$ ⁸⁸) do not oxidize BrO_3^- to BrO_4^- . This apparent discrepancy has been discussed by Appelman.^{81,86} The sluggish oxidizing nature of the perbromate ion implies that there is a considerable activation barrier to the reduction of BrO_4^- to BrO_3^- . Conversely then, the overall barrier to the formation of BrO_4^- from BrO_3^- is the sum of the overall free energy change of the reaction plus the activation barrier to reduction of perbromate. On this basis, only the very strongest oxidizing agents would be capable of producing perbromate by oxidation of bromate. The inability of earlier workers to synthesize perbromates is then a reflection of the kinetic barrier to the reaction rather than the thermodynamic unfavourability of the process. The reasons why electrolytic preparations of perbromates are so unfavourable are not clear, but Appelman has suggested⁸⁴ that an extremely unstable Br(VI) intermediate may occur in the reaction and that this causes a prohibitively high activation energy.

Two other Br (VII) species have been reported. BrO_3F can be prepared by fluorination of BrO_4^- with SbF_5 .⁶⁸ Although this oxyfluoride is considerably more reactive towards hydrolysis than the analogous ClO_3F , it is nonetheless a rather stable species. Similarly, the BrF_6^+ ion can be prepared by the reaction of BrF_5 with the extremely powerful fluorinating agents KrF^+ or Kr_2F_3^+ .⁷ Salts of the BrF_6^+ ion

have been shown to be rather stable at room temperature, although they are very powerful oxidizing agents and will convert O_2 to O_2^+ and Xe to XeF^+ . The stability of the three Br(VII) species prepared to date suggest that some of the other Br(VII) compounds listed in Table 1.1 should also be stable, isolable species.

F. Purpose of the Present Work.

The almost complete lack of information on the oxyfluoro species of bromine compared with our rather extensive knowledge of the corresponding compounds of chlorine and iodine at the outset of the present work was rather surprising. Although this could be taken to indicate a relatively low stability for the oxyfluoro compounds of bromine, such a conclusion would not be valid as no systematic attempt to synthesize such compounds has yet been reported. The object of the present work was, therefore, to attempt to prepare and characterize new oxyfluoro compounds of bromine, and to study their stabilities relative to those of the analogous chlorine and iodine compounds. It was also of interest to determine whether the structures of any such species are consistent with the structures of the corresponding chlorine and iodine compounds and with the predictions of the VSEPR theory. Although a complete X-ray structural study would be desirable for such new compounds, it was anticipated that their expected reactivity and physical properties might create considerable difficulties in a crystallographic study. The structures proposed in this thesis are, therefore, based on spectroscopic (Raman and ^{19}F nmr) evidence.

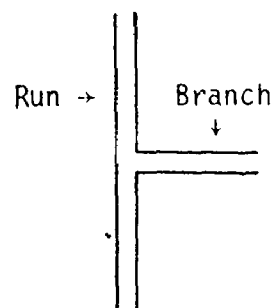
CHAPTER II

EXPERIMENTAL

A. Vacuum Techniques and Sample Handling.

Because the compounds used and prepared during the course of this work were sensitive to moisture, they were handled in a vacuum system or in the inert atmosphere of a dry-box. The vacuum lines used were constructed of glass or of Monel metal. Due to the corrosive nature of the reagents employed, reactions were carried out in fluoroplastic tubes. Kel-F tubes (2 cm o.d. x 15 cm long with a wall thickness of 1 mm), available from Argonne National Laboratories, were used for large-scale preparations or for storage of solvents. Smaller reaction vessels were made by heat-sealing one end of a short length of fluoroplastic tubing. The other end was then flared for attachment to a Teflon valve through a Kel-F, Teflon or FEP adaptor. Several sizes of fluoroplastic tubing were employed: FEP: 1/4" o.d. x 1/32" wall from the Fluoro-carbon Company, California; 0.154" o.d. x 0.02" wall from Warehoused Plastics Sales, Toronto. Kel-F: 0.132" o.d. x 0.008" wall from Adam Spence Corporation, New Jersey. The 0.154" o.d. FEP, and 0.132" o.d. Kel-F tubes were used to record ^{19}F nmr spectra. The fluoroplastic valves and adaptors used, as well as the vacuum systems, are described in more detail elsewhere.^{7,89} A method was developed (with Dr. G. J. Schrobilgen) for fusing together thin walled 1/4" o.d. FEP tubes. A TEE was constructed out of 7 mm i.d.

glass tubing (approximately 6" overall size). A length of 1/4" FEP tubing (~ 2 ft.) was inserted into the run of the TEE, with a hole (~ 1/4" diameter) cut in the side of the FEP tube at the branch of the TEE. A second 1/4" tube (~ 2 ft.) was inserted in



the branch of the TEE, and 4 mm glass rods were inserted into the 1/4" FEP tubes. The junction of the TEE was then gently heated over a Bunsen burner to melt the FEP, and the plastic tubes were pushed inwards during this heating to fill the junction section of the TEE with molten plastic. The inner glass rods prevented the molten FEP from collapsing. The system was allowed to cool and the glass rods could be removed just after the plastic had solidified but was still slightly warm. The outer glass TEE was then broken away. The FEP TEE produced was reamed out with a 5/32" drill bit silver-soldered to a long 5/32" metal rod. In this way, all-plastic double-armed reaction vessels could be made. 0.154" o.d. FEP spaghetti tubing could also be fused end-on to 1/4" o.d. FEP tubing by heating and drawing out the 1/4" FEP tube to approximately the same diameter as the spaghetti tubing. Then using a suitable glass outer jacket (a section of 5 mm thin-walled nmr tubing) and inner rod (2 mm diameter) the spaghetti tubing could be fused to the drawn-out 1/4" FEP tube over a very low flame. In this way, a section of spaghetti tubing (suitable for ^{19}F nmr spectroscopy) could be fused to the side-arm of a double-armed FEP reaction vessel. These vessels were convenient for transferring solutions at low temperature. The more conventional method of building a multi-armed

reaction vessel using Teflon compression fittings to hold the components together cannot be used to transfer solutions which must remain cold since the compression fittings cannot be cooled to very low temperatures without leaking.

The fluoroplastic reaction vessels used were conditioned with anhydrous HF , BrF_5 and F_2 before being used.

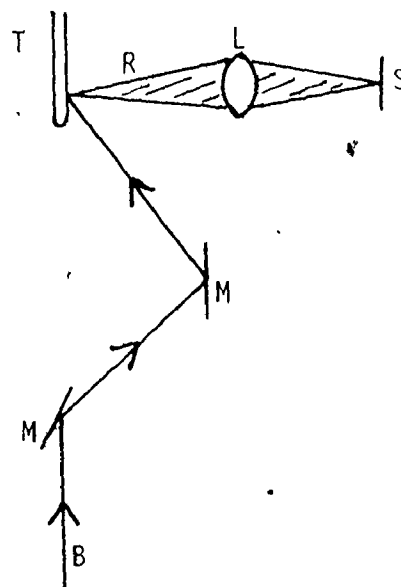
Certain samples could be handled in quartz tubes. 6 mm o.d. quartz tubes were connected to Teflon valves using 6 mm Teflon ferrules.

B. Instrumentation.

(i) Laser Raman Spectroscopy.

The laser Raman instrumentation used has been extensively described elsewhere.^{90,91}

In the early part of the work, the sample tube was positioned horizontally, at right angles to the laser beam, and the Raman-scattered radiation was observed perpendicular to both these directions. Low temperature spectra (down to $\sim -120^\circ\text{C}$) could be recorded using a technique described elsewhere.⁹⁰ For the major part of the work, however, the set-up shown in the schematic diagram was used. The sample tube (T) was mounted vertically, parallel to the entrance slit (S) of the spectrometer. The laser beam (B) was directed by means of two mirrors (M) to strike the sample at an angle of 45° ,



at the same level as the entrance slit on the spectrometer. The scattered radiation (R) was focussed onto the slit by the lens (L). The sample tube, the entrance slit, and the laser beam were all in one plane. This arrangement was found to produce more intense spectra than the previously described set-up, particularly for solid samples. Coloured samples could also be very conveniently rotated to avoid overheating of the sample due to absorption of the laser radiation. Polarization ratios were found not to be affected by this arrangement and were checked using a sample of liquid CCl_4 . Low temperature (down to -120°C) spectra could be obtained by passing cold N_2 through an unsilvered Pyrex double-walled Dewar. The cold gas was produced by boiling off liquid nitrogen from a Dewar at a controlled rate by an electric heater. The temperature was monitored with a copper-constantan thermocouple positioned close to the sample. Spectra could be obtained at -196°C by placing the sample against the inside wall of an unsilvered Pyrex Dewar filled with liquid nitrogen. Raman spectra were generally recorded using the green 514.5 nm line of an Argon ion laser using an output power between 50 and 300 mW. For some highly coloured samples (those containing Br_2^+ , see Chapter V), the red 632.8 nm line of an He-Ne laser was used. The Raman shifts quoted are estimated to be accurate to $\pm 2 \text{ cm}^{-1}$. Spectra were often recorded in Kel-F or FEP sample tubes and Raman lines due to the tubes were often observed. Their prominence in the overall spectrum depended on the efficiency of the sample as a Raman scatterer. In those cases where tube lines were observed, these have been subtracted out of the spectra in the

Tables but not in the Figures. (The only exception is Table 5.1 where the FEP lines have been listed). The characteristic spectra of FEP and Kel-F were recorded at various temperatures between room temperature and -196°C , and the positions and relative intensities of the peaks were found to be relatively constant in these spectra and in a number of spectra of different samples contained in FEP and Kel-F tubes. The tube lines subtracted from a sample spectrum at a given temperature were taken from reference spectra recorded at a similar temperature.

The use of fluoroplastic tubes to record Raman spectra also interfered, at times, with the measurement of polarization ratios. With some tubes the polarization ratios varied greatly when the spectra were recorded at different positions on the tube. This problem was more severe for some tubes than for others, and Kel-F tubes generally gave more consistent results than those made of FEP. Before being used for an experiment in which polarization ratios were to be determined, sample tubes were therefore filled with CCl_4 and the effect of the tube on the polarization ratios of CCl_4 was determined. Only tubes which did not have a significant effect were used.

The resolution of spectral curves shown in Figure 6.1 was carried out on a Dupont Model 310 curve resolver and curve plotter.

(ii) Nuclear Magnetic Resonance Spectroscopy.

^{19}F nmr spectra were usually recorded using a Varian DA-60 IL spectrometer operating at 56.4 or 58.3 MHz and modified as described elsewhere.^{89, 90, 92} Some spectra were recorded using a Varian HA-100 spectro-

meter operating at 94.1 MHz (samples of BrOF_3 in SO_2ClF and SO_2F_2 (Chapter IV) and the spectrum of a solution of BrO_3F in HF at room temperature (Chapter VII)), and the ^{19}F nmr spectrum of KBrOF_4 in CH_3CN was obtained using a Bruker WH90 spectrometer. All chemical shifts were measured relative to CFCl_3 as an external standard. Resonances to low field of CFCl_3 are assigned negative chemical shifts. The chemical shifts are estimated to be accurate to ± 2 ppm. For samples contained in FEP tubes, integration of the peaks in the spectrum was found to be very inaccurate. The fluorine nuclei in the sample tube give rise to a very broad ^{19}F nmr signal extending several hundred ppm to high and low field of CFCl_3 . The presence of this broad signal causes the integrator to continually drift. Because of this, the accuracy of the integration is at best $\pm 10\%$ and can be much worse if the two peaks being compared have widely differing chemical shifts.

C. Preparation and Purification of Starting Materials.

(i) Gases.

(a) Fluorine: F_2 gas (Matheson) was passed through two Matheson model 68-1008 hydrogen fluoride traps connected in series and admitted to a Monel vacuum line,⁸⁹ through 1/4" o.d. copper tubing.

(b) Inert atmospheres: Extra dry nitrogen (Canadian Liquid Air, 99.9%, < 10 ppm H_2O) was used for the dry-box atmosphere and for maintaining a pressure greater than atmospheric over Br(V) containing samples while they were being stored. Argon (Matheson, 99.998%) was used when

Br(VII) containing samples were being stored.

(ii) Solvents.

(a) HF: For the Br(V) work, anhydrous HF (Harshaw Chemical Co.) was distilled directly from the cylinder to a Kel-F storage vessel and was used without further purification. For the Br(VII) work, the unpurified HF was introduced into a 2 litre nickel can fitted with a Monel valve (Autoclave Engineers). F_2 was then admitted to the can (approximately 200-300 psi) and the mixture allowed to stand for several weeks. The non-condensable gases present were then removed at $-196^\circ C$ and the HF distilled into a Kel-F storage vessel.

(b) SO_2ClF and SO_2F_2 : SO_2ClF (Baker and Adamson) was distilled onto SbF_5 and allowed to stand at room temperature for an hour. The SO_2ClF was then distilled onto NaF where it was kept until used. Since the commercial product contained SO_2F_2 impurity, the most volatile fraction of each distillate was discarded. The purity of the SO_2ClF was verified by its ^{19}F nmr spectrum which showed only one line. SO_2F_2 was obtained from Matheson Gas Products and was used directly.

(c) Acetonitrile: CH_3CN (Fisher Scientific Co.) was purified by distillation from P_2O_5 , followed by distillation from dry K_2CO_3 . The distilled material was stored over molecular sieves until used.

(iii) Lewis Acids.

BF_3 (Matheson Co.) was purified by bubbling it through 100% sulphuric acid containing B_2O_3 .

AsF_5 (Ozark-Mahoning Co.) was used without further purification.

Some of the AsF_5 used was prepared by the direct interaction of powdered As metal (Alpha Inorganics, 99.5%) with excess F_2 at 300°C for several hours in a 1440 ml nickel can fitted with a stainless steel valve (Autoclave Engineers). The AsF_5 produced was used without further purification.

AsF_5 and BF_3 were transferred into reaction mixtures using a grease-free vacuum line of known volume.


SbF_5 (Ozark Mahoning Co.) was purified by double distillation in an atmosphere of dry nitrogen using an all-glass apparatus, and was stored in glass vessels in a desiccator. The distillation apparatus and procedure are described in detail elsewhere.⁹³

(iv) Other Reagents.

(a) Metal Fluorides: KF (BDH, 99%), NaF (Allied Chemical, reagent grade), and CsF (K & K, 99.9%) were dried under vacuum at 250°C for several days in a glass tube and stored under an atmosphere of dry N_2 until used.

(b) BrF_5 and IF_5 : BrF_5 (Ozark Mahoning Co.) was purified by bubbling fluorine through it until the liquid became colourless. It was then distilled onto dry NaF to remove traces of HF . IF_5 was purified in a similar manner.

(c) KBrO_3 and KBrO_4 : KBrO_3 (Allied Chemical, 99.8%) was dried under vacuum at 250°C for several days. KBrO_4 was generously provided by Dr. E. H. Appelman (Argonne National Laboratories), and was used without purification. It was, however, dried under vacuum at 120°C for several days.



(d) SeO_2 and SO_2 : Anhydrous SeO_2 (J.T.Baker, 99%) was used directly. SO_2 (Matheson) was distilled from P_2O_5 .

(e) Iodine Oxides and Oxyfluoro Species: I_2O_5 (Alfied Chemical, 99.5%) was dried under vacuum at 150°C for several days. IOF_3 and IO_2F were prepared by the method of Aynsley et al.⁵² IO_2F_3 was supplied by Dr. J. P. Krasznai and had been prepared by the method of Engelbrecht.¹⁰ $\text{IO}_2\text{F}_3 \cdot \text{AsF}_5$ and $\text{IO}_2\text{F}_3 \cdot \text{SbF}_5$ (prepared by direct reaction of IO_2F_3 with the Lewis acid²⁶) were also supplied by Dr. J. P. Krasznai, as was the sample of $\text{IO}_2\text{SO}_3\text{F}$. $\text{IOF}_2^+ \text{SbF}_6^-$ was prepared by the direct reaction of IOF_3 with excess SbF_5 using SO_2ClF as a solvent.

(f) KrF_2 : This was prepared with the assistance of Dr. G. J. Schrobilgen using the method reported by Schreiner et al.¹⁴

(g) KBrF_6 : 0.906 g (15.71 mmol) of KF and 11.06 g (63.2 mmol) of BrF_5 were stirred at room temperature for a week in a Kel-F tube, the excess BrF_5 was removed under vacuum leaving a white solid which weighed 3.750 g, which corresponds to 98% KBrF_6 . The Raman spectrum of this solid showed only the three lines reported by Shamir and Yaroslavsky.¹⁵ KBrF_6 is stable indefinitely when kept in well passivated Kel-F tubes. The decomposition reported by Shamir and Yaroslavsky for CsBrF_6 was, therefore, probably due to their use of storage vessels made of glass. KBrF_6 is very soluble in CH_3CN , but was found to decompose slowly in this solvent. A white solid, identified as KBrF_4 , from its Raman spectrum,^{15,16} was deposited. This decomposition proceeded in Kel-F, FEP, glass and quartz sample tubes so the decomposition is not due to attack on the walls

of the container. The other products of the decomposition could not be positively identified. A ^{19}F nmr spectrum of the decomposing solution did not show any peaks attributable to fluorinated solvent species. A gas was produced by the decomposing solution which turned moist starch I^- paper dark. Although it is perhaps somewhat surprising, the simplest explanation of our observations is that the decomposition proceeds according to equation (2.1). The rate of the decomposition can be mini-



mized by rigorously drying the CH_3CN , indicating that the above reaction may be catalyzed by traces of moisture.

(h) CsSO_2F : CsSO_2F was prepared following the method of Seel and Boudier,⁹⁷ by shaking CsF in liquid SO_2 for two days, followed by removal of the excess SO_2 under vacuum.

(i) $\text{KrF}^+\text{AsF}_6^-$ and $\text{BrF}_6^+\text{AsF}_6^-$: $\text{KrF}^+\text{AsF}_6^-$ was made by the direct interaction of KrF_2 with excess AsF_5 .⁹⁰ $\text{BrF}_6^+\text{AsF}_6^-$ was prepared by dissolving $\text{KrF}^+\text{AsF}_6^-$ in BrF_5 and allowing the solution to warm up to room temperature. The purity of both products was monitored by Raman spectroscopy.

CHAPTER III

PREPARATION AND CHARACTERIZATION OF KBrO_2F_2 AND KBrOF_4

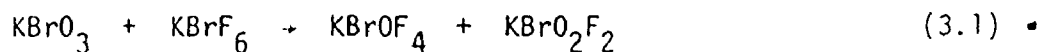
A. Introduction

At the outset of this work, no reliable evidence for the existence of the anionic species BrO_2F_2^- and BrOF_4^- had been reported. The compounds KBrO_2F_2 , NaBrO_2F_2 and $\text{Ba}(\text{BrO}_2\text{F}_2)_2$ had been reported by Mitra,⁹⁸ but this claim was withdrawn when the results were found to be irreproducible.⁹⁹ Independently of the present work, Bougon and his co-workers have recently reported the preparation and characterisation of KBrOF_4 ⁴³ and KBrO_2F_2 .^{45,46}

In this chapter, the preparation of the compounds KBrO_2F_2 and KBrOF_4 by several methods is described. Their Raman spectra have been observed and tentatively assigned. The ^{19}F nmr spectrum of KBrOF_4 has also been recorded.

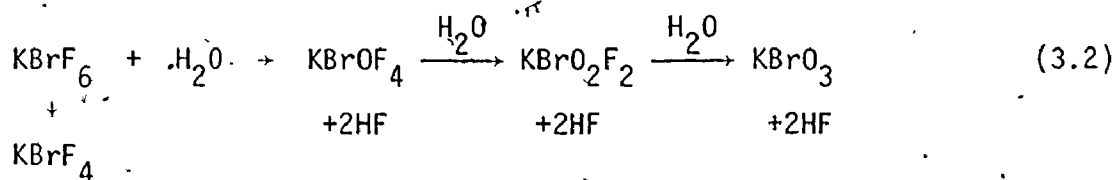
B. Preparation and Properties of KBrO_2F_2 and KBrOF_4

KBrO_2F_2 and KBrOF_4 can be most conveniently prepared by the reaction of KBrO_3 and KBrF_6 in CH_3CN (equation (3.1)). They can then be



separated by extraction of the mixture with CH_3CN . The KBrO_2F_2 is insoluble in CH_3CN , whereas the KBrOF_4 is slightly soluble. In this way reasonable amounts (0.3-0.5 g) of each product can be conveniently obtained.

Both KBrO_2F_2 and KBrOF_4 are also produced in the hydrolysis of KBrF_6 in CH_3CN . The hydrolysis is, however, not a smooth reaction and mixtures of products are obtained. When approximately 0.02 mmol of H_2O (dissolved in CH_3CN) is added to a solution of 0.22 mmol of KBrF_6 in CH_3CN , and the solvent is removed under vacuum, the resulting solid consists of mostly unreacted KBrF_6 with small amounts of KBrOF_4 and KBrO_2F_2 . Thus even when a 10:1 mole ratio of $\text{KBrF}_6:\text{H}_2\text{O}$ is used, both KBrOF_4 and KBrO_2F_2 are observed as products. It might have been expected that when KBrF_6 reacts with small amounts of H_2O , only KBrOF_4 would be formed, but this was not observed. When larger quantities of water were added, the amounts of KBrOF_4 and KBrO_2F_2 increased, but KBrF_4 also appeared as a major product (probably from the decomposition of KBrF_6 , which, in Chapter II, is shown to be catalysed by H_2O). When even more water was added KBrO_3 became the major product. These observations are consistent with the hydrolysis scheme (3.2). This hydrolysis cannot be used as a



convenient source of KBrOF_4 and KBrO_2F_2 because of the relatively large amounts of KBrF_4 produced. The reason that both BrOF_4^- and BrO_2F_2^- are observed even when small quantities of water are used is probably that the BrOF_4^- ion hydrolyses more rapidly than BrF_6^- . The maximum coordination number of bromine appears to be six, so that attack by water on the BrF_6^- ion would be expected to be slow. On the other hand, BrOF_4^- has a

vacant coordination site and would probably be rapidly attacked by water. A similar result has been reported for the hydrolysis of CsIF_6 with an equimolar amount of H_2O using CH_3CN as a solvent,⁵⁸ where the CsIOF_4 product is always contaminated with CsIO_2F_2 . The extent of contamination in this case is smaller than in the bromine system, reflecting the relative ease with which iodine can expand its coordination number to seven or more (e.g., IF_7 and IF_8^- ¹⁰⁰ are known) which would increase the relative rate of hydrolysis of the IF_6^- ion.

KBrO_2F_2 and KBrOF_4 are also produced in the reaction of KBrO_3 with BrF_5 (see Section E), and also by the reaction of the parent oxy-fluoride (BrO_2F or BrOF_3) with a fluoride ion donor (see Chapter IV).

Both KBrOF_4 and KBrO_2F_2 are white solids that are stable at room temperature and can be stored indefinitely in FEP, Kel-F or glass containers. They are, however, very sensitive to moisture and must be stored in rigorously dried vessels. When exposed to small amounts of moisture, the solids evolved a brown gas, presumably Br_2 .

Some other reactions of the Br(V) anions were also studied. When KBrOF_4 was shaken with excess KBrO_3 in CH_3CN overnight, the resultant product contained no KBrOF_4 , but only KBrO_2F_2 and KBrO_3 . This indicates that in CH_3CN , equilibrium (3.3) lies to the right. This may be due in



part to the extremely small solubility of KBrO_2F_2 in CH_3CN . This means that when excess KBrO_3 is used in the reaction of KBrO_3 with KBrF_6 , a

reduced amount of KBrOF_4 is obtained since the excess KBrO_3 reacts with some of the KBrOF_4 produced by equation (3.1). In BrF_5 as a solvent, KBrOF_4 and KBrO_3 also reacted to give KBrO_2F_2 , but not all the KBrOF_4 was consumed.

Although KBrOF_4 is stable in CH_3CN , and does not decompose to KBrO_2F_2 and KBrF_6 , it nevertheless cannot be prepared by the reaction of these two compounds, i.e. reaction (3.4) was found not to have proceeded to the right to any appreciable extent, even after 28 hours. This is



again probably due to the extremely low solubility of KBrO_2F_2 in CH_3CN .

C. Characterization of KBrO_2F_2 and KBrOF_4 by Raman Spectroscopy

Figure 3.1 shows the Raman spectrum of solid KBrO_2F_2 and Table 3.1 lists the observed lines and their assignments, together with those of some related molecules. The Raman spectrum corresponds well with that reported by Bougon and his coworkers.^{45,46} Because no solvent could be found for KBrO_2F_2 (it is insoluble in BrF_5 , CH_3CN and SO_2ClF , and a reaction occurs with HF [see Chapter IV]), no polarization data could be obtained. The assignments (Table 3.1) were made by comparison with the related molecules IO_2F_2^- ,^{54,55} ClO_2F_2^- ,³⁵ $\text{SeO}_2\text{F}_2^{2-}$ (Chapter VI) and XeO_2F_2 .¹⁰¹ On the basis of VSEPR theory and the geometries of the related molecules, BrO_2F_2^- is expected to have a C_{2v} structure with the lone pair and two oxygen atoms occupying the equatorial positions of a trigonal bipyramid. The nine fundamentals [$\Gamma = 4A_1 + A_2 + 2B_1 + 2B_2$] for

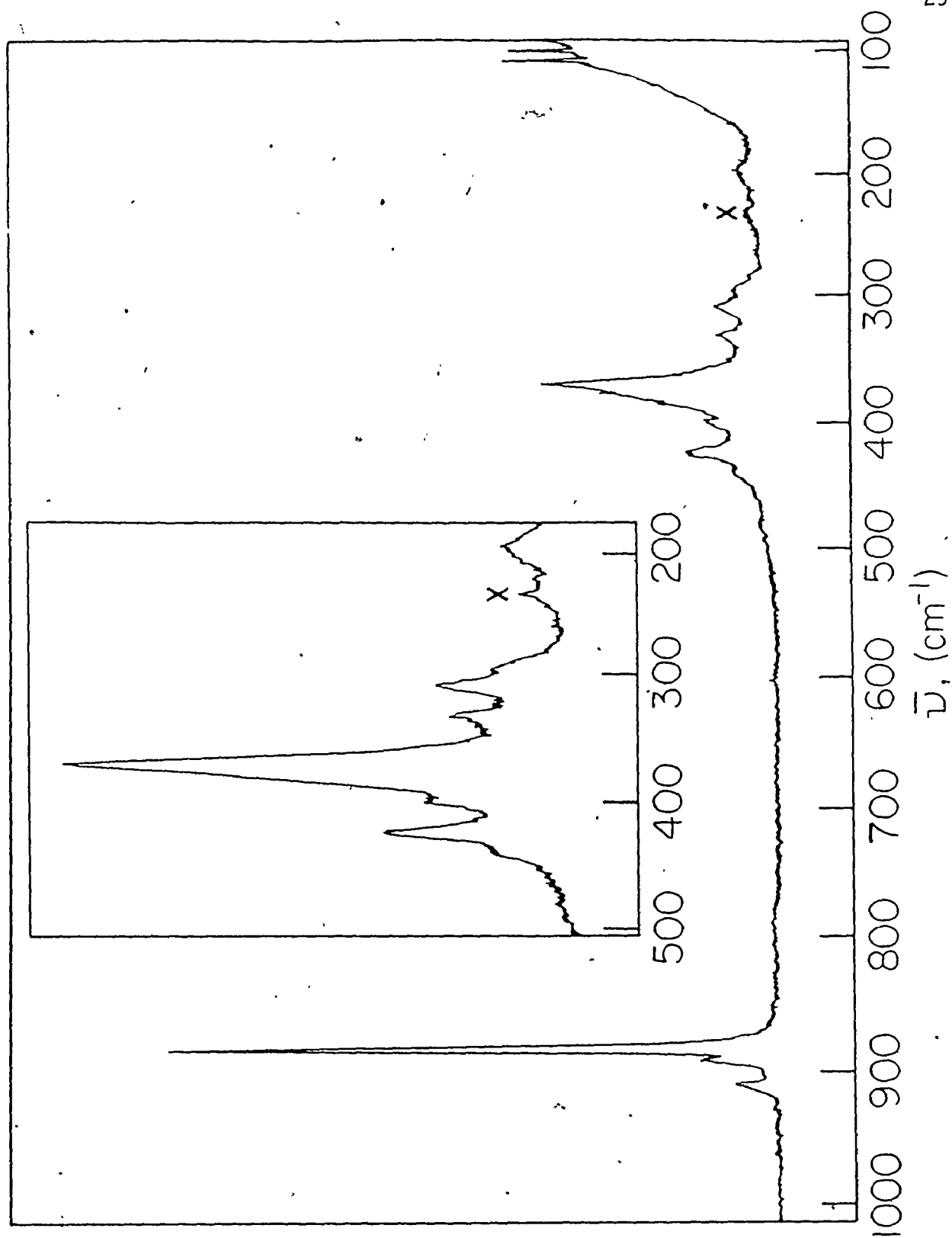


Figure 3.1. Raman spectrum of solid KBrO_2F_2 at 25°C . Peaks labelled X are due to an unidentified impurity (see Text)

TABLE 3.1

Raman Frequencies of BrO_2F_2^- and Some Related Molecules (cm^{-1})

BrO_2F (a)	XeO_2F_2 (b)	$\text{SeO}_2\text{F}_2^{2-}$ (c)	$\text{ClO}_2\text{F}_2^{-(d)}$	$\text{IO}_2\text{F}_2^{-(e)}$	$\text{BrO}_2\text{F}_2^{-(f)}$	Assignments
953(14)(g)	902 w ^(h)	833(25) 823(sh)	1221 (8)	838 w	910(7)	ν_8 (B_2) $\nu_{\text{asym}} \text{XO}_2$
908(100)	845 v.s	868(sh) 859(100)	1076(100) 1064 1055	817 v.s 804 w.sh	892(7) sh 884(100)	ν_1 (A_1) $\nu_{\text{sym}} \text{XO}_2$
-	578 w	-	-	456 v.w	442(sh)	ν_6 (B_1) $\nu_{\text{asym}} \text{XF}_2$
394(14)	333 m.s	445(10)	559(12)	360 m	424(14)	ν_2 (A_1) δXO_2
-	-	-	480(10)	-	400(2)	ν_5 (A_2) Torsion τ
-	490 s	396(15)	363(100)	479 s	380(sh) 369(35)	ν_3 (A_1) $\nu_{\text{sym}} \text{XF}_2$
-	313 m.s ⁽ⁱ⁾	304(20)	337(80) ⁽ⁱ⁾	323 s	338(8)	ν_7 (B_1) δ rock
-	313 m.s	-	337(80)	346 w	307(9) 293(sh)	ν_9 (B_2) δ wag
-	198 w	241(12)	198 (7)	194 v.w	197(4)	ν_4 (A_1) δXF_2
-	-	-	-	-	118 br	Lattice mode

a See Chapter IV. b Reference 101. c See Chapter VI. d Reference 35. e References 54,55

f KBrO_2F_2 g Numbers in parentheses give relative intensities.

h s, strong; v.s, very strong; m, medium; w, weak; v.w, very weak; sh, shoulder; br, broad.

i ν_7 and ν_9 are coincident in these molecules.

such a structure are all expected to be Raman active.

The three highest frequency lines can be readily

assigned to the BrO_2 symmetric and asymmetric

stretching frequencies, with $\nu_{\text{sym}} \text{BrO}_2$ being split

by solid state effects. The XO_2 ($\text{X} = \text{Cl}, \text{Br}, \text{I}$)

stretching frequencies in the XO_2F_2^- anions decrease in the order $\text{Cl} > \text{Br} > \text{I}$,

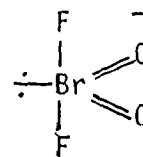
which is due to the increasing mass of the central atom X and the decrease in bond strength as the electronegativity of X decreases. The $-\text{BrO}_2$

stretching frequencies are also lower than those in BrO_2F which is consis-

tent with a decreased BrO double bond character due to the negative charge

of the anion. Finally the BrO_2 frequencies in BrO_2F_2^- are higher than the

SeO_2 frequencies in the isoelectronic SeO_2F_2^- , reflecting the additional bond weakening by the extra negative charge in the selenium compound.



(1)

These three assignments agree with those of Bougon et al.⁴⁶ and our previously published work.¹⁰² The remaining assignments are less definitive. They differ from our previously published interpretation and agree with those of Bougon et al. The strongest remaining line at 369 cm^{-1} was previously assigned to δ_{rock} whereas $\nu_{\text{sym}} \text{BrF}_2$ was assigned to the line at 424 cm^{-1} . Bougon et al. on the other hand, assigned the strong lines at 369 cm^{-1} to $\nu_{\text{sym}} \text{BrF}_2$. Since $\nu_{\text{sym}} \text{BrF}_2$ is an A_1 mode and is a strong line in the spectra of the related molecules, it seems reasonable to assign it to the line at 369 cm^{-1} (along with a shoulder at 380 cm^{-1}).

The lowest frequency peak at 197 cm^{-1} is assigned to δBrF_2 which occurs as the lowest frequency fundamental in all the related molecules.

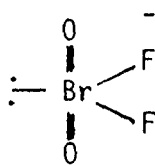
The remaining assignments are more arbitrary. The 307 cm^{-1} peak (and the shoulder at 293 cm^{-1}) are assigned to δ_{wag} , and are in the same region as the corresponding motions in IO_2F_2^- and ClO_2F_2^- . Since in all the related molecules, $\delta_{\text{rock}} < \nu_{\text{sym}}\text{XF}_2$, the peak at 338 cm^{-1} is assigned to δ_{rock} . This also places δ_{rock} and δ_{wag} close together in frequency, which is also observed in IO_2F_2^- , XeO_2F_2 and ClO_2F_2^- (in the last two, these two modes have the same frequency). $\nu_{\text{asym}}\text{XF}_2$, which should be a very weak peak in the Raman, has been assigned to the shoulder at 424 cm^{-1} .

This leaves only two fundamentals, $\delta_{\text{s}}\text{BrO}_2$ and the torsion mode τ , to be assigned. In ClO_2F_2^- (which is the only molecule where τ has been assigned), δXO_2 is more intense and also at higher frequency than τ . Therefore, the stronger peak at 424 cm^{-1} is assigned to δBrO_2 with the weak peak at 400 cm^{-1} assigned to τ . This assignment for δBrO_2 places it between the values found for ClO_2F_2^- and IO_2F_2^- and in the same region as the analogous motion in BrO_2F [In ClO_2F_2^- and ClO_2F ,³¹ and in XeO_2F_2 and XeO_2F^+ ,¹⁰³ the δXO_2 motions occur at similar frequencies].

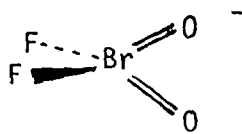
A small peak (<3% relative intensity) appeared on several spectra at about 230 cm^{-1} . However, since the relative intensity of this peak varied from one spectrum to the next and since it was absent on some spectra, it has been assigned to an unidentified impurity. The broad shoulder at 118 cm^{-1} has been attributed to a lattice mode and the two sharp spikes at 111 cm^{-1} and 100 cm^{-1} are associated with the glass sample tube (and have not been listed in Table 3.1).

Other geometries for the BrO_2F_2^- ion such as (2) and (3) are possible

(if the analogy with the related ions ClO_2F_2^- and IO_2F_2^- and the predictions of VSEPR are ignored). Although both structures have C_{2v} symmetry and would be expected to show the same number of Raman lines as a molecule of structure (1), these alternative geometries are not as consistent with



(2)



(3)

the observed Raman spectrum as the structure (1) proposed above. In the case of (2), $\nu_{\text{asym}} \text{BrO}_2$ would be predicted to be extremely weak in the Raman spectrum, and for both (2) and (3), $\nu_{\text{asym}} \text{BrF}_2$ would not be expected to be one of the weakest lines in the spectrum. The vibrational spectrum is, therefore, more consistent with the suggested structure (1) than with the alternative structures (2) and (3).

Figures 3.2 and 3.3 show the Raman spectra of KBrOF_4 at room temperature and liquid nitrogen temperature respectively. The low temperature spectrum is much better resolved and shows a few extra peaks. The room temperature spectrum is very similar to that obtained recently by Bougon et al.⁴⁹ Table 3.2 lists the observed frequencies along with those of some related molecules and ions. Our assignments agree quite well with those reported by Bougon and his coworkers. Although KBrOF_4 is slightly soluble in CH_3CN , the solubility is not large enough to allow a solution spectrum of KBrOF_4 to be obtained. BrF_5 , SO_2ClF and HF also proved unsuitable as solvents so no polarization data is available. The assignments

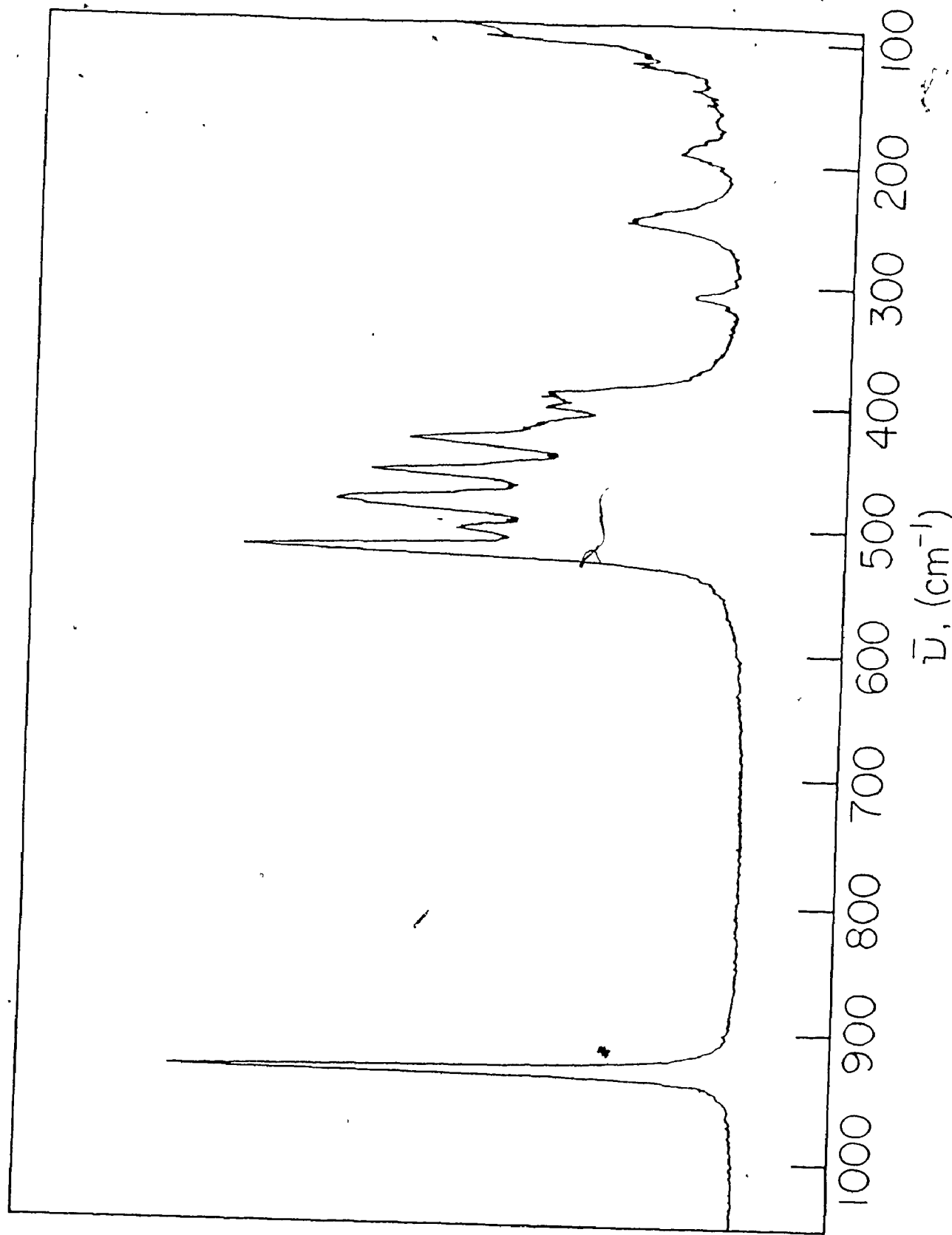


Figure 3.2. Raman spectrum of solid KBrOF_4 at 25°C.

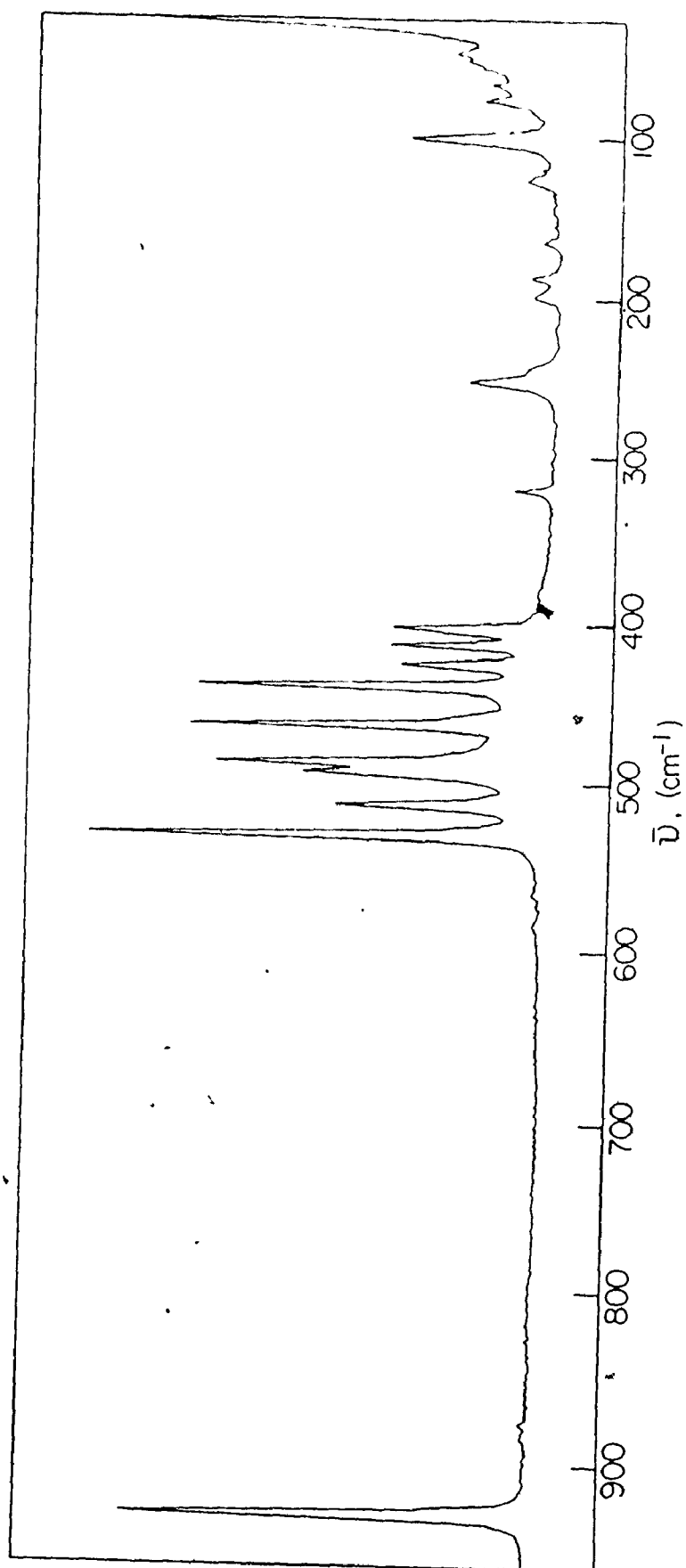


Figure 3.3. Raman spectrum of solid KBrOF_4 at -196°C .

TABLE 3.2

Raman Frequencies of BrOF_4^- and Some Related Molecules (cm^{-1})

BrF_4^- Infra Raman red	XeOF_4 (b) (liquid)	ClF_5 (b) (liquid)	ClOF_4^- (c) (gas)	IF_5 (d) (gas)	IOF_4^- (e) (liquid)	BrF_5 (b) (liquid)	BrOF_4^- (g) solid (f) at 10°K Room temp.	Assignments
-	920(20) ^(h)	709(30)	1211 (6)	710 (5)	888 v.s. ⁽ⁱ⁾	682(70)	930(100)	$\nu_1 A_1$, X=0
-	530	567(100)	461(100)	614 v.s	533 v.s	570(100)	523(100)	$\nu_2 A_1$ $\nu_{\text{sym}} \text{XF}_4$ in phase
570	-	[608] ^(j)	599 (1) 557 (4)	631 sh	475 m,sh	[644]	503(50)	506(47) 486(55)sh $\nu_7 E \nu_{\text{asym}} \text{XF}_4$
-	455	527(40)	350(43) ^(k)	602 sh	485 m	535(100)	478(70) 454(70)	$\nu_4 B_1$ $\nu_{\text{sym}} \text{XF}_4$ out-of-phase
-	-	354(20)	416(14) 395(1)	370 w	365 m.s	414(10)	429(60) 417(sh) 403(35) 392(35)	$\nu_8 E \delta \text{OXF}$
302	-	285(0+) ^(l)	[350]	318 m	273 m	365(20)	310(12)	$\nu_3 A_1$ $\nu_{\text{sym}} \text{XF}_4$ out-of-plane
-	242	233(10)	285(4)	318 m	214 w	312(10)	241(25)br 239(sh)	$\nu_6 B_2$ $\nu_{\text{sym}} \text{XF}_4$ in plane
-	-	161(0+)	213(16)	200 w	144 w,br	237(0+)	187(10) 196(5) 184(5)	$\nu_9 E \delta_{\text{asym}} \text{XF}_4$ in plane

continued.....

TABLE 3.2 (continued)

Raman Frequencies of BrOF_4^- and Some Related Molecules (cm^{-1})

BrF_4^- (a) Infra Raman red	XeOF_4 (b)	ClF_5 (b) (liquid)	ClOF_4^- (c)	IF_5 (d) (gas)	IOF_4^- (e)	BrF_5 liquid (b) solid (f) at 10°K	BrOF_4^- (g) Room temp. -196°C	Assignments
-	-	[230]	[346]	-	-	[281]	-	$\nu_5 \delta_1 \delta_{\text{asym}} \text{XF}_4$ out-of-plane
-	-	-	-	-	-	-	119(10)	Lattice modes
-	-	-	-	-	-	53	161(3)	
-	-	-	-	-	-	51	122(5)	
-	-	-	-	-	-	48	97(30)	
-	-	-	-	-	-	38	74(8)	
-	-	-	-	-	-	36	66(3)	
-	-	-	-	-	-	-	46(6)	

a Reference 96. b Reference 105. c Reference 42. d Reference 106. e Reference 58. f Reference 104.
g KBrOF_4 h Numbers in parentheses give relative intensities.

i s, strong; v.s, very strong; m, medium; w, weak; br, broad; sh, shoulder.

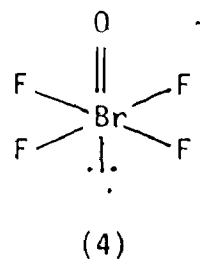
j Frequencies in brackets were not observed directly in the Raman spectrum but were obtained from the infra-red spectrum or estimated from combination bands or force constant calculations.

k ν_3 and ν_4 are coincident in these molecules.

l Intensity too small to be measured.

in Table 3.2 are thus based only on comparison with the related molecules BrF_5 (solid ¹⁰⁴ and liquid ¹⁰⁵), IOF_4^- ,⁵⁸ ClOF_4^- ,⁴² XeOF_4 ¹⁰⁵ and BrF_4^- .⁹⁶ The assignments were also made so that the differences in frequency between BrF_5 and BrOF_4^- were similar to differences between ClF_5 ¹⁰⁵ and ClOF_4^- , and IF_5 ¹⁰⁶ and IOF_4^- . The BrOF_4^- ion is expected to have a square pyramidal geometry (structure (4)) of C_{4v} symmetry. All the related molecules have this geometry and the ¹⁹F nmr

spectrum of BrOF_4^- (see Section D) also supports this. The nine fundamental modes are classified as $3A_1 + 2B_1 + B_2 + 3E$, and all are Raman active. The asymmetric XF_4



bending mode would, however, be expected to be very weak (this mode is inactive in D_{4h} symmetry), and has not been observed in any of the related molecules. This mode is, therefore, assumed not to be observed for BrOF_4^- .

The single line at 930 cm^{-1} is obviously the BrO stretching motion which, as expected, is intermediate in strength between those of IOF_4^- and ClOF_4^- . The fact that this frequency is very close to the mean of the BrO_2 stretching motions in BrO_2F (931 cm^{-1}) indicates that the bond weakening effect of the negative charge is offset by the greater electron withdrawing power of four fluorines in BrOF_4^- as compared to the single fluorine and one oxygen in BrO_2F .

The strongest Raman band should be the BrF_4 symmetric stretch, ₂ and the line at 523 cm^{-1} in the room temperature spectrum (529 cm^{-1}

at -196°C) is assigned to this motion. This frequency is quite similar to that in BrF_4^- (530 cm^{-1}) and lower than that in BrF_5 (570 cm^{-1}). The next strongest band should be the symmetric out-of-phase stretching mode ν_4 . This motion should come in roughly the same region as the similar motion in BrF_4^- (455 cm^{-1}), and the peaks at 478 cm^{-1} and 454 cm^{-1} (room temperature) and 481 and 459 cm^{-1} (-196°C) are both possible. In solid BrF_5 this motion is split into two components (at 525 cm^{-1} and 539 cm^{-1}). Both 478 cm^{-1} and 454 cm^{-1} are, therefore, assigned to ν_4 in BrOF_4^- . The peak at 503 cm^{-1} in the room temperature spectrum is assigned to $\nu_{\text{asym}}^{\text{XF}_4}$. In the -196°C spectrum a line at 486 cm^{-1} appears in addition to the line at 506 cm^{-1} , and both lines are assigned to $\nu_{\text{asym}}^{\text{XF}_4}$, with the E mode split into its two components by solid state effects.

The five deformations remain to be assigned; $\nu_8(\text{E})$ should be the highest frequency deformation, since it involves motion of the doubly bonded oxygen atom, and it is assigned to the peaks at 429 cm^{-1} (along with the shoulder at 417 cm^{-1}), 403 cm^{-1} and 392 cm^{-1} in the room temperature spectrum. These lines are well resolved at -196°C and are at 434 cm^{-1} , 421 cm^{-1} , 409 cm^{-1} , and 399 cm^{-1} . These values are close to those in BrF_5 ($425, 417$, and 414 cm^{-1}), IOF_4^- (365 cm^{-1}) and ClOF_4^- (416 cm^{-1} and 395 cm^{-1}), and it is assumed that the E mode is extensively split by solid state effects. Similarly extensive splittings have been observed for ν_8 and ν_9 of solid BrF_5 at 10°K .¹⁰⁴ As in all related molecules, ν_9 should have the lowest frequency of all and the broad line at 187 cm^{-1} in the room temperature spectrum is thus assigned to ν_9 . At -196°C , this

line is split into two components at 196 cm^{-1} and 184 cm^{-1} . ν_3 can be assigned to the line at 310 cm^{-1} (314 cm^{-1} at -196°C) and ν_6 to the line at 241 cm^{-1} (a shoulder at 239 cm^{-1} appears in the low temperature spectrum). Both these assignments place the frequency found for BrOF_4^- between those in IOF_4^- and ClOF_4^- and similar to the frequency in BrF_4^- . As was mentioned earlier, it was assumed that ν_5 was too weak to be observed.

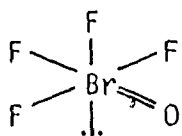
A line was observed at 161 cm^{-1} in the low temperature spectrum which was not observed at room temperature. This line is assigned to a lattice mode as it is too low in frequency to be a fundamental. Several other lattice modes (122 , 97 , 74 , 66 , and 46 cm^{-1}) were also observed in the low temperature spectrum.

The main difference between our assignments and those reported by Bougon et al. are as follows. They have assigned the peaks at 506 cm^{-1} and 478 cm^{-1} as the two components of $\nu_{\text{asym}}\text{BrF}_4(\text{E})$. However, the rather large intensity of the 478 cm^{-1} peak makes this assignment dubious. Furthermore, in our low temperature spectrum, the 478 cm^{-1} line splits into two lines at 486 cm^{-1} and 481 cm^{-1} , which also favours our assignment. Bougon et al. assign the peak at 161 cm^{-1} as a component of $\delta_{\text{asym}}\text{XF}_4(\text{E})$, with the broad peak at 187 cm^{-1} as the second component. However, at low temperature, the 187 cm^{-1} peak is split into two components which we have attributed to the splitting of the E mode, leaving 161 cm^{-1} as a lattice vibration. The fact that 161 cm^{-1} is not observed on our room temperature spectrum also supports this assignment. Finally, Bougon et al. attribute the shoulder at 239 cm^{-1} to ν_5 , the mode which we assumed to be unobserved.

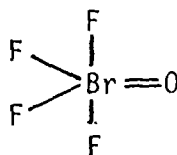
This value is close to what would be expected by comparison with the calculated value for BrF_5 , and may be observable if the BrOF_4^- is distorted in the solid. However, ν_5 is not observed in solid BrF_5 ¹⁰⁴ or in solid RbClOF_4 and CsClOF_4 ⁴² and we have, therefore, assigned the shoulder at 239 cm^{-1} as a component of $\delta_{\text{sym}}\text{XF}_4$ in-plane, leaving ν_5 unobserved.

D. ^{19}F N.M.R. Spectrum of KBrOF_4 .

The ^{19}F nmr spectrum of a saturated solution of KBrOF_4 in CH_3CN at room temperature showed a single peak at -104 ppm (width at half height $\sim 275\text{ Hz}$). This peak is in the F on Br(V) region and is slightly upfield from the resonance due to the basal fluorines (-132 ppm ¹⁰⁷) of the iso-electronic molecule BrF_5 . It is also slightly upfield of the chemical shift for the parent molecule BrOF_3 which occurs at -160 ppm (see Chapter IV). The observation of a single line for BrOF_4^- is in agreement with the equivalence of the four fluorine atoms in the proposed structure (4). Other possible structures such as (5) or (6) (which do not conform to the predictions of VSEPR) would be expected to exhibit more than one F-on-Br(V) resonance.



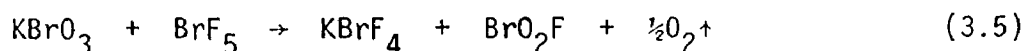
(5)



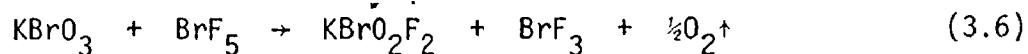
(6)

E. The Reaction of KBrO_3 and BrF_5 .

The reaction of KBrO_3 and BrF_5 has been reported by Schmeisser and Pammer²³ to occur at -50°C according to equation (3.5). Independently of our work, Bougon and Tantot⁴⁵ have reported that this reaction at room



temperature gives different products and proceeds according to equation (3.6) when approximately equimolar amounts of BrF_5 and KBrO_3 are used.

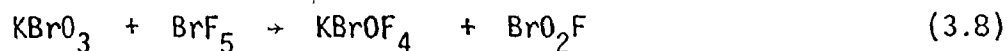
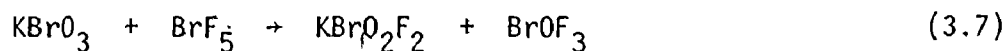


When $\text{BrF}_5:\text{KBrO}_3$ ratios higher than 1:1 were used, they reported that the reaction was slow, whereas when lower ratios were used, KBrF_4 was the main product and the reactions were at times violent. Bougon and his coworkers⁴⁹ also showed that when a 15:1 molar ratio mixture of BrF_5 and KBrO_3 was refluxed in the presence of 8.7 atmospheres of fluorine, KBrOF_4 is obtained as a solid product after 16 hours. The other products were not identified and no reactions were proposed. Because the reaction of KBrO_3 with BrF_5 had been reported²³ to be the most convenient preparation for BrO_2F , it was studied in the present work. Our results were not compatible with either those of Schmeisser and Pammer or those of Bougon et al. It was found that when pure reagents are used, KBrO_3 and BrF_5 do not react appreciably at -50°C when $\text{BrF}_5:\text{KBrO}_3$ ratios between 1.24:1 and 3.7:1 were used. Even after the mixtures had stood at this temperature for several hours, Raman spectroscopy showed that the white solid remaining after the BrF_5 was removed under vacuum was essentially pure KBrO_3 .

The Raman spectra generally had a small peak at 884 cm^{-1} due to KBrO_2F_2 . When a mixture of BrF_5 and KBrO_3 (2.62:1) was allowed to react at room temperature for six hours, a larger (but still relatively minor) amount of KBrO_2F_2 was produced, and a very small amount of BrO_2F was obtained.

We have found, however, that when a very small amount of HF is added the reaction is much more rapid and substantial amounts of BrO_2F are obtained, and the solid product of the reaction consists mostly of KBrO_2F_2 with variable amounts of KBrOF_4 being present (usually between 0% and 20%, as estimated from the Raman spectra). In most cases the KBrO_3 is completely consumed. The amount of KBrOF_4 produced varied considerably from one reaction mixture to the next. Our results are not consistent with the reaction scheme proposed by Schmeisser and Pammer as KBrF_4 is not usually observed as a solid product. Our results are also not consistent with those of Bougon and Tantot as they did not observe BrO_2F as a product. Furthermore, neither of the previously proposed reactions explain the formation of KBrOF_4 .

Our results can be explained by the following reaction schemes. Two first steps are possible. Which of these steps occurs will depend on

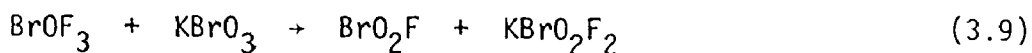


whether BrO_2F or BrOF_3 is the stronger fluoride ion acceptor. In the related chlorine system, ClOF_3 is a stronger F^- acceptor than ClO_2F .⁴³ Also, when a mixture of KBrOF_4 and KBrO_2F_2 is reacted with a deficit of

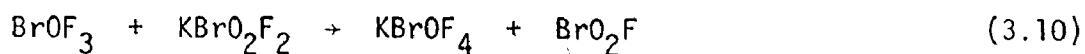
As F_5 in BrF_5 , all the KBrO_2F_2 reacts whereas some KBrOF_4 is left unreacted. These two facts, as well as the facile reaction of BrOF_3 with KHF_2 (see Chapter IV) suggest that BrOF_3 is a stronger F^- acceptor than BrO_2F , and that reaction (3.8) is the first step. Since KBrO_2F_2 is the main solid product, reaction (3.8) must be followed by another step. A reasonable reaction would be (3.3) which has earlier been shown to proceed to the right in BrF_5 . The fact that reactions (3.3) and (3.8) occur at the same time and that their rates may depend on the exact composition of the reaction mixture could account for the variable ratios of KBrO_2F_2 and KBrOF_4 formed in different reactions.

The role of HF in promoting the reaction is not clear, but it must be involved in the first step rather than in the second step, since this second step (reaction (3.3)) has already been shown to occur in BrF_5 in the absence of HF.

If the relative Lewis acidities of BrOF_3 , and BrO_2F are ignored in choosing the first step of the reaction, another possible reaction scheme would be equation (3.7), followed by a rapid reaction such as (3.9)

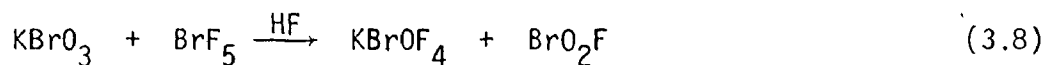


so that BrOF_3 would not be observed as a product. This would be analogous to the situation found in the reaction of BrF_5 with water or IO_2F , where BrOF_3 is not observed as a product (see Chapter IV). Reaction (3.10) would have to proceed to a small extent in order to account for the KBrOF_4

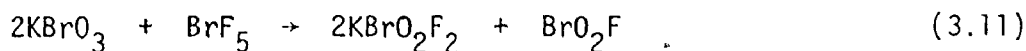


observed in the products. This scheme is made unlikely by the fact that when the reaction of KBrO_3 with BrF_5 was carried out in the presence of KF (mole ratio (1:1.9:1)), a normal (i.e. $\sim 10\%$) amount of KBrOF_4 was observed. If BrOF_3 were present as an intermediate, this would have reacted rapidly with the KF present to produce an unusually large amount of KBrOF_4 .

The first mechanistic scheme given is thus more likely and the proposed reaction scheme is thus (3.8) followed by (3.3).



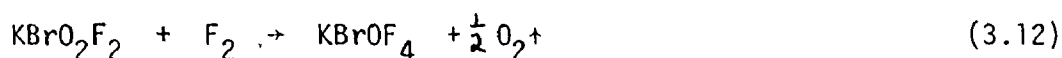
If (3.3) proceeds to completion, then the overall reaction becomes (3.11).



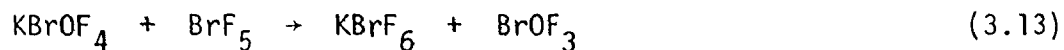
On the basis of (3.11), one mole of KBrO_2F_2 should be produced per mole of KBrO_3 used. Comparison of the weights of KBrO_2F_2 product and the KBrO_3 used showed that this was indeed the case (see Section F). The yield of BrO_2F obtained from this reaction was typically about 50% of theoretical yield calculated for equation (3.11). Also, the reaction mixture usually turned quite dark brown due to evolution of bromine. Thus the low yield of BrO_2F can be attributed to its decomposition in the reaction mixture. The products reported by Bougon and Tantot for the reaction of KBrO_3 with BrF_5 (equation (3.6)) may be attributable to the complete decomposition of the BrO_2F in the reaction mixture which would

produce Br_2 , BrF_3 and O_2 (however, Bougon and Tantot do not specifically mention the production of Br_2). This decomposition of BrO_2F would be favoured by the rather small amount of BrF_5 solvent present at low $\text{BrF}_5:\text{KBrO}_3$ ratios.

Bougon and his coworkers have also reported that heating a mixture of BrF_5 with KBrO_3 (15:1 mole ratio) in the presence of F_2 produces KBrOF_4 as the only solid product.⁴⁹ It is likely that the fluorination of KBrO_2F_2 to KBrOF_4 in this case is due to the F_2 (e.g. equation (3.12)) and not due to a reaction between BrF_5 and KBrO_2F_2 .



Bougon et al. report the formation of O_2 gas and add that under more vigorous conditions, KBrF_6 is obtained. The fluorination of KBrO_2F_2 to KBrF_6 must employ F_2 as the fluorinating agent since BrF_5 is a much weaker fluoride ion acceptor than BrOF_3 , so that reaction (3.13) would not proceed to the right. The direct reaction of F_2 with KBrO_2F_2 to give

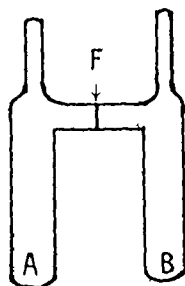


KBrOF_4 and ultimately KBrF_6 is in agreement with our observation that BrO_2F can be fluorinated to BrOF_3 and then BrF_5 by the strong fluorinating agent KrF_2 (see Chapter IV).

F. Experimental Section

(i) Preparation of KBrOF_4 and KBrO_2F_2 by the Reaction of KBrO_3 and KBrF_6 .

0.216 g (1.30 mmol) of KBrO_3 and 0.250 g (1.42 mmol) of KBrF_6 were shaken with 1.3 g of CH_3CN for 12 hours in a Kel-F tube. The solvent was removed under vacuum and a white solid resulted which showed only lines attributable to KBrOF_4 and KBrO_2F_2 . The separation of KBrOF_4 from KBrO_2F_2 relies on the slight solubility of KBrOF_4 in CH_3CN compared to the insolubility of KBrO_2F_2 . 0.315 g of a mixture of KBrO_2F_2 and KBrOF_4 and 2.4 g of CH_3CN were placed in ampoule A of the glass apparatus shown.



The mixture was shaken for 2 hours. The liquid was then filtered over to side B, through the glass frit F, and the CH_3CN distilled back to side A. A small amount of white solid was deposited in B. This operation was then repeated several times. The progress of the extraction can be monitored by Raman spectroscopy. The white material in B was KBrOF_4 . Calc. for KBrOF_4 : K, 18.53%; Br, 37.87%; F, 36.02%. Found: K, 18.88%; Br, 37.46%; F, 38.14%. KBrO_2F_2 was obtained when a mixture of KBrO_2F_2 and KBrOF_4 was extracted with CH_3CN , as described above, and all the KBrOF_4 removed in this way. Calc. for KBrO_2F_2 : K, 20.69%; Br, 42.48%;

F, 20.10%. Found: K, 20.40%; Br, 42.57%; F, 20.25%. The analyses were performed by Schwarzkopf Microanalytical Laboratories, Woodside, New York.

(ii) Hydrolysis of KBrF_6 .

A solution of 10 ml of H_2O in 200 ml of dry CH_3CN was prepared using a 10 ml syringe (Hamilton Co. Inc., Whittier, California). Aliquots of this stock solution were then syringed into a solution of KBrF_6 (0.051 g, 0.22 mmol) dissolved in CH_3CN (0.3 g) in a 6 mm o.d. quartz tube. After each addition the solvent was removed under vacuum, and the Raman spectrum of the solid produced was recorded.

(iii) Reactions of KBrOF_4 and KBrO_3 , and KBrF_6 and KBrO_2F_2 :

(a) KBrOF_4 and an unmeasured excess of KBrO_3 were placed in an FEP nmr tube and CH_3CN was distilled in. The mixture was allowed to stand at room temperature overnight. The solvent was then removed under vacuum. The Raman spectrum of the resulting solid showed only lines attributable to KBrO_3 and KBrO_2F_2 . This reaction was also done using BrF_5 as a solvent. KBrOF_4 (0.026 g, 0.12 mmol) and KBrO_3 (0.051 g, 0.31 mmol) were allowed to react for five hours at room temperature in the presence of BrF_5 (0.94 g) as a solvent. The solvent was removed under vacuum. The Raman spectrum of the resultant solid showed that in addition to excess KBrO_3 , approximately equal amounts of KBrO_2F_2 and KBrOF_4 were present.

(b) Approximately equal amounts of KBrF_6 and KBrO_2F_2 were placed in a Kel-F tube and CH_3CN was distilled in. The mixture was agitated at room temperature for 28 hours, and the CH_3CN was removed under vacuum, leaving a white solid. Raman spectroscopy indicated that no KBrOF_4 had

been produced. There was, however, some KBrF_4 produced, probably from the decomposition of KBrF_6 .

(iv) Reaction of KBrO_3 with BrF_5 .

In a typical reaction 2.756 g (16.5 mmol) of KBrO_3 , 7.56 g (42.0 mmol) of BrF_5 and 0.0124 g (0.6 mmol) of HF were allowed to mix at room temperature for 3-5 hours in a Kel-F tube. The resulting mixture was brown in colour due to production of Br_2 by partial decomposition. The volatile products were then pumped through a -48°C trap (n-hexyl alcohol slush bath). 0.590 g of white material (BrO_2F) was collected in the -48°C trap, which corresponds to 4.51 mmol of BrO_2F (55% yield based on the proposed reaction scheme). The low yield is presumably due to decomposition of BrO_2F in the reaction mixture. A white solid remained in the reaction vessel which was identified from its Raman spectrum as consisting mostly of KBrO_2F_2 (with about 10% KBrOF_4). The weight of this solid was 3.11 g which corresponds to 16.4 mmol of KBrO_2F_2 (ignoring the presence of the KBrOF_4).

CHAPTER IV

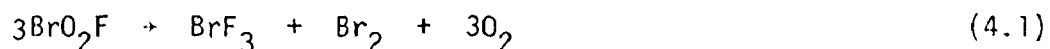
THE PREPARATION AND THE CHEMICAL AND SPECTROSCOPIC PROPERTIES OF BrO_2F AND BrOF_3 .

A. Introduction

When the present work began, BrO_2F had been reported in the literature but had never been characterized, and evidence for the existence of BrOF_3 was very tenuous. Ruff and Menzel²⁴ obtained a deep red liquid from the reaction of BrF_5 with H_2O . They showed, however, that this was not BrOF_3 as might have been expected since all of the oxygen present was evolved as O_2 . Irsa and Friedman¹⁰⁸ examined mass spectra of mixtures of BrF_5 and O_2 and observed bromine oxyfluoride ions including BrO_2^+ , BrO_2F^+ and BrOF_2^+ , from which they concluded that both BrOF_3 and BrO_2F must have been present in these mixtures. Sloth et al.¹⁰⁹ on the other hand examined the hydrolysis of BrF_5 by mass spectrometry and observed a number of bromine oxides and oxyfluorides including BrO_2F , but did not obtain any evidence for BrOF_3 as a product.

BrO_2F was isolated by Schmeisser and his coworkers who used several preparative methods,⁸ including the fluorination of BrO_2 with F_2 or BrF_5 , the reaction of KBrO_3 with BrF_5 or BrF_3 and the reaction of a mixture of Br_2 and BrF_5 with O_3 . BrO_2F was also obtained as a product in the reactions of BrF_5 with Cl_2O_6 and N_2O_5 , as well as in the reaction of BrO_2NO_3 with NO_2F . BrO_2F was reported to form colourless crystals melting at -9°C . At room temperature, the liquid slowly turned yellow

due to decomposition, while at +56°C, vigorous decomposition occurred which it was suggested could be described by equation (4.1) ²³



BrO_2F attacks glass rapidly and was shown to react explosively with water and organic substances.²² No spectroscopic data was reported however.

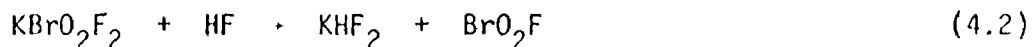
In this chapter, Raman and ^{19}F nmr spectroscopic data is reported for BrO_2F along with some of its reaction chemistry. Also the preparation of BrOF_3 is reported for the first time and its characterization by Raman and ^{19}F nmr spectroscopy is described. Independently from our work, Bougon and Bui Huy have very recently reported the preparation and vibrational spectrum of BrOF_3 ,⁴⁸ and their results will be discussed.

Some reactions in which BrO_2F and BrOF_3 are the products will be described as well, along with an attempted preparation of $\text{BrO}_2\text{SO}_3\text{F}$.

B. Preparation and Properties of BrO_2F

The preparation of BrO_2F by the reaction of KBrO_3 with BrF_5 has been described in Chapter III. The yield of BrO_2F was typically about 50% based on the amount of KBrO_3 used.

A more convenient method of obtaining small quantities of BrO_2F is to dissolve KBrO_2F_2 in HF. The reaction occurring is (4.2)



After removal of the HF under vacuum at low temperature, the BrO_2F is separated from the KHF_2 by allowing the mixture to warm up to room temperature under dynamic vacuum and collecting the BrO_2F in a -48°C trap. This method is convenient since it avoids the use of BrF_5 and the long time required for the reaction of KBrO_3 with BrF_5 . The BrO_2F obtained melted at approximately -10°C and the liquid was found to be stable for short periods of time (~ 30 min) at room temperature when kept in well-passivated Kel-F or FEP tubes.

Transferring BrO_2F by static distillation was found to be difficult because small amounts of O_2 are produced by decomposition (see above) which greatly slows down the static distillation which in turn leads to further decomposition. For this reason, BrO_2F is best transferred by dynamic distillation or by pouring a solution containing BrO_2F into the reaction vessel.

BrO_2F is quite soluble in BrF_5 , and the solutions are stable at room temperature for several hours. During an attempt to prepare a concentrated solution of BrO_2F in BrF_5 , a white solid was deposited in the tube at room temperature. Since BrO_2F melts at about -10°C , the solid produced cannot be BrO_2F . It is presumably an adduct of BrO_2F and BrF_5 . When the excess BrF_5 was removed under vacuum at -48°C , a white solid was produced which was identified as BrO_2F from its Raman spectrum. The adduct must, therefore, be rather labile since it dissociates even at -48°C . The exact nature of this adduct was not investigated further. IF_5 has been shown to form a number of molecular adducts such as $\text{KIO}_2\text{F}_4 \cdot 2\text{IF}_5$,²⁶ $\text{CsF} \cdot 3\text{IF}_5$,¹¹⁰ $\text{XeF}_2 \cdot \text{IF}_5$,¹¹¹ where the interaction has been

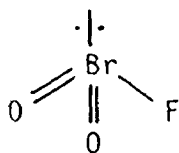
presumed to be due to a weak O or F bridge to the iodine atom of IF_5 . A similar interaction has also been proposed between KrF_2 and BrF_5 .⁸⁹ The adduct between BrO_2F and BrF_5 may be of a similar nature, with BrO_2F forming a weak bridge to the Br atom of BrF_5 .

BrO_2F was found to be soluble in SO_2ClF , even at low temperatures (-120°C). BrO_2F is also quite soluble in HF at room temperature, but these solutions decompose with evolution of Br_2 and production of BrF_3 . The other product is presumably O_2 and these observations are consistent with the thermal decomposition (4.1) which Schmeisser has suggested.²³ The solubility of BrO_2F in HF is only slight at -78°C , but at this temperature the solutions appear to be stable.

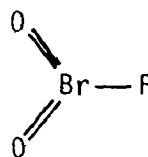
C. Characterization of BrO_2F by Raman and ^{19}F N.M.R. Spectroscopy.

(i) Raman Spectroscopy

Figures 4.1 and 4.2 show the Raman spectra of solid and molten BrO_2F . Table 4.1 lists the frequencies obtained from these spectra, as well as those obtained from spectra of BrO_2F in various solvents. Also listed in Table 4.1 are the fundamental frequencies of the related species ClO_2F ,³¹ and SeO_2F^- (see Chapter VI). BrO_2F is expected to have a pyramidal geometry (structure 1) with C_s symmetry. The six fundamentals ($1 = 4\text{A}' + 2\text{A}''$) are all Raman active. Six lines are observed in



(1)



(2)

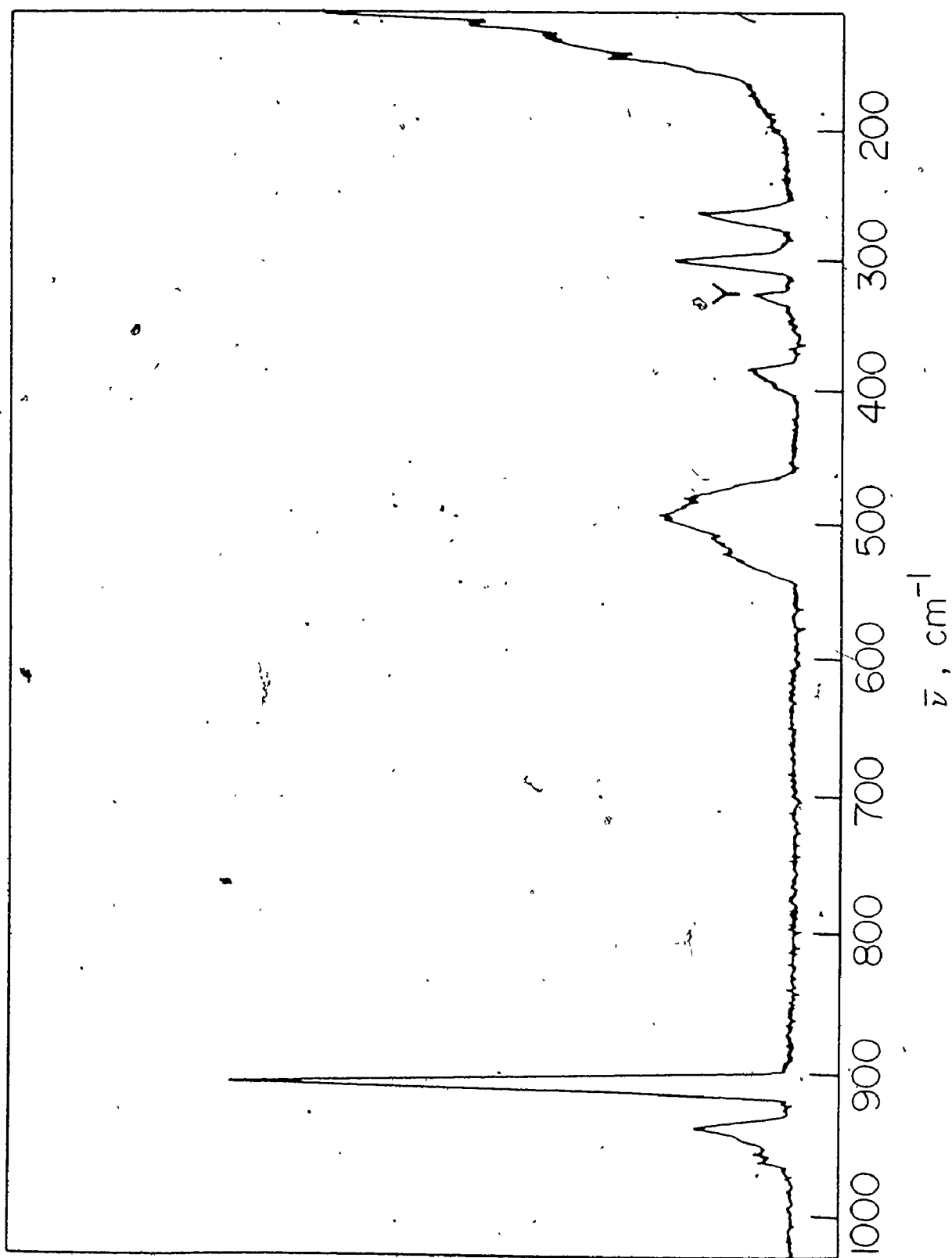


Figure 4.1. Raman spectrum of solid BrO_2F recorded at -75°C in a Kel-F tube. The band marked γ is due to Br_2 impurity.

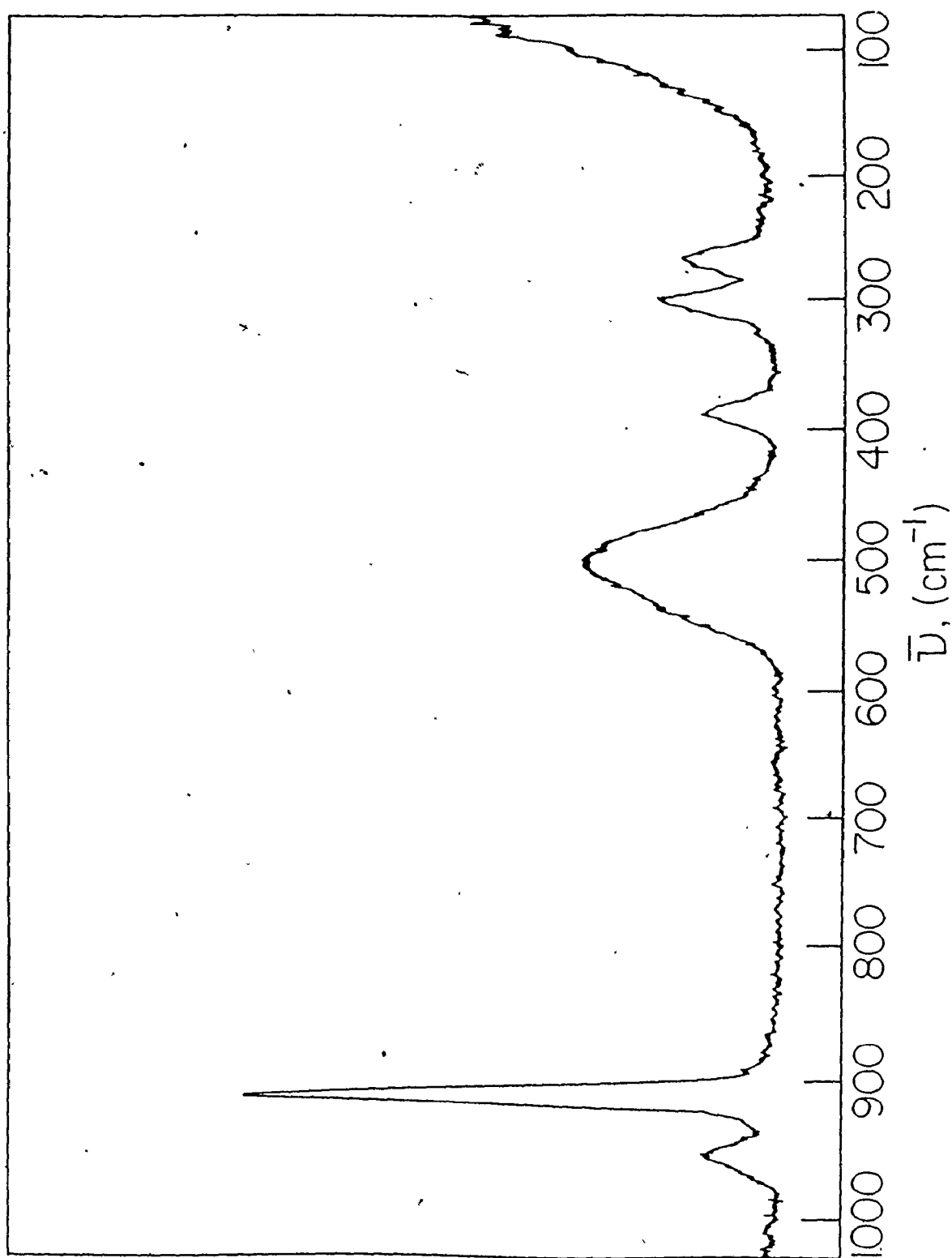


Figure 4.2. Raman spectrum of liquid BrO_2F recorded at -9°C in a Kel-F tube.

TABLE 4.1

Raman Spectra of BrO_2F , ClO_2F and SeO_2F^- (cm^{-1})

$\text{ClO}_2\text{F}^{(a)}$	$\text{SeO}_2\text{F}^{-(b)}$	BrO_2F in BrF_5 solution. (e) (Room temp.)	BrO_2F in SO_2ClF solution. (f) (-100°C)	BrO_2F in HF solution. (g) (-20°C)	Liquid BrO_2F (-10°C)	Solid BrO_2F (-75°C)	Assignment
1253(4) ^(c) dp	888(45)	962 (8)	955(13)	964(15)	953(14)	963 (5) 940(20)	ν_5 ; ν_{BrO} asym
1097(100)	p	916(100)	911(100)	915(100)	908(100)	908(100)	ν_1 ; ν_{BrO} sym
602(20)	p	-	523(20) br	531(25)	506(36)	524(sh) ⁽²⁵⁾ 496 487(sh) v.br	ν_2 ; $\nu_{\text{Br-F}}$
533(50)	p	-	-	395 (?)	394(14)	400(sh)(10) 386	ν_3 ; δ_{OBrO}
98(30)	p(?)	-	-	310 (?)	305(21)	305 294(sh)(20)	ν_4 ; δ_{OBrF} sym
51(0 ⁺)(h)	238 (2)	-	-	276 (?)	271(16)	267(15)	ν_6 ; δ_{OBrF} asym

a) Reference 31. (b) see Chapter VI. (c) Numbers in parentheses give relative intensities

d) dp: depolarized; p: polarized; sh: shoulder; v.br: very broad.

(e) The BrO_2F spectrum below 900 cm^{-1} is obscured by the very strong BrF_5 lines.

(f) Bending modes were obscured by FEP tube lines.

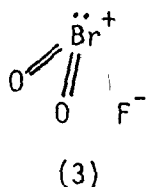
(g) The relative intensities of the three bending modes cannot be accurately measured due to the proximity of FEP tube lines.

(h) Intensity too small to be measured.

the spectrum of liquid BrO_2F and in the HF solution spectrum. Of the six lines observed for molten BrO_2F , four are polarized and two are depolarized. The planar structure (2) with C_{2v} symmetry can, therefore, be ruled out since only three polarized lines ($\Gamma = 3A_1 + B_1 + 2B_2$) would have been expected. The six lines observed can be satisfactorily assigned to a monomeric, pyramidal BrO_2F molecule by analogy with the known spectrum of ClO_2F . The BrO_2F frequencies are lower than those of ClO_2F , which is consistent with the decrease in bond strength as the electronegativity of the central atom decreases and with the larger mass of Br compared to Cl. Direct comparison with IO_2F is not possible since the latter is polymeric and gives a complex Raman structure.^{50,51} The BrO_2F frequencies are slightly higher than those of the isoelectronic SeO_2F^- which reflects the bond weakening effect of the negative charge on the anion.

The BrF stretching frequency in BrO_2F is relatively low when compared to other fluorine containing bromine species. The frequency for BrO_2F (506 cm^{-1}) is similar to the mean of the Br-F stretching frequencies in the anions BrF_4^- (531 cm^{-1}),⁹⁶ BrF_6^- (487 cm^{-1}),⁹⁵ and BrOF_4^- (498 cm^{-1}) (Chapter III), and considerably lower than that in the neutral molecules BrF_3 (613 cm^{-1}),¹¹² BrF_5 (615 cm^{-1}),¹⁰⁵ and BrO_3F (605 cm^{-1}).⁶² The mean value for BrOF_3 (see below) is 574 cm^{-1} if the frequency of the asymmetric F-Br-F stretch reported by Bougon and Bui Huy⁴⁸ is used. A force constant calculation for ClO_2F ³¹ has revealed an unusually low Cl-F stretching force constant, although this has been disputed on the basis of a more recent calculation.¹¹³ A similar

unexpectedly low stretching frequency has been found for the Se-F bond in SeO_2F^- (see Chapter VI). The results obtained in the present work indicate that the Br-F bond in BrO_2F is also rather weak, and presumably this may be attributed to a large contribution from the ionic resonance structure (3) in addition to the covalent structure (1).



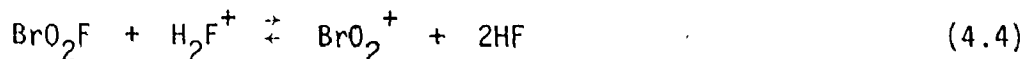
The mean of the BrO stretching frequencies in liquid BrO_2F (931 cm^{-1}) is similar to that for BrO_3F (941 cm^{-1}) but higher than those of other related species: BrO_3^- (829 cm^{-1}),¹¹⁴ $\text{Br}_2\text{O}_4(\text{A})$ (893 cm^{-1}),¹² BrO_2F_2^- (895 cm^{-1}) and BrO_2^+ (899 cm^{-1}) (see Chapter V). As the stretching frequency for a Br(VII) compound is expected to be significantly higher than for a similar Br(V) compound, it appears that the BrO stretching frequencies in BrO_2F are abnormally high. This is also consistent with an important contribution from structure (3) above, which places a positive charge on bromine, thereby increasing the BrO stretching frequencies. This suggestion is in agreement with the results of a recent force constant calculation for BrO_2F .⁴⁶ The Br-F stretching constant ($2.24 \text{ m dyn } \text{\AA}^{-1}$) was found to be considerably smaller than that of the weaker Br-F bond in BrF_5 ($3.19 \text{ m dyn } \text{\AA}^{-1}$ ¹⁰⁵) and BrF_3 ($3.01 \text{ m dyn } \text{\AA}^{-1}$ ¹¹⁵) and similar to that found in BrF_4^- ($2.38 \text{ m dyn } \text{\AA}^{-1}$ ¹¹⁶). Moreover, the Br=O stretching constant in BrO_2F ($6.78 \text{ m dyn } \text{\AA}^{-1}$) is

similar to the values reported for BrO_3F ($6.88 \text{ m dyn } \text{\AA}^{-1}$ ¹¹⁷ and $6.92 \text{ m dyn } \text{\AA}^{-1}$ ¹¹⁸).

The spectra of BrO_2F in the solid and liquid phases and in solution are quite similar (Table 4.1). The molecule thus has the same pyramidal monomeric structure in all these phases. The Br-F stretching frequency is, however, significantly greater in solution than in the solid or in the melt, indicating that there is possibly weak intermolecular fluorine bridging in the solid and in the melt. In ClO_2F , the Cl-F stretching frequency increases by 28 cm^{-1} on going from the liquid to the gas, indicating that fluorine bridging may be present in the liquid here also.

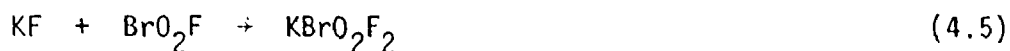
(ii) ^{19}F N.M.R. Spectroscopy

The ^{19}F nmr spectrum of BrO_2F in BrF_5 at -35°C consists of a sharp line at $-210 \pm 4 \text{ ppm}$. The chemical shift depends slightly on the composition and temperature of the solution. It lies between the chemical shifts of the two resonances of BrF_5 (-132 and -270 ppm ¹⁰⁷) and in the same region as the isoelectronic BrOF_2^+ ion (-192 ppm for the BF_4^- salt at -78°C , see Chapter V). In SO_2ClF solution, the chemical shift for BrO_2F was found to be $-205 \pm 2 \text{ ppm}$ at temperatures from -78°C to -123°C , which is in good agreement with the value found for the BrF_5 solution. In HF solution, no separate ^{19}F nmr signal was observed for BrO_2F at all temperatures down to the freezing point of the solution, indicating that BrO_2F and HF are undergoing rapid fluorine exchange. This exchange may occur via reactions such as (4.3) or (4.4) since BrO_2F_2^- and BrO_2^+ are both known species (Chapters III and V).



D. The Reaction of BrO₂F with KF

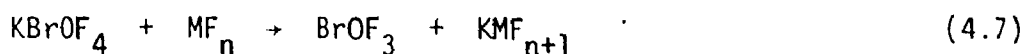
The reaction of BrO₂F with KF at room temperature was found to give a mixture of KBrF₄ and KBrO₂F₂. The KBrF₄ is probably produced by decomposition of BrO₂F to BrF₃ (equation(4.1)) followed by reaction with KF. Only 12% of the available KF was consumed by the reactions (4.5) and (4.6). Thus the reaction of KF with BrO₂F proceeds only to a small



extent (<12%) after twenty-four hours. This is probably due to the reaction being kinetically controlled rather than to any inherent instability of the KBrO₂F₂, since the latter can be obtained pure by other methods and is stable indefinitely at room temperature.

E. Preparation and Properties of BrOF₃

BrOF₃ can, in principle, be prepared from the reaction of KBrOF₄ with a Lewis acid MF_n, according to equation (4.7). However, the

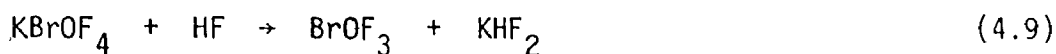


considerable F⁻ donor ability of BrOF₃ (see Chapter V) according to equation (4.8) makes the use of strong Lewis acids undesirable. A weaker



Lewis acid which is capable of causing reaction (4.7) but not (4.8) would be more useful. This is the basis of the methods used in the present work and by Bougon and Bui Huy ⁴⁸ for the preparation of BrOF_3 .

We have found that BrOF_3 is most conveniently prepared by dissolving KBrOF_4 in HF at low temperature. Removal of the HF under vacuum at -78°C leaves a white solid whose Raman spectrum is consistent with BrOF_3 . Subsequent removal of the BrOF_3 (see below) left a white solid whose Raman spectrum contained the lines characteristic of KHF_2 . Reaction (4.9), in which HF acts as a Lewis acid, had therefore occurred



when excess HF is present. This reaction is analogous to (4.2) by means of which BrO_2F is prepared from KBrO_2F_2 . However, unlike the BrO_2F reaction, when the $\text{BrOF}_3/\text{KHF}_2$ mixture is allowed to warm up to room temperature under dynamic vacuum, a rather small amount of volatile material (BrOF_3) is collected in a -78° trap. The Raman spectrum of the solid residue shows it to consist of mostly KBrOF_4 , indicating that the reverse reaction (4.10) occurs in the absence of a solvent. Removal of the HF under vacuum drives this reaction to the right, and it occurs even

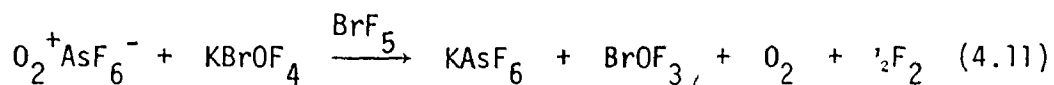


at -20°C . The fact that (4.10) occurs whereas the analogous reaction with BrO_2F (i.e. the reverse of (4.2)) does not under similar conditions

indicates that BrOF_3 is a stronger fluoride ion acceptor than BrO_2F , just as ClOF_3 is a stronger fluoride ion acceptor than ClO_2F .⁴³

In order to isolate BrOF_3 from KHF_2 , the BrOF_3 was dissolved in BrF_5 and the insoluble KHF_2 removed. The BrF_5 could then be removed under vacuum at -48°C leaving BrOF_3 as a white solid.

The reaction used by Bougon and Bui Huy⁴⁸ to prepare BrOF_3 employs $\text{O}_2^+\text{AsF}_6^-$ as the Lewis acid (equation (4.11)). The O_2 and F_2



are removed under vacuum at low temperature and the BrOF_3 can be isolated by distillation of the BrF_5 and BrOF_3 (leaving KAsF_6 and excess KBrOF_4 behind) followed by removal of the BrF_5 under vacuum at -30 to -40°C . Although this preparation involves a simpler purification procedure, it nevertheless requires the preparation of $\text{O}_2^+\text{AsF}_6^-$,¹¹⁹ whereas the method described in the present work requires only the use of HF .

The BrOF_3 prepared according to reaction (4.9) has a melting range of approximately -5°C to 0°C and formed a clear colourless liquid. The liquid slowly decomposed at room temperature even in a well-seasoned FEP tube, turning pale yellow and forming bubbles of gas. Reacting the decomposed liquid with excess KF produced a white solid identified as KBrF_4 from its Raman spectrum. Thus the decomposition of BrOF_3 at room temperature appears to proceed according to equation (4.12)



This is analogous to the thermal decomposition of ClOF_3 which has been

shown to proceed as follows ³⁹

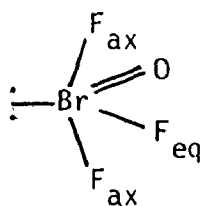


Although Bougon and Bui Huy have reported that the vapour pressure of BrOF_3 is less than 5 mm Hg at room temperature, it was found in this work that BrOF_3 can be readily distilled statically by letting the solid warm up to room temperature. The reason for this apparent discrepancy is not known.

F. Characterization of BrOF_3 by Raman and ^{19}F N.M.R. Spectroscopy.

(i) Raman Spectroscopy

The Raman spectra of solid (Figure 4.3) and liquid (Figure 4.4) BrOF_3 and of a solution of BrOF_3 in HF (Figure 4.5) have been recorded, and the observed peaks are listed in Table 4.2. A monomeric BrOF_3 would be expected to have the structure (4) which has AX_4E geometry and C_s symmetry. Such a molecule would be expected to have nine fundamental



(4)

modes ($r = 6A' + 3A''$) which should all be Raman active. The spectrum of solid BrOF_3 contains thirteen lines without including the low frequency peaks which can be assigned to lattice modes. The spectrum of molten

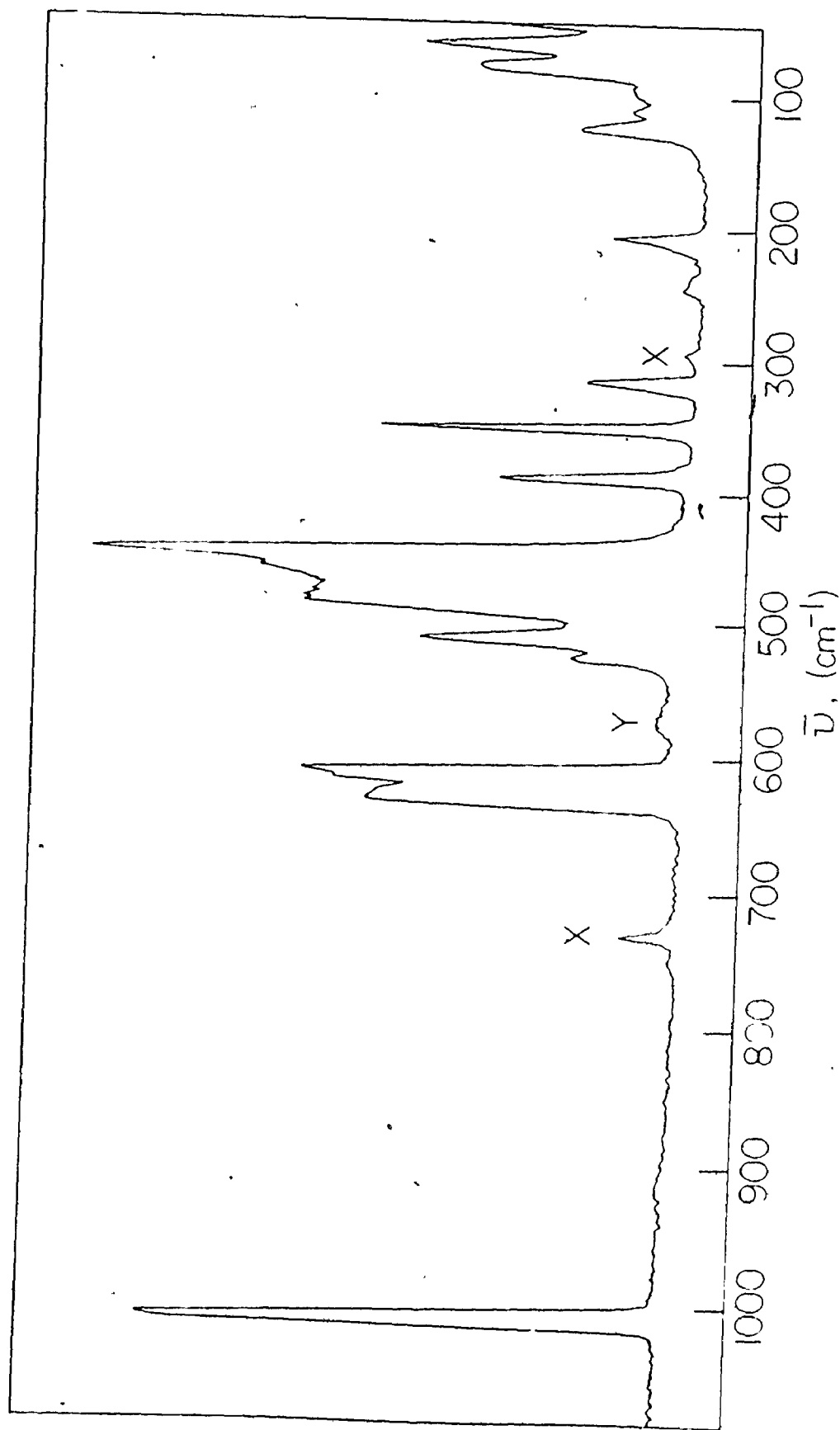


Figure 4.3. Raman spectrum of solid BrOF_3 at -195°C . Peaks labelled X are due to the FEP container and Y is due to an unidentified impurity.

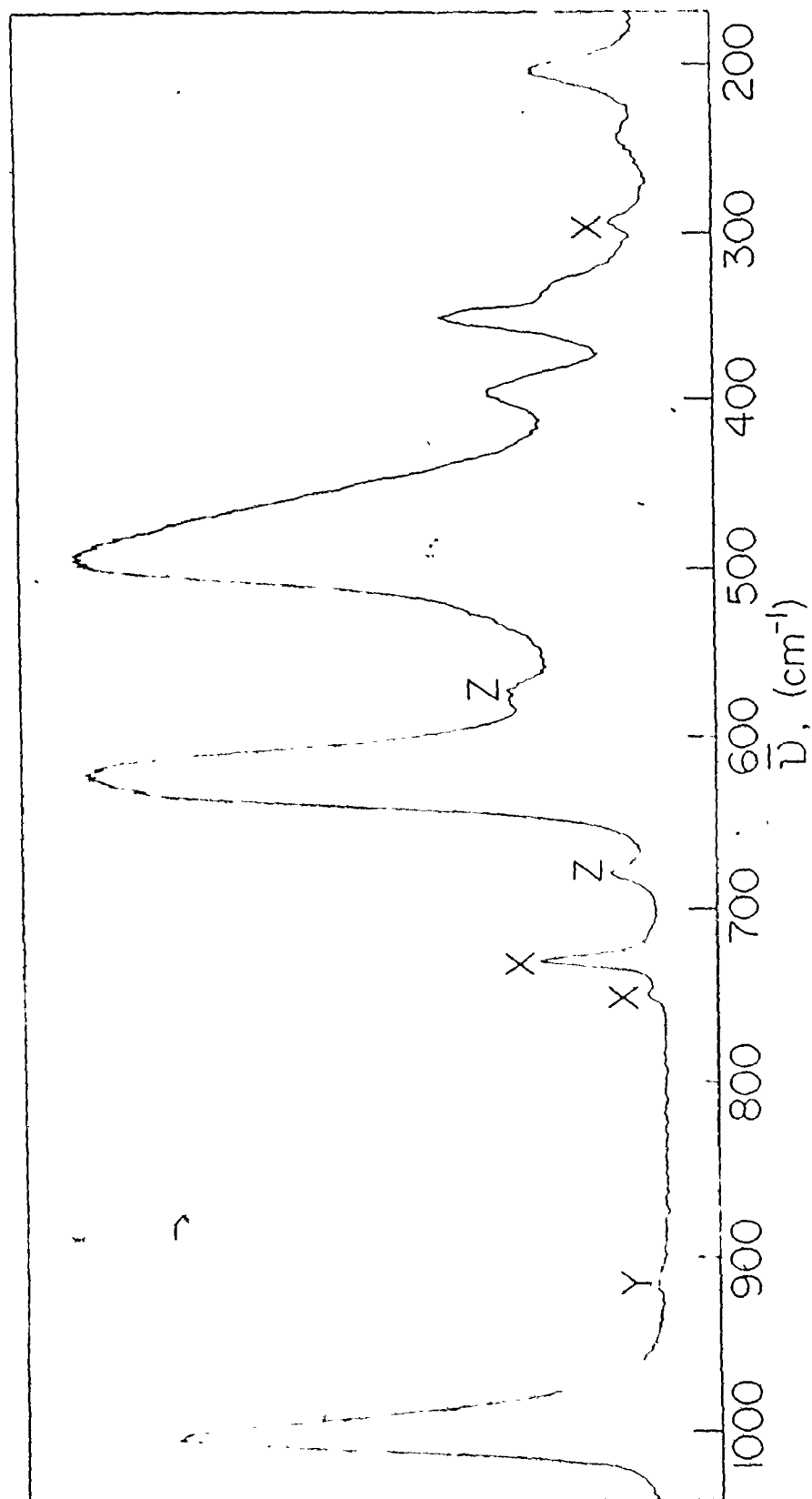


Figure 4.4. Raman spectrum of liquid BrOF_3 at 0°C . Peaks marked X are due to the FEP container, Y is due to BrO_2F , and Z are due to BrF_3 decomposition product.

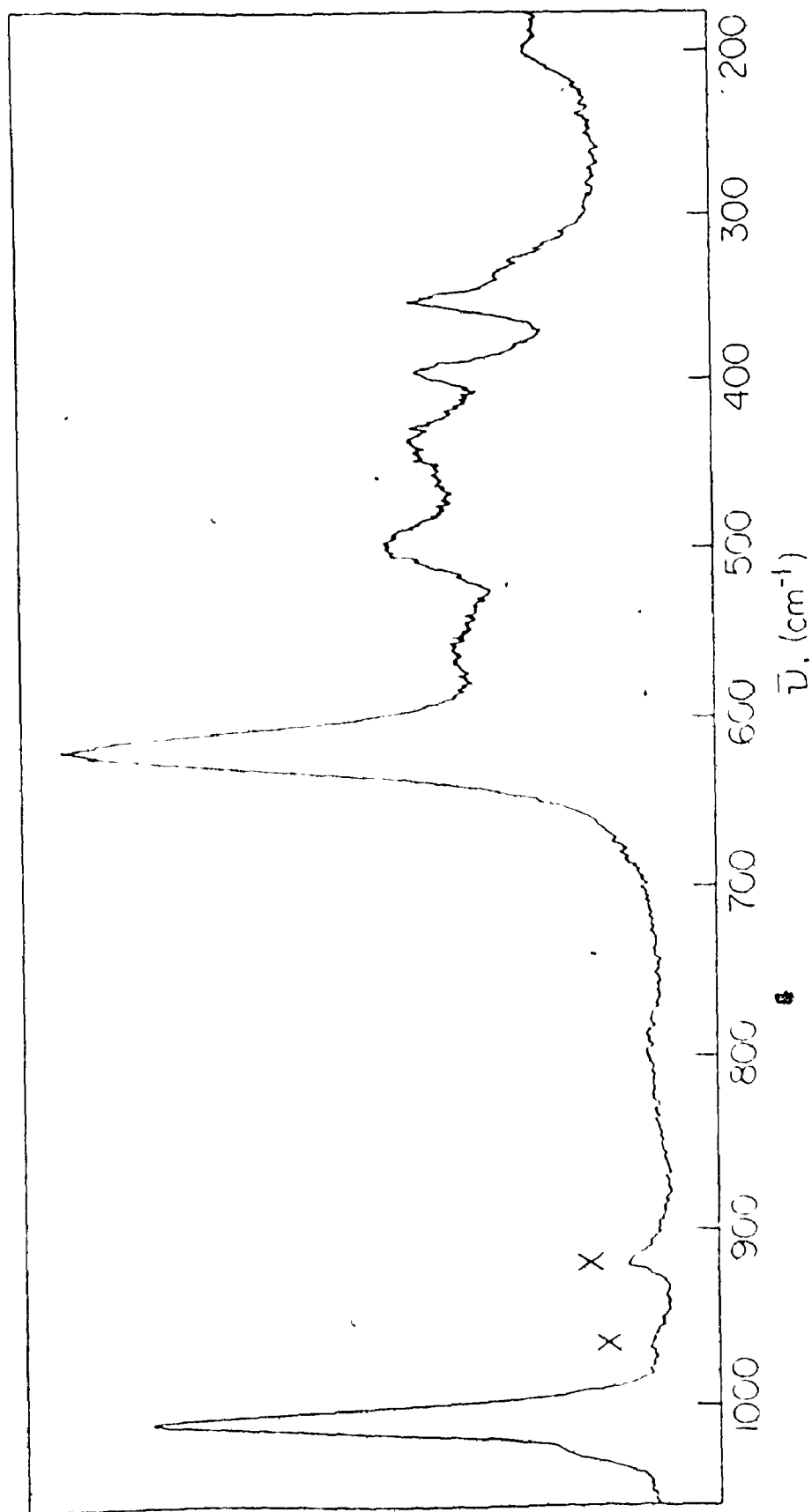


Figure 4.5. Raman spectrum of a solution of BrOF_3 in HF at -78°C in a quartz tube. Peaks marked X are due to BrO_2F produced by attack on the container.

TABLE 4.2
Raman Spectra of BrOF_3 (cm^{-1})

HF solution (-78°C)	Liquid (0°C)	Solid (-196°C)	Tentative Assignment
1011(85) p ^(a)	1004(90) p ^(b)	1010(100)	ν_{BrO}
619(100)p	624(100)p	627(60) 614(70)	$\nu_{\text{BrF}_{\text{eq}}}$
557(15)dp	-	526(sh) 510(25)	$\nu_{\text{asym F}_{\text{ax}} \text{BrF}_{\text{ax}}}$
499(25) p	493(100)p v.br	479(70) 460(sh)	$\nu_{\text{sym F}_{\text{ax}} \text{BrF}_{\text{ax}}}$
435(20) p	-	447(100)	
393(20)dp	396(20)dp	387(35)	
353(25) p	351(30) p	350(45)	
333(sh)dp	333(sh)dp?	315(17)	
234(1)?	243(4)?	245(2)	
200(7)?	199(20) p?	206(15)	
		123(15)	Lattice modes
		74(20)	
		63(25)	

(a) Numbers in parentheses give relative intensities.

(b) p: polarized; dp: depolarized; ?: degree of polarization is uncertain.

BrOF_3 has eight bands and agrees well with the one reported by Bougon and Bui Huy.⁴⁸ However, the bands at 493 cm^{-1} and 624 cm^{-1} are asymmetric and appear to consist of at least two overlapping bands which gives a total of at least ten lines for liquid BrOF_3 . That these two bands in the liquid state spectrum consist of several overlapping peaks is supported by the fact that both split into several components in the solid state spectrum. The HF solution spectrum contains ten bands. Also, the appearance of the HF spectrum depends on the temperature and concentration of the solution. At room temperature the 499 cm^{-1} and 435 cm^{-1} lines appear as a single, very broad band. At a concentration of 27 mole %, this peak has a frequency of 488 cm^{-1} and an intensity of approximately 65% of that of the 619 cm^{-1} peak. As the concentration of BrOF_3 decreases, the 488 cm^{-1} peak decreases in relative intensity and broadens towards the low frequency side. At a concentration of 3.1 mole %, the relative intensity is only 20% of that of the 619 cm^{-1} peak. That the spectrum of molten BrOF_3 and of solutions of BrOF_3 in HF exhibit a greater number of lines than expected can only be explained by postulating that BrOF_3 is associated in the liquid state and in HF solution (as well as in the solid). The changes in the Raman spectrum of the HF solution with varying temperature and concentration must reflect changes in the nature or extent of the polymerization of the BrOF_3 solute. The complexity of the HF solution spectra cannot be due to reaction of the BrOF_3 with the HF solvent to form either BrOF_4^- or BrOF_2^+ , since the characteristic $\text{Br}=\text{O}$ stretching frequencies (see Chapters III and V) for these ions were not observed.

The conclusion that liquid BrOF_3 is associated has also been reached by Bougon and Bui Huy,⁴⁸ and is consistent with the fact that ClOF_3 has been shown to be associated in the liquid and solid,⁴¹ and IOF_3 is strongly associated in the solid phase⁵⁶ (it decomposes without melting and no suitable solvent has been found to allow it to be examined in solution⁵¹). Association is presumed to be present in liquid IF_5 at room temperature,¹²⁰ since two Raman lines which are observed at this temperature do not appear in the spectra of either the liquid at $+130^\circ\text{C}$ or the gas. These lines have been assigned to polymer bands. The spectrum of molten BrOF_3 was recorded at $+45^\circ\text{C}$ in an attempt to detect the disappearance of any bands. Rather poor spectra were obtained for BrOF_3 at $+45^\circ\text{C}$ due to bubbling of the liquid (presumably due to decomposition and refluxing). No significant differences could, however, be detected between the spectra run at 0°C , 25°C and 45°C ; none of the lines could, therefore, be readily assigned to polymer bands.

Since the nature of the association in BrOF_3 is unknown, it is not possible to make a complete assignment of the observed spectra, but some useful conclusions can be drawn. It is clear that the highest frequency band at 1004 cm^{-1} must be assigned to the BrO stretching mode; this is in the normal Br=O stretching region and indicates that this bond is probably not involved (or at least not strongly involved) in the intermolecular association that is presumed to be present.

The strong band at 624 cm^{-1} is too high in frequency to be a bending mode and can, therefore, be assigned to a terminal fluorine stretching mode. Likewise, the strong band at 493 cm^{-1} can be assigned, at least in part, to a Br-F stretching motion, and the lower frequency

of this line suggests that it is associated with the fluorines involved in the bridging between molecules. The fact that it is this band which is the most markedly affected on going from the solid to the liquid to the HF solution supports this assignment, since the bridging Br-F bands would be expected to be most drastically affected by the changes in the extent of intermolecular interactions which accompany changes in phase. If the association in BrOF_3 is similar to that which has been suggested for the related molecules ClOF_3 ,⁴¹ SF_4 , BrF_3 , and ClF_3 ,¹¹⁵ then the association involves only the axial bonds. In this case the 624 cm^{-1} line can be described as a Br-F_{eq} stretch and one of the components of the 493 cm^{-1} line can be assigned as a $\nu_{\text{sym}} \text{F}_{\text{ax}}\text{-Br-F}_{\text{ax}}$ stretching motion, which would be expected to be lower in frequency than $\nu_{\text{Br-F}_{\text{eq}}}$ due to the inherent weakness of the axial bonds and their further weakening by the bridging. The depolarized line at 557 cm^{-1} in the HF solution spectrum may be described as the $\nu_{\text{asym}} \text{F}_{\text{ax}}\text{-Br-F}_{\text{ax}}$ stretching mode. It is to be noted however that this frequency is considerably shifted from the value of $\sim 605\text{ cm}^{-1}$ reported by Bougon and Bui Huy for this mode on the basis of a partial gas-phase infra-red spectrum. Since the exact nature of the association, and hence the nature of the species present, is not known, it is not possible to assign the remaining lines in the spectrum which must correspond to bending modes. Bougon and Bui Huy have completely assigned the liquid phase spectrum on the basis of a monomeric BrOF_3 molecule of C_s symmetry, but the assignments attribute the broad line at 493 cm^{-1} entirely to $\nu_{\text{sym}} \text{F}_{\text{ax}}\text{-Br-F}_{\text{ax}}$. However, the asymmetry of this band and its splitting into two components in HF solution indicate that there are two

or more fundamentals responsible for this line, and cast doubt on the assignments. Indeed the assignment of even a component of this 493 cm^{-1} line to $\nu_{\text{sym}} \text{F}_{\text{ax}}-\text{Br}-\text{F}_{\text{ax}}$ (as was proposed above) is not totally satisfactory as it is not clear why the intensity of such a mode should decrease dramatically when BrOF_3 is dissolved in HF. A further investigation of the vibrational spectra of BrOF_3 by other techniques, such as matrix isolation, was beyond the scope of this work.

(ii) ^{19}F N.M.R. Spectroscopy

Although two signals of intensity ratio 2:1 would be expected for a BrOF_3 molecule with C_s symmetry, the ^{19}F nmr spectrum of molten BrOF_3 at room temperature shows only a single line in the F on Br (V) region at -152 ppm. There must be rapid exchange between the non-equivalent fluorines which may be a result of the association present in the liquid. Bougon and Bui Huy have reported similar results. BrOF_3 is quite soluble in HF even at low temperature, but no ^{19}F nmr signal attributable to BrOF_3 could be observed, even down to the freezing point of the solution. It appears, therefore, that BrOF_3 undergoes rapid fluorine exchange with the solvent, presumably by reactions such as (4.14) and (4.15). In SO_2ClF solution at -80°C to -100°C a single broad line



(peak width $\sim 600\text{ Hz}$) was observed at -164 ppm , and at -120°C the peak shifted to -160 ppm , and the line width increased to $\sim 1600\text{ Hz}$. Similarly

in SO_2F_2 at -136°C , only a single broad line was observed for BrOF_3 at -162 ppm. The small difference in chemical shift of BrOF_3 in the molten state and in solution in SO_2ClF and SO_2F_2 suggests that BrOF_3 is associated in a similar fashion both in the molten state and in solution in these non-polar solvents. That only a single line is observed in these solvents indicates that exchange of non-equivalent fluorines occurs rapidly and probably intermolecularly, even at low temperature, between the units of an associated cluster of BrOF_3 molecules.

G. Reaction of BrF_5 with H_2O and Iodine Oxyfluoro Species

(i) Hydrolysis of BrF_5 .

Equimolar amounts of BrF_5 and H_2O were allowed to react at -63°C using HF as a solvent, and the solution was cooled to -78°C . A white precipitate was formed whose Raman spectrum consisted of lines attributable to BrO_2F and BrF_5 . Although the formation of BrO_2F presumably proceeds via the intermediate formation of BrOF_3 (equations (4.16) and (4.17)), no BrOF_3 was in fact observed. The solution was pale yellow,



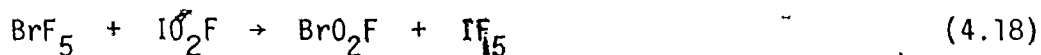
indicating that some decomposition had occurred, but no Raman lines attributable to decomposition products (such as BrF_3 or Br_2) were observed, which indicates that only a small amount of decomposition had occurred. Removal of HF and BrF_5 under vacuum left a pale yellow solid

identified as BrO_2F . Two very weak Raman lines attributable to BrF_3 were observed and this may account for the yellow colour of the solid. It must be concluded that if BrOF_3 is indeed an intermediate, it must hydrolyse considerably faster than BrF_5 . The BrF_3 observed was produced either by decomposition of BrOF_3 or BrO_2F . These results are in agreement with mass spectral data obtained by Sloth et al.¹⁰⁹ who reported finding no evidence for BrOF_3 in the products of the hydrolysis of BrF_5 in the absence of a solvent.

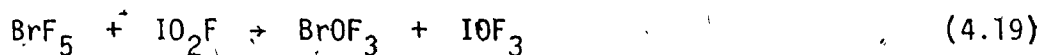
ii) Reaction of BrF_5 with Iodine Oxides and Oxyfluorides.

BrF_5 rapidly fluorinates I(V) oxides and oxyfluorides and as in the case of the hydrolysis of BrF_5 , BrO_2F rather than BrOF_3 is the product.

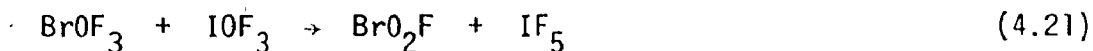
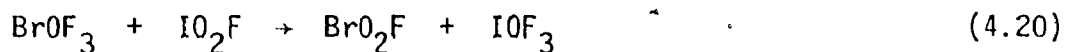
BrF_5 reacted with IO_2F at -48°C . If a large enough excess of BrF_5 was used, a clear solution was obtained (otherwise the adduct between BrO_2F and BrF_5 precipitated out). A ^{19}F nmr spectrum of this solution showed, in addition to the BrF_5 107 solvent peaks, the characteristic peaks due to IF_5 121 and BrO_2F , and integration of these signals showed that IF_5 and BrO_2F were present in equal amounts. Thus the overall reaction can be written as (4.18). On removing the excess BrF_5 at



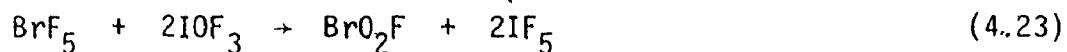
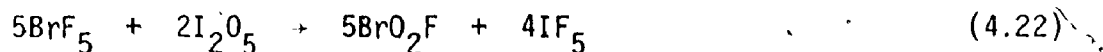
-48°C , a solid was produced whose Raman spectrum consisted of a mixture of BrO_2F and IF_5 ,¹⁰⁶ containing no BrOF_3 . The BrOF_3 , which is presumably produced as an intermediate according to equation (4.19) must fluorinate



the I (V) species present more rapidly than the BrF_5 solvent, i.e. it is removed by rapid reactions such as (4.20) and (4.21).



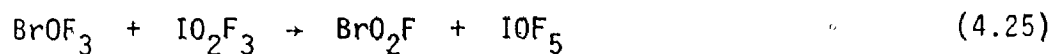
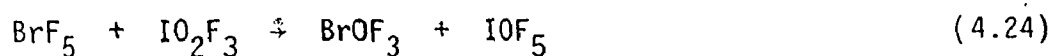
Similar results were obtained in the reactions of BrF_5 with I_2O_5 and IOF_3 , except that some decomposition of a bromine species was evident from the formation of the characteristic brown colour of Br_2 and some gas evolution. In both cases, ^{19}F nmr spectra of the resulting solutions showed only BrF_5 , IF_5 and BrO_2F . Because of the decomposition which had occurred, integration of the BrO_2F and IF_5 signals showed amounts of BrO_2F that were less than would be required according to equations (4.22) and (4.23). When the solvent was removed under vacuum



from the $\text{I}_2\text{O}_5/\text{BrF}_5$ reaction mixture, a solid was obtained whose Raman spectrum showed lines attributable to only BrO_2F and IF_5 , but not to BrOF_3 . As in the case of the $\text{IO}_2\text{F}/\text{BrF}_5$ reaction, the BrOF_3 presumably formed as an intermediate must be removed by rapid reaction with the I(V) species present.

When IO_2F_3 and BrF_5 were reacted at room temperature, the ^{19}F nmr spectrum showed (in addition to the AX_4 pattern of BrF_5) the AB_4 pattern of IOF_5 ⁷⁶ and a very weak AX_4 pattern assigned to IF_5 . Removal

of BrF_5 and IOF_5 under vacuum at -40°C produced a solid which consisted of mostly BrO_2F with some BrOF_3 (approximately 10% according to the Raman spectrum), a small amount of IF_5 , and possibly a very small amount of BrF_3 . The BrF_3 may have been produced by decomposition of either BrO_2F or BrOF_3 , while the IF_5 was probably due to photochemical decomposition of IO_2F_3 to IOF_3 ,⁷⁰ followed by fluorination to IF_5 by the solvent. Thus the reaction of BrF_5 with IO_2F_3 can be written as equations (4.24) and (4.25). The formation of a mixture of BrO_2F and



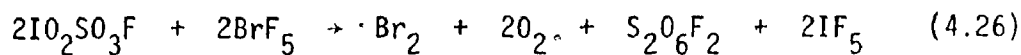
BrOF_3 can be accounted for if reaction (4.25) does not go to completion. That BrOF_3 is observed as a product in the fluorination of IO_2F_3 by BrF_5 supports the supposition made earlier that it must be an intermediate in the fluorination of IO_2F , I_2O_5 and IOF_3 by BrF_5 .

The solid mixture of BrO_2F , BrOF_3 , IF_5 (and possibly BrF_3) was redissolved in BrF_5 to produce a solution more concentrated than the original reaction mixture. The ^{19}F nmr spectrum of this solution at -60°C showed BrF_5 and IF_5 , and a weak, very broad (~ 200 Hz) peak at a chemical shift of approximately -209 ppm. This signal is presumably due to BrO_2F undergoing exchange at an intermediate rate with BrOF_3 . BrF_5 and IF_5 cannot be involved in the exchange since the expected spin-spin coupling is observed for these molecules. The -209 ppm peak does not represent the limiting fast-exchange average peak for BrO_2F and

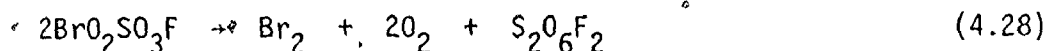
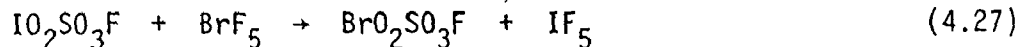
BrOF_3 , since a chemical shift of approximately -199 ppm would be expected for the average of a 10:1 mixture of $\text{BrO}_2\text{F}:\text{BrOF}_3$ (involvement of BrF_3 would move the peak further upfield). Also, raising the temperature to -40°C (thereby increasing the rate of exchange) caused the peak to broaden (to ~ 370 Hz) and move upfield (to ~ -204 ppm). The resonance due to BrOF_3 expected in the -60°C spectrum could not be observed, presumably due to its weakness and/or breadth.

(iii) Reaction of BrF_5 with $\text{IO}_2\text{SO}_3\text{F}$.

BrF_5 reacted with $\text{IO}_2\text{SO}_3\text{F}$ at -48°C to give a brown solution. A non-condensable gas was produced during the reaction. The ^{19}F nmr spectrum of the reaction mixture showed (in addition to the BrF_5 solvent lines) the AX_4 pattern of IF_5 and a sharp singlet at a chemical shift of -41 ppm. The chemical shift of $\text{S}_2\text{O}_6\text{F}_2$ has been reported as -40.4 ppm for the pure liquid,¹²² and -39.5 ppm for a solution in BrF_5 .¹²³ The intensity of the singlet at -41 ppm relative to one component of the IF_5 doublet was estimated to be approximately 1:2 on the basis of peak height. These observations are consistent with equation (4.26). Thus



if $\text{BrO}_2\text{SO}_3\text{F}$ is produced (4.27), it must decompose rapidly (4.28). Schack

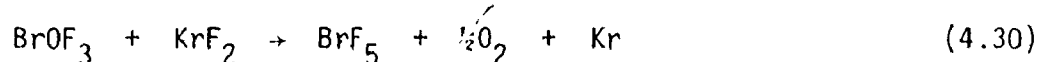
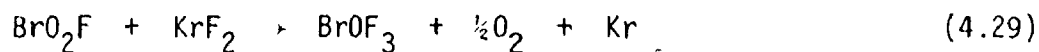


and Christie¹²⁴ have reported that they failed to obtain $\text{BrO}_2\text{SO}_3\text{F}$ from

the reaction of BrOSO_3F and O_3 (whereas the same reaction with ClOSO_3F produces $\text{ClO}_2\text{SO}_3\text{F}$). Carter et al.¹²⁵ have also proposed $\text{BrO}_2\text{SO}_3\text{F}$ as an unstable intermediate in the reaction of KBrO_3 with $\text{S}_2\text{O}_6\text{F}_2$ which produces $\text{K}[\text{Br}(\text{OSO}_2\text{F})_4]$ (whereas the analogous reactions with KClO_3 and KIO_3 produced $\text{ClO}_2\text{SO}_3\text{F}$ and $\text{IO}_2\text{SO}_3\text{F}$, respectively). That attempts to prepare $\text{BrO}_2\text{SO}_3\text{F}$ by three different methods have failed suggest it is of low stability. It cannot, however, be definitely concluded that $\text{BrO}_2\text{SO}_3\text{F}$ is unstable since its formation and subsequent decomposition has not been established in any of the unsuccessful preparations reported.

H. Reaction of BrO_2F with KrF_2

BrO_2F can be fluorinated using the strong oxidising agent KrF_2 with HF as a solvent. The ^{19}F nmr spectrum of a solution of BrO_2F with excess KrF_2 at -45°C showed singlets at -52 ppm and $+183$ ppm which were assigned to KrF_2 ⁹⁴ and HF (exchanging with BrO_2F). The Raman spectrum of the solution at -45°C showed only a single peak at 467 cm^{-1} due to KrF_2 and the BrO stretches of BrO_2F . Gas evolution occurred when the sample was warmed to $+2^\circ\text{C}$. The Raman spectrum of the solution showed BrO_2F and BrOF_3 to be present in comparable amounts, along with a small amount of BrF_5 .¹²⁶ After an hour at $+2^\circ\text{C}$, the BrOF_3 and BrF_5 lines had increased in intensity relative to those of BrO_2F . After another hour at $+2^\circ\text{C}$, no BrO_2F was observed. After an hour at room temperature, the BrF_5 lines had grown in intensity. A ^{19}F nmr spectrum showed KrF_2 , HF and BrF_5 to be present. Thus BrO_2F is fluorinated to BrOF_3 (equation (4.29)) which is in turn fluorinated to BrF_5 (equation (4.30)).



I. Experimental Section

(i) Preparation of BrO₂F.

The preparation of BrO₂F by the reaction of KBrO₃ with BrF₅ was described in Chapter III. BrO₂F can also be prepared by dissolving KBrO₂F₂ in anhydrous HF. In a typical experiment 0.087 g (0.46 mmole) of KBrO₂F₂ was placed in an FEP nmr tube and approximately 0.4 g of HF was distilled in. The mixture was warmed to -78°C to melt the HF and then warmed further to dissolve the KBrO₂F₂. On cooling the solution to -78°C, a white precipitate was formed which was identified as BrO₂F from its Raman spectrum. The HF was removed under vacuum at -78°C, leaving a white solid. This solid was warmed to room temperature under dynamic vacuum and the volatile component was trapped at -48°C and identified as BrO₂F by its Raman spectrum. The involatile residue was identified as KHF₂ from its Raman spectrum.

(ii) Decomposition of BrO₂F in HF.

When a solution of KBrO₂F₂ in HF was allowed to stand at room temperature for thirty minutes, it became brown, suggesting Br₂ formation. When the solvent was removed under vacuum at -78°C, and the remaining solid allowed to warm up to room temperature under dynamic vacuum, a white solid remained which was identified as KBrF₄ from its Raman spectrum.^{95,96} Thus when a solution of BrO₂F in HF decomposes it

produces Br_2 and BrF_3 , and presumably O_2 .

(iii) Preparation of BrO_2F Samples for Raman and ^{19}F N.M.R. Spectroscopy.

BrO_2F was distilled dynamically into FEP nmr tubes, trapped at -48°C , and the solvent then added by distillation.

(iv) Reaction of BrO_2F with KF .

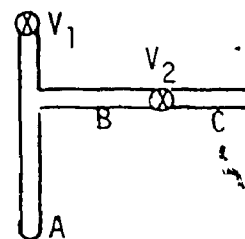
0.133 g (2.29 mmol) of KF was shaken at room temperature with 0.592 g (4.52 mmol) of BrO_2F for 24 hours in a Kel-F trap. Some decomposition occurred since Br_2 was liberated in the tube. The excess BrO_2F was removed under vacuum, and a Raman spectrum of the white solid which remained showed it to be a mixture of KBrO_2F_2 and KBrF_4 . The weight of the white solid in the tube had increased by 0.037 g (which corresponds to 0.28 mmol of BrO_2F or BrF_3).

(v) Preparation and Properties of BrOF_3 .

In a typical preparation, 0.219 g (1.04 mmol) of KBrOF_4 was placed in an FEP nmr tube, and approximately 0.6 g of HF was distilled in. The mixture was warmed to -78°C to melt the HF and then to a slightly higher temperature to dissolve the KBrOF_4 . The HF was removed under vacuum at -78°C , leaving a white solid whose Raman spectrum was consistent with BrOF_3 . 1.3 g of BrF_5 was distilled in, and the mixture warmed to -48°C . This produced a clear solution with a translucent solid (KHF_2) floating on it (density of BrF_5 : 2.47 g cm^{-3} , KHF_2 : 2.37 g cm^{-3}). It was possible to separate the solution from the solid by carefully manipulating the reaction vessel in such a way that the solution slowly

flowed to one end of the nmr tube while the solid adhered to the walls at the other end of the tube. The section of tube containing the solid was then sealed off and removed. The BrF_5 was removed under vacuum at -48°C , and a white solid (BrOF_3) resulted. For larger scale preparations

the reaction was carried out in a double armed FEP vessel. The KBrOF_4 was placed in arm A, and HF was added. The HF was removed under vacuum at low temperature. BrF_5 was distilled



in and a solution of BrOF_3 in BrF_5 with KHF_2 floating on it was formed.

The apparatus was tipped sideways and the mixture introduced into section B. Careful opening of the Teflon valve V_2 allowed the solution to trickle into tube C. When the solid KHF_2 reached V_2 , the latter was closed and all the solution wetting the solid KHF_2 in B was removed under vacuum through valve V_1 . V_2 could then be safely disconnected from B,

and the BrF_5 solvent present in C removed under vacuum. In this way, BrOF_3 could be conveniently isolated. The melting range of BrOF_3 , which was found to be approximately -5°C to 0°C , was determined by placing a

solid sample of BrOF_3 contained in an FEP nmr tube in a glass dewar

which was kept cold by a flow of cold nitrogen through the dewar. The temperature was varied by controlling the nitrogen flow and was measured

using a copper-constantan thermocouple. In another experiment a

sample of solid BrOF_3 in an FEP tube was placed in a salt-water/ice bath

at -10°C and the bath was slowly allowed to warm up to 0°C over a period

of 2 hours while the temperature was monitored using a mercury thermometer.

The melting range determined by this method was -4°C to 0°C .

On standing at room temperature, liquid BrOF_3 began to bubble and turned yellowish. After two hours at room temperature, the liquid was chilled to -196°C , excess KF was added and the mixture was allowed to warm up to room temperature. A reaction took place which produced a white solid identified as KBrF_4 from its Raman spectrum.

(vi) Reaction of BrOF_3 and KHF_2 .

A mixture of BrOF_3 and KHF_2 (produced by dissolving KBrF_4 in HF and removing the HF under vacuum) was allowed to warm up under vacuum to approximately -20°C , and then chilled to -196°C . The Raman spectrum showed the resulting solid to consist mostly of KBrF_4 , with only a small amount of BrOF_3 remaining. In another experiment 0.012 g of KBrF_4 was dissolved in HF , and the solvent removed under vacuum at -78°C . The resulting $\text{BrOF}_3/\text{KHF}_2$ mixture was allowed to warm up to room temperature under reduced pressure. The remaining white solid weighed 0.010 g and was identified as KBrF_4 from its Raman spectrum. Using a good dynamic vacuum, some BrOF_3 can be distilled out of a $\text{BrOF}_3/\text{KHF}_2$ mixture, but the residual KBrF_4 still accounts for most of the BrOF_3 originally present.

(vii) Preparation of N.M.R. and Raman Samples of BrOF_3 .

The Raman and ^{19}F nmr spectra of liquid BrOF_3 were obtained from a sample prepared in an FEP nmr tube as described above. An HF solution of BrOF_3 for nmr was obtained by dissolving KBrF_4 in HF in an FEP nmr tube. An HF solution of BrOF_3 for Raman spectroscopy was prepared by dissolving KBrF_4 in HF in a 6 mm quartz tube. These solutions often attack the quartz tube (the solution rapidly turns brown, and the Raman

spectrum of the solution shows large amounts of BrO_2F . Raman spectra of BrOF_3 in HF were also recorded in FEP and Kel-F containers, but in these cases the Raman lines associated with the container obscured many of the BrOF_3 lines. For the investigation of the dependence of the Raman spectrum on the concentration of a solution of BrOF_3 in HF, 0.075 g (0.50 mmole) of BrOF_3 was placed in an FEP nmr tube. Preweighed amounts of HF were then distilled in to give solutions with mole percentages of BrOF_3 of 27.0%, 15.0%, 11.0%, 8.0%, 6.0%, 4.5% and 3.1%. The Raman spectrum of each solution was recorded at room temperature. In addition to the changes in the BrOF_3 lines, weak lines due to BrF_3 also appeared due to the slow thermal decomposition of BrOF_3 . The Raman spectrum of BrOF_3 at $+45^\circ\text{C}$ was recorded by positioning an FEP nmr tube containing liquid BrOF_3 against the inside wall of an unsilvered Pyrex Dewar (the same one used for recording Raman spectra at -196°C). The Dewar was then filled with hot water ($+45^\circ\text{C}$) and the temperature was monitored using a mercury thermometer. ^{19}F nmr samples of BrOF_3 in SO_2ClF and SO_2F_2 were prepared by statically distilling BrOF_3 into an FEP nmr tube, and then distilling in the solvent. The mixtures were warmed to -78°C to allow dissolution of the BrOF_3 . Saturated solutions were used.

(viii) Hydrolysis of BrF_5

0.213 g (1.22 mmol) of BrOF_5 was distilled into a 1/4" o.d. FEP tube, and 21.9 μl (1.22 mmol) of H_2O was syringed into the tube (kept at -196°C) and formed a frozen bead above the level of the frozen BrF_5 . Approximately 1.3 g of HF was then distilled in. The mixture was warmed to -78°C to melt the HF, and then to -63°C for ten minutes giving a light

yellow solution. On cooling the sample to -78°C , a white solid was formed. The Raman spectrum of the solid was recorded at -196°C and showed it to consist of BrO_2F and BrF_5 , with no BrOF_3 being present. The sample was left at -63°C for one hour and then at -78°C for two days. The Raman spectrum of the solid in the bottom of the tube was again run and still found to consist only of lines attributable to BrF_5 and BrO_2F . The solvent and excess BrF_5 were removed under vacuum at -72°C and then at -48°C , leaving a yellow solid whose Raman spectrum showed lines attributable to BrO_2F with possibly a very small amount of BrF_3 . No BrOF_3 was present.

(ix) Reaction of I(V) Oxides and Oxyfluorides with BrF_5 .

(a) IO_2F : 0.0571 g (0.32 mmol) of IO_2F was placed in an FEP nmr tube, and 1.61 g (9.2 mmol) of BrF_5 was distilled in. The mixture was warmed to -48°C to give a clear solution together with a white solid. The mixture was allowed to react at room temperature for fifteen minutes and a solid was still present in the tube (presumably the adduct between BrO_2F and BrF_5). A ^{19}F nmr spectrum at -45°C showed only BrF_5 , IF_5 and BrO_2F . The solvent was removed under vacuum at -48°C and a white solid resulted whose Raman spectrum contained lines attributable to BrO_2F and IF_5 , but no BrOF_3 . In another experiment a much larger (and unmeasured) excess of BrF_5 was used and complete dissolution occurred at -48°C . The ^{19}F nmr spectrum of this solution at -40°C showed BrF_5 , IF_5 , and BrO_2F , and the integration of the spectrum gave the following results:

$$\text{BrO}_2\text{F}:\text{IF}_5:\text{BrF}_5 = 30:32:117 \approx 1:1:4$$

(b) I_2O_5 : 0.114 g (0.342 mmol) of I_2O_5 was placed in an FEP nmr tube, and 1.81 g (10.3 mmol) of BrF_5 was distilled in. The mixture was warmed to -48°C and an orange solution was formed with a white solid still present in the tube. Decomposition seemed to occur since the solution was orange in colour and bubbles of gas were evolved. The solid dissolved when the sample was warmed to room temperature and a ^{19}F nmr spectrum at this temperature showed signals due to BrF_5 , IF_5 , and BrO_2F . Integration of the spectrum gave the following results:

$$\text{BrO}_2\text{F}:\text{IF}_4:\text{IF}_4 = 23:30:125 \approx 0.75:1:4$$

The solvent was removed under vacuum at -48°C , and then at -30°C . The Raman spectrum of the remaining material consisted of lines attributable to BrO_2F and IF_5 , with no BrOF_3 being present.

(c) IOF_3 : A large excess of BrF_5 was distilled onto IOF_3 and the mixture became brown on warming to -63°C . Further warming to -35°C caused complete dissolution and a darkening of the brown colour. The nmr spectrum of the solution showed BrF_5 , IF_5 , and a relatively small amount of BrO_2F ($\text{BrO}_2\text{F}:\text{IF}_5 < 1:10$) to be present.

(x) Reaction of IO_2F_3 and BrF_5 .

1.04 g (5.95 mmol) of BrF_5 was distilled onto 0.150 g (0.694 mmol) of IO_2F_3 , and the mixture was warmed to -18°C and then to room temperature for forty minutes to get a complete reaction. A Raman spectrum of the solution showed peaks attributable to BrF_5 , IOF_5 ,⁷⁵ BrO_2F and a small amount of BrOF_3 . The ^{19}F nmr spectrum of this solution at -50°C showed the characteristic multiplets of BrF_5 and IOF_5 , and a small amount of IF_5 .

No peaks other than those due to BrF_5 were observed in the F on Br(V) region. The BrF_5 and IOF_5 were removed under vacuum at -48°C and the Raman spectrum of the remaining solid showed lines attributable to a large amount of BrO_2F , some BrOF_3 and very weak lines due to IF_5 and possibly BrF_3 . BrF_5 was distilled into the tube and a more concentrated solution was prepared. The 94.1 MHz ^{19}F nmr spectra of this solution were recorded at -60°C , -50°C , and -40°C .

(xi) Reaction of $\text{IO}_2\text{SO}_3\text{F}$ and BrF_5 .

Excess BrF_5 was distilled onto 0.062 g (0.24 mmol) of $\text{IO}_2\text{SO}_3\text{F}$ in an FEP nmr tube and the mixture was allowed to warm up to -48°C . A brown solution was formed. The mixture was cooled to -196°C . A non-condensable gas was present in the tube. This was detected by opening the tube to the manifold of the vacuum line and observing a change in the reading of the vacuum gauge. The ^{19}F nmr spectrum of the solution was recorded at -48°C .

(xii) Reaction of BrO_2F and KrF_2 .

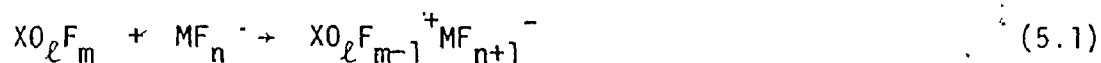
Approximately 0.1 g of KBrO_2F_2 was placed in an FEP nmr tube and excess KrF_2 was distilled in. Approximately 0.5 g of HF was then distilled in and the mixture warmed to -78°C to melt the HF. All the solid in the tube dissolved at -45°C . The tube was then warmed while the reaction was monitored by ^{19}F nmr and Raman spectroscopy.

CHAPTER V

PREPARATION AND CHARACTERIZATION OF THE CATIONS BrO_2^+ AND BrOF_2^+

A. Introduction.

Many fluorides and oxyfluorides react with Lewis acids according to the general equation (5.1). In some cases, the product is best described



as an ionic salt with discrete cations and anions. For example, the complex $\text{SF}_4 \cdot \text{SbF}_5$ appears to be best formulated as $\text{SF}_3^+ \text{SbF}_6^-$.^{128,129,130} In other cases, however, strong fluorine bridges link the "cation" and the "anion" and the product is best described as a covalent adduct. For example, the complex between NbF_5 and SbF_5 has been shown¹³¹ to contain very strong fluorine bridges between the Nb and Sb atoms; the adduct is therefore best written as $\text{NbF}_5 \cdot \text{SbF}_5$ with the ionic form $\text{NbF}_4^+ \text{SbF}_6^-$ making only a small contribution.

It was of interest to examine the reactions between BrO_2F and a number of Lewis acids. Schmeisser and Brändle⁸ had reported that BrO_2F does not form complexes with BF_3 , AsF_5 or SbF_5 . In this chapter, it will be shown that BrO_2F does in fact react with BF_3 and AsF_5 to produce salts containing the BrO_2^+ cation. Independently of our work Jacob⁴⁴ has reported the preparation of the compounds $\text{BrO}_2^+ \text{AsF}_6^-$ and $\text{BrO}_2^+ [\text{SbF}_6(\text{SbF}_5)_{1.24}]^-$.

He has, however, only reported the vibrational frequencies for the cation in the $[\text{SbF}_6(\text{SbF}_5)_{1.24}]^-$ salt. Although he states that "the characteristic frequencies of $\text{Sb}_2\text{F}_{11}^-$ and $\text{Sb}_3\text{F}_{16}^-$ " were observed, this must be regarded with some skepticism since the extremely complex spectra for these anions are not well characterized (see Table 5.5).

It was also of interest to examine the reaction between BrOF_3 and various Lewis acids, and these reactions are also described in this chapter. Bougon et al.³² have also studied the $\text{BrOF}_3/\text{AsF}_5$ system and their results are essentially in agreement with ours.

B. Preparation and Properties of the BrO_2^+ Salts.

The reaction of BrO_2F with the Lewis acids BF_3 and AsF_5 at -72°C using HF as a solvent produces cream to light-brown coloured solids which in Section C are shown to contain the BrO_2^+ cation. The products are however often coloured orange or reddish as a result of partial decomposition (see Section C). The compound $\text{BrO}_2^+\text{BF}_4^-$ is quite soluble in HF whereas $\text{BrO}_2^+\text{AsF}_6^-$ is much less soluble. Both salts can also be made using BrF_5 as a solvent.

Interaction of BrO_2F with AsF_5 at -120°C using SO_2ClF as a solvent produces the same cream coloured product. The reaction of BrO_2F with excess SbF_5 in SO_2ClF also produces solid products, but these were generally more highly coloured and Raman spectra could not be obtained. Moreover, the tendency of SbF_5 to form polymeric anions of the type $\text{Sb}_n\text{F}_{5n+1}^-$ meant that the products were probably mixtures since exactly equimolar amounts of reagents were not used.

The BrO_2^+ salts were found to be unstable at room temperature. Rapidly warming a sample of $\text{BrO}_2^+\text{BF}_4^-$ to room temperature under vacuum in an FEP tube caused the solid to melt, turn very deep purple in colour, and bubble vigorously. No solid residue was left after ten minutes. The compound $\text{BrO}_2^+\text{AsF}_6^-$ does not melt at room temperature but the red colour of the solid deepens and the Raman lines associated with the decomposition product increase in intensity. Both materials therefore had to be kept at low temperature. For this reason, no analytical data were obtained for these products. The fact that BrO_2F was observed in small amounts or not observed at all in the Raman spectra of the products indicates that the formation of BrO_2^+ was essentially complete.

Solutions of $\text{BrO}_2^+\text{BF}_4^-$ in HF and BrF_5 appear to be stable at low temperatures for extended periods of time. At room temperature however, a solution of $\text{BrO}_2^+\text{BF}_4^-$ in BrF_5 became dark brown in colour after ten minutes, indicating that decomposition had occurred.

Solid $\text{BrO}_2^+\text{AsF}_6^-$ reacts very vigorously with H_2O at room temperature and a cloud of brown gas, presumably Br_2 , is evolved.

C. Characterization of $\text{BrO}_2^+\text{BF}_4^-$ and $\text{BrO}_2^+\text{AsF}_6^-$ by Raman and ^{19}F N.M.R. Spectroscopy.

.. (i) Raman Spectroscopy

Figure 5.1 shows the Raman spectrum of a slightly orange solid obtained from the reaction of BrO_2F with excess BF_3 in HF. The spectrum was run in an FEP tube at -196°C using the green 514.5 nm line of the Ar

ion laser. Figure 5.2 shows the Raman spectrum of an orange solid obtained from the reaction of BrO_2F with AsF_5 in HF. This spectrum was run at -196°C using the red 632.8 nm line of an He-Ne laser. Table 5.1 lists the frequencies obtained from these spectra, along with the fundamental frequencies of the BrO_2^+ cation in $\text{BrO}_2^+[\text{SbF}_6(\text{SbF}_5)_{1.24}]^-$,⁴⁴ and the related molecules SeO_2 ¹³³ and BrO_2F (see Chapter IV). When the solid used to obtain the spectrum in Figure 5.1 was dissolved in HF, the Raman spectrum of the solution showed only two lines at 876 cm^{-1} and 937 cm^{-1} . The line at 876 cm^{-1} was polarized whereas the line at 937 cm^{-1} had too low an intensity to allow definitive polarization data to be obtained. The other lines expected were too weak to observe or were masked by the very intense lines due to the FEP tube. The solution spectrum could not be recorded in a quartz container since attempts to transfer the solid product to a quartz tube failed due to decomposition of the sample. Similarly, attempts to prepare the sample in a quartz tube led to extensive attack on the walls of the tube and very intense fluorescence was observed. The lines in the $\text{Br}=\text{O}$ region (884 cm^{-1} and 947 cm^{-1} in Figure 5.1 and 862 cm^{-1} and 931 cm^{-1} in Figure 5.2) correspond reasonably well with the BrO_2^+ frequencies reported by Jacob (865 cm^{-1} and 932 cm^{-1}) which suggests that the reaction of BrO_2F with BF_3 or AsF_5 produced salts containing the BrO_2^+ cation. In Figure 5.2, the peak at 907 cm^{-1} is assigned to a small amount of unreacted BrO_2F , whereas the weak line at 827 cm^{-1} is of unknown origin and was only observed in one spectrum of $\text{BrO}_2^+\text{AsF}_6^-$. When the solid product of the reaction between BrO_2F and BF_3 was mixed with excess KF in HF, the

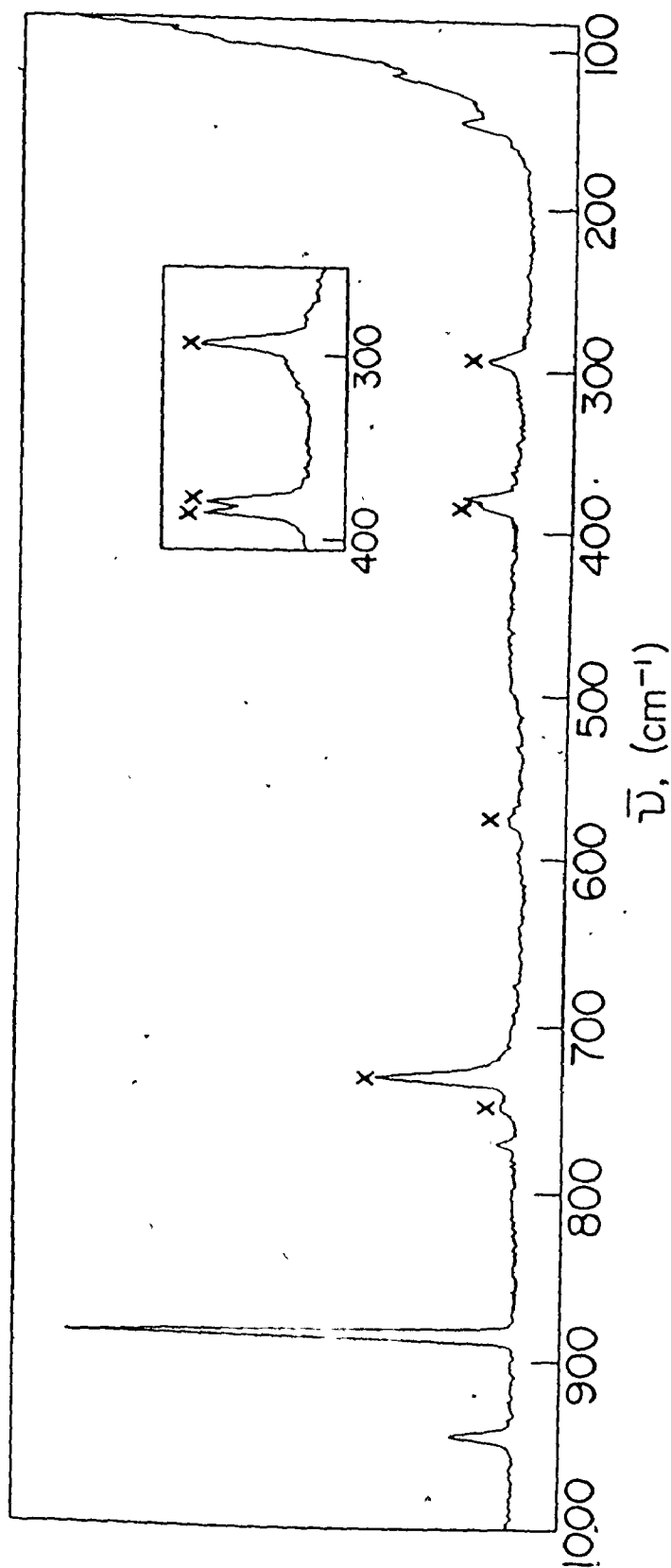


Figure 5.1. Raman spectrum of solid $\text{BrO}_2^+\text{BF}_4^-$ recorded at -196°C . Peaks labelled X are due to the FEP sample tube.

The inset shows the Raman spectrum of an empty FEP tube at -196°C between 250 and 400 cm^{-1} .

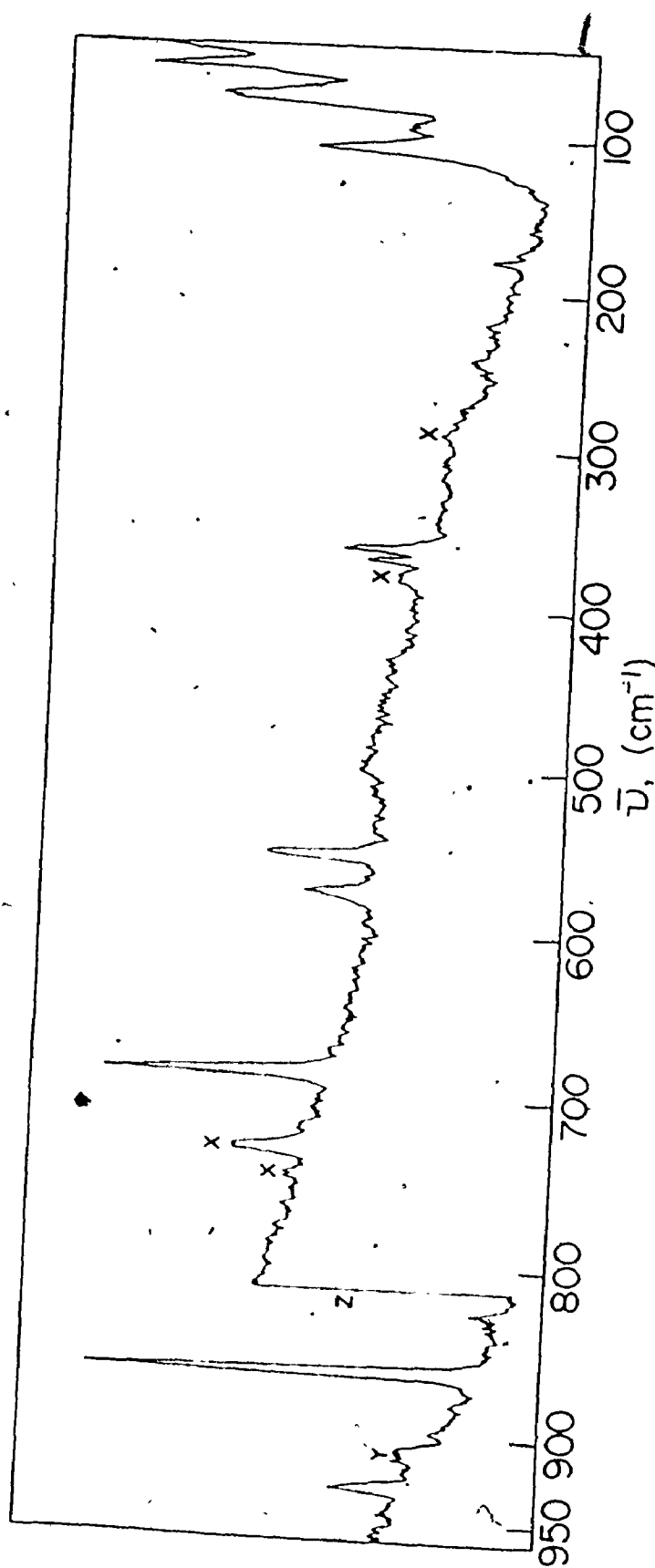


Figure 5.2. Raman spectrum of solid $\text{BrO}_2^+\text{AsF}_6^-$ recorded at -196°C using 632.8 nm exciting radiation. Peaks marked with an X are due to the FEP sample tube and Y is due to unreacted BrO_2F . Z denotes an adjustment to the baseline of the spectrum. The weak peak at 827 cm^{-1} is of unknown origin (see text).

TABLE 5.1

Raman Frequencies of BrO_2^+ Salts and Some Related Molecules (cm^{-1})

$\text{BrO}_2\text{F(a)}$ (liquid)	$\text{SeO}_2\text{(b)}$	BrO_2^+ in $[\text{SbF}_6(\text{SbF}_5)_{1.24}]^+$ salt	(c) $\text{BrO}_2^+\text{AsF}_6^-$ solid	$\text{BrO}_2^+\text{BF}_4^-$ soln. in HF	$\text{BrO}_2^+\text{BF}_4^-$ solid	Assignments BF_4^- AsF_6^- (e) Other
953 (14)	967 m(g)	932 m	931(20)	937(25)	947(13)	XO_2^+ $\nu_3(\text{B}_1)$ $\nu_{\text{asym}} \text{XO}_2$
908(100)	922 s	865 s	907(10) 862(100)	876(100) p	884(100)	$\nu_1(\text{A}_1)$ $\nu_{\text{sym}} \text{XO}_2$ $\nu_1(\text{A}_1)$
			749 (2) 731(20) 685(60)		771 (4) 749 (4) 731(30)	$\nu_1(\text{A}_1)$
			576(18)} 552(28)}		575 (3)	$\nu_1(\text{A}_{1g})$
394(14)	382 m	375 m	382 (6)		384(sh)	$\nu_2(\text{E}_g)$
			368(15) 361(20) 293 (2)		379(11)	$\nu_2(\text{A}_1)$
					293 (8)	$\nu_5(\text{T}_{2g})$
						Br_2^+

TABLE 5.1 (continued)

Raman Frequencies of BrO_2^+ Salts and Some Related Molecules (cm^{-1})

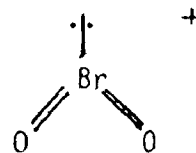
$\text{BrO}_2\text{F}^{(a)}$ (liquid)	SeO_2 (b)	BrO_2^+ in $[\text{SbF}_6(\text{SbF}_5)_{1.24}]^-$ salt	(c)	$\text{BrO}_2^+\text{AsF}_6^-$ solid	$\text{BrO}_2^+\text{BF}_4^-$ soln. in HF.	$\text{BrO}_2^+\text{BF}_4^-$ solid	Assignments
							$\text{BF}_4^-(e)$ $\text{AsF}_6^-(e)$ Other
				179 (6)		145 (7)	Lattice modes
				106(40)		115 (4)sh	
				92 (6)			
				76(40)			
				54(40)			

- a see Chapter IV. b Reference 133. c Reference 44; The lines due to the anion were not reported.
- d The remaining lines were either too weak to observe or masked by the very strong lines due to the FEP container.
- e Assignments are based on T_d symmetry for BF_4^- and O_h symmetry for AsF_6^- .
- f Numbers in parentheses give relative intensities.
- g m, medium; s, strong; p, polarized.

884 cm^{-1} and 947 cm^{-1} lines in the Raman spectrum disappeared and were replaced by the characteristic BrO_2^+ lines. This further confirms our supposition that BrO_2^+ is responsible for these Raman lines.

In Figure 5.1, the 771 cm^{-1} peak has a frequency very close to the value reported for ν_1 of the BF_4^- ion (769 cm^{-1}) in KBF_4 .^{134,135} The other fundamentals were too weak to be observed. Despite the fact that excess BF_3 was used in the syntheses, there were no lines attributable to the complex anion B_2F_7^- ^{136,137} in the Raman spectra of the products. The compound formed by BrO_2F and BF_3 is, therefore, formulated as $\text{BrO}_2^+\text{BF}_4^-$. In Figure 5.2, the strong line at 685 cm^{-1} has a frequency identical with that of ν_1 (A_{1g}) for AsF_6^- in CsAsF_6 .¹³⁸ The two lines at 576 cm^{-1} and 552 cm^{-1} are assigned to ν_2 (E_g) of AsF_6^- (576 cm^{-1} in CsAsF_6) with the E mode split by a solid state effect. Finally, ν_5 (T_{2g}) of AsF_6^- (372 cm^{-1} in CsAsF_6) is assigned to the line at 368 cm^{-1} . Once again there was no evidence for the formation of the complex anion $\text{As}_2\text{F}_{11}^-$ ^{137,139} despite the fact that excess AsF_5 was used in several of the preparations. Thus the compound formed by BrO_2F and AsF_5 is $\text{BrO}_2^+\text{AsF}_6^-$.

Since both the symmetric and asymmetric BrO_2 stretching frequencies are observed for BrO_2^+ both in the solid BF_4^- and AsF_6^- salts and in HF solution, the cation must be bent (structure (1)) rather than linear.



(1)

This is in agreement with the predictions of VSEPR

theory and with the assignment of a bent geometry

to the related species SeO_2 ,¹⁴⁰ ClO_2^+ ,³⁰ and IO_2^+ .⁵¹ The OBrO bending mode

in BrO_2^+ was reported to be at 375 cm^{-1} in the $[\text{SbF}_6(\text{SbF}_5)_{1.24}]^-$ salt.⁴⁴ In Figures 5.1 and 5.2, the OBrO bending mode coincides with one of the lines due to the FEP container. Evidence for this can be obtained by comparing the relative intensities of the 382 cm^{-1} and 293 cm^{-1} lines of FEP. In the reference spectrum of FEP, the 382 cm^{-1} and 293 cm^{-1} lines at -196°C are of equal intensity, and the 382 cm^{-1} band is often split into a doublet with branches of equal intensity at 384 and 376 cm^{-1} (see inset in Figure 5.1). In Figure 5.1, the peak at 379 cm^{-1} is stronger than the shoulder at 384 cm^{-1} and the FEP line at 293 cm^{-1} , indicating the presence of a sample line at approximately 379 cm^{-1} . Similarly, in Figure 5.2, the broad band at 382 cm^{-1} is considerably more intense than the broad FEP line at 293 cm^{-1} , indicating that again a sample line must coincide with the 382 cm^{-1} line of FEP. The OBrO bending mode of BrO_2^+ is assigned to this line at approximately 379 cm^{-1} for the BF_4^- salt and approximately 382 cm^{-1} for the AsF_6^- salt. Further evidence for this was obtained from a sample of $\text{BrO}_2^+\text{BF}_4^-$ prepared in a quartz tube. Although the Raman spectrum of this product was complex since extensive decomposition had occurred, a weak Raman line was observed at 378 cm^{-1} which was assigned to δ_{OBrO} of BrO_2^+ .

The line at 361 cm^{-1} in Figure 5.2 is assigned to the decomposition product of the BrO_2^+ salts. This line was found to increase in intensity in samples of $\text{BrO}_2^+\text{AsF}_6^-$ that had been warmed to room temperature or stored for extended periods of time. The same line was found to be more intense in more highly coloured samples of both the BF_4^- and AsF_6^- salts. When

samples of $\text{BrO}_2^+\text{AsF}_6^-$ and $\text{BrO}_2^+\text{BF}_4^-$ were allowed to decompose extensively, the intensity of the 361 cm^{-1} line increased, and peaks appeared at $\sim 720\text{ cm}^{-1}$ and $\sim 1080\text{ cm}^{-1}$. The intensities decreased in the order $361\text{ cm}^{-1} > 720\text{ cm}^{-1} > 1080\text{ cm}^{-1}$. These observations are consistent with the formation of $\text{Br}_2^+\text{BF}_4^-$ and $\text{Br}_2^+\text{AsF}_6^-$ as decomposition products. The vibrational frequency of the Br_2^+ cation is 360 cm^{-1} ¹⁴¹ and it shows an absorption band at 510.0 nm. Therefore, when 514.5 nm radiation is used to record the Raman spectrum of a sample containing Br_2^+ , the resonance Raman spectrum of the Br_2^+ cation is observed which has a strong fundamental at 360 cm^{-1} and overtones at 720 cm^{-1} and 1080 cm^{-1} . This was verified by recording the Raman spectrum of a sample of $\text{BrO}_2^+\text{AsF}_6^-$ using 632.8 nm exciting radiation. The relative intensity of the 361 cm^{-1} line was 20% of that of the 862 cm^{-1} line (Figure 5.2). When the spectrum was recorded using 514.5 nm exciting radiation, the relative intensity of this peak increased to 60% of that of the 862 cm^{-1} line. The decreased intensity of the 361 cm^{-1} line when observed using 632.8 nm radiation is consistent with the suggestion that 514.5 nm excitation gives a resonance Raman spectrum whereas 632.8 nm radiation gives only a weaker pre-resonance Raman spectrum.

The BrO_2^+ stretching frequencies are unusual in several respects. On going from BrO_2F to BrO_2^+ , it would be expected that the BrO stretching frequencies would increase, as a positive charge on the Br atom should cause a decrease in the electronegativity difference between bromine and oxygen, which should result in an increase in the Br=O stretching frequency. However, this is not observed (see Table 5.2) since the mean BrO stretching

TABLE 5.2
Comparison of BrO_2^+ Stretching Frequencies
to Some Related Molecules (cm^{-1})

SO_2 (a)	ClO_2^+ (b)	ClO_2F (c)	SeO_2 (d)	BrO_2^+ (e)	BrO_2F (f)	
1362	1296	1253	967	937	953	$\nu_{\text{asym}} \text{XO}_2$
1151	1044	1097	922	876	908	$\nu_{\text{sym}} \text{XO}_2$
1256	1170	1175	944	907	931	Mean XO stretching frequency

a Reference 114; gaseous infra-red spectrum.

b Reference 29; Raman of solid $\text{ClO}_2^+\text{AsF}_6^-$.

c Reference 31; Raman of liquid

d Reference 133; matrix isolated infra-red.

e HF solution of $\text{BrO}_2^+\text{BF}_4^-$.

f see Chapter IV; Raman of liquid.

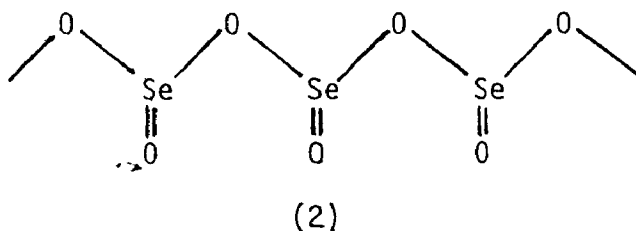
frequency in BrO_2^+ in solution in HF (907 cm^{-1}) is considerably lower than that of BrO_2F (931 cm^{-1}). In the related Cl system, the mean ClO stretching frequencies (ClO_2^+ : 1170 cm^{-1} ; 29 ClO_2F : 1175 cm^{-1} 31) and stretching force constants (ClO_2^+ : $8.96\text{ mdyn \AA}^{-1}$; 29 ClO_2F : $9.07\text{ mdyn \AA}^{-1}$ 31) are comparable, and this was attributed to the large contribution of the ionic ClO_2^+F^- form to the overall bonding in ClO_2F .²⁶ In BrO_2F , there is also probably a large contribution from the ionic form BrO_2^+F^- but this cannot account for a higher stretching frequency in BrO_2F than in BrO_2^+ .

An unusual trend is also observed when BrO_2^+ is compared to the isoelectronic SeO_2 . Again contrary to expectations, the mean BrO stretching frequency in BrO_2^+ is lower than the mean SeO stretching frequency in SeO_2 (944 cm^{-1}).¹³³ This is contrary to the observation¹⁴² that within a series of isoelectronic molecules the force constant increases as the magnitude of the positive charge on the central atom increases. Comparison of the mean stretching frequencies in ClO_2^+ (1170 cm^{-1}) and SO_2 (1256 cm^{-1})¹¹⁴ shows that these molecules also do not conform with the expected trend. This has been rationalized^{29,143} by assuming that in such molecules with a rather electronegative central atom X in a high oxidation state, the bond polarity is in the direction $\text{X}^{\delta-}-\text{O}^{\delta+}$ and that introducing a formal positive charge on X, therefore weakens the bond by further increasing the bond polarity. This argument however does not seem entirely satisfactory for the less electronegative elements Se and Br, and does not hold in the isoelectronic pair of molecules SeOF_2 and BrOF_2^+ ($\nu_{\text{X=O}} = 1012\text{ cm}^{-1}$ 144 and 1052 cm^{-1} , respectively) where the expected trend is

observed.

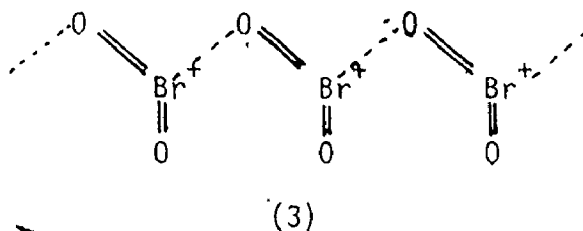
The low BrO stretching frequencies in the solid BrO_2^+ salts could be explained if extensive fluorine bridging occurs between the anions and the cations. Donation of electron density from the anion to the bromine atom of the cation would result in a weakening of the Br-O bonds. Comparison of the BrO frequencies in the $[\text{SbF}_6(\text{SbF}_5)_{1.24}]^-$, AsF_6^- and BF_4^- salts are not in complete agreement with this interpretation however, since these frequencies are significantly higher in the BF_4^- salt than in the other two, whereas BF_4^- is the most basic of these anions and would have been expected to bridge the most strongly to the cation. Furthermore, the vibrational frequencies observed for the BF_4^- and AsF_6^- anions in the BrO_2^+ salts are close to the values found for the K^+ and Cs^+ salts of these anions. It would have been expected that very strong anion-cation interaction would have shifted the anion frequencies from their normal values.

Another form of bridging which could occur in the solid BrO_2^+ salts is bridging between cations. In the isoelectronic SeO_2 , the structure of the solid has been shown¹⁴⁵ to consist of an infinite chain of Se atoms linked by O-bridges, with each Se bearing a terminal oxygen (structure 2)



A similar structure involving weaker bridging (structure 3) between the BrO_2^+

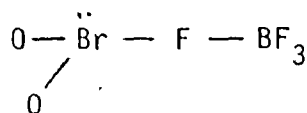
cations is possible. The Br-O-Br bridges are certainly not symmetric as is



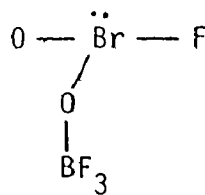
the case in SeO_2 since such a structure would produce only a single line in the $\text{Br}=\text{O}$ region of the vibrational spectrum, and peaks in the $\text{Br}-\text{O}-\text{Br}$ stretching region ($400 - 600 \text{ cm}^{-1}$)^{13,19} would have been expected. In the case of rather weak bridging such as in structure (3), symmetric and asymmetric BrO_2 stretching frequencies would be expected, and this is consistent with the observed spectrum. However, it is again not obvious why the BrO_2^+ stretching frequencies should increase when AsF_6^- is replaced with BF_4^- .

(ii) ^{19}F N.M.R. Spectroscopy.

When $\text{BrO}_2^+\text{BF}_4^-$ is dissolved in HF , the BrO stretching frequencies decrease by $8 - 10 \text{ cm}^{-1}$ which also is unusual. To investigate the possibility that these solutions contain bridged species such as (4) or (5) rather than simple BrO_2^+ and BF_4^- ions, the ^{19}F nmr spectrum of the solution was recorded. The nmr parameters obtained from these spectra are recorded in Table 5.3. At -45°C , two broad singlets were observed at $+152 \text{ ppm}$



(4)



(5)

TABLE 5.3

Chemical Shifts (δ , ppm from CFCl_3) and Coupling Constants
 J (Hz) for $\text{BrO}_2^+ \text{BF}_4^-$ Dissolved in HF.

Temp. °C	BF_4^-		HF		
	δ	width (a)	δ	J (b)	width (a)
-45°C	+152	410	+194	— (c)	514
-53°C	+152	175	+194	276	— (d)
-68°C	+152	75	+194	476	250
-78°C	+152	<50 (e)	+193	525	103

a Linewidth at half-height (Hz). These values are estimated to be accurate to ± 10 Hz.

b Estimated to be accurate to ± 10 Hz.

c Single line observed for HF.

d Extensive overlap of the peaks made the measurement of width at half-height impossible.

e Exact linewidth could not be measured.

and +194 ppm. As the temperature was lowered, the +152 ppm singlet became sharper and the one at +194 ppm split into a doublet with branches of equal intensity. At -78°C , the coupling constant of the doublet at +193 ppm was 525 Hz. The +152 ppm line is assigned to BF_4^- and is in excellent agreement with the value of +153.6 ppm found for BF_4^- when KBF_4 is dissolved in HF.¹³⁰ No fluorine to boron coupling was observed and this is probably due to the very small value of this coupling constant. The value of $J_{\text{B-F}}$ has been shown to decrease with decreasing concentration and also to vary depending on the nature of the cation involved.¹⁴⁶ For $\text{NH}_4^+\text{BF}_4^-$ in aqueous solution, $J_{\text{B-F}}$ for BF_4^- was found to be 1.15 Hz at infinite dilution and to be relatively independent of concentration. For Na^+BF_4^- in aqueous solution, a value of approximately 1.4 Hz was found for solutions with concentrations of less than 1 M, but the splitting increased rapidly at higher concentrations. Since the concentration of $\text{BrO}_2^+\text{BF}_4^-$ in HF used was approximately 0.6 M, the coupling constant can be expected to be between 1.1 and 1.4 Hz. Such a small coupling would not have been observed under the conditions used to record the nmr spectrum. ✕

. The high field singlet at +194 ppm at -45°C , which split into a doublet when the solution was cooled, is assigned to HF. The splitting at low temperature is due to H-F coupling and the observed coupling constant ($J_{\text{HF}} = 525 \text{ Hz}$) is in good agreement with the previously reported values of 526 Hz¹⁴⁷ and 521 Hz.¹⁴⁸ This splitting can only be observed when the total number of ions formed by dissociation of the solvent is at a minimum,¹⁴⁸ i.e. when $[\text{H}_2\text{F}^+] = [\text{HF}_2^-]$. The observation of HF coupling indicates that

the HF is not involved in any rapid exchange processes with other species in solution. If non-labile complexes such as (4) or (5) were present in solution, extra peaks would have been observed in the F on Br (V) region of the spectrum. If complexes such as (4) or (5) were present in equilibrium with BrO_2^+ and BF_4^- , and the exchange was rapid, only a single F on B resonance would be observed; however, the chemical shift of this resonance would not be expected to coincide with that of free BF_4^- in HF. The nmr spectra thus are most consistent with discrete BF_4^- and presumably BrO_2^+ ions in solution.

(iii) Discussion

The spectroscopic data obtained in the present work suggests that the adducts between BrO_2F and Lewis acids are essentially ionic salts containing the BrO_2^+ cation. The rather low BrO_2 stretching frequencies may be attributable to some secondary bonding to the bromine atom of the cation. Whether this bridging involves only the cations or whether it links the anions and the cations cannot be decided on the basis of the vibrational spectra. Comparison with the related IO_2^+ and ClO_2^+ ions favours the latter explanation however. In $\text{ClO}_2^+\text{Sb}_2\text{F}_{11}^-$, X-ray crystallography has shown that several fluorine bridges link the ClO_2^+ cation to the anions surrounding it.³⁰ In $\text{IO}_2^+\text{AsF}_6^-$, the suggestion that the cation is polymeric through oxygen bridges has been made,⁵⁰ but later work⁵¹ has shown this conclusion to be incorrect and has demonstrated that discrete IO_2^+ and AsF_6^- ions are present, linked by fluorine bridges. It therefore seems more likely that the bridging in BrO_2^+ salts is between the anions and the

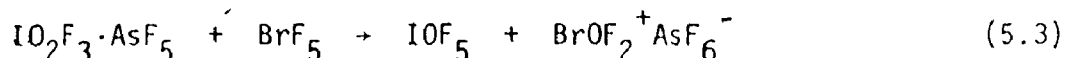
cations. The bridging cannot be very strong since the AsF_6^- and BF_4^- frequencies are close to the values found in the K^+ and Cs^+ salts of these anions. The observed splitting of ν_2 of AsF_6^- may be due to this bridging between this anion and the cation. The higher value of the BrO_2^+ stretching frequencies in the BF_4^- salt than in the AsF_6^- salt may be due to more favourable bridging interactions in the latter case, perhaps caused by packing considerations. This might offset the lower basicity of AsF_6^- when compared to BF_4^- . More definitive conclusions about this will have to await a determination of the crystal structure of some BrO_2^+ salts. In HF solution, BrO_2^+ and BF_4^- ions appear to be present. The low BrO_2^+ frequencies observed in solution may possibly be accounted for by strong solvation of the ion.

D. Preparation and Properties of the BrOF_2^+ Salts.

The reaction of BrOF_3 with an excess of AsF_5 using HF as a solvent produces a white solid product. A product with an identical Raman spectrum can also be obtained using BrF_5 as a solvent. The Raman spectrum of this adduct (see Section E) indicates that it is best formulated as $\text{BrOF}_2^+\text{AsF}_6^-$. The reaction is therefore (5.2). Another preparative route used to obtain



this adduct was the reaction of $\text{IO}_2\text{F}_3 \cdot \text{AsF}_5$ ²⁶ with BrF_5 at room temperature, which proceeds according to equation (5.3). In Chapter IV, it was shown

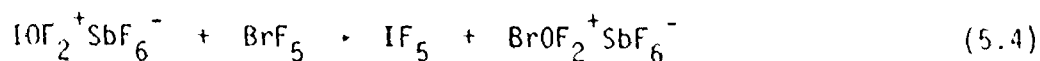


that BrOF_3 is an intermediate in the fluorination of IO_2F_3 by BrF_5 (equations (4.24) and (4.25)) and that the BrOF_3 is almost completely consumed by reaction with IO_2F_3 (equation (4.25)). When AsF_5 is present however, reaction (5.2) occurs instead of reaction (4.25) and $\text{BrOF}_2^+\text{AsF}_6^-$ is formed as a precipitate. That $\text{BrOF}_2^+\text{AsF}_6^-$ is only very slightly soluble in BrF_5 is shown by the observation that the $\text{Br}=\text{O}$ stretching frequency is very weak in the Raman spectrum of a saturated solution at room temperature. It is also slightly soluble in HF and Bougon and his coworkers¹³ have recorded the Raman spectrum of this solution (see Table 5.4). Solid $\text{BrOF}_2^+\text{AsF}_6^-$ slowly turns pink and is therefore only marginally stable at room temperature (see Section E).

BrOF_3 also reacts with BF_3 at low temperature, using HF as a solvent, to form an adduct which can be formulated as $\text{BrOF}_2^+\text{BF}_4^-$ according to its Raman and ^{19}F nmr spectra (see Section E). This adduct is much more soluble in HF than the AsF_6^- salt, and the solid obtained by removal of the HF solvent under vacuum is often coloured yellow or orange by the presence of decomposition products. When the solid is allowed to warm up to room temperature under dynamic vacuum, it darkens in colour. No solid residue is left after 15 minutes indicating that the decomposition products are volatile.

Because of the difficulty in measuring out stoichiometric quantities of BrOF_3 and SbF_5 , the direct reaction between these two was not investigated. Use of excess SbF_5 would have resulted in mixtures of SbF_6^- and $\text{Sb}_2\text{F}_{11}^-$ anions being produced, and would have complicated the Raman spectra. Instead

of a direct reaction of BrOF_3 and SbF_5 , the fluorination of $\text{IO}_2\text{F}_3 \cdot \text{SbF}_5$ with BrF_5 was investigated to see if a reaction analogous to (5.3) would occur. A crystalline product was obtained which showed the characteristic $\text{Br}=\text{O}$ stretching frequency of BrOF_2^+ , but the remainder of the spectrum was rather complicated. The decomposition of $\text{BrOF}_2^+\text{Sb}_n\text{F}_{5n+1}^-$ differs from that of the AsF_6^- and BF_4^- salts (Section E) in that BrF_2^+ is the major decomposition product. Another reaction that was tried in order to obtain $\text{BrOF}_2^+\text{SbF}_6^-$ was that of $\text{IOF}_2^+\text{SbF}_6^-$ with BrF_5 . In Chapter IV it was shown that IOF_3 is fluorinated to IF_5 by BrF_5 (equation (4.23)), and that the intermediate BrOF_3 must react rapidly with the M(V) oxyfluoro species present. Since in the reaction of $\text{IO}_2\text{F}_3 \cdot \text{MF}_5$ ($\text{M} = \text{As, Sb}$) with BrF_5 , the BrOF_3 intermediate is trapped as $\text{BrOF}_2^+\text{MF}_6^-$, it was thought that the BrOF_3 intermediate in the $\text{IOF}_3/\text{BrF}_5$ reaction might be trapped by the presence of a Lewis acid, i.e. reaction (5.4) was expected. However, when



$\text{IOF}_2^+\text{SbF}_6^-$ was reacted with excess BrF_5 at -37°C , IF_5 was indeed observed as a product but no $\text{BrOF}_2^+\text{SbF}_6^-$ was obtained. The only solid product observed was $\text{BrF}_2^+\text{SbF}_6^-$. It is unlikely that the $\text{BrF}_2^+\text{SbF}_6^-$ was produced by the decomposition of $\text{BrOF}_2^+\text{Sb}_n\text{F}_{5n+1}^-$ since the latter decomposes only slowly at low temperatures. It is more likely that one of the intermediates involved in reaction (5.4) is decomposing to BrF_2^+ .

E. Characterization of the BrOF_2^+ Salts by Raman and ^{19}F N.M.R.

Spectroscopy.

(i) Raman Spectroscopy

The Raman spectra of solid $\text{BrOF}_2^+\text{AsF}_6^-$ and solid $\text{BrOF}_2^+\text{BF}_4^-$ as well as a solution of $\text{BrOF}_2^+\text{BF}_4^-$ in HF are shown in Figures 5.3, 5.4 and 5.5, respectively. The vibrational frequencies obtained from these spectra are listed in Table 5.4. Also listed are the results obtained by Bougon and his coworkers for $\text{BrOF}_2^+\text{AsF}_6^-$ in the solid phase and in HF solution,¹⁴ along with the vibrational frequencies of the related species SeOF_2 ,¹⁴ SOF_2 ,¹⁴ and ClOF_2 .^{17, 18} The spectra shown in Figures 5.3, 5.4 and 5.5 were recorded in quartz tubes to avoid interference from Raman lines due to FEP or Kel-F sample tubes. However there was some attack on the quartz tube in each case. On Figure 5.5, the lines at 937 cm^{-1} and 876 cm^{-1} are due to a small amount of BrO_2^+ produced by attack of BrOF_2^+ on the quartz vessel (the other lines expected for $\text{BrO}_2^+\text{BF}_4^-$ would be much too weak to influence the remainder of the spectrum), and the broad band which appears in the baseline between 400 cm^{-1} and 540 cm^{-1} is a fluorescence peak often observed in spectra of samples which have attacked quartz or glass containers. The fluorescence band is observed as a very broad, weak peak in the spectrum shown in Figure 5.4. In Figure 5.3 the broad line at 490 cm^{-1} is also attributed to attack on the quartz tube. None of these features were observed in spectra of samples contained in FEP tubes.

The highest frequency line on all three spectra can readily be assigned to a Br=O stretching motion. The fact that this band is shifted to

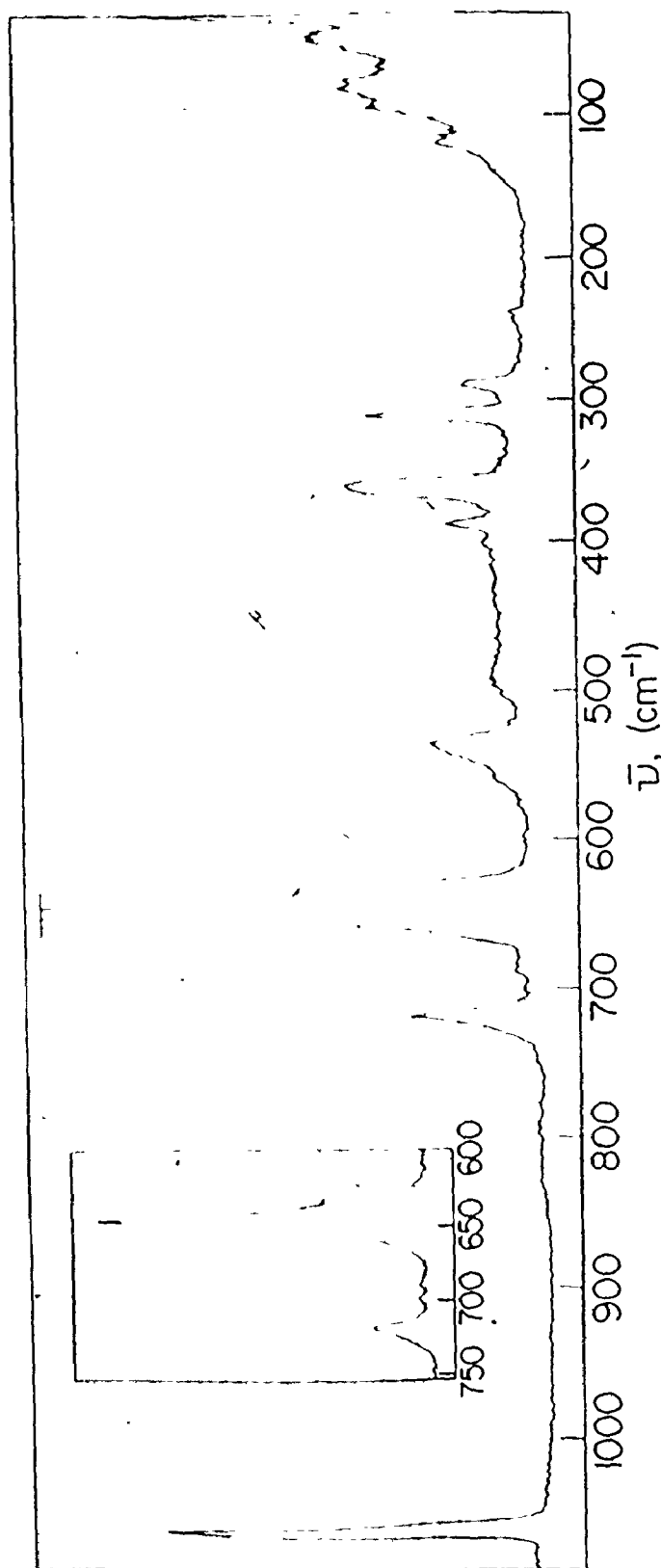


Figure 5.3. Raman spectrum of solid $\text{BrOF}_2^+\text{AsF}_6^-$ recorded at -196°C in a quartz tube. The broad peak at 490 cm^{-1} is due to attack on the quartz.

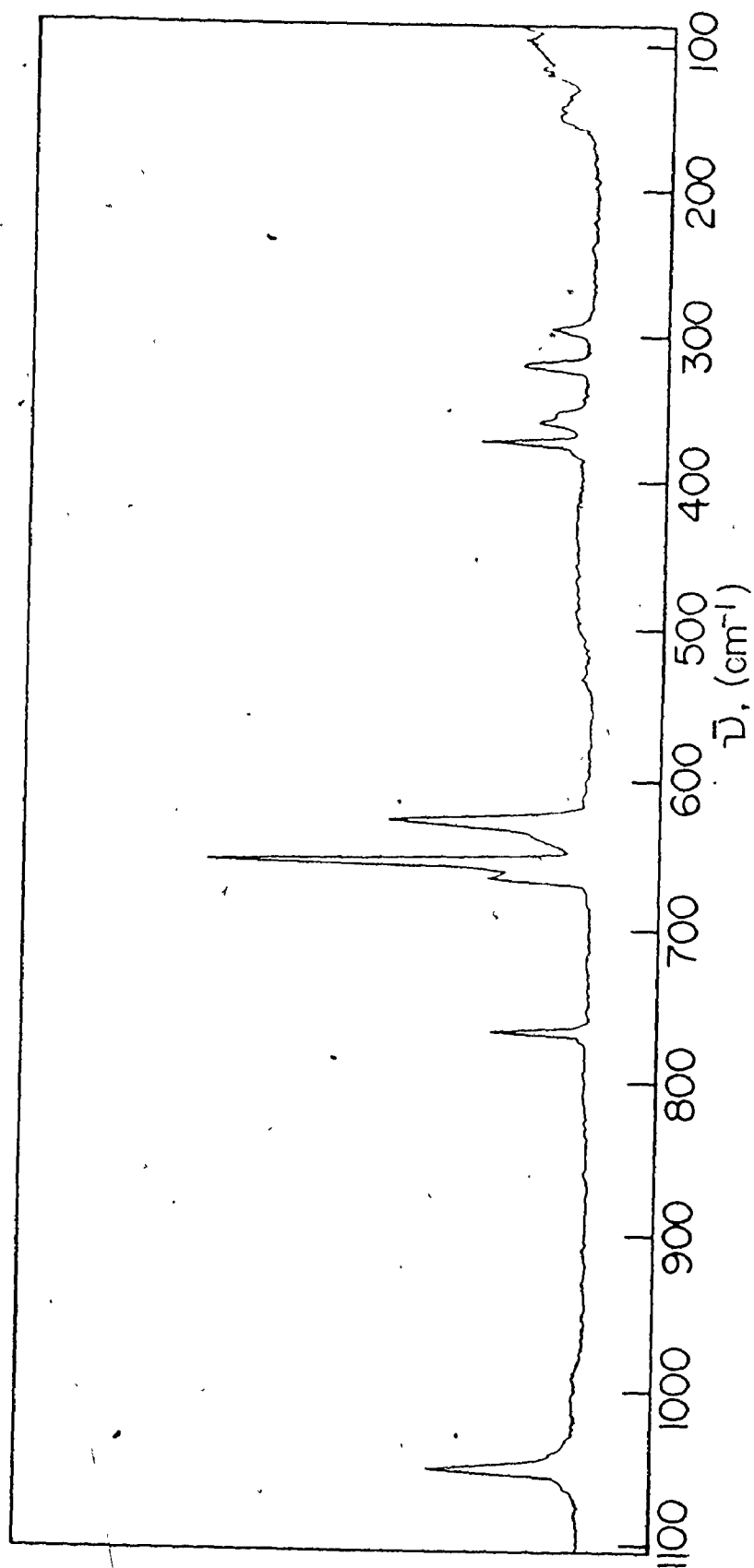


Figure 5.4. Raman spectrum of solid $\text{BrOF}_2^+\text{BF}_4^-$ recorded at -196°C in a quartz tube.

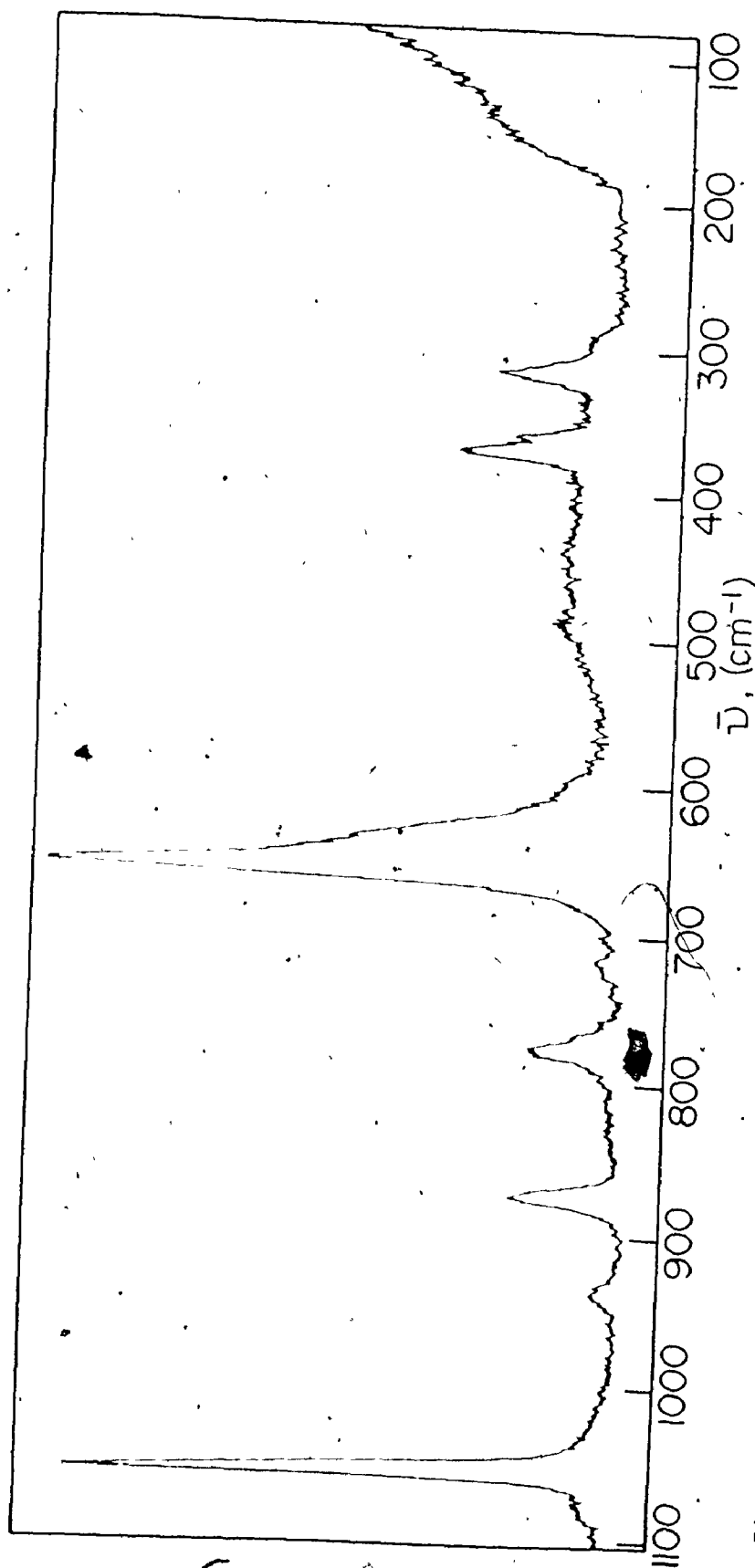


Figure 5.5. Raman spectrum of a solution of $\text{BrOF}_2^+\text{BF}_4^-$ in HF recorded at -72°C in a quartz tube. The peaks at 876 and 937 cm^{-1} are due to $\text{BrO}_2^+\text{BF}_4^-$ produced by attack on the container.

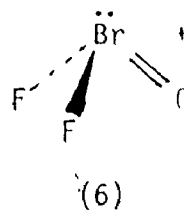
TABLE 5.4 (continued)

- | | | | | | | | |
|---|---|---|----------------|---|---------------|---|----------------|
| a | Reference 144. | b | Reference 149. | c | Reference 37. | d | Reference 132. |
| e | Assignments given for AsF_6^- of O_h symmetry, but the actual symmetry in the solid is much lower since the selection rules for O_h are not obeyed. | | | | | | |
| f | Low frequency range limited by the absorption of the AgBr plates. | | | | | | |
| g | Numbers in parentheses give relative intensities. | | | | | | |
| h | p, polarized; s, strong; m, medium; w, weak; sh, shoulder; br, broad. | | | | | | |
| i | State of polarization of the five low frequency lines could not be determined. | | | | | | |

a considerably higher frequency than the corresponding motion in BrOF_3 (1004 cm^{-1} in the liquid, see Chapter IV), along with the occurrence of bands characteristic of the corresponding anions BF_4^- and AsF_6^- suggest that the adducts should be formulated as $\text{BrOF}_2^+\text{BF}_4^-$ and $\text{BrOF}_2^+\text{AsF}_6^-$. As was the case for the BrO_2^+ salts, there was no evidence for the occurrence of the complex anions $\text{As}_2\text{F}_{11}^-$ or B_2F_7^- in this work despite the fact that excess Lewis acid was used in both cases. (In Raman spectra of HF solutions of $\text{BrOF}_2^+\text{AsF}_6^-$ containing excess AsF_5 , Bougon and his coworkers¹¹ have observed lines which they assigned to $\text{As}_2\text{F}_{11}^-$).

The Raman spectrum of solid $\text{BrOF}_2^+\text{AsF}_6^-$ observed in this work corresponds well with the spectrum reported by Bougon and his collaborators, (see Table 5.4). The major difference is that in the present work only a single, broadened line was seen at 360 cm^{-1} , whereas Bougon and his coworkers have observed two peaks (360 cm^{-1} and 366 cm^{-1}) in the same region. The reason for this is probably the presence of a small amount of the decomposition product Br_2^+ which would produce a peak at 360 cm^{-1} and might obscure the resolution of the two distinct peaks at 360 cm^{-1} and 366 cm^{-1} due to $\text{BrOF}_2^+\text{AsF}_6^-$.

The BrOF_2^+ cation is expected to have the pyramidal structure (6) of C_s symmetry. The six fundamental vibrational modes expected [$\Gamma = 4\text{A}' + 2\text{A}''$] are all Raman active. Definitive polarization data could only be obtained for the three highest frequency lines in the spectrum of $\text{BrOF}_2^+\text{BF}_4^-$ in HF solution.



The three stretching modes of the BrOF_2^+ cation can be identified by comparison of the spectra of the AsF_6^- and BF_4^- salts, and can be readily assigned. As expected, the frequencies are similar to those in SeOF_2 , and lower than those in ClOF_2^+ . The bending modes cannot be assigned with equal certainty since polarization measurements for these lines were inconclusive. For all the related molecules, ν_3 is the highest frequency bending mode. The line at 369 cm^{-1} in the HF solution of $\text{BrOF}_2^+\text{BF}_4^-$ (373 cm^{-1} in solid $\text{BrOF}_2^+\text{BF}_4^-$; one component of the broad 360 cm^{-1} line in solid $\text{BrOF}_2^+\text{AsF}_6^-$) is therefore assigned to ν_3 . Two bending modes (ν_6 and ν_4) remain to be assigned. Since a motion involving the doubly bonded $\text{Br}=\text{O}$ would be expected to occur at higher frequency than one involving only the single $\text{Br}-\text{F}$ bonds, ν_6 would be expected to occur at higher frequency than ν_4 . This has been found for SeOF_2 and SOF_2 , and is in agreement with the force constant calculation for ClOF_2^+ . The assignments of ν_6 and ν_4 in Table 5.4 were made on this basis. However, they could possibly be reversed since Bougon et al.³⁸ have concluded on the basis of a statistical analysis of polarization ratios for ClOF_2^+ that the 402 cm^{-1} peak shows a significantly lower polarization ratio than the 383 cm^{-1} peak, and that therefore the assignments of ν_6 and ν_4 for ClOF_2^+ should be the reverse of those given in Table 5.4. The assignment of these two modes in BrOF_2^+ is therefore tentative.

The anion lines in the Raman spectra of $\text{BrOF}_2^+\text{BF}_4^-$ can be readily assigned and are very similar to the BF_4^- lines in $\text{ClOF}_2^+\text{BF}_4^-$. The BF_4^- ion is expected to have tetrahedral symmetry and the four fundamentals

($\Gamma = A_1 + E + 2T_2$) are all Raman active. In the spectrum of solid $\text{BrOF}_2^+\text{BF}_4^-$, six lines are observed which can be assigned to BF_4^- if it is assumed that there is some splitting of the degenerate modes ν_2 and ν_3 . The 360 cm^{-1} line is assigned to ν_2 of the anion and not to the Br_2^+ decomposition product because the solid was only slightly coloured, and because no line was observed at 720 cm^{-1} . In solution, only ν_1 of BF_4^- can be unambiguously assigned. The shoulder at 360 cm^{-1} has been assigned to ν_2 of BF_4^- . This assignment is uncertain however since some Br_2^+ is probably present (a weak, broad peak is present at 716 cm^{-1}) and this may be responsible for the shoulder at 360 cm^{-1} . The two fundamentals ν_3 and ν_4 of BF_4^- are too weak to be observed in the solution spectrum.

The anion lines for $\text{BrOF}_2^+\text{AsF}_6^-$ are more difficult to assign. An octahedral AsF_6^- anion has six normal modes of vibration ($\Gamma = A_{1g} + E_g + 2T_{1u} + T_{2g} + T_{2u}$). Of these the A_{1g} , E_g , and T_{2g} modes are only Raman active, the two T_{1u} modes are only infra-red active while the T_{2u} mode is inactive. The anion lines for $\text{BrOF}_2^+\text{AsF}_6^-$ have been assigned on the basis of O_h symmetry in Table 5.4, but the actual symmetry in the solid must be lower since the selection rules are not obeyed and several of the degenerate modes are split. All six fundamentals of AsF_6^- were observed in the Raman spectrum (if ν_1 of AsF_6^- is assumed to coincide with ν_2 of BrOF_2^+ , see below) and Bougon and his coworkers have observed three "forbidden" modes (A_{1g} , E_g and T_{2g}) in the infra-red spectrum (see Table 5.4). In the assignments given below, the infra-red data reported by Bougon and his coworkers are used to support the assignments of the Raman data obtained in the

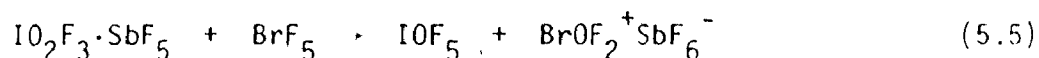
present work. The Raman line at 720 cm^{-1} and the weak peak at 688 cm^{-1} are assigned to the Raman "forbidden" mode ν_3 (T_{1u}). This mode is observed in the infra-red as a strong band at 688 cm^{-1} with a shoulder at 730 cm^{-1} . The Raman line at 531 cm^{-1} (and the shoulder at 558 cm^{-1}) are attributed to ν_2 (E_g), which is observed as a medium intensity line in the infra-red spectrum. The Raman "forbidden" fundamental ν_4 (T_{1u}) is assigned to the lines at 387 cm^{-1} and 398 cm^{-1} , which is observed as a relatively intense line at 385 cm^{-1} (with a shoulder at 405 cm^{-1}) in the infra-red spectrum. The Raman "allowed" vibration ν_5 (T_{2g}) is attributed to a component of the broad 360 cm^{-1} band (Bougon et al. observed it as a separate line at 360 cm^{-1}) and is present in the infra-red spectrum as a shoulder at 355 cm^{-1} .

Despite the fact that the decomposition product Br_2^+ shows Raman lines at 360 cm^{-1} and 720 cm^{-1} , the lines observed at these frequencies in the spectrum of solid $\text{BrOF}_2^+\text{AsF}_6^-$ were not assigned to Br_2^+ for several reasons. First, the sample used to record the Raman spectrum was only slightly coloured suggesting that only a relatively small amount of Br_2^+ was present. Second, the relative intensity of the 720 cm^{-1} line is too large compared to the 360 cm^{-1} for the former to be entirely due to Br_2^+ . Also, no band was observed at 1080 cm^{-1} again suggesting that no large amounts of Br_2^+ were present. Finally, lines at 730 cm^{-1} and 355 cm^{-1} are also observed in the infra-red spectrum indicating that these lines must be due to $\text{BrOF}_2^+\text{AsF}_6^-$ since the Br_2^+ vibration is inactive in the infra-red. The possibility that some Br_2^+ is present in the sample cannot be eliminated on the basis of the vibrational spectra however. Moreover, the fact that

only a single broad line at 360 cm^{-1} was observed in the present work (rather than the two lines in this region observed by Bougon and his co-workers) is attributed to the presence of a small amount of Br_2^+ .

The very weak line at 239 cm^{-1} is assigned to ν_6 (T_{2u}) which is formally forbidden in both the Raman and infra-red spectra. This leaves only ν_1 (A_{1g}) unaccounted for, and this is assumed to be coincident with the strong peak due to ν_2 of the BrOF_2^+ cation. A weak line at 660 cm^{-1} is observed in the infra-red spectrum and has been assigned to ν_1 of AsF_6^- , and this supports the supposition that ν_1 of AsF_6^- and ν_2 of BrOF_2^+ are superimposed in the Raman spectrum. This would correspond to a considerable decrease in frequency for ν_1 of AsF_6^- between solid $\text{BrOF}_2^+\text{AsF}_6^-$ and the "free ion" value of 683 cm^{-1} for $\text{BrOF}_2^+\text{AsF}_6^-$ in HF (see Table 5.4). The fact that all the fundamentals of AsF_6^- are observed in the Raman spectrum indicates a considerable lowering of the symmetry of the anion in the solid. A similar effect has been found in a number of $\text{ClOF}_2^+\text{MF}_6^-$ salts. Also, the crystal structure of $\text{SeF}_3^+\text{NbF}_6^-$,¹⁵⁰ where the cation is isoelectronic with BrOF_2^+ , has shown that there is bridging between the anion and the cation which results in very distorted NbF_6^- octahedra. A similar situation may exist in $\text{BrOF}_2^+\text{AsF}_6^-$. However, since the cation frequencies are very similar in the solid AsF_6^- and BF_4^- salts and in HF solution, discrete ions must be present in both solid adducts.

The reaction of $\text{IO}_2\text{F}_3 \cdot \text{SbF}_5$ with BrF_5 has also been studied. By analogy with equation (5.3), this should proceed according to (5.5). The



^{19}F nmr spectrum of the solution indicates that IOF_5 is indeed produced and that all the $\text{IO}_2\text{F}_3 \cdot \text{SbF}_5$ is consumed. A solid product is formed in the reaction, and Figure 5.6 shows the Raman spectrum of this solid product recorded in a Kel-F sample tube. The Raman lines due to the Kel-F tube are indicated with an X in Figure 5.6. The reaction was repeated in an FEP tube to ensure that the Kel-F tube lines did not conceal any Raman lines due to the sample. The vibrational frequencies obtained from Figure 5.6 are listed in Table 5.5. The characteristic Br-O stretch of the BrOF_2^+ cation is observed at 1061 cm^{-1} . The remainder of the spectrum must therefore be due to the remaining BrOF_2^+ lines and the lines due to the anion. This anion should be SbF_6^- from equation (5.5). However, the $\text{IO}_2\text{F}_3 \cdot \text{SbF}_5$ used contained a slight excess of SbF_5 . In view of the tendency of SbF_6^- to form polymeric anions $\text{Sb}_n\text{F}_{5n+1}^-$, mixtures of SbF_6^- and $\text{Sb}_2\text{F}_{11}^-$ anions may be present in this sample.

Table 5.5, therefore, lists the Raman frequencies attributed to the BrOF_2^+ cation in the AsF_6^- salt (see Table 5.4). Also listed in Table 5.5 are the vibrational frequencies for the SbF_6^- anion in KSbF_6 . Clearly, the anion lines in $\text{BrOF}_2^+ \text{Sb}_n\text{F}_{5n+1}^-$ cannot be assigned on the basis of a free octahedral SbF_6^- anion. It is known that formation of a fluorine bridge between the anion and the cation can lower the symmetry of the SbF_6^- from O_h to C_{4v} , and this distortion has been successfully used to assign the Raman spectra of a number of SbF_6^- salts. Several sets of frequencies which have been assigned to C_{4v} symmetry SbF_6^- units have been included in Table 5.5. Finally, a number of Raman spectra for the $\text{Sb}_2\text{F}_{11}^-$

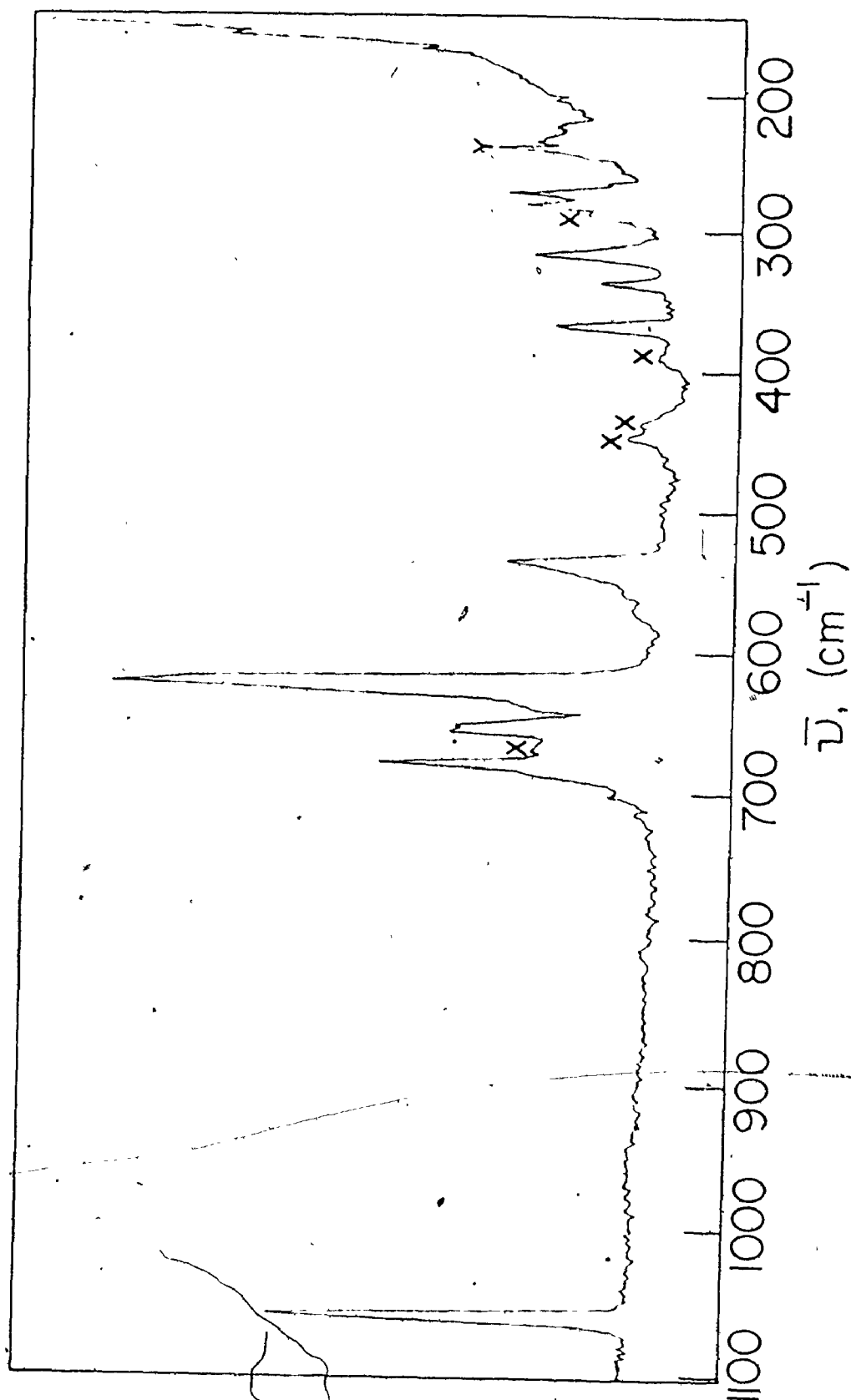


Figure 5.6. Raman spectrum of $\text{BrOF}_2^+ \text{SbF}_{5n+1}^-$ recorded at -95°C . Peaks marked X are due to the KCl-F container and Y is due to the glass of the dewar which surrounded the sample.

TABLE 5.5 (continued)

Vibrational Frequencies of $\text{GrOF}_2^+ \text{SbF}_6^-$ and Some related SbF_6^- Systems (cm^{-1})

- ^a Only anion lines are shown, and the intensities shown in parentheses have been normalized with respect to the strongest anion line.
- ^b Reference 151; m, medium; s, strong; v.s, very strong; sh, shoulder.
- ^c Solid AsF_6^- salt. ^d Reference 7. ^e Reference 152. ^f Reference 103.
- ^g Approximate position since two or more lines are coincident.
- ^h Relative intensity not reported.

ion have been reported ^{1,90,152,153,154} and some of these have been included in Table 5.5. The Raman frequencies and relative intensities reported for the C_{4v} SbF_6^- ions and $Sb_2F_{11}^-$ ions vary drastically when the cation is varied. For this reason and since mixtures of anions may be present, it is not possible to identify the anion lines in the spectrum of $BrOF_2^+ Sb_n F_{5n+1}^-$. It seems that the best fit is obtained with the SbF_6^- lines observed for the β - XeF_3^+ salt ¹⁵² and that the amount of $Sb_2F_{11}^-$ present must be small since no intense peaks are seen at $\sim 690\text{ cm}^{-1}$ (as in $XeF^+ Sb_2F_{11}^-$ and $CsSb_2F_{11}^-$ ¹⁵³) and no peaks are observed at about $\sim 740\text{ cm}^{-1}$ (as in $BrF_4^+ Sb_2F_{11}^-$). Identification of the cation lines in the spectrum of $BrOF_2^+ Sb_n F_{5n+1}^-$ is not entirely satisfactory either. Although $\nu_{X=O}$, $\nu_{asym} XF_2$, $\delta_{sym} OXF$, $\delta_{asym} OXF$, and $\delta_{sym} XF_2$ can be readily identified (if it is assumed that $\delta_{sym} XF_2$ coincides with an anion line to account for the high relative intensity of the 278 cm^{-1} line), the assignment of $\nu_{sym} XF_2$ is less certain. On the basis of intensity the 624 cm^{-1} peak appears to be due to $\nu_{sym} XF_2$. However, this assignment would imply an $\sim 25\text{ cm}^{-1}$ shift to higher frequency from $\nu_{sym} XF_2$ in the SbF_6^- salt to that in the BF_4^- and AsF_6^- salts. Also, assigning the 624 cm^{-1} peak to $\nu_{sym} XF_2$ would mean that $\nu_{asym} XF_2 = \nu_{sym} XF_2$ whereas the reverse is true in the other $BrOF_2^+$ salts. The alternative assignment indicated in Table 5.5 attributes the 656 cm^{-1} peak to $\nu_{sym} XF_2$. The cation frequencies are then quite similar in all the $BrOF_2^+$ salts. However, the intensity of the 656 cm^{-1} line relative to the 1061 cm^{-1} band is rather low compared to the relative intensity of $\nu_{sym} BrF_2$ to $\nu_{Br=O}$ in the other salts. This assignment therefore has to be regarded

as tentative. No attempt was made to assign the anion lines. It is clear, however, that the SbF_6^- anion is distorted from O_h symmetry and that this distortion reduces the symmetry to C_{4v} or quite possibly to an even lower symmetry if there is more than one fluorine bridge between the anion and cation. The lines assigned to the bending modes of BrOF_2^+ are probably coincident with anion lines but this has not been indicated in Table 5.5. The decomposition product ($\text{BrF}_2^+ \text{SbF}_6^-$) is not present in the sample used to record the spectrum shown in Figure 5.6 since the characteristic strong line at 704 cm^{-1} due to $\text{BrF}_2^+ \text{SbF}_6^-$ ⁹⁶ is not observed.

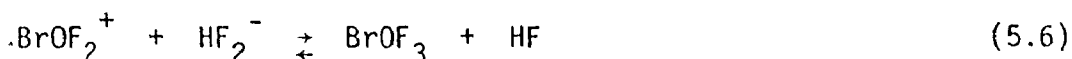
Both $\text{BrOF}_2^+ \text{AsF}_6^-$ and $\text{BrOF}_2^+ \text{BF}_4^-$ decompose at room temperature. $\text{BrOF}_2^+ \text{AsF}_6^-$ becomes pink when allowed to stand at room temperature for a few hours. The decomposition product exhibits a strong Raman line at 360 cm^{-1} with weaker lines at 720 cm^{-1} (coincident with ν_3 of AsF_6^-) and 1080 cm^{-1} . $\text{BrOF}_2^+ \text{BF}_4^-$ rapidly turns a very dark brownish colour when allowed to warm up to room temperature, and all the decomposition products are volatile. Even samples prepared at low temperature were often coloured and Raman lines at 360 cm^{-1} and $\sim 720 \text{ cm}^{-1}$ were observed. The decomposition products for the two salts can be identified as $\text{Br}_2^+ \text{BF}_4^-$ and $\text{Br}_2^+ \text{AsF}_6^-$ on the basis of these Raman lines (see Section C).

$\text{BrOF}_2^+ \text{SbF}_6^-$ appears to decompose to a different product however. After a sample had been kept at room temperature for four hours, its Raman spectrum contained a number of lines which could be readily assigned to $\text{BrF}_2^+ \text{SbF}_6^-$ ⁹⁶. However, the decomposition of the SbF_6^- salt is slower than that of the AsF_6^- and BF_4^- salts since even after the sample was left for

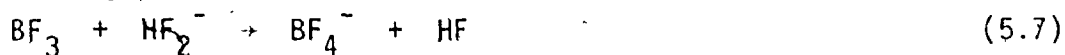
several days at room temperature, the characteristic $\text{Br}=\text{O}$ stretching frequency of BrOF_2^+ was still observable in the Raman spectrum of the decomposing material. After approximately 10 days at room temperature, the solid consisted entirely of $\text{BrF}_2^+\text{SbF}_6^-$ according to its Raman spectrum. This solid was however pinkish in colour, presumably indicating that some Br_2^+ was formed, although it could not be observed in the Raman spectrum. This Br_2^+ does not necessarily come from the decomposition of BrOF_2^+ however, since $\text{BrF}_2^+\text{SbF}_6^-$ has also been reported to turn pink on prolonged storage.¹⁵⁵

(ii) ^{19}F N.M.R. Spectroscopy

$\text{BrOF}_2^+\text{BF}_4^-$ is quite soluble in HF, and the ^{19}F nmr spectrum of the BrOF_2^+ cation was observed. Excess BF_3 was introduced into the solution to prevent exchange between the cation and the HF solvent,^{130,156} which probably occurs by a reaction such as (5.6). Addition of excess BF_3 slows



down this exchange reaction because the HF_2^- is removed from solution by reaction (5.7). Bougon and his collaborators¹³² have reported that the



^{19}F nmr spectrum of a solution of $\text{BrOF}_2^+\text{AsF}_6^-$ in HF did not show a separate signal in the F on Br (V) region at $+10^\circ\text{C}$. When excess AsF_5 was added, they observed a sharp singlet at -202 ppm which was attributed to BrOF_2^+ . This singlet was found to shift to high field as the temperature was lowered

(-199 ppm at -60°C). In the present work, the ^{19}F nmr spectrum of a solution of $\text{BrOF}_2^+\text{BF}_4^-$ and BF_3 in HF (mole ratio $\approx 1:1.2:70$) was recorded at -79°C . A sharp singlet was observed at -192 ppm (linewidth $\sim 20 \pm 3$ Hz) which can be assigned to BrOF_2^+ , and a strong singlet was observed at +190 ppm which was assigned to the HF solvent. No separate signal was observed in the F on B region, and the BF_3 and BF_4^- were therefore exchanging rapidly with the HF solvent. When the sample was warmed to -69°C and then to -59°C , the chemical shift of the BrOF_2^+ singlet did not change significantly, but the peak broadened considerably (70 ± 5 Hz at -69°C and 180 ± 15 Hz at -59°C). This line broadening is probably due to exchange between the BrOF_2^+ and the HF solvent.

The singlet observed for BrOF_2^+ is in agreement with the equivalence of the fluorine atoms in the proposed structure (6) and its chemical shift is in the same region as that found for the isoelectronic BrO_2F (-210 ppm).

The ^{19}F nmr resonances of the related molecules BrOF_4^- ($\delta = -104$ ppm, Chapter III), BrOF_3 ($\delta = -162$ ppm, Chapter IV), and BrOF_2^+ ($\delta = -192$ ppm) shift to lower field on going from the anion to the parent molecule to the cation. A similar trend is observed in the series BrF_6^- ($\delta = -96$ ppm for KBrF_6 dissolved in CH_3CN at room temperature), BrF_5 ($\delta_{\text{av}} = -160$ ppm, the weighted mean of $\delta_{\text{FBrF}_4} = -270$ and $\delta_{\text{FBrF}_4} = -132^{107}$) and BrF_4^+ ($\delta = -180.4$ ppm⁷). The same trend is observed for the Xe(IV) and Xe(VI) cations^{157,158} and for ClOF_2^+ ,¹⁵⁶ where the ^{19}F resonances occur to low field of the parent molecule. However a large number of cases have been

reported in which the opposite trend is observed and cation formation causes the resonance to shift to high field (IF_6^+ and IF_7 ,¹⁵⁹ KrF^+ and KrF_2 ,⁹⁰ XeF^+ and XeF_2 ,⁹⁰ ClF_2^+ and ClF_3 ,¹⁵⁶ ClF_4^+ and ClF_5 ,¹⁵⁶ SOF_3^+ and SOF_4 ,¹⁴⁷ SeF_3^+ ¹³⁰ and SeF_4 ¹²¹). The reasons for the differing trends in these groups of molecules are not clear. The dominant contribution to the shielding of the fluorine nucleus, and therefore to the chemical shift, is the paramagnetic term $\sigma_{\text{FF}}^{\text{par}}$.¹⁶⁰ This term arises as a consequence of mixing of the ground and excited electronic states. It can be expressed¹⁶¹ in terms of ground-state molecular orbitals and is inversely proportional to the mean excitation energy (ΔE). In a very general manner, the $\sigma_{\text{FF}}^{\text{par}}$ term can be described as a measure of the asymmetry in the electron distribution about the fluorine nucleus. In the case of a spherically symmetrical F^- ion, the $\sigma_{\text{FF}}^{\text{par}}$ term is zero, whereas in the case of molecular F_2 , the electronic distribution is very asymmetric and $\sigma_{\text{FF}}^{\text{par}}$ assumes a very large negative value. This causes the chemical shift for the F_2 molecule to be 630 ppm to low field of that for the F^- nucleus in liquid HF. The magnitude of the paramagnetic term is dependent on the degree of ionic character in the bond between fluorine and the atom to which it is bound (M). A large contribution from the ionic M^+F^- form results in a small $\sigma_{\text{FF}}^{\text{par}}$ term and (since $\sigma_{\text{FF}}^{\text{par}}$ is negative) a relatively high chemical shift for the fluorine. Since the degree of ionic character in the bond depends mainly on the electronegativity (x_{M}) of the atom M, the chemical shift of the fluorine in an M-F system should depend on x_{M} as well. This has indeed been found for a number of binary fluorides (such

as MF_3 : $M = \text{N, P, As, Sb}$; MF_4 : $M = \text{S, Se, Te}$; MF_5 : $M = \text{P, As, Sb}$) where the chemical shift of the fluorine ligands decreases as χ_M increases. On this basis, one might expect the chemical shifts in a series MF_{n-1}^+ , MF_n and MF_{n-1}^- to increase on going from the cation to the neutral molecule to the anion since the ionic nature of the MF bond increases along the series (as is reflected for example by a lowering of the M-F stretching frequency). This is indeed observed in the BrOF_2^+ , BrOF_3 , BrOF_4^- series examined in this work, but does not seem to be generally the case. The reason for this is that other factors also affect the paramagnetic shielding term. The variation in the chemical shift of the fluorine atoms in compounds containing the same central atom in different oxidation states has been attributed to changes in the hybridization of the central atom. The trends are not clear however. Thus, the chemical shifts of AsF_3 and SbF_3 are greater than those of AsF_5 and SbF_5 , respectively, and this is attributed to the involvement of higher energy d orbitals in the hybridization of the As and Sb atoms in the higher oxidation state.¹⁶⁰ The same does not apply to the halogen fluorides however, since here the chemical shifts increase with increasing oxidation state. Since cation or anion formation involves a change in the hybridization of the central atom, this should have some effect on the chemical shift of the fluorine ligands, but whether the change will be to high or low field cannot be predicted a priori. Other factors such as the occurrence of π bonding between the central atom and the fluorine ligand or the occurrence of low energy excited states capable of mixing with the ground state will vary also when anions or cations are

formed from a neutral molecule, and the effects on the chemical shifts of the resultant species are not obvious. It appears that the factors which govern ^{19}F - chemical shifts are not understood well enough to rationalize the trends which have been observed in the present work and which have been reported in the literature.

F. Experimental Section.

(i) Preparation of BrO_2^+ Salts.

(a) $\text{BrO}_2^+\text{AsF}_6^-$: Approximately 0.135 g (1.03 mmol) of BrO_2F was dynamically distilled into a U-tube constructed of 1/4" o.d. thin-walled FEP tubing and fitted with an FEP nmr tube as a side-arm. Enough HF was added to dissolve the BrO_2F at room temperature and the solution was washed into the side-arm. The HF was removed under vacuum at -72°C and solid BrO_2F was obtained. Approximately 0.4 g of HF and 1.1 mmol of AsF_5 were condensed into the side-arm. The mixture was allowed to react at -78°C for an hour, giving a yellowish solution with an orange solid in the bottom of the tube. The solvent was removed under vacuum, and an orange powder was obtained. This powder was used to record the Raman spectrum shown in Figure 5.2. The colour of the samples prepared by this method varied from cream coloured to rather deep reddish-orange. In other preparations, larger excesses of AsF_5 were used but products with identical Raman spectra were obtained.

In another experiment, 0.155 g (1.18 mmol) of BrO_2F was dissolved in 2.7 g of BrF_5 , and approximately 2.2 mmol of AsF_5 was slowly admitted

to the tube kept at -62°C . A brown solution standing over a brownish solid was produced. The solvent and excess AsF_5 were removed under vacuum at -62°C , and a brown powder was left behind. The Raman spectrum of this powder showed the lines characteristic of $\text{BrO}_2^+\text{AsF}_6^-$ along with the 360 cm^{-1} line due to Br_2^+ which is the decomposition product. The sample was briefly warmed to room temperature, and the Raman spectrum was again recorded. The 360 cm^{-1} line was now the dominant line in the spectrum, and weaker lines at 720 cm^{-1} and 1080 cm^{-1} were also present.

(b) $\text{BrO}_2^+\text{BF}_4^-$: Approximately 0.704 mmol of BrO_2F (estimated from the amount of KBrO_2F_2 used) was dynamically distilled into a 1/4" o.d. FEP U-tube fitted with an FEP nmr tube side-arm. Approximately 0.6 g of HF and 1.1 mmol of BF_3 were distilled in. The mixture was allowed to react at -72°C and an orange solution was formed after 30 minutes. The solution was concentrated by removal of some of the HF and the excess BF_3 under vacuum. A portion of this solution was decanted into the side-arm and (after subsequent dilution with HF) was used to record the ^{19}F nmr spectrum. The concentration of the sample used to record the nmr spectrum was calculated from the integration of the peaks due to BF_4^- and HF. The remainder of the solution in the U-tube was pumped to dryness at -72°C , and an orange powder was formed. This sample was used to record the Raman spectrum shown in Figure 5.1.

A very similar procedure was used for the reaction of BrO_2F and BF_3 using BrF_5 as a solvent, except that the side-arm on the U-tube consisted of a 6 mm o.d. quartz tube. Most of the solution of $\text{BrO}_2^+\text{BF}_4^-$ in BrF_5 was

decanted into the side-arm. The solution which remained in the U-tube was allowed to stand at room temperature for 10 minutes and turned dark brown in colour. The volatile components of the solution in the side-arm were removed under vacuum at -48°C , and an orange solid resulted. The Raman spectrum of this solution contained the lines characteristic of $\text{BrO}_2^+\text{BF}_4^-$, but showed a number of additional lines as well, indicating that decomposition (probably as a result of attack on the quartz) had occurred. This impure sample of $\text{BrO}_2^+\text{BF}_4^-$ was dissolved in HF and a large excess of KF added. The mixture was rapidly warmed to dissolve all the solid present, and then cooled to -78°C . A large mass of white precipitate was formed. The Raman spectrum of this white solid showed the lines characteristic of BrO_2F .

(ii) Preparation of BrOF_2^+ Salts.

(a) $\text{BrOF}_2^+\text{AsF}_6^-$: In a typical preparation, approximately 0.77 mmol of BrOF_3 was placed in a 10 mm o.d. quartz ampoule. Approximately 0.5 g of HF and 1.4 mmol of AsF_5 were distilled in at -196°C . The mixture was warmed to -72°C to give a cream coloured solid under a brownish solution. Removal of the solvent under vacuum produced a cream coloured solid. This solid was used to record the Raman spectrum shown in Figure 5.3. When this solid was allowed to stand at room temperature for an hour, it turned pink in colour and the Raman lines at 360 cm^{-1} and 720 cm^{-1} increased in relative intensity. After four hours at room temperature, the solid was even more darkly coloured and the Raman lines at 360 cm^{-1} , 720 cm^{-1} and 1080 cm^{-1} then dominated the spectrum.

BrF_5 was also used as a solvent for the preparation of $\text{BrOF}_2^+\text{AsF}_6^-$. 0.076 g (0.50 mmol) of BrOF_3 was dissolved in 1.3 g of BrF_5 in a 1/4" o.d. FEP tube, and 0.6 mmol of AsF_5 was distilled in. The mixture was warmed to -62°C , and then briefly to room temperature to get complete reaction. A light brown solution and a white solid were present in the tube. The Raman spectrum of the solution showed a weak line at 1053 cm^{-1} indicating that $\text{BrOF}_2^+\text{AsF}_6^-$ is slightly soluble in BrF_5 . Removal of the BrF_5 under vacuum produced a white solid whose Raman spectrum was identical with that of $\text{BrOF}_2^+\text{AsF}_6^-$ produced using HF as a solvent.

$\text{IO}_2\text{F}_3 \cdot \text{AsF}_5$ was dissolved in an excess of BrF_5 (mole ratio ~ 1:20) in an FEP nmr tube, and warmed to room temperature. After ten minutes, a white crystalline solid was deposited in the tube. The ^{19}F nmr spectrum of the supernatant solution showed signals due to BrF_5 , IOF_5 , and a small amount of IF_5 . No signals due to $\text{IO}_2\text{F}_3 \cdot \text{AsF}_5$ were observed. The IF_5 is probably produced by thermal or photochemical decomposition of the $\text{IO}_2\text{F}_3 \cdot \text{AsF}_5$ adduct to $\text{IOF}_2^+\text{AsF}_6^-$,²⁶ followed by fluorination to IF_5 by the BrF_5 solvent. The volatile components of the mixture were removed under vacuum and a white solid was produced whose Raman spectrum showed it to be $\text{BrOF}_2^+\text{AsF}_6^-$.

(b) $\text{BrOF}_2^+\text{BF}_4^-$: In a typical preparation, 0.28 mmol of BrOF_3 was dissolved in 0.4 g of HF in an FEP nmr tube, and 0.63 mmol of BF_3 was distilled in at -196°C . The mixture was warmed to -72°C , and a clear, yellowish solution was formed. This solution was used to record the ^{19}F nmr spectrum. The HF and excess BF_3 were then removed under vacuum at

-72°C, and a yellowish solid resulted whose Raman spectrum was consistent with $\text{BrOF}_2^+\text{BF}_4^-$. Samples were prepared in a similar manner in Kel-F and quartz vessels.

$\text{BrOF}_2^+\text{BF}_4^-$ was also prepared by the direct reaction of KBrOF_4 (0.058 g, 0.27 mmol) with excess BF_3 (0.70 mmol) at -72°C using HF (0.8 g) as a solvent. The reaction was done in a 10 mm o.d. quartz ampoule fitted with a 6 mm o.d. quartz tube as a side-arm. The reaction produced a mixture of KBF_4 and $\text{BrOF}_2^+\text{BF}_4^-$. Potassium tetrafluoroborate is much less soluble in HF than $\text{BrOF}_2^+\text{BF}_4^-$, and the latter can be isolated by pouring the solution into the side-arm and removing the HF under vacuum.

(c) $\text{BrOF}_2^+\text{SbF}_6^-$: 0.203 g (0.47 mmol) of $\text{IO}_2\text{F}_3 \cdot \text{SbF}_5$ was dissolved in 1.75 g of BrF_5 , and the mixture was warmed to room temperature. A white microcrystalline solid was produced after ten minutes. The ^{19}F nmr spectrum of the solution showed lines due to BrF_5 , IOF_5 , and a small amount of IF_5 (see section F (ii) (a)). The volatile components of the mixture were removed under vacuum, and a white solid was produced. Raman spectroscopy showed this solid to contain the BrOF_2^+ cation. $\text{BrOF}_2^+\text{Sb}_n\text{F}_{5n+1}^-$ is slightly soluble in BrF_5 since a weak peak at 1051 cm^{-1} appeared in the Raman spectrum of the BrF_5 standing over solid $\text{BrOF}_2^+\text{Sb}_n\text{F}_{5n+1}^-$.

When a sample of $\text{BrOF}_2^+\text{Sb}_n\text{F}_{5n+1}^-$ was allowed to stand at room temperature for four hours, extra lines appeared in the Raman spectrum and these could be assigned to $\text{BrF}_2^+\text{SbF}_6^-$. After several days, extensive decomposition had occurred. After the sample had stood for ten days, the Raman spectrum could be entirely attributed to $\text{BrF}_2^+\text{SbF}_6^-$.

(d) Reaction of $\text{IOF}_2^+\text{SbF}_6^-$ with BrF_5 : 0.026 g (0.062 mmol) of $\text{IOF}_2^+\text{SbF}_6^-$ was allowed to react with excess BrF_5 (0.79 g, 4.5 mmol) in an FEP nmr tube at -48°C and then at -37°C . There was a white solid present in the tube, and the solution was coloured slightly brown. The ^{19}F nmr spectrum of the solution showed that IF_5 had been produced in the reaction. A weak, broad line at +113 ppm was also present in the nmr spectrum, and this is presumably due to SbF_6^- . The cation associated with this SbF_6^- anion (BrF_2^+ , see below) could not be observed as a separate resonance however. The volatile species present were removed under vacuum at -37°C and then briefly at room temperature. A slightly yellowish solid was produced. Its Raman spectrum could be attributed to $\text{BrF}_2^+\text{SbF}_6^-$.

CHAPTER VI

A REINVESTIGATION OF THE VIBRATIONAL SPECTRUM OF SeO_2F^-

AND THE PREPARATION AND RAMAN SPECTRUM OF $\text{SeO}_2\text{F}_2^{2-}$

A. Introduction.

During the course of our work on BrO_2F (see Chapter IV), it was of interest to compare its vibrational spectrum to that of the isoelectronic species SeO_2F^- . Paetzold and Aurich¹⁶² have reported the synthesis of KSeO_2F by the direct reaction of KF and SeO_2 at a temperature of 250°C (reaction (6.1)) and have recorded its infra-red and Raman



spectra. However, their assignments were unusual in several respects and did not seem consistent with our findings for BrO_2F . We have repeated this preparation of SeO_2F^- and in this chapter the Raman spectrum will be described and reassigned. Milne and Moffett^{163, 164} have shown that MSeO_2F ($\text{M} = \text{K}$ and Cs) can be prepared by other methods such as the reaction of the appropriate metal fluoride with SeO_2 in DMSO or $48\% \text{HF}$ as solvent.

It was also of interest to attempt the preparation of the dioxodifluoroselenate (IV) ion, $\text{SeO}_2\text{F}_2^{2-}$, since the reaction of TeO_2 with CsF or RbF gives only the $\text{TeO}_2\text{F}_2^{2-}$ ion,¹⁶⁵ with no evidence for the TeO_2F^- ion. Also, the $\text{SeO}_2\text{F}_2^{2-}$ ion is isoelectronic with the BrO_2F_2^- ion prepared

in the present work and a comparison between the two would be of interest. Finally, the reaction between SO_2F^- and excess CsF was studied in an attempt to find evidence for the corresponding $\text{SO}_2\text{F}_2^{2-}$ anion.

B. Vibrational Spectrum of the SeO_2F^- Ion.

The Raman spectrum of the product of the reaction of equimolar quantities of SeO_2 and KF at approximately 280°C is shown in Figure 6.1. The Raman bands are listed in Table 6.1. Also listed are the Raman and infra-red bands for SeO_2F^- reported by Paetzold and Aurich, along with the fundamental frequencies for the isoelectronic species BrO_2F (see Chapter IV) and $\text{SeO}_2(\text{OH})^-$,¹⁶⁶ and the related ion SO_2F^- .¹¹¹ An isolated SeO_2F^- ion is expected to have a pyramidal geometry which corresponds to C_s symmetry. The six fundamentals ($\Gamma = 4\text{A}' + 2\text{A}''$) should all be Raman and infra-red active. This agrees well with the number of lines observed if the peak at 424 cm^{-1} and the shoulders at 450 cm^{-1} and 408 cm^{-1} observed in the Raman spectrum are all assigned to the same normal mode. In the infra-red spectrum, the two lines at 440 cm^{-1} and 403 cm^{-1} are assigned to this mode. The assignments proposed in the present work are based on comparison with the assignments of the related molecules $\text{SeO}_2(\text{OH})^-$, BrO_2F , and SO_2F^- . As expected the frequencies for SeO_2F^- are considerably lower than those for SO_2F^- . The SeO_2F^- frequencies are also slightly lower than those of BrO_2F , which is consistent with a slight weakening of the bonds due to the negative charge on the anion. Several of the assignments proposed in the present work differ from those of

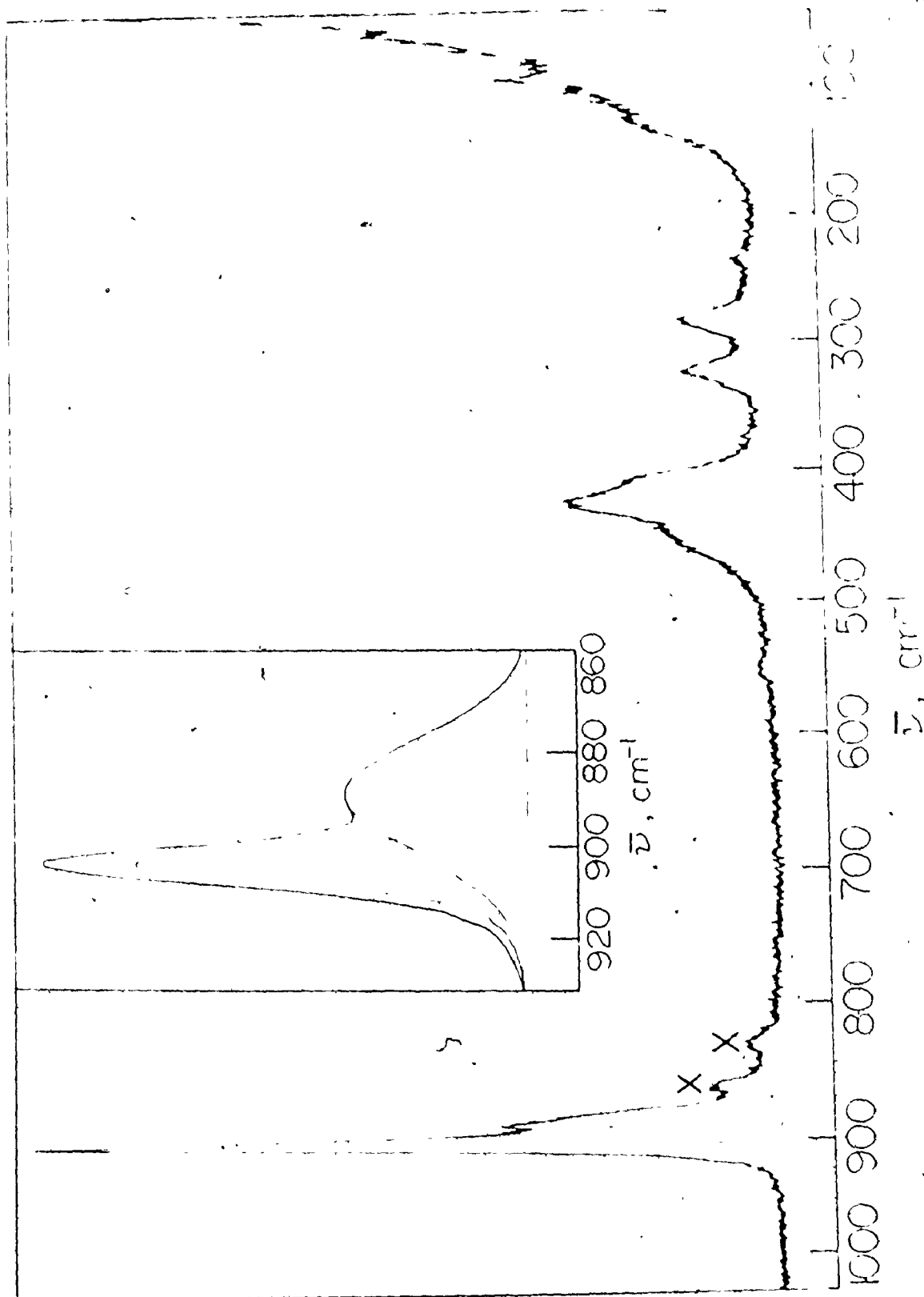


Figure 6.1. Raman spectrum of YSeO_2F . Bands marked X are due to $\text{Y}_2\text{SeO}_2\text{F}_2$.

The inset shows the resolved spectrum of the SeO_2 stretching region.

TABLE 6.1

Fundamental Frequencies of SeO_2F^- and Some Related Molecules.

$\text{SO}_2\text{F}^-(a)$	$\text{SeO}_2(\text{OH})^-(b)$	$\text{BrO}_2\text{F}^-(c)$	SeO_2F^-		Raman	I.R.	This work (i)	Assignments	
			Paetzold & Aurich (d)	Milne et al. (h)				Present results	Paetzold & Aurich (d)
			I.R.	I.R.					
1102 vs (e)	855 s	908(100) (f)	909 vs	912 vs	903(100)	912 vs	903(100)	$\nu_{\text{sym}} \text{XO}_2 \text{A}''$	$\nu_{\text{sym}} \text{XO}_2$
1180 vs	790 w	963 (25) 940	882 vs	884 vs	887(80)	884 vs	888(45) br	$\nu_{\text{asym}} \text{XO}_2 \text{A}'$	$\nu_{\text{sym}} \text{XO}_2$
593 s	615 m	524sh 496 (25)vbr 487sh	440 s, vbr 415	440 s 403 vs	415(25)	440 s 403 vs	450sh 424 (25)vbr 408sh	$\nu_{\text{X-F}} \text{A}'$	$\nu_{\text{X-F}} \text{A}'$ δXO_2
498 s	410 w	400sh 386	-	320 ms	348(25)	320 ms	324(10)	$\delta \text{XO}_2 \text{A}'$	δFXO_2
350 m	345 w	305 (20) 294sh	-	280sh	282(25)	280sh	283(10)	$\delta_{\text{sym}} \text{OXF A}'$	δFXO_2
265 m	320 w	267(15)	-	ca. 250	227(0)? (g)	ca. 250	238 (2)	$\delta_{\text{asym}} \text{OXF A}''$	-

a Reference 113.

b Reference 166.

c

See Chapter IV.

d

Reference 162.

e vs, very strong; s, strong; m, medium; w, weak; vbr, very broad; br, broad; sh, shoulder.

f Numbers in parentheses give relative intensities.

g Intensity too small to be measured.

h References 163 and 164.

i KSeO_2F .

Paetzold and Aurich.

The broad and asymmetric high frequency peak can be resolved into two peaks (see Figure 6.1). It is found to consist of a sharp intense line at 903 cm^{-1} which is assigned to $\nu_{\text{sym}} \text{SeO}_2$ and a broad band centred at 888 cm^{-1} which is assigned to $\nu_{\text{asym}} \text{SeO}_2$. Although $\nu_{\text{sym}} \text{XO}_2$ is generally lower in frequency than $\nu_{\text{asym}} \text{XO}_2$, the reverse is true in a number of related selenium compounds such as $\text{SeO}_2(\text{OH})^-$ (see Table 6.1), SeO_3^{2-} ($\nu_1 = 807 \text{ cm}^{-1}$, $\nu_3 = 737 \text{ cm}^{-1}$) and $\text{SeO}_2\text{-O-SeO}_2^{2-}$ ($\nu_{\text{sym}} \text{SeO}_2 = \sim 855 \text{ cm}^{-1}$, $\nu_{\text{asym}} \text{SeO}_2 = \sim 800 \text{ cm}^{-1}$), and this tends to support the present assignment.

The second main difference between our results and those of Paetzold and Aurich is the assignment of the Se-F stretching mode. They have assigned the 440 cm^{-1} line in their infra-red spectrum to the Se-F stretch, and report that this mode is not observed in the Raman. This is not satisfactory as the Se-F stretch is an A' mode and should certainly be visible in the Raman spectrum. Also, this leaves four Raman peaks whereas only three bending modes remain to be assigned. They, therefore, leave the weak line at 238 cm^{-1} unassigned. In the present work, the broad asymmetric peak centred at 424 cm^{-1} in the Raman spectrum is assigned to the Se-F stretching motion, with the shoulder being attributed to solid state splittings. A very similar asymmetric peak appears in the Raman spectrum of solid BrO_2F (Figure 4.1) and was assigned to the Br-F stretch. In the melt, this peak was found to lose its asymmetry which supports the suggestion that the shoulders on the peak in the

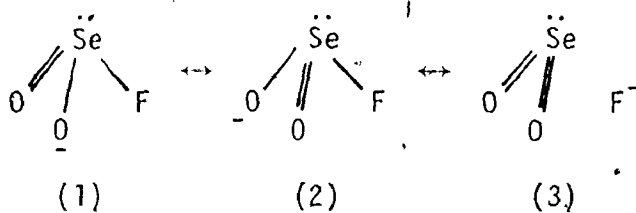
spectrum of the solid are due to solid state effects. Assignment of the Se-F stretch in SeO_2F^- to the complex peak at 424 cm^{-1} leaves three lines in the Raman spectrum which can be assigned to the three bending motions, with the very weak line at 238 cm^{-1} being assigned to the A'' mode

$\epsilon_{\text{asym}}^{\text{OSeF}}$.

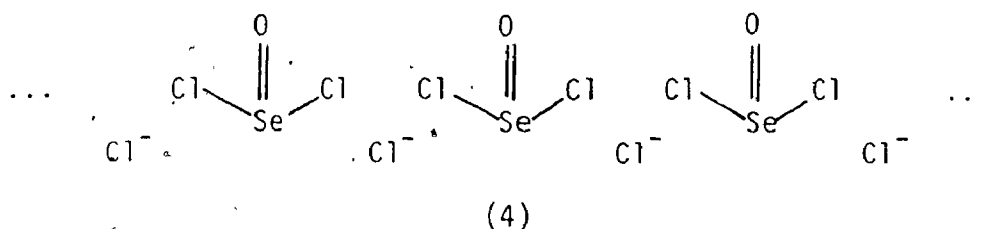
A number of solvents were tried in an attempt to obtain polarization data for SeO_2F^- . KSeO_2F was found to be insoluble in SO_2ClF and CH_3CN and only very slightly soluble in dimethyl sulfoxide. Trifluoroacetic acid, formamide, and IF_5 dissolved substantial quantities of KSeO_2F but produced solutions with rather complicated Raman spectra, indicating that in each case the solvent reacted with some of the SeO_2F^- . Raman spectra of molten KSeO_2F were recorded at $260^\circ\text{--}280^\circ\text{C}$. The melt obtained at these temperatures was very viscous and also appeared to be inhomogeneous since a small amount of white solid was still present in the tube. Higher temperatures (to obtain a more homogeneous mixture) could not be attained. The SeO_2F^- peaks which appeared in the melt spectra were rather broad and no polarization data could be obtained.

The Se-F stretching frequency in SeO_2F^- (424 cm^{-1}) is rather low compared to the mean of the Se-F frequencies of SeOF_3^- (527 cm^{-1})¹⁶⁷ and SeF_5^- (520 cm^{-1})¹⁶⁸; in the analogous sulphur system, the S-F stretching frequencies are comparable in SO_2F^- (593 cm^{-1}) and SF_5^- (587 cm^{-1})¹⁶⁸ indicating that an Se-F frequency of about 520 cm^{-1} could have been expected for SeO_2F^- . Paetzold and Aurich¹⁶² reached a similar conclusion

by examining the variation in the $\nu\text{Se-OCH}_3$ frequency in a series of molecules $\text{CH}_3\text{O-SeO-X}$ as X varies from F to OCH_3 to O^- , and assuming that a similar change in the $\nu\text{Se-F}$ frequency will occur in the series F-SeO-X as X is similarly varied. In this way Paetzold and Aurich estimated an Se-F frequency of approximately 500 cm^{-1} . The observed value of 424 cm^{-1} is thus considerably lower than would be expected. Similarly weak X-F bonds have been found for BrO_2F (see Chapter IV) and ClO_2F ³¹ and have been attributed to large ionic contributions to the X-F bond, and this is consistent with the relatively high XO_2 stretching frequencies found in these molecules. The mean XO_2 stretching frequency in SeO_2F^- (895 cm^{-1}) is relatively high when compared to that in SeO_2 (944 cm^{-1}).¹³³ In the analogous sulphur system the difference between SO_2F^- (1140 cm^{-1})¹¹³ and SO_2 (1256 cm^{-1})¹¹⁴ is considerably larger. The value found in SeO_2F^- (895 cm^{-1}) is also relatively high compared to SeOF_5^- (921 cm^{-1})¹⁶⁹ since the latter is an Se(VI)oxyfluoroanion whereas SeO_2F^- contains Se(IV). There is a much larger change in the SeO frequencies on going from the Se(IV) species SeO_2 (944 cm^{-1}) to the Se(VI) species SeO_2F_2 (1015 cm^{-1}).^{170,171} The relatively high SeO_2 stretching frequencies and the relatively low Se-F stretching frequency found in SeO_2F^- are both consistent with a large contribution from structure (3) in addition to structures (1) and (2)



Paetzold and Aurich have suggested that the low value of the Se-F stretching frequency may be due in part to bridging between the anions in the crystal. The crystal structure of 8-hydroxyquinolinium trichloroselenate,¹⁷² which contains the SeOCl_3^- anion, has revealed chlorine bridging between the anions, with the immediate environment of the Se consisting of an oxygen at 1.59Å, two cis chlorines at 2.2Å and two bridging chlorines at about 3.0Å. The ionic form (4) thus makes a large contribution to the overall structure and can account for the small



difference in the Se=O stretching frequencies of SeOCl_3^- (924 cm^{-1})¹⁶⁷ and the parent molecule SeOCl_2 (949 cm^{-1}).¹⁷³ Weak fluorine bridging between the SeO_2F^- anions may exist in KSeO_2F , but the bridges are certainly not symmetric as in SeOCl_3^- as this would not be consistent with our observed vibrational data. Also, the Se-F vibrational frequency in molten SeO_2F^- (approximately 411 cm^{-1}) is not very different from that in solid KSeO_2F whereas a much larger change would have been expected for a very heavily fluorine bridged structure in the solid.

C. Purity of the KSeO_2F Samples.

Paetzold and Aurich have reported that their KF/SeO_2 melts were

often coloured pink due to the facile reduction of SeO_2 to elemental Se. This was not found to be a problem in the present work. However, when the KF and SeO_2 were not used in exactly equimolar amounts, impurity lines appeared in the Raman spectra of the products. When KF was present in excess, or when SeO_2 sublimed out of a 1:1 = KF: SeO_2 reaction mixture, Raman lines assigned to $\text{K}_2\text{SeO}_2\text{F}_2$ appeared (see Section D). When excess SeO_2 was present, a number of very broad bands appeared in the spectra of the products at approximately 880 cm^{-1} , 655 cm^{-1} , 530 cm^{-1} , 460 cm^{-1} , and 250 cm^{-1} . These lines cannot be assigned to solid SeO_2 however, since the latter has a characteristic strong line at 595 cm^{-1} .¹⁶⁶ Also, no SeO_2 could be extracted from the mixture using benzene as a solvent, in which SeO_2 is soluble.¹²⁷ The lines characteristic of excess SeO_2 could, however, be eliminated by melting the sample with a small amount of KF. These observations suggest that the excess selenium dioxide is not present as free SeO_2 in the solid, and yet is still capable of reacting with KF. Walrafen¹⁶⁶ has reported that in Raman spectra of molten H_2SeO_3 , a number of broad lines ($855, 800, 535, 410, 365, 330, 250\text{ cm}^{-1}$) appear which he has assigned to the $\text{Se}_2\text{O}_5^{2-}$ ion. It is therefore possible that excess SeO_2 reacts with SeO_2F^- according to (6.2) and that the complex anion $\text{Se}_2\text{O}_4\text{F}^-$ is



responsible for the impurity lines in the spectra of KSeO_2F containing excess SeO_2 . Addition of excess KF results in reaction (6.3) and



elimination of the additional lines.

D. Preparation and Raman Spectrum of $K_2SeO_2F_2$

When a slight excess of KF was used in an attempted preparation of $KSeO_2F$, extra lines appeared weakly in the $Se=O$ stretching region (see for example Figure 6.1). As the $KF:KSeO_2F$ ratio was increased, the additional peaks grew in intensity. The intensity of the additional lines could be decreased if the mixture was heated with SeO_2 . These observations are consistent with the following equilibria involving the $SeO_2F_2^{2-}$ ion ((6.4) and (6.5)). The same peaks were also observed when a



sample of $KSeO_2F$ was heated to $180^\circ C$ under vacuum for several days. A white solid sublimed out, and this solid was identified as SeO_2 by its Raman spectrum. It would appear that the other product of the decomposition is $K_2SeO_2F_2$ formed according to the disproportionation



Unfortunately, it was not possible to prepare a pure sample of $K_2SeO_2F_2$. Even when a $KF:SeO_2$ ratio as high as 20:1 was used, the product always contained $KSeO_2F$ as well as $K_2SeO_2F_2$. At high $KF:SeO_2$ ratios however, the mixture did not melt at $300^\circ C$, and this may be partly responsible for the mixture of products obtained. Heating $KSeO_2F$ under

vacuum at temperatures above 200°C also always gave a product containing both KSeO_2F and $\text{K}_2\text{SeO}_2\text{F}_2$. In addition the mixture developed a red colour at these high temperatures indicating that some decomposition, possibly to elemental selenium, had taken place.

The Raman lines associated with $\text{SeO}_2\text{F}_2^{2-}$ are listed in Table 6.2. These lines were obtained from the spectra of a number of different samples, some containing considerable amounts of SeO_2F^- and others containing unknown quantities of decomposition products. The four high frequency lines were always easily distinguishable in these spectra. The lower frequency $\text{SeO}_2\text{F}_2^{2-}$ fundamentals were much more difficult to identify because of the presence of the SeO_2F^- . The four frequencies listed in Table 6.2 were distinguishable in the spectra of all the samples containing large quantities of $\text{SeO}_2\text{F}_2^{2-}$. The possibility that some of these lines may be due to impurity cannot be eliminated however. For this reason, the attribution of these lines to $\text{SeO}_2\text{F}_2^{2-}$ is somewhat uncertain, and the assignments given for these lines are therefore tentative.

The assignments given in Table 6.2 were made on the basis of the C_{2v} structure (5) with the lone pair and the oxygen atoms occupying the equatorial positions of a trigonal bipyramid. A similar structure has been suggested for the related ions XO_2F_2^- ($\text{X} = \text{Cl}, \text{I}, \text{Br}$) (see Chapter III) and $\text{TeO}_2\text{F}_2^{2-}$.¹⁶⁵ The nine fundamentals ($\Gamma = 4\text{A}_1 + \text{A}_2 + 2\text{B}_1 + 2\text{B}_2$) for such a structure are all expected to be Raman active.

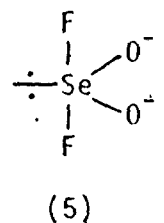


TABLE 6.2

Raman Spectrum of $\text{SeO}_2\text{F}_2^{2-}$ and Some Related Ions (cm^{-1})

$\text{ClO}_2\text{F}_2^{-(a)}$	$\text{BrO}_2\text{F}_2^{-(b)}$	$\text{IO}_2\text{F}_2^{-(c)}$	$\text{TeO}_2\text{F}_2^{2-(d)}$	$\text{SeO}_2\text{F}_2^{2-(e)}$	Assignments and approx. description
1076(100)(f)					
1064	892(7)sh(g)	817 vs	796 vs	868 sh	$\nu_1 \text{XO}_2$ (A_1)
1055	884(100)	804	781	859(100)	
1221 (8)	910 (7)	838 w	758 m	833(25)	$\nu_8 \text{XO}_2$ (B_2)
559(12)	424(14)	360 m	353 mw	823 sh	$\nu_2 \delta \text{XO}_2$ (A_1)
363(100)	380 sh 369(35)	479 s	404 mw 385 sh	396(15)	$\nu_3 \text{XF}_2$ (A_1)
337(80)	307 (9) 293 sh	346 w	326 w	-	$\nu_9 \delta \text{wag}$ (B_2)
-	442 sh	456 vw	315 sh	-	$\nu_6 \text{XF}_2$ (B_1)
337(80)	338 (8)	323 s	279 mw	304(20)	$\nu_7 \delta \text{rock}$ (B_1)
198 (7)	197 (4)	194 vw	197 vw	241(12)	$\nu_4 \delta \text{XF}_2$ (A_1)
480(10)br	400 (2)	-	150(h)	-	$\nu_5 \text{Torsion}$ (A_2)

a Reference 35. b See Chapter III. c References 54 and 55.

d Reference 165: The assignments of ν_4 and ν_9 have been reversed from those given in Reference 165 to be consistent with the assignments for ClO_2F_2^- and IO_2F_2^- .e $\text{K}_2\text{SeO}_2\text{F}_2$. f Numbers in parentheses give relative intensities.

g s, strong; vs, very strong; m, medium; w, weak; sh, shoulder; br, broad;

h Calculated from $\nu_5 + \nu_7$ combination.

The four high frequency lines which are always observed have been assigned to the SeO_2 symmetric and asymmetric stretching modes split by solid state effects. The assignment of the high frequency lines to $\nu_{\text{sym}} \text{SeO}_2$ was made on the basis of the intensity of the lines in this region and is analogous to the assignments for $\text{TeO}_2\text{F}_2^{2-}$. The four other bands which could be attributed to $\text{SeO}_2\text{F}_2^{2-}$ have been assigned by comparison with the related molecules. Several of the fundamentals could not be observed, either due to interference from the Raman lines associated with the SeO_2F^- present in the sample or due to their weakness.

E. Attempted Preparation of the $\text{SO}_2\text{F}_2^{2-}$ Ion.

$\text{M}^+\text{SO}_2\text{F}^-$ salts can be readily prepared from the appropriate metal fluoride and liquid SO_2 .^{97,113,174} These salts dissociate into MF and SO_2 however when heated (100-150°C for KSO_2F ¹⁷⁴), and high temperature reactions can, therefore, not be used to investigate the formation of $\text{SO}_2\text{F}_2^{2-}$. The reaction between $\text{M}^+\text{SO}_2\text{F}^-$ and excess MF ($\text{M} = \text{Cs}^+, \text{N}(\text{CH}_3)_4^+$) has been examined using CH_3CN as a solvent.¹⁷⁵ However, no definitive evidence for $\text{M}_2\text{SO}_2\text{F}_2$ was obtained since hydrolysis of the products occurred while infra-red spectra were being recorded. In the present work, the reaction between CsSO_2F and excess CsF in CH_3CN has been monitored by Raman spectroscopy, and no peaks attributable to $\text{SO}_2\text{F}_2^{2-}$ were observed.

The behaviour of selenium appears to be intermediate between that of sulphur and of tellurium. SO_2F^- is a stable species that appears to show no tendency to form the $\text{SO}_2\text{F}_2^{2-}$ ion. SeO_2F^- is also a stable

species but it will give $\text{SeO}_2\text{F}_2^{2-}$ in the presence of excess fluoride, and it is also slightly disproportionated at high temperature to give SeO_2 and $\text{SeO}_2\text{F}_2^{2-}$. In the case of tellurium, on the other hand, there is no evidence for TeO_2F^- as a stable species but $\text{TeO}_2\text{F}_2^{2-}$ is readily prepared. When equimolar mixtures of TeO_2 and F^- are heated, the product is a mixture of TeO_2 and $\text{TeO}_2\text{F}_2^{2-}$.¹⁶⁵ Thus if TeO_2F^- is formed it is completely disproportionated to TeO_2 and $\text{TeO}_2\text{F}_2^{2-}$.

F. Experimental Section.

(i) KSeO_2F :

KSeO_2F was prepared following the method described by Paetzold and Aurich¹⁶² by mixing SeO_2 and KF in a platinum crucible, which was then placed inside a glass tube under a slow stream of dry nitrogen and heated until a melt was formed. In a typical experiment, 1.59 g (14.3 mmol) of SeO_2 and 0.825 g (14.2 mmol) of KF were used. The white crystalline product which resulted when the melt was allowed to cool was crushed in a mortar in the dry-box and transferred to 1/4" o.d. glass or 6 mm o.d. quartz tubes, and Raman spectra were recorded.

The solubility of KSeO_2F in various solvents was tested by introducing a solvent onto some solid KSeO_2F in a 1/4" o.d. glass tube (SO_2ClF , CH_3CN and IF_5 were distilled in; DMSO , HCONH_2 and $(\text{CF}_3\text{CO})_2\text{O}$ were poured in). The Raman spectrum of the solution was then recorded and compared with that of the pure solvent.

The Raman spectrum of molten KSeO_2F was recorded in a 1/4" o.d. glass tube. The sample was placed in a glass Dewar and a stream of nitrogen, heated by a Nichrome resistance wire, was passed through the Dewar. The temperature was monitored using a copper-constantan thermocouple placed near the sample. The maximum temperature which could be attained was 280°C .

A sample of KSeO_2F , which had been prepared using excess SeO_2 , was placed in a glass double-ampoule (see Chapter III, section F(i)) and benzene was introduced onto the solid. The mixture was shaken overnight, and the solvent was filtered into the empty side of the double-ampoule. The benzene was then distilled back onto the $\text{KSeO}_2\text{F}/\text{SeO}_2$ mixture. No residue was left behind indicating that no SeO_2 had been extracted out of the mixture.

(ii) $\text{K}_2\text{SeO}_2\text{F}_2$

Mixtures containing KF and SeO_2 in mole ratios as high as 20:1 were heated to 300°C in a platinum crucible under a stream of dry nitrogen. After being allowed to cool, the products were crushed in a mortar and introduced into 1/4" o.d. glass tubes to record the Raman spectrum. A sample of KSeO_2F in a glass tube was heated under dynamic vacuum to 180°C overnight, and a white material appeared in a cool section of the tube. The Raman spectra of the sublimed material and of the white involatile residue were both recorded. Another similar experiment was carried out, but a temperature of 230°C was maintained for three days. The involatile residue remaining was coloured red and its Raman spectrum was recorded.

(iii) Attempted Preparation of $\text{SO}_2\text{F}_2^{2-}$

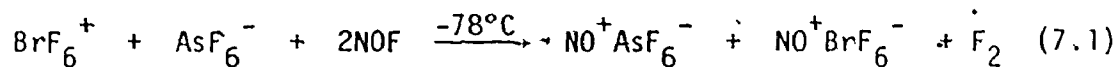
0.423 g (1.95 mmol) of CsSO_2F and 0.487 g (3.18 mmol) of CsF were placed in a 10 mm o.d. ampoule and 1 g of CH_3CN was distilled in. The ampoule was sealed off and the mixture was shaken at room temperature. After three weeks, the Raman spectrum of the solid present in the bottom of the ampoule was recorded and found to be identical to that of CsSO_2F starting material. The Raman spectrum of the CH_3CN solution did not show any peaks other than those due to CH_3CN solvent.

CHAPTER VII

CHARACTERIZATION OF BrO_2F BY ^{19}F N.M.R. SPECTROSCOPY, AND SOME ATTEMPTED PREPARATIONS OF Br(VII) OXYFLUORO SPECIES.

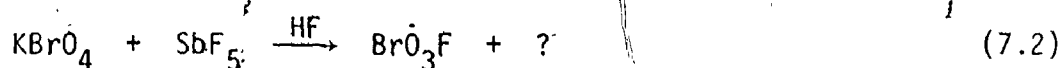
A. Introduction.

Only three species of bromine in the +7 oxidation state have been prepared and characterized. These are the BrO_4^- ion (in several salts,^{84, 176, 177} HBrO_4 ^{84, 178} and in isopropyl perbromate¹⁷⁹), the BrF_6^+ ion (in the $\text{Sb}_2\text{F}_{11}^-$ and AsF_6^- salts) and perbromyl fluoride BrO_3F .¹⁸⁰ BrO_2F_3 has been detected by mass spectrometry as a product of the hydrolysis of BrF_5 ,¹⁰⁹ but has not been isolated or characterized (and was not detected in the hydrolysis of BrF_5 described in Chapter IV). The reaction of BrO_2F with the strong oxidant PtF_6 was originally thought to produce $\text{BrO}_2\text{F}_2^+\text{PtF}_6^-$.¹⁸⁰ The reaction was proposed to be analogous to that by which $\text{ClO}_2\text{F}_2^+\text{PtF}_6^-$ was prepared from ClO_2F and PtF_6 .⁶⁶ However, the vibrational spectrum of the product of the reaction of BrO_2F and PtF_6 indicates that it contains the BrOF_2^+ cation rather than the BrO_2F_2^+ cation. Fogle and Rewick¹ have claimed the preparation of BrF_7 by the reaction of BrF_5 with F_2 at 110°-340°C using a CsF catalyst, but subsequent work² showed that a displacement reaction between $\text{BrF}_6^+\text{AsF}_6^-$ and NOF at low temperature failed to produce BrF_7 , and proceeded according to equation (7.1). In view



of the apparent instability of BrF_7 at -78°C , Fogle and Rewick's claim to have prepared it by a high temperature reaction is rather dubious. Pilipovich and his coworkers¹⁸¹ were unable to obtain BrF_7 from mixtures of BrF_5 and F_2 which they exposed to u.v. radiation for several hours at -40°C to -60°C . They were also unable to prepare BrOF_5 by a similar procedure using mixtures of BrF_5 and O_2 . In both cases, only the unchanged starting materials were recovered.

Alkali metal salts of BrO_4^- are most conveniently prepared by bubbling fluorine gas through an aqueous BrO_3^- solution.⁸⁴ The BrF_6^+ ion is prepared by reaction of BrF_5 with a KrF^+ salt at room temperature.⁷ These preparative methods are oxidations of a Br(V) compound to a Br(VII) compound. On the other hand, BrO_3F is prepared by the fluorination of KBrO_4 with SbF_5 in HF ⁶⁸ (equation(7.2)). The other products of the



reaction were not identified. This reaction is not a redox process but a ligand exchange reaction involving a compound which already contains bromine in the +VII state.

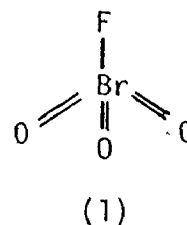
In the present work, both of these types of reactions were employed in attempting to prepare new oxyfluoro compounds of Br(VII) , although the ligand exchange method was more extensively used. The unsuccessful attempt to use KrF_2 to oxidize BrO_2F and BrOF_3 to BrO_2F_3 and BrOF_5 , respectively, has been described in Chapter IV. In this chapter some other reactions (all of which proved incapable of producing new oxyfluorides of Br(VII)) will be described. Also the ^{19}F nmr spectrum of

BrO_3F has been recorded for the first time, and the Raman spectra of solid and liquid BrO_3F and of a solution of BrO_3F in HF have been obtained.

B. Raman and ^{19}F N.M.R. Spectra of BrO_3F .

(i) Raman Spectroscopy.

The vibrational spectrum of gaseous BrO_3F has been studied by Appelman and Claassen.⁶² A pseudo-tetrahedral structure (1) of C_{3v} symmetry is predicted by the VSEPR theory and has been confirmed by electron diffraction studies.¹¹⁸ The six fundamental modes ($\Gamma = 3A_1 + 3E$) are all infra-red and Raman active. Although Appelman and Claassen could readily identify and assign the three stretching vibrations in the infra-red and Raman spectra of gaseous BrO_3F , the frequencies of the bending modes were not unequivocally determined. In the Raman spectrum, the presence of HF and Br_2 impurities largely obscured the low frequency region of the spectrum. In the infra-red spectrum, the bending modes could be observed but this region was complicated by the appearance of rotational fine structure. The lines which were attributed to the bending modes were assigned on the basis of rather poor polarization data and by comparison with the vibrational spectra of ClO_3F and BrO_4^- . Since the identification of the fundamental bending modes and their assignments were not unequivocal, the Raman spectrum of BrO_3F was reinvestigated. Spectra of liquid BrO_3F (Figure 7.1), solid BrO_3F (Figure 7.2) and of a solution of BrO_3F in HF were recorded



and the frequencies obtained from these spectra are listed in Table 7.1.

The Raman spectra of the liquid and the HF solution clearly show the expected six lines. The frequencies and relative intensities of the peaks in the spectra of liquid BrO_3F and of the solution in HF are very similar.

They are also similar to those of gaseous BrO_3F with the exception of ν_2 ($\nu_{\text{Br-F}}$) which appears as a sharp line at 605 cm^{-1} in the gas phase spectrum and as a broad line at 596 cm^{-1} in the spectrum of the liquid

(594 cm^{-1} in HF solution). A similar broadening has been reported for ν_2 of ClO_3F on going from the gas phase spectrum⁶² to the liquid spectrum.¹⁸² Polarization data obtained from spectra of liquid BrO_3F and solutions of BrO_3F in HF clearly showed the lines at 868 cm^{-1} and 596 cm^{-1} (in the liquid spectrum) to be polarized, whereas the line at 971 cm^{-1} is depolarized. These three lines are the three stretching vibrations. The three remaining lines at 378 cm^{-1} , 355 cm^{-1} and 289 cm^{-1} (in the spectrum of the liquid) are, therefore, the three bending modes which have symmetry designations $A_1 + 2E$. The 355 cm^{-1} line was found to have a significantly lower polarization ratio than the other two, suggesting that this line is due to ν_3 (A_1). Further evidence for this is obtained from the Raman spectrum of solid BrO_3F (Figure 7.2). In the low frequency region, doublets are observed at 381 cm^{-1} and 373 cm^{-1} , and at 297 cm^{-1} and 293 cm^{-1} , and this suggests that these pairs of lines are due to E modes where the degeneracy of the two components has been removed in the crystal lattice. The E mode at 971 cm^{-1} in the liquid is also split into a doublet at 979 cm^{-1} and 964 cm^{-1} . The 351 cm^{-1} line is not split however, and this is consistent with its assignment to a fundamental of A_1 .

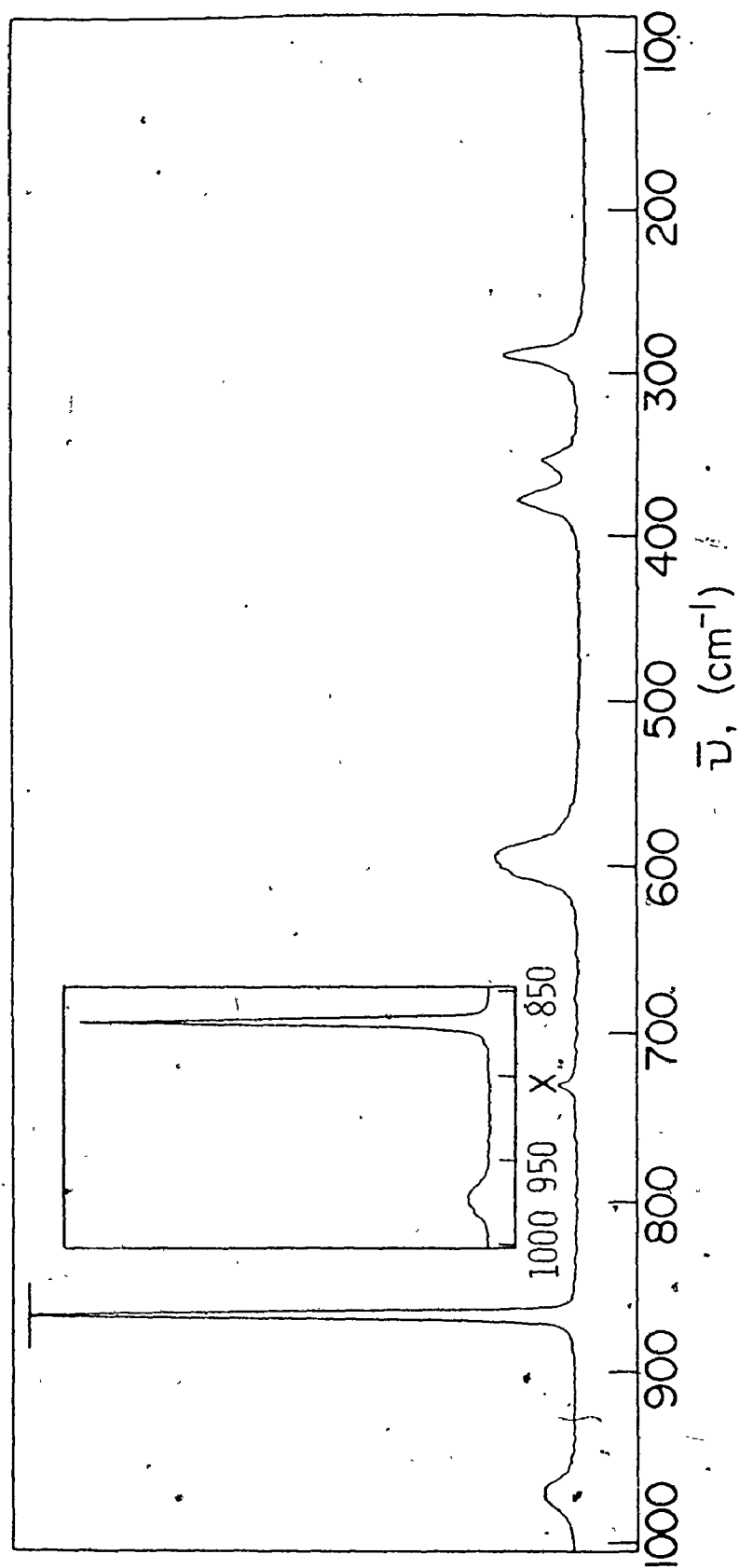


Figure 7.1. Raman spectrum of liquid BrO_3F recorded at -72°C . 'X' denotes a peak due to the FEP container.

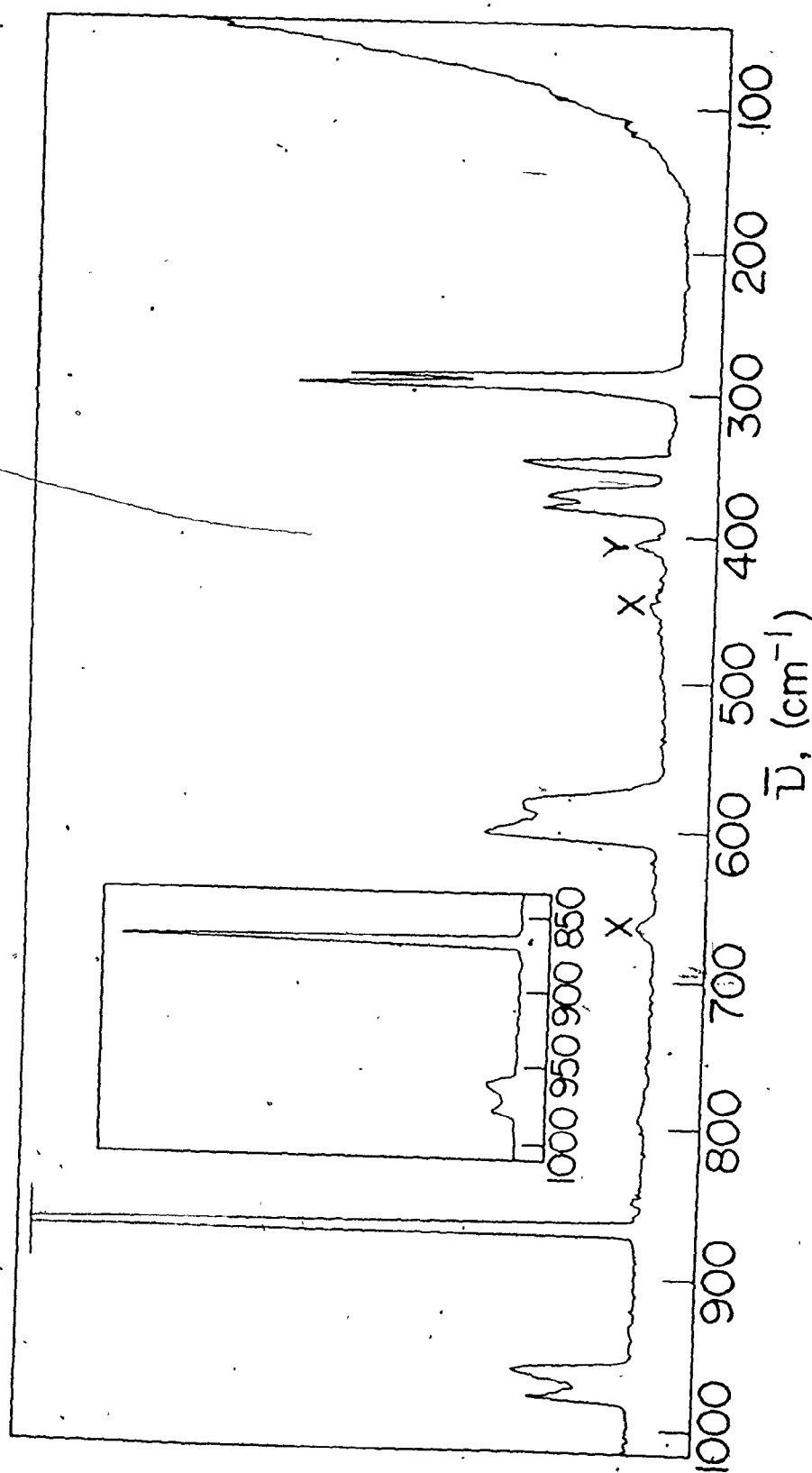


Figure 7.2. Raman spectrum of solid BrO_3F recorded at -196°C . Peaks marked X are due to the XeI-F sample tube and Y is due to an unidentified impurity.

TABLE 7.1

Vibrational Frequencies of BrO_3F (cm^{-1})

i.r.	Gas ^(a)	Liquid	Solution in HF	Solid	Assignments (a) and approximate descriptions.
	Raman	Raman	Raman	Raman	
976.5 v.s	(b) 974 w	971(5) ^(c) dp	976(7)	979 (6) 964 (7)	ν_4 (E) BrO_3 asym. stretch
975.5 v.s	875.2 v.s	868(100) p	871(100).	868(100)	ν_1 (A_1) BrO_3 sym. stretch
606 v.s	605 v.s	596(13) br p	594(14)	602(11) 581 (8) sh 405 (2)	ν_2 (A_1) BrF stretch Impurity
382.0 s	376 ? ^(d) w	378(9) dp	380(12) ^(e)	381-(7) 373 (7)	ν_5 (E) BrO_3 asym. deformation
359.8 m	354 ? ^(d) w	355(6) p	361(10)	351 (9)	ν_3 (A_1) BrO_3 sym. deformation
286 w	296 ? ^(d) v.w	289(13) dp	291(14) ^(e)	297(23) 293(20)	ν_6 (E) Rocking mode

a Reference 62.

b v.s, very strong; s, strong; m, medium; w, weak; v.w, very weak; sh, shoulder.

c Numbers in parentheses give relative intensities.

d ? = the frequencies of these fundamentals were regarded as uncertain due to the presence of impurities.

e These peaks coincide with FEP lines. The intensities shown have been corrected.

symmetry. $\nu_1(A_1)$ appears as a sharp line at 868 cm^{-1} , and $\nu_2(A_1)$ consists of a broad line at 602 cm^{-1} with a second broad component at 581 cm^{-1} . The profiles of the Raman bands in solid BrO_3F are very similar to those found in the spectrum of solid ClO_3F ,¹⁸³ and this further confirms the assignments for BrO_3F . The very weak line at 405 cm^{-1} in Figure 7.2 was absent in other spectra of solid BrO_3F and is therefore assigned to a small amount of an unidentified impurity. The assignments of the bending modes proposed in the present work confirm Appelman and Claassen's assignments.

(ii) ^{19}F N.M.R. Spectroscopy.

The ^{19}F nmr spectrum of liquid BrO_3F was recorded at -80°C and a single broad line at -274 ppm was observed. The linewidth was approximately $70 \pm 5\text{ Hz}$. There was no evidence for any fine structure. A saturated solution of BrO_3F in HF at -80°C was prepared. The solubility of BrO_3F was calculated to be less than $0.8\text{ mole}/1000\text{ g}$ of HF from the weight of KBrO_4 used in the preparation and the amount of HF required to just dissolve the BrO_3F obtained. The accuracy of this solubility determination depends on the efficiency of the conversion of KBrO_4 into BrO_3F and the transfer of BrO_3F into the nmr tube, and on the accuracy of the estimate of the amount of HF added. Reaction (7.2) has been reported to give a 97% yield of BrO_3F .⁶⁸ Also, only a very small peak due to ν_1 of BrO_3F was visible in the Raman spectrum of the $\text{KBrO}_4/\text{SbF}_5/\text{HF}$ reaction mixture after the BrO_3F used for this ^{19}F nmr work had been distilled out. Both of these facts suggest that the solubility of BrO_3F in HF at -78°C is

close to the upper limit (0.8 mole/1000 g of HF) which was calculated.

The ^{19}F nmr spectrum of the solution of BrO_3F in HF at -80°C showed in addition to the solvent peak (at +194 ppm) a weak, broad line at -269 ppm which had a linewidth (at half-height) of 194 ± 10 Hz. Warming the solution to -66°C caused the singlet to broaden slightly to 217 ± 10 Hz. The 94.1 MHz ^{19}F nmr spectrum of a saturated solution of BrO_3F in HF was recorded at $+37^\circ\text{C}$ and the BrO_3F resonance was again observed as a single broad line (linewidth = 710 ± 50 Hz). The brown colour of the sample at this temperature indicated that some decomposition had occurred. No fine structure could be observed.

The difference in chemical shift of liquid BrO_3F and BrO_3F dissolved in HF is substantial. Evans¹⁸⁴ has reported a rather large ^{19}F nmr solvent shift (up to 10 ppm) for a number of fluoro-carbons dissolved in a variety of solvents. In these cases, the solvent shift was too large to be attributed to a change in the bulk diamagnetic susceptibility (for which Evans corrected), and he has suggested that the solvent can influence the magnitude of the paramagnetic contribution to the ^{19}F shift, probably by altering the average energy ΔE between the ground state and the excited states which contribute to the paramagnetic term. Such a change could be brought about by the differences in van der Waals forces or dipolar forces between the fluorine compound and the different solvents. In the case of BrO_3F , the 6 ppm difference in chemical shift between the liquid and the HF solution may be rationalized on a similar basis.

The broadness of the ^{19}F resonance of BrO_3F is attributed to partial

coupling between the fluorine and the central atom bromine. The two naturally occurring isotopes of bromine ^{79}Br (50.57%) and ^{81}Br (49.43%) both have $I = 3/2$ and rather large quadrupole moments ($Q = 0.33$ and 0.28 in units of $e \times 10^{-24} \text{ cm}^2$).¹⁶⁰ The rate of relaxation of a nucleus depends directly on the electric field gradient present at the nucleus and upon the magnitude of the quadrupole moment. If this relaxation is very rapid, coupling is not observed between this nucleus and adjacent nuclei. When an atom with a large quadrupole moment (such as Br) is situated in a molecule in which the ligands do not have an arrangement of cubic symmetry there will, in general, be a large field gradient and hence a very rapid quadrupolar relaxation of the Br nucleus and no coupling will be observed between the Br and the ligands. Examples are BrO_2F , BrOF_2^+ and BrF_5 where sharp ^{19}F nmr lines are observed with no evidence for any coupling between the ^{19}F and Br nuclei. On the other hand, if the bromine is placed in a completely symmetrical environment, the electric field gradient at the central atom will be zero and quadrupolar relaxation will not occur; coupling between the bromine and the ligands may then be observed. The ion BrF_6^+ is an example in which the central atom is octahedrally surrounded by fluorine atoms. Coupling between the bromine and fluorines produces a quartet⁷ (all lines equal intensity) in the ^{19}F nmr spectrum (Two overlapping quartets are actually observed because the two coupling constants $J_{^{79}\text{Br}-\text{F}}$ and $J_{^{81}\text{Br}-\text{F}}$ are slightly different). Some similar cases which have been reported are IF_6^+ ,¹⁵⁹ ClF_6^+ ,¹⁵⁶ and BF_4^- .¹⁴⁶ In these ions, the electric field gradient at the central atom is zero by

symmetry in the free ion, and coupling is observed. In some cases, well resolved coupling can be observed even if the central atom is not completely symmetrically surrounded. In $^{11}\text{BF}_3\text{OH}^-$, coupling between the ^{11}B and ^{19}F is observed¹⁴⁶ despite the fact that the ^{11}B atom is strictly speaking not in a tetrahedral environment. Presumably the similarity between an F and an OH ligand (which means the electric field gradient at B will be small) and the rather small value of the quadrupole for ^{11}B (0.0355 in multiples of $e \times 10^{-24} \text{ cm}^2$) produce a slow rate of relaxation for the ^{11}B nucleus which allows the ^{11}B - ^{19}F coupling to be observed. In other cases however, coupling is not observed even when the central nucleus is in a seemingly symmetric environment. In octahedral $^{102}\text{F}_4^-$ (which is isoelectronic with IF_6^+), no ^{127}I - ^{19}F coupling is observed.²⁶ Presumably the slight difference in the electronegativities of the oxygen and fluorine ligands produces a small electric field gradient at iodine and this combined with the large quadrupole moment (-0.75 in units of $e \times 10^{-24} \text{ cm}^2$) of ^{127}I produces a rapid rate of relaxation for this nucleus.

Intermediate rates of quadrupole relaxation of the central atom (A) will affect the ^{19}F spectrum of the ligands. If the rate of relaxation is relatively slow, then the multiplets caused by the A- ^{19}F coupling will broaden. As the rate of quadrupolar relaxation increases, these multiplets coalesce into broad lines. For very rapid relaxation, the ^{19}F nmr spectrum will show only sharp lines. It is believed that the broad line found for BrO_3F is the result of intermediate rate quadrupolar relaxation of the central atom. The Br in BrO_3F is tetrahedrally surrounded by three

oxygen atoms and one fluorine atom. The small resultant electric field gradient causes the ^{79}Br and ^{81}Br nuclei to undergo relaxation so that the two sets of overlapping quartets expected for BrO_3F are coalesced into a single broad line. The rate of relaxation is not sufficient however to completely eliminate the $\text{Br}-^{19}\text{F}$ coupling since in that case a sharp line would have been observed. Intermolecular exchange of the F^- ligands could also account for the broadness of the ^{19}F resonance, but this is unlikely in view of the relative inertness of BrO_3F (see below). The broadening of the ^{19}F nmr resonance of BrO_3F in HF when the temperature was raised from -80°C to -66°C and then to $+37^\circ\text{C}$ can be explained in terms of a slower rate of quadrupole relaxation at the higher temperatures which causes the $\text{Br}-\text{F}$ coupling to be less collapsed. A similar temperature dependence has been observed in the nmr spectrum of ClO_3F , and this has been discussed in detail by Bacon et al.¹⁸⁵ In general terms, the rate of quadrupolar relaxation for an atom in a rapidly tumbling molecule varies directly with the rotational correlation time τ_c , which can be thought of as the length of time required (on the average) for a molecule to rotate through an angle of a radian.^{160,186} As the temperature is raised, the molecule tumbles more rapidly. The rate of quadrupole relaxation therefore decreases (since τ_c decreases) and a better resolved spectrum is observed. The difference in the linewidths of the BrO_3F resonance at -80°C for the pure liquid and for the HF solution is presumably also attributable to the difference in the value of τ_c since this will depend on the viscosity of the medium.¹⁶⁰

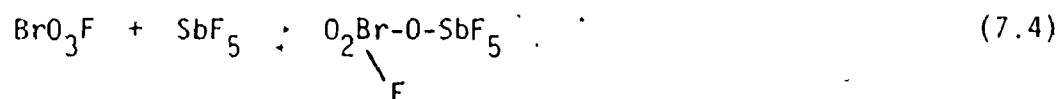
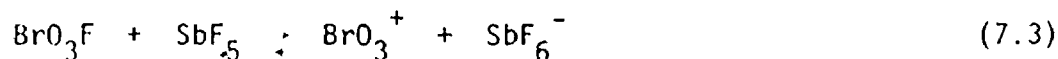
The singlet observed for BrO_3F in HF at $+37^\circ\text{C}$ was rather similar in shape to the ^{19}F nmr resonance observed for ClO_3F at -131°C .¹⁸⁵ This indicates that the rate of quadrupole relaxation in BrO_3F is much more rapid than that in ClO_3F at any given temperature. This can be attributed at least in part to the considerably larger quadrupole moments of both of the bromine isotopes than of the chlorine isotopes ($Q = 0.080$ for ^{35}Cl and 0.062 for ^{37}Cl in units of $e \times 10^{-24} \text{ cm}^2$). There may also be differences in the electric field gradients at the central atoms chlorine and bromine, but the magnitude of these electric field gradients cannot be estimated easily. Comparison with IO_3F is not possible since the latter has been only poorly characterized,⁶⁹ and no ^{19}F nmr data has been reported.

The similarity between the ^{19}F nmr resonances of BrO_3F at $+37^\circ\text{C}$ and ClO_3F at -131°C suggests that a considerable increase in temperature would be required in order to resolve the coupling in BrO_3F . In ClO_3F , the broad singlet at -131°C was found to split into a doublet at -79°C and the expected four lines could only be observed at room temperature.^{185,187} Thus it can be anticipated that an HF solution of BrO_3F would have to be heated above 100°C in order to observe the expected splittings due to Br-F coupling. However, in view of the decomposition which began to occur at $+37^\circ\text{C}$, it is unlikely that a solution of BrO_3F would be of sufficient thermal stability to survive at such a high temperature.

(iii) Reaction of BrO_3F with SbF_5 and AsF_5 .

No evidence was found for any interaction between BrO_3F and the

strong Lewis acids SbF_5 and AsF_5 . The Raman spectrum of a solution of BrO_3F in HF containing excess SbF_5 was recorded at -78°C , and the three stretching frequencies of BrO_3F were observed. These three frequencies were not significantly different from those found for a sample of BrO_3F dissolved in HF in the absence of a Lewis acid. Adduct formation via either (7.3) or (7.4) would have resulted in a shift in the stretching



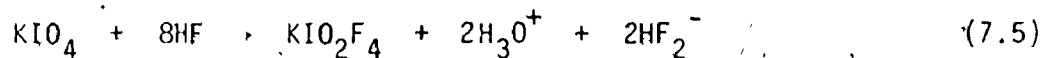
frequencies of the BrO_3F . Equation (7.3) would produce a BrO_3^+ cation with higher $\text{Br}=\text{O}$ stretching frequencies than BrO_3F and no $\text{Br}-\text{F}$ stretching mode would be seen. Formation of an adduct through oxygen would also have changed the BrO region of the spectrum in that two high frequency Raman bands would have been expected for the terminal BrO bonds, whereas one lower frequency peak due to the bridging BrO would have been seen. It can, therefore, be concluded that BrO_3F does not form an adduct with SbF_5 at low temperature in HF solvent. Similarly, the ^{19}F nmr spectrum of an HF solution of BrO_3F containing excess AsF_5 was recorded at -80°C . The peak attributable to BrO_3F was at the same chemical shift as that in a sample of BrO_3F in HF in the absence of AsF_5 . No separate signal in the F on As(V) region was observed and the AsF_5 was therefore undergoing rapid F^- exchange with the HF solvent. Thus no evidence for any interaction between BrO_3F and AsF_5 was obtained. The inertness of BrO_3F towards Lewis

acids is analogous to the lack of complex formation between ClO_3F and the Lewis acids BF_3 , PF_5 , AsF_5 , SbF_5 and SO_3 .²¹

C. Reactions Involving KBrO_4 .

(i) Solution in Hydrofluoric Acid.

When KBrO_4 is dissolved in HF, the Raman spectrum of the solution shows only a single broad peak at 800 cm^{-1} , which is close to the value of ν_1 for BrO_4^- found in the spectrum of the solid (798 cm^{-1}).⁸⁴ The other Raman lines are presumably too weak to be observed. The ^{19}F nmr spectrum of the solution shows only the single strong line due to the HF solvent. These results indicate that KBrO_4 does not react with HF. In this behaviour, BrO_4^- resembles ClO_4^- which is also inert towards HF, but differs from IO_4^- which has been shown to react with HF according to (7.5)¹⁸⁸



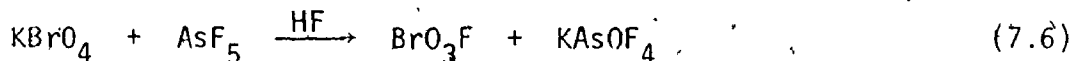
This reaction is attributable to the ease with which iodine can expand its valence shell to achieve octahedral coordination. Bromine does not appear to be capable of doing this readily. In aqueous solution, it has been shown that perbromate is not hydrated⁸⁴ whereas IO_4^- readily forms hydrated species such as H_4IO_6^- .¹⁸⁸ That the Raman frequency observed for a solution of KBrO_4 in HF should be very similar to that of ν_1 of the BrO_4^- ion suggests that this ion is not protonated to give perbromic acid HOBBrO_3 . The possibility that the 800 cm^{-1} peak is actually ν_1 of HOBBrO_3 is made unlikely by the fact that the formal BrO bond order in HOBBrO_3 is higher.

than that in BrO_4^- and that ν_1 of HOBrO_3 should be at a higher frequency than ν_1 of BrO_4^- . This is shown by comparison of the XO symmetric stretching frequency in the related pairs of molecules HSeO_3^- (862 cm^{-1})¹⁸⁹ and SeO_4^{2-} (833 cm^{-1}),¹¹⁴ HOCIO_3 (1031 cm^{-1})¹⁹⁰ and ClO_4^- (928 cm^{-1}).¹¹⁴ Also, in the Raman spectrum of HClO_4 the Cl-OH stretching frequency is more intense than the $\nu_{\text{symmetric ClO}_3}$ stretching mode. In the Raman spectrum of KBrO_4 dissolved in HF, no peak was observed which could be attributed to $\nu_{\text{Br-OH}}$ of HBrO_4 . The results obtained are therefore most consistent with the BrO_4^- ion being mostly-unprotonated in anhydrous HF. This is a rather surprising result since the value of the Hammett acidity function H_0 for HF containing 0.05% H_2O has been recently determined to be -10.8 ¹⁹¹ (although previously determined values of -10.2 ¹⁹² and -10.4 ¹⁹³ indicate a slightly lower acidity) and has been estimated to be -15.1 for HF in the absence of any water impurity.¹⁹¹ Thus anhydrous HF is, strictly speaking, a stronger acid than 100% H_2SO_4 ($H_0 = -11.93$)¹⁹⁴ but since the last traces of H_2O are virtually impossible to remove from the HF, the acidity of experimentally available HF is slightly lower than that of H_2SO_4 . It has been shown¹⁹⁵ that ClO_4^- is extensively (or perhaps even completely) protonated to HClO_4 in 100% H_2SO_4 . It would, therefore, have been expected that BrO_4^- , which might be expected to be a stronger base than ClO_4^- , would be protonated to HBrO_3 in HF. However, the acidity of the HF used in this work may have been considerably lower than that of the extensively purified HF used in the H_0 value determinations due to the presence of H_2O . This may in part be responsible for the rather surprising result found in the present work.

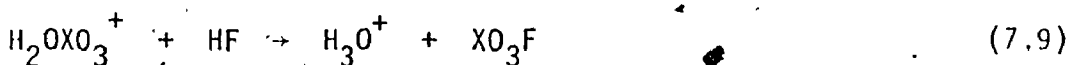
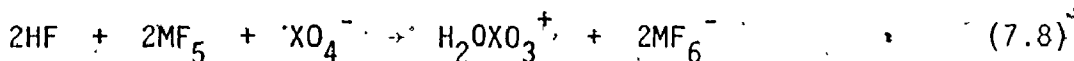
(ii) Reactions with some Fluorinating Agents.

The reactions of various fluorinating agents with KBrO_4 were investigated:

(a) AsF_5 : Appelman and Studier have shown that KBrO_4 can be fluorinated by SbF_5 to give BrO_3F (equation (7.2)). In the present work, it was found that AsF_5 will also fluorinate KBrO_4 using HF as a solvent. The BrO_3F produced was identified by its ^{19}F nmr spectrum. The Raman spectrum of the white solid which remained after the HF, BrO_3F and excess AsF_5 were removed under vacuum from the reaction vessel showed only lines attributable to the AsF_6^- anion. The reaction is therefore not simply (7.6) since the Raman spectrum of KAsOF_4 has been reported ¹⁹⁶ and was



not observed in our work. AsOF_3 was not a product of the reaction either since its Raman spectrum ¹⁹⁷ was not observed. An alternative explanation may be put forward if a mechanism analogous to the one proposed for the formation of ClO_3F from ClO_4^- in superacid media ²¹ is assumed. This mechanism involves the participation of the protonated acid H_2OXO_3^+ ($\text{X} = \text{Cl}, \text{Br}$) produced by reaction (7.8) where MF_5 is a Lewis acid such as AsF_5 or SbF_5 . This is followed by reaction of this cation with HF (7.9).



The overall reaction is therefore (7.10). Invoking the involvement of

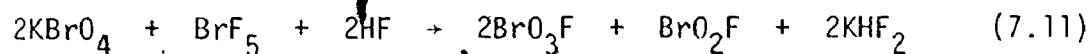


protonated HBrO_4 in this reaction scheme is not inconsistent with the fact that BrO_4^- does not appear to be protonated in pure HF since MF_5/HF mixtures have been shown to be very much more acidic than pure HF ($H_0 = -21.1$ for a 0.6 mole % solution of SbF_5 in HF ¹⁹¹). Reaction (7.9) would most likely be a nucleophilic displacement of H_2O by HF rather than cleavage of the H_2OXO_3^+ ion into H_2O and XO_3^+ , followed by reaction of XO_3^+ with HF. Involvement of ClO_3^+ in the reaction of ClO_4^- has been rejected as being unlikely because of the lack of complex formation between ClO_3F and various Lewis acids, ²¹ and the same argument can be applied to BrO_3F (see above). In the case of the reaction of BrO_4^- with AsF_5 , removal of the volatile components BrO_3F , HF and excess AsF_5 would leave a 1:1 mixture of KAsF_6 and $\text{H}_3\text{O}^+\text{AsF}_6^-$ ¹⁹⁸ (which has been shown to be stable at room temperature). Both of these products would display only Raman lines characteristic of the AsF_6^- anion as observed. (The H_3O^+ lines cannot be observed in the Raman spectrum of solid $\text{H}_3\text{O}^+\text{AsF}_6^-$ because of their broadness and low intensity ¹⁹⁸). If the $\text{H}_3\text{O}^+\text{AsF}_6^-$ decomposed for some reason during the reaction or as the HF solvent was being removed, the decomposition products ($\text{H}_2\text{O} + \text{HF} + \text{AsF}_5$) would also be volatile and would not affect the Raman spectrum of the solid residue. Thus, although the exact equation for the reaction cannot be written (since the presence of $\text{H}_3\text{O}^+\text{AsF}_6^-$ is uncertain), the data obtained can be rationalized. The fact that no Raman lines due to KBrO_4 were observed in the Raman spectrum

of the residue suggests that the reaction goes to completion (which was also observed when SbF_5 was used as a fluorinating agent⁶⁸).

(b) BrF_5 : The reaction between KBrO_4 and BrF_5 has also been examined. KBrO_4 and excess BrF_5 were mixed at room temperature and the solid KBrO_4 did not dissolve to any significant extent. After the reaction mixture had stood for 30 minutes at room temperature, ^{19}F nmr and Raman spectra of the liquid BrF_5 layer failed to show the presence of any oxygen-containing Br(VII) species in solution. Thus the direct reaction between KBrO_4 and BrF_5 is at least rather slow (and may not occur at all). A small amount of HF was introduced into the mixture, since in the $\text{KBrO}_3/\text{BrF}_5$ system, this was found to be a catalyst for this reaction (see Chapter III). After 1 1/2 hours at room temperature, still no reaction could be detected based on the Raman and ^{19}F nmr spectra of the BrF_5 solvent. Removal of the volatile materials under vacuum left a white solid whose Raman spectrum was identical with that of KBrO_4 .⁸⁴ That apparently no reaction occurs between KBrO_4 and BrF_5 is surprising in view of the fact that BrF_5 is a fairly powerful fluorinating agent. The lack of reaction is probably due to the insolubility of KBrO_4 in BrF_5 (and in BrF_5 containing some HF). Indeed, KBrO_4 and BrF_5 react readily in the presence of HF as a solvent (in which both KBrO_4 and BrF_5 are soluble). When KBrO_4 and excess BrF_5 were combined with a large excess of HF, all the solid present dissolved at -48°C . The Raman spectrum of the solution showed lines attributable to BrF_5 ,¹²⁶ and BrO_3F and a line at 916 cm^{-1} which could be attributed to BrO_2F (see Chapter IV). The other Raman lines

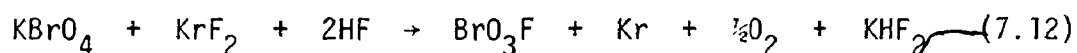
expected for BrO_2F were too weak to be observed. No BrOF_3 was present in the sample since its characteristic $\text{Br}=\text{O}$ stretching frequency was not observed. The ^{19}F nmr spectrum of the solution showed the AX_4 pattern of BrF_5 in addition to the HF solvent line. Careful examination of the quintet of BrF_5 ($\delta = -270$ ppm) showed that the quintet was skewed and suggested that a weak broad line (assigned to BrO_3F) was present at roughly the same chemical shift as the quintet of BrF_5 . No separate signal could be observed for BrO_2F since this has been shown, in Chapter IV, to undergo rapid fluorine exchange with HF at low temperature. The reaction can therefore be written as (7.11). As was the case in the reaction of



BrF_5 with the iodine (V) oxides and oxyfluorides, any BrOF_3 produced as an intermediate in (7.11) must be removed by rapid reaction with KBrO_4 to account for the production of BrO_2F and the absence of BrOF_3 as a product. When the volatile components of the reaction mixture were removed under vacuum, a white solid was obtained which was identified as KHF_2 from its Raman spectrum. Since no lines attributable to KBrO_4 were observed in the Raman spectra of the HF solution reaction mixture or in the solid residue obtained, (7.11) must go to completion at -48°C . In another $\text{KBrO}_4/\text{BrF}_5/\text{HF}$ experiment, the mixture of BrO_3F , BrF_5 and BrO_2F was allowed to warm up to room temperature and the Raman spectrum of the solution was used to detect changes in the sample. After 1 1/2 hours, the $\text{BrO}_3\text{F}:\text{BrF}_5$ ratio had not changed, but the BrO_2F signal had become weaker (probably due to

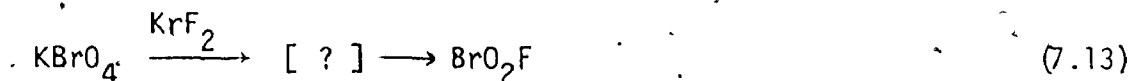
thermal decomposition, see Chapter IV). Thus BrO_3F is apparently not fluorinated by BrF_5 at room temperature.

(c) KrF_2 : The reaction of KBrO_4 with KrF_2 was investigated. In Chapter IV it was shown that KrF_2 fluorinates BrO_2F to BrOF_3 and BrOF_3 to BrF_5 . It was therefore thought that reaction (7.12) might occur. The

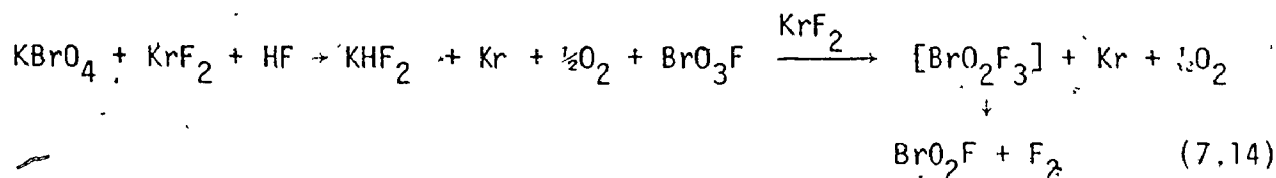


results obtained were ambiguous however, but show that (7.12) does not occur. A mixture of KrF_2 and KBrO_4 (mole ratio 1.40:1) in HF was allowed to react at a temperature slightly higher than -78°C for a few minutes. The Raman spectrum of the solution showed large peaks attributable to KrF_2 and BrO_4^- , along with a rather weak peak at 916 cm^{-1} which could be assigned to BrO_2F . The sample was allowed to warm up slowly to room temperature to dissolve all the solid present. Bubbles of gas were formed as the sample warmed up, indicating that a reaction was taking place. After ten minutes at room temperature, all the solid in the tube had dissolved. The Raman spectrum of the solution showed that the sample consisted mainly of BrO_2F . A weak peak due to unreacted KBrO_4 was also present, along with three very weak lines which could be assigned to BrF_5 (presumably formed by reaction of BrO_2F with KrF_2 [see Chapter IV]). There was no KrF_2 or BrO_3F present in the product. That BrO_2F is the major product is rather surprising since this represents a reduction of Br (VII) to Br (V) in the presence of the strong oxidant KrF_2 . The only reasonable explanation for this is that the BrO_4^- was fluorinated to an unstable oxy-fluoro compound of Br (VII) by KrF_2 , and that this unstable species

decomposes to BrO_2F , (equation (7.13)). It is possible that the unstable



species is BrO_2F_3 (equation (7.14)) which could conceivably lose F_2



to produce BrO_2F . This reaction would explain the presence of the unreacted KBrO_4 (since less than a 2:1 ratio of KrF_2 to KBrO_4 was used).

The reaction was repeated and this time the mixture was allowed to remain at low temperature for an extended period of time to see if any BrO_3F or the unstable species responsible for the appearance of BrO_2F could be detected. A mixture of KBrO_4 and KrF_2 (mole ratio 1.21:1) in HF was allowed to stand at -78°C for two hours. A large amount of solid was present in the bottom of the tube, and no effort was made to dissolve this solid by warming the sample. The Raman spectra of the solid and of the solution consisted only of lines attributable to KBrO_4 and KrF_2 . No BrO_2F was observed. Since both BrO_4^- and KrF_2 were present in solution but no products were formed, the reaction must be slow at low temperature, (i.e. the slowness of the reaction was not due to the insolubility of one of reagents). The reaction mixture was warmed to -72°C for twelve hours. Raman spectra indicated that the major components of the mixture were still KBrO_4 and KrF_2 , but very weak lines attributable to BrO_2F were observed. After a further 24 hours at -72°C , the amount of BrO_2F present

had increased but was still rather small. Warming the sample to -63°C caused bubbling to occur and after 2 1/2 hours the amount of BrO_2F had again increased. Leaving the sample at -63°C for 18 hours and then warming it to -48°C for 4 hours each caused an increase in the amount of BrO_2F present. In order to attempt to observe the product distribution at the end of the reaction, the tube was warmed quickly to room temperature to allow the reaction to go to completion. As the mixture was warming up however, it detonated violently and ruptured the tube. The reason for the explosion is not clear in view of the fact that the previous time this reaction was done, the mixture warmed smoothly up to room temperature. The more rapid rate of warming in the second case may have been a factor in promoting the explosion. Since the product mixture present after completion of the reaction could not be observed, no further information could be obtained about the stoichiometry of the reaction. It was, however, established that KBrO_4 and KrF_2 react rather slowly at low temperature, and that the only observable product of the reaction is BrO_2F . No Raman lines due to BrO_3F or any other oxygen containing bromine species were observed. This would mean that if (7.14) represents the process that is occurring, the reaction of BrO_3F with KrF_2 and the decomposition of BrO_2F_3 would have to be very rapid even at -72°C in order to account for the BrO_2F produced at this temperature. The reaction of BrO_3F with KrF_2 was therefore examined. Approximately equimolar amounts of BrO_3F and KrF_2 were allowed to react (using HF as a solvent) for 20 hours at -78°C , and then for 20 hours at -72°C . Raman spectra of the solution present showed the

presence of BrO_3F and KrF_2 in solution, but there was no sign of BrO_2F or any other changes in the Raman spectra that would suggest that a reaction had occurred. The mixture was warmed to -63°C for 4 hours, then -48°C for 8 hours and then -22°C for 4 hours. The Raman spectra recorded during this procedure again showed mainly KrF_2 and BrO_3F , and rather weak lines due to BrF_5 became visible. The sample was allowed to stand at room temperature for 45 minutes and then cooled back down to -78°C . The Raman spectra of the mixture again indicated that no significant change had taken place in the sample, with the exception of a slight increase in the amount of BrF_5 present. The ^{19}F nmr spectrum of the solution at -20°C (the lowest temperature at which no precipitate was present) showed single peaks at +197 ppm due to HF , -52 ppm due to KrF_2 , a doublet at -133 ppm due to BrF_5 and a broad line at -270 ppm representing BrO_3F and the quintet resonance due to BrF_5 . Integration of the signals showed the molar ratios to be $\text{KrF}_2:\text{BrO}_3\text{F}:\text{BrF}_5 = 13:11:1$. This is in agreement with the approximately equimolar amounts of BrO_3F and KrF_2 used. The BrF_5 produced probably arises from the partial thermal decomposition of BrO_3F to Br_2 ⁶² followed by fluorination to BrF_5 by KrF_2 . The apparent inertness of BrO_3F towards KrF_2 is consistent with its inertness towards BrF_5 , AsF_5 and SbF_5 and eliminates equation (7.14) as a possible explanation of the $\text{KBrO}_4/\text{KrF}_2$ reaction, since the rapid reaction between BrO_3F and KrF_2 which is required by (7.14) does not occur. The $\text{KBrO}_4/\text{KrF}_2$ reaction was not investigated further since even at the lowest temperatures used, no evidence could be found as to the identity of the unstable intermediate which is presumed to

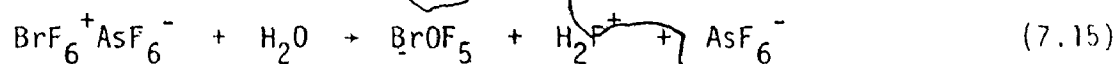
be decomposing to BrO_2F . A low temperature matrix isolation experiment may be useful to trap unstable intermediates in the reaction but this was beyond the scope of the present work.

D. Reactions Involving $\text{BrF}_6^+\text{AsF}_6^-$.

$\text{BrF}_6^+\text{AsF}_6^-$ can be conveniently synthesized from the reaction of BrF_5 with $\text{KrF}^+\text{AsF}_6^-$.⁷ $\text{BrF}_6^+\text{Sb}_2\text{F}_{11}^-$ was not used in this work since this is always formed with $\text{BrF}_4^+\text{Sb}_2\text{F}_{11}^-$ as an impurity, and the presence of BrF_4^+ would substantially complicate the reactions and product mixtures formed.

(i) Hydrolysis.

The hydrolysis of BrF_6^+ was examined as a possible method of preparing BrOF_5 (equation (7.15)). Although in theory $\text{BrOF}_4^+\text{AsF}_6^-$ could be



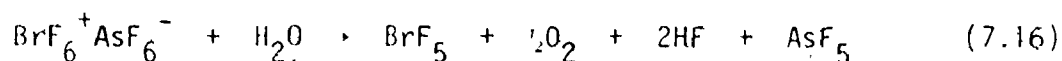
formed, the fact that IOF_5 has been shown to form oxygen bridged adducts with the Lewis acids rather than ionic salts containing the IOF_4^+ cation suggests that BrOF_4^+ is unlikely to be stable and would abstract a fluoride ion from the solvent to form BrOF_5 .

When $\text{BrF}_6^+\text{AsF}_6^-$ and an equimolar amount of H_2O were allowed to react at -72°C using HF as a solvent, bubbles of gas were formed. After 2 hours at -72°C , all the solid $\text{BrF}_6^+\text{AsF}_6^-$ had dissolved and the bubbling had ceased. The Raman spectrum of the solution was recorded. The strongest lines in the spectrum could be unequivocally assigned to BrF_5 , and nothing appeared in the BrO stretching region. A weak peak appeared which could

be assigned to a small amount of KrF_2 (this was the starting material for the preparation of $\text{KrF}^+\text{AsF}_6^-$ and may not have completely reacted). The region from 1770 cm^{-1} to 1900 cm^{-1} was examined but no peak appeared which could be attributed to O_2^+ (1858 cm^{-1} in solid $\text{O}_2^+\text{AsF}_6^-$ ¹⁹⁹). The ^{19}F nmr spectrum of the solution recorded at the freezing point of the solution (approximately -80°C) showed, in addition to a strong singlet at $+194\text{ ppm}$ due to HF , a doublet at -131 ppm ($J = 77 \pm 5\text{ Hz}$) and a broad line at -268 ppm which were assigned to BrF_5 ($\delta = -132$ and -270 ppm ¹⁰⁷ and $J_{\text{FF}} = 76\text{ Hz}$ ¹⁰⁰). The intensity of the broad line at -268 ppm was too small to allow the expected quintet splitting pattern to be observed. In addition, a broad, weak line at $\sim +68\text{ ppm}$ was observed and this was assigned to the F on As of AsF_6^- ($\delta = 58.4\text{ ppm}$)¹²¹ and/or AsF_5 ($\delta = 65.2\text{ ppm}$)¹²¹ undergoing slow F^- exchange with the HF solvent to account for the slightly higher than expected chemical shift. No other peaks which could be attributed to BrOF_5 were observed.

The spectroscopic data suggests that the hydrolysis of $\text{BrF}_6^+\text{AsF}_6^-$ does not proceed according to (7.15) but that BrF_5 is the major product. The bubbling of the solution during the reaction and the failure to observe the characteristic O_2^+ line in the Raman spectrum of the solution suggest that O_2 and not O_2^+ is a product. This is further supported by the fact that removal of the volatile components under vacuum did not produce any solid residue, whereas had O_2^+ been present the white salt $\text{O}_2^+\text{AsF}_6^-$ would have been left behind. Thus, although BrF_6^+ will oxidize O_2 to O_2^+ at room temperature,⁷ this process apparently does not take

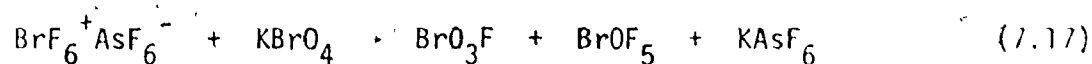
place at low temperature in HF solution. The exact nature of the fluoro-arsenic species present could not be determined by ^{19}F nmr or Raman spectroscopy. The single line observed at $\delta = +68$ ppm in the ^{19}F nmr spectrum was interpreted in terms of fluoride exchange between the fluoro-arsenic species and the HF solvent. In the Raman spectra, ν_1 of AsF_6^- (685 cm^{-1}) would have been coincident with the broad line assigned to ν_1 of BrF_5 (680 cm^{-1}) whereas ν_1 of AsF_5 (733 cm^{-1}) would have been coincident with the very strong line due to the FEP tube (733 cm^{-1}). The equation for the reaction can be written as (7.16). Although Dean et al.¹³⁹ have



shown that dilute solutions of AsF_5 in HF are largely ionized to $\text{As}_2\text{F}_{11}^-$ and H_2F^+ , no Raman lines due to $\text{As}_2\text{F}_{11}^-$ ^{132,137,138} were observed in this work. It is possible that at the higher concentrations used in this work, the extent of ionization of the AsF_5 is rather small and the main fluoro-arsenic species present is AsF_5 (which would not be directly observable due to interference from the FEP tube). The amount of $\text{As}_2\text{F}_{11}^-$ present would then be too small to be detectable in the Raman spectrum.

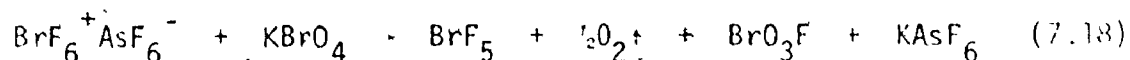
(ii) KBrO_4

The reaction of $\text{BrF}_6^+ \text{AsF}_6^-$ with KBrO_4 was investigated as a possible means of making BrOF_5 according to equation (7.17). $\text{BrF}_6^+ \text{AsF}_6^-$ and

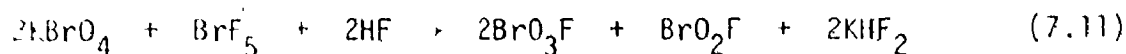


an approximately equimolar amount of KBrO_4 were placed in an FEP nmr tube

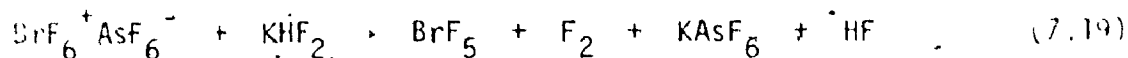
and HF distilled in as a solvent. The tube was warmed to -72°C for 40 minutes and bubbles of gas were formed in the mixture. The sample consisted of a clear solution with a white solid lying under it. Raman spectra were recorded for both the solution and the solid. The species present in solution were identified as BrO_3F and BrF_5 with a small amount of BrO_2F . The solid on the other hand consisted of mainly KAsF_6 and BrO_2F . The characteristic stretching frequency of the O_2^+ cation was not observed. These observations suggest that the reaction does not proceed according to (7.17) but rather that (7.18) is the primary reaction. The formation



of gas bubbles in the reaction mixture is due to the O_2 being evolved. The presence of BrO_2F as a product can be rationalized by a secondary reaction of BrF_5 with KBrO_4 (equation (7.11)). The KHF_2 produced by this reaction



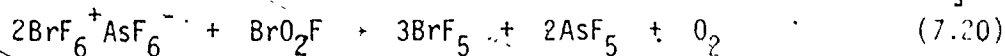
would also react with BrF_6^+ according to (7.19). Thus some of the gas



evolved may have been F_2 rather than O_2 . As was mentioned, no O_2^+ was observed and, as in the case of the hydrolysis of BrF_6^+ , it must be concluded that BrF_6^+ is incapable of oxidizing O_2 at low temperature in HF solution. The ^{19}F nmr spectrum of the reaction mixture was recorded at -79°C . In addition to the strong HF solvent line at +193 ppm, two other

signals were observed; a doublet at -132 ppm and a broad line at -269 ppm. The doublet is assigned to the X_4 portion of the AX_4 pattern of BrF_5 , whereas the broad peak at -269 ppm is assigned to a superposition of the broad BrO_3F signal and the quintet of BrF_5 . Integration of the -132 and -269 ppm signals showed their relative intensities to be approximately 2:1. From this, the relative mole ratios of BrF_5 and BrO_3F can be calculated to be approximately equal, which is in agreement with equation (7.18). If reactions (7.11) followed by (7.19) occur, this would increase the relative amount of BrO_3F since two moles of BrO_3F are produced for every mole of BrF_5 generated. It must be assumed that these reactions do not proceed to a sufficient extent to noticeably alter the 1:1 $BrO_3F:BrF_5$ ratio expected on the basis of equation (7.18). In view of the rather poor accuracy of the integration of the spectrum (at best $\pm 10\%$, see Chapter II), substantial contributions from equations (7.11) and (7.19) could go undetected. Any BrO_2F or AsF_6^- present in solution must be undergoing rapid fluoride exchange with the HF solvent as no separate signals are seen for these species. The sample was warmed briefly to room temperature and then cooled to $-40^\circ C$. Raman spectra of the solid and solution present were identical to those recorded after the mixture had been warmed only to $-72^\circ C$. The reaction was, therefore, complete after 40 minutes at $-72^\circ C$. The volatile components of the mixture were removed under vacuum and a white solid remained. The Raman spectrum of this white solid consisted of lines attributable to $KAsF_6$. No lines due to $KBrO_4$ or $BrF_6^+AsF_6^-$ were observed, indicating that both were completely consumed in the reaction.

Since the $\text{BrF}_6^+ \text{AsF}_6^-$ was apparently present in slight excess some of it must have been consumed by reactions other than (7.18) and (7.19). A possible reaction is (7.20) between BrF_6^+ and BrO_2F . This would be in



agreement with the behaviour of BrO_2F towards KrF_2 . Alternatively, warming the sample to room temperature may have caused some decomposition of BrO_3F or BrO_2F (or both) to Br_2 which would be rapidly fluorinated by BrF_6^+ , and this could also account for the lack of $\text{BrF}_6^+ \text{AsF}_6^-$ in the residue. However, the presence of an excess of $\text{BrF}_6^+ \text{AsF}_6^-$ is not definitive due to the uncertainties in the weighings, and these suggestions about possible side reactions must be regarded as rather speculative. If in fact KBrO_4 was the reagent present in slight excess, then the failure to observe KBrO_4 in the solid residue of the reaction is readily explained since the excess will be entirely consumed by reaction (7.11).

(iii) BrO_3F

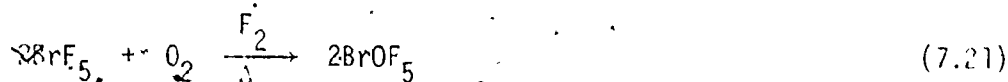
The reactivity of BrO_3F towards BrF_6^+ has been tested. $\text{BrF}_6^+ \text{AsF}_6^-$ and BrO_3F were allowed to interact in the presence of HF as a solvent (and some BrF_5 impurity was present also). The reaction was monitored by Raman spectroscopy on the solution and on the solid present at low temperature. After 45 minutes at -72°C and 20 minutes at -62°C , no reaction had occurred and the solution contained BrO_3F and BrF_5 whereas the solid consisted of $\text{BrF}_6^+ \text{AsF}_6^-$. The tube was allowed to warm up to room temperature for 15 minutes. All the solid dissolved to give a clear, colourless solution.

Cooling the sample back down to -80°C caused a large amount of precipitate to be formed. The solid was identified as $\text{BrF}_6^+ \text{AsF}_6^-$ whereas the solution was still found to contain only BrO_3F and BrF_5 . Only Raman lines attributable to these three species were observed. However, the Raman spectrum of the sample did exhibit fluorescence which indicates that at room temperature a reaction occurs which produces a small amount of a fluorescent product. The exact nature of this material was not investigated further. It can be concluded that BrO_3F does not react rapidly with BrF_6^+ even at room temperature.

E. Miscellaneous Reactions.

(i) Attempted Preparation of BrOF_5 .

An attempt was made to prepare BrOF_5 by a high pressure reaction. A mixture of BrF_5 and a stoichiometric amount of O_2 required for equation (7.21) were placed in a Monel bomb along with a large excess of F_2 gas to give a total pressure of approximately 1400 psi at room temperature. The



mixture was heated to 175°C for several days. After removal of the non-condensable gases at -196°C , the contents of the bomb were distilled into a Kel-F trap, and some of the material was transferred to an FEP nmr tube. The ^{19}F nmr spectrum of this material showed only lines attributable to BrF_5 , indicating that reaction (7.21) had not occurred.

(ii) Reaction of BrO_3F and KrF^+

The reaction of BrO_3F with the very powerful fluorinating agent KrF^+ was also briefly studied using HF as a solvent. To an approximately equimolar mixture of BrO_3F and KrF_2 was added an excess of AsF_5 . The mixture was kept at -72°C for approximately 72 hours. A large amount of white solid was present in the bottom of the tube and Raman spectroscopy showed this solid to be mostly $\text{KrF}^+\text{AsF}_6^-$ with some unreacted KrF_2 in it. The ν_1 stretching mode of BrO_3F was also visible due to the presence of some of the HF solution intermingled with the solid. No extra lines were observed in the Br-O stretching region and it was concluded that no reaction had occurred. When the sample was allowed to warm up to room temperature, vigorous gas evolution began to take place and the solution rapidly turned brown. The reaction was immediately quenched by cooling the sample to -196°C . The frozen sample was then warmed to -72°C . This produced a brown solution standing over a solid. The Raman spectrum of the solid indicated that some $\text{KrF}^+\text{AsF}_6^-$ was still present but the main lines could now be attributed to $\text{O}_2^+\text{AsF}_6^-$. The spectrum of the solution showed that BrO_3F was also still present but that BrF_5 had been produced. BrO_3F therefore does react with KrF^+ at room temperature, but decomposition occurs. The BrF_5 produced probably arises as a result of fluorination of the Br_2 produced by the decomposition (since the solution was brown). A number of other weak Raman lines were observed which are presumably due to decomposition products which were not identified. No lines were observed in the Br-O region of the spectrum however. This indicates that if

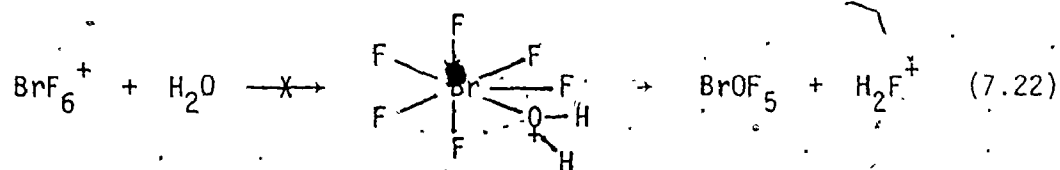
BrO_2F_2^+ or BrO_2F_3 were produced in the reaction, these species were at least in part responsible for the decomposition which was seen to occur.

F. Discussion.

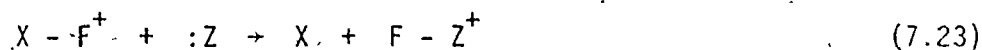
The perbromate ion has been found to be readily fluorinated to BrO_3F by a number of fluorinating agents such as AsF_5 , BrF_5 , BrF_6^+ and presumably BrOF_3 . BrO_3F is stable with respect to these fluorinating agents and KrF_2 also, and this relative inertness is analogous to the remarkable stability and inertness of ClO_3F . For ClO_3F , this has been attributed to the favourable pseudotetrahedral geometry of the molecule and its strong covalent Cl-F bond.²¹ These arguments presumably apply to BrO_3F as well. BrO_3F is attacked by the extremely strong fluorinating agent KrF^+ however, but only the decomposition products O_2^+ , BrF_5 and Br_2 could be detected. No evidence could be found for the production of BrO_2F_3 or BrO_2F_2^+ which might have been expected as products. Similarly, the reaction of KBrO_4 with KrF_2 is apparently anomalous since although the reaction proceeds smoothly at low temperature, only BrO_2F can be observed as a product. The most reasonable explanation involves the production of an unstable intermediate which is decomposing to BrO_2F . No information as to the nature of this intermediate could be obtained.

The reaction of the BrF_6^+ ion with potential oxygen donors such as H_2O and BrO_4^- failed to give BrOF_5 as a product. Instead BrF_5 was formed. This may be due largely to the inability of Br(VII) to accommodate seven ligands around it. Evidence for this comes from the apparent instability

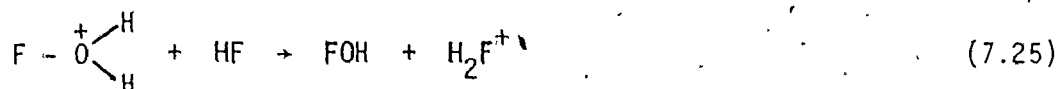
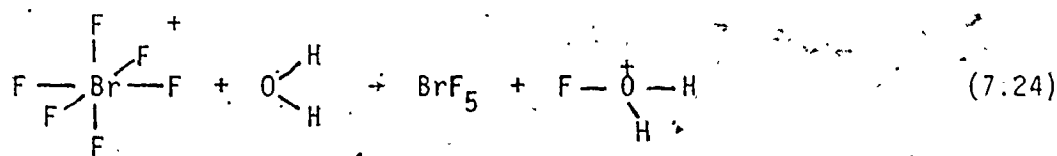
of BrF_7 . Thus in the case of the hydrolysis, reaction according to scheme (7.22) cannot occur due to the inability to form the seven coordinate intermediate. Instead, the H_2O molecule may attack at a fluorine



atom. The reaction may be an SN_2 displacement on fluorine of Class 4 as catalogued by Liebman and Jarvis²⁰² (equation (7.23)). Applying



this to $\text{X} = \text{BrF}_5$ and $:\text{Z} = \text{H}_2\text{O}$, one gets (7.24) where BrF_5 and protonated



hypofluorous acid^{81,203} are produced. Loss of a proton to the solvent (7.25) would produce HOF . This would then decompose to HF and O_2 (to account for the bubbles of gas which were observed). The factors which affect the rate of this decomposition are poorly understood. Such a reaction scheme would account for all the products observed. It also suggests that attempts to prepare BrOF_5 by reaction of BrF_6^+ with oxygen donors are

unlikely to succeed since the BrF_6^+ ion will be attacked at a fluorine ligand rather than at the central Br atom.

Attempts to produce the Br (VII) oxyfluorides BrOF_5 and BrO_2F_3 by oxidation of the Br (V) species BrOF_3 and BrO_2F with KrF_2 or by the high pressure reaction of BrF_5 with oxygen were unsuccessful. This lack of success does not, however, imply that these two Br (VII) species are inherently unstable. A very high activation barrier could equally well be responsible for the failure of the reactions attempted. A similar situation exists in the case of the preparation of the BrO_4^- ion (see Chapter I).

G. Experimental Section.

(i). BrO_3F .

BrO_3F was prepared by the method of Appelman and Studier.¹⁴ In a typical preparation, 0.359 g (1.65 mmol) of SbF_5 was dissolved in 0.27 g of HF in an FEP nmr tube and the mixture cooled to -196°C . 0.079 g (0.43 mmol) of KBrO_4 was added in a dry box. The mixture was warmed to -72°C for several hours and then to room temperature for a few minutes. When the sample was cooled to -30°C , a white slurry was produced. The Raman spectrum of this mixture showed BrO_3F to be present (in solution) and a strong line at 660 cm^{-1} was assigned to SbF_6^- (see Table 5.5). A number of additional weak lines appeared which could possibly be due to $\text{Sb}_2\text{F}_{11}^-$ or other $\text{Sb}_n\text{F}_{5n+1}^-$ ions. No BrO_4^- was observed in the Raman spectrum. The tube (A) was cooled to -63°C and a static distillation into another

FEP nmr tube (B) at -196°C was set up. Some white material (presumably the rather volatile BrO_3F) distilled over very rapidly, whereas other white material (presumably HF) came over more slowly. Only a small part of the liquid in the original reaction tube (A) was distilled into tube (B). The Raman spectrum of the material remaining in tube (A) showed that only a small amount of BrO_3F remained. When the second tube (B) was warmed to -78°C , the white solid melted and two immiscible layers were formed. The Raman and ^{19}F nmr spectra of both layers were recorded, with much stronger signals being obtained from the lower layer. Also, when more HF was added, the upper layer in the tube increased in volume while the lower layer decreased. Both these facts suggest that the upper layer was a saturated solution of BrO_3F in HF, whereas the lower layer was liquid BrO_3F (with some HF dissolved in it). Enough HF was added to form a saturated solution at -78°C , and the amount of HF required to achieve complete dissolution was estimated on the basis of the volume of the solution formed.

(ii) Reactions of KBrO_4

(a) KBrO_4 and AsF_5 : 0.026 g (0.14 mmol) of KBrO_4 was dissolved in 0.2 g of HF in an FEP nmr tube, and 0.78 mmol of AsF_5 was distilled in. The mixture was warmed to -78°C to give a clear solution and a white solid. The volatile components of this mixture were distilled into a second FEP nmr tube, and the ^{19}F nmr spectrum of the solution was recorded at -77°C . A singlet at +150 ppm was assigned to HF undergoing rapid exchange with AsF_5 , and a broad, weak line at -270 ppm was assigned to BrO_3F . The

final traces of HF were removed under vacuum from the white solid which remained in the original reaction tube, and the Raman spectrum of the solid was recorded. Three lines at 693 cm^{-1} , 582 cm^{-1} , and 378 cm^{-1} were observed which indicated the presence of AsF_6^- .¹⁵¹

(b) KBrO_4 and BrF_5 : 0.088 g (0.48 mmol) of KBrO_4 was placed in an FEP nmr tube, and 1.14 g (6.55 mmol) of BrF_5 was distilled in. The sample was allowed to warm up to room temperature for 30 minutes, and then cooled to -60°C . A solid was present in the bottom of the tube at low temperature and at room temperature. ^{19}F nmr and Raman spectra recorded on the liquid showed only peaks due to BrF_5 .

Approximately 0.003 g of HF (estimated on the basis of volume of gaseous HF) was distilled into the sample, and the mixture was allowed to warm up to room temperature for one hour. The sample was cooled to -48°C and ^{19}F nmr and Raman spectroscopy indicated that no detectable amount of reaction had occurred. The volatile components of the mixture were removed under vacuum and a white solid was formed. This solid was identified as KBrO_4 on the basis of its Raman spectrum.

In another experiment, 0.107 g (0.582 mmol) of KBrO_4 was dissolved in 0.62 g of HF in an FEP nmr tube, and 0.459 g (2.63 mmol) of BrF_5 was distilled in. The tube was warmed to -48°C to dissolve all the solid present and then cooled back down to -65°C . The Raman spectrum of the solution was recorded at this temperature, and the ^{19}F nmr spectrum was recorded at -70°C . The sample was pumped to dryness under vacuum at room temperature and the white solid which was formed was identified as KHF_2 .

by its Raman spectrum.

(c) KBrO_4 and KrF_2 : In one experiment, 0.050 g (0.27 mmol) of KBrO_4 was mixed with 0.13 g of HF in an FEP nmr tube, and 0.047 g (0.38 mmol) of KrF_2 was distilled in. The sample was warmed to -78°C and a large amount of solid was present in the tube. The sample was removed from the cold bath, rapidly warmed for a few seconds and then cooled back to -78°C . After several of these heating and cooling cycles, the Raman spectrum of the solution was recorded (there was still solid present). When the sample was allowed to warm up to room temperature, gas bubbles were evolved. A clear, colourless solution was obtained after ten minutes and its Raman spectrum was recorded.

In a different experiment, 0.075 g (0.41 mmol) of KBrO_4 was mixed with 0.12 g of HF and 0.041 g (0.34 mmol) of KrF_2 was distilled in. The sample was warmed to -78°C for 2 hours, -72°C for 36 hours, -63°C for 8 hours and -48°C for 4 hours. The Raman spectra of the solution and of the solid present in the bottom were periodically monitored. The ^{19}F nmr spectrum of the solution was also recorded after the tube had stood at -63°C , and only signals due to HF (exchanging with any BrO_2 that was present) and KrF_2 were observed. The sample was then warmed rapidly towards room temperature. Vigorous bubbling occurred and before the sample reached room temperature it detonated with a bright red flash.

(iii) Reactions of $\text{BrF}_6^+ \text{AsF}_6^-$

(a) Hydrolysis: 0.0435 g (0.113 mmol) of $\text{BrF}_6^+ \text{AsF}_6^-$ was prepared in a 1/4" o.d. FEP tube fitted with an FEP nmr tube side-arm. A layer of

HF (0.4 g) was placed over the $\text{BrF}_6^+\text{AsF}_6^-$ to avoid reaction of the latter with the small amount of O_2 present in the dry box atmosphere. The mixture was cooled to -196°C and 2.0 μl (0.11 mmol) of H_2O was syringed into the tube (in a dry box) and formed a frozen bead. The N_2 in the tube was removed under vacuum and the frozen bead of H_2O was knocked down onto the layer of frozen HF. The mixture was warmed to -72°C and bubbles of gas were formed. After 2 hours at -72°C , all the solid in the tube had dissolved and a clear solution was present. A portion of the solution was decanted into the nmr tube side-arm, and Raman and ^{19}F nmr spectra were recorded. The volatile components of the solution were removed under vacuum at -72°C and then at room temperature. No solid residue was left behind.

(b) $\text{BrF}_6^+\text{AsF}_6^-$ and KBrO_4 : 0.061 g (0.16 mmol) of $\text{BrF}_6^+\text{AsF}_6^-$ was prepared in an FEP nmr tube, and a layer of HF (~ 0.1 g) was distilled in. 0.026 g (0.14 mmol) of KBrO_4 was then introduced into the tube kept at -196°C . The mixture was warmed to -72°C to give a clear solution and a white solid. Bubbles of gas were also formed. Raman spectra of the solid and of the solution were recorded, and the ^{19}F nmr spectrum of the solution was recorded as well. The sample was warmed briefly to room temperature, cooled to -40°C , and Raman spectra recorded on both the solid and solution.

(c) $\text{BrF}_6^+\text{AsF}_6^-$ and BrO_3F : 0.050 g (0.13 mmol) of $\text{BrF}_6^+\text{AsF}_6^-$ was prepared in an FEP nmr tube. The solution resulting from the reaction of $\text{BrF}_6^+\text{AsF}_6^-$ with KBrO_4 (section (b)) was used as a source of BrO_3F . This

solution was cooled to -62°C and the components which were volatile at this temperature (HF , BrO_3F and BrF_5) were distilled onto the freshly made $\text{BrF}_6^+\text{AsF}_6^-$. This mixture was allowed to warm up to -72°C , and a clear colourless solution standing over a white solid was obtained. Raman spectroscopy showed BrO_3F and BrF_5 to be present in solution, whereas the solid consisted of $\text{BrF}_6^+\text{AsF}_6^-$. The tube was kept at -72°C for 45 minutes, -62°C for 20 minutes and then room temperature for 15 minutes. Raman spectroscopy was used to attempt to detect any reaction which might have occurred. No significant changes were observed in the spectra, other than the fact that fluorescence was observed in the Raman spectrum after the sample had been warmed to room temperature.

(iv) Reactions of BrO_3F with KrF_2 and $\text{KrF}^+\text{AsF}_6^-$.

Approximately 0.43 mmol of BrO_3F (estimated on the basis of the amount of KBrO_4 used in its preparation) was dissolved in 0.5 g of HF in an FEP nmr tube and 0.054 g (0.44 mmol) of KrF_2 was distilled in. The mixture was warmed to -78°C (for 20 hours), -72°C (for 20 hours), -63°C (for 4 hours), -48°C (for 8 hours) and -22°C (for 4 hours). Raman spectra of the solution and of the solid present were recorded. The sample was allowed to warm to room temperature for 45 minutes, then cooled to -70°C and the Raman spectra of solution and solid again recorded. The ^{19}F nmr spectrum of the sample was obtained at -20°C .

Since no reaction had apparently taken place, 1.1 mmol of AsF_5 was distilled into the tube. The sample tube was sealed off (to prevent the possibility of air leaking in and reacting with the KrF^+) and warmed to

-72°C for several days. A large amount of solid was obtained and this was shown to be mainly $\text{KrF}^+\text{AsF}_6^-$ from its Raman spectrum. Some unreacted KrF_2 was also present, as was BrO_3F . Vigorous gas evolution occurred as soon as the tube was allowed to warm up to room temperature. The sample also turned brown in colour. The tube was immediately cooled to -196°C, and then rewarmed to -72°C. A brown solution with a solid in it was formed. The Raman spectrum of the solid was recorded.

(v) BrF_5 , F_2 and O_2 at High Temperature and Pressure.

A Monel bomb (volume 44 cm³) fitted with a Monel valve was conditioned with 1500 psi of F_2 at room temperature and was then evacuated overnight. 2.56 g (14.6 mmol) of BrF_5 was distilled in. 7.85 mmol of and 168 mmol of F_2 were condensed in to give an overall pressure of approximately 1400 psi at room temperature and the bomb was heated to 175°C for several days. The non-condensable gases were removed at -196°C and the contents of the bomb were distilled into a Kel-F trap. A white solid was trapped out at -196°C. This material was still a solid at -78°C. Warming the tube to +48°C however caused the solid to melt (m.p. of BrF_5 -61.3°C). Some of this liquid was distilled into an FEP nmr tube and the ^{19}F nmr spectrum recorded at room temperature showed lines attributable to BrF_5 .

CHAPTER VIII

CONCLUSIONS

A. Introduction.

This thesis describes the first detailed study of the oxyfluorides of bromine. Prior to this work, BrO_2F was the only oxyfluoro species of Br (V) which had been reported, and it had not been spectroscopically characterized. The preparation of BrOF_3 and of the ions BrO_2^+ , BrOF_2^+ , BrOF_4^- and BrO_2F_2^- has been accomplished in this work, and these (along with BrO_2F) have been characterized by Raman and ^{19}F nmr spectroscopy. During the course of this project, other workers have also reported evidence for these molecules and ions. Where there is overlap, our results agree well with those of these other workers but in some cases our interpretations of the data differ.

A number of reactions involving Br (VII) oxyfluoro species are described, but none led to the formation of any new molecules. These reactions nevertheless increase our knowledge of Br (VII) chemistry and provide a basis for future work in this rather poorly explored field of halogen chemistry.

B. Comparison of the Oxyfluorides of Bromine with those of Chlorine and Iodine.

A direct comparison of the oxyfluoro species of chlorine, bromine and iodine is most readily made for the halogens in the + (V) oxidation state

since all the neutral molecules and the corresponding singly charged anions and cations are now known. The bromine compounds appear to resemble the chlorine compounds more closely than those of iodine in many respects. Whereas BrO_2F and ClO_2F ³¹ are both monomeric in the solid and liquid phases, IO_2F is a highly associated solid which decomposes without melting. This presumably reflects the tendency of iodine to achieve high coordination numbers through secondary bonding in the solid. Similarly ClOF_3 ³¹ and BrOF_3 both form associated liquids at room temperature, whereas IOF_3 is a polymeric solid.⁵⁶ In this case however, BrOF_3 can be considered as intermediate between ClOF_3 and IOF_3 . Although it is probably not as heavily bridged as IOF_3 , the bridging in liquid BrOF_3 is extensive enough to cause more Raman lines than would be expected for the monomer. This association apparently persists in HF solution (from the Raman spectra) and at low temperature in SO_2ClF and SO_2F_2 (from the ^{19}F nmr spectra). For ClOF_3 , on the other hand, the Raman spectrum of the liquid can be satisfactorily assigned on the basis of a monomer.⁴¹ The decomposition of the oxide trihalides of the halogens show a discontinuity between bromine and iodine. Whereas ClOF_3 ³¹ and BrOF_3 decompose thermally according to equation (8.1)



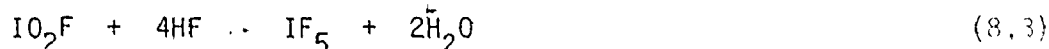
IOF_3 disproportionates according to (8.2).⁵² Finally, the behaviour of the



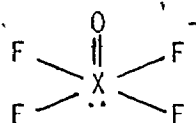
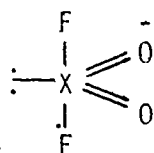
compounds XO_2F and XOF_3 ($\text{X} = \text{Cl, Br, I}$) in HF solution provides another

example of the difference between iodine and the other two halogens.

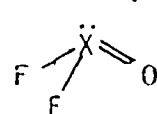
Whereas IO_2F and IOF_3 both react with anhydrous HF (reactions (8.3) and (8.4))⁵¹, ClO_2F , ClOF_3 , BrO_2F and BrOF_3 are inert towards fluorination by HF.



The cations and anions derived from the oxyfluorides XO_2F and XOF_3 ($\text{X} = \text{Cl}, \text{Br}$ and I) seem to have many common features. In all three cases, the structures of the anions XO_2F_2^- and XOF_4^- appear to be based on trigonal bipyramidal and octahedral arrangements of electron pairs about the central atom. This is in accord with the predictions of the VSEPR theory.



The structures of the two iodine compounds were established by crystallography,^{5,57} whereas for the bromine and chlorine anions, Raman and ^{19}F nmr spectroscopy were used. These idealized geometries appear to be somewhat distorted in the solid state, however, since more lines are observed in the Raman spectra than would be expected. The three XOF_2^+ cations have been studied ($\text{X} = \text{Cl}$,^{37,38} I ,⁵¹ Br (Chapter V)) and a pyramidal geometry has been suggested. In all three cases, there appear to be significant anion-cation interactions in the solid. Similarly, the



XO_2^+ cations are all bent molecules. Anion-cation bridging has been established crystallographically for $ClO_2^+Sb_2F_{11}^-$ ²⁰ and spectroscopically for $IO_2^+AsF_6^-$.⁵¹ Similar bridging is presumably responsible for the anomalously low Br=O stretching frequencies in the AsF_6^- , BF_4^- and $[SbF_6(SbF_5)_{1.24}]^-$ salts of the BrO_2^+ cation. In the XO_2^+ and XOF_2^+ salts, discrete cations appear to be present (in contrast to the polymeric oxygen bridged cation which was suggested for $IO_2^+AsF_6^-$ ⁵⁰ but disproved in later work⁵¹).

In certain respects, the bromine system differs from both the analogous chlorine and iodine systems, particularly in the stabilities of the products. For instance, BrO_2^+ and $BrOF_2^+$ salts decompose at room temperature whereas the corresponding Cl and I cations have been shown to be stable at this temperature. The stabilities of the oxidetrifluorides appear to follow a similar pattern, with $BrOF_3$ slowly liberating oxygen at room temperature whereas IOF_3 and $ClOF_3$ are considerably more stable. A final example is the failure (both in this work and in previous work⁵²) to prepare BrO_2SO_3F . This can be contrasted with the ready preparation of ClO_2SO_3F ⁵³ and IO_2SO_3F ⁵⁴ and suggests that bromyl fluorosulphate may be much less stable than its chloryl or iodyl analogues. A similar situation exists in the oxides of the halogens. Although chlorine and iodine form stable, well characterized oxides, those of bromine are poorly understood and tend to be much less stable. That most of the oxyfluoro species of Br (V) had not been reported or characterized at the outset of this work may therefore be due to the somewhat lower stability of many of these species

when compared to their Cl and I analogues and also to the fact that the oxides of Br were not well known, while the oxides of Cl and I have been used as convenient starting materials for the synthesis of the oxyfluorides of these elements.

C. Future Directions for Research.

(i) Br(V).

Although all the possible Br (V) oxyfluoro species have been shown to exist and have been characterized, a number of questions remain unanswered. A determination of the crystal structures of KBrO_2F_2 and KBrOF_4 would provide information on the more subtle features of the structures of these two anions and would be useful for verifying the assignments of the Raman frequencies. Comparisons could be made with the crystal structures of the analogous iodine compounds. It was found in this work that the KBrOF_4 prepared was crystalline in nature (whereas KBrO_2F_2 was generally produced as a powder). Although no crystals suitable for a complete structure determination could be found, it appears likely that careful crystallization of KBrOF_4 from CH_3CN will eventually yield good crystals.

Similarly, X-ray crystallographic studies would be very useful to resolve some of the ambiguities associated with the Raman spectra of the BrOF_2^+ and BrO_2^+ salts. Specifically, both the large shift of ν_1 of AsF_6^- in $\text{BrOF}_2^+\text{AsF}_6^-$ and the low value of the BrO_2^+ stretching frequencies have been attributed to fluorine bridging between the anion and the cation which can only be detected with certainty by X-ray crystallography. The

difficulty in this case is the decomposition of these salts at room temperature, which requires that the structure determination and the manipulations of the crystals be performed at low temperature. A thorough investigation of the $\text{BrOF}_3/\text{SbF}_5$ system would also be useful in order to shed light on the apparent discrepancies in the Raman spectrum of " $\text{BrOF}_2^+ \text{SbF}_6^-$ ". Finally, work on the reactions of BrO_2F and BrOF_3 with other Lewis acids (such as BiF_5 , NbF_5 or TaF_5) would also help in understanding these systems. Bougon and his coworkers²⁰ have found that adducts of BrOF_3 with PF_5 and BiF_5 are not stable at room temperature, but a low temperature investigation might yield useful results.

Perhaps the most intriguing structural problem relating to the Br (V) oxyfluorides is the nature of the association in BrOF_3 . In Chapter IV, it was suggested that the association may be similar to that found in SF_4 and ClOF_3 . A careful study of the temperature and concentration dependence of the Raman spectra of BrOF_3 dissolved in HF (and in other solvents as well) might show which bands are the most affected by changes in the extent of association. Similarly, gas phase spectra or matrix isolation spectra might yield the fundamental frequencies of a monomeric BrOF_3 molecule, and comparison of these with the lines due to associated BrOF_3 would certainly be helpful. These experiments are complicated however by the apparently low volatility of BrOF_3 and its instability at room temperature.

Finally, the nature of the adduct between BrO_2F and BrF_5 encountered in this work was not pursued in detail, and this system should be investigated further.

(ii) Br (VII).

Although several new oxyfluorides of Br (V) were prepared, no new oxyfluorides of Br (VII) were obtained in this work. A number of possible preparative reactions were investigated however. It was found, not unexpectedly, that the fluorinating agents AsF_5 , BrF_5 and BrF_6^+ will convert BrO_4^- to BrO_3F , and that BrO_3F is stable towards further fluorination. Similarly, attempts to prepare BrOF_5 from BrF_6^+ were unsuccessful and this has been attributed to the inability of the reaction to proceed through a seven-coordinate intermediate. Two of the reactions attempted should be reinvestigated. The reaction of KBrO_4 with KrF_2 produced BrO_2F and this unexpected result led to the suggestion that an unstable intermediate is involved in the reaction. By working at lower temperatures in a different solvent (or perhaps in a matrix) it might be possible to obtain evidence as to the nature of this intermediate. Also, BrO_3F was found to react with the strong fluorinating agent $\text{KrF}^+\text{AsF}_6^-$, but only decomposition products could be observed. Again, a further investigation of this reaction might lead to new oxyfluorides of Br (VII), possibly BrO_2F_2^+ .

Another approach which should be pursued is the reaction of Br (V) oxyfluorides or oxides with powerful fluorinating agents. It was shown in this work that KrF_2 is incapable of oxidizing BrO_2F or BrOF_3 to the Br (VII) species BrO_2F_3 and BrOF_5 . Adelhelm and Jacob¹⁸⁰ have attempted the reaction of BrO_2F with PtF_6 and their results are consistent with BrOF_2^+ as a product (rather than BrO_2F_2^+). The fluorinating agents KrF^+ and Kr_2F_3^+ have been shown to oxidize BrF_5 to BrF_6^+ however, and may be capable of

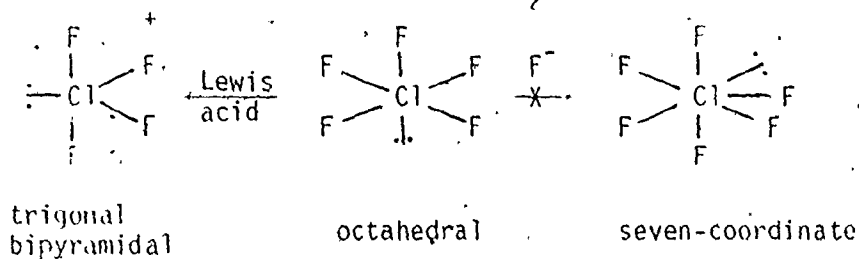
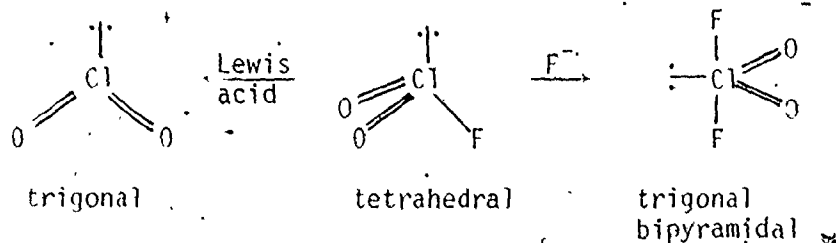
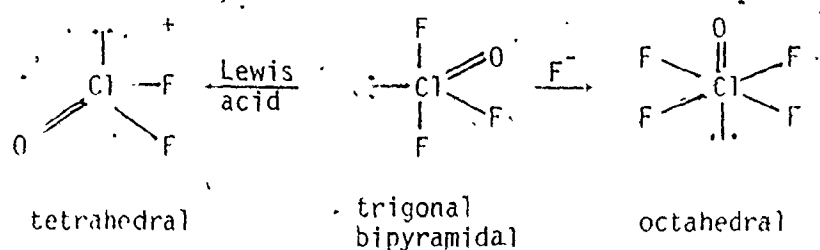
producing BrO_2F_2^+ and BrOF_4^+ (or BrOF_5) from BrO_2F and BrOF_3 . Experimental difficulties arise here however, since any decomposition of BrO_2F (or BrOF_3) to O_2 or Br_2 may lead to formation of O_2^+ or Br_2^+ salts which could complicate the Raman spectra of the products. Despite these difficulties, these reactions are perhaps the most likely to succeed in overcoming the apparently high kinetic barrier to formation of the Br (VII) oxyfluorides.

D. The Relation of Reactivity to Geometry in Oxyfluoro Compounds.

The structures suggested in this thesis are consistent with the theory that the geometry of a molecule is determined by the number of electron pairs on the valence shell of the central atom of the molecule (the Valence Shell Electron Pair Repulsion theory).

Christe et al.⁴³ have suggested that the arrangement of the electron pairs about the central atom also influences the reactivity of the molecule towards Lewis acids and bases. They have noted that among the fluorides and oxyfluorides of chlorine, those molecules which are derived from a trigonal bipyramidal arrangement of ligands and lone pairs about the central atom react readily with Lewis acids and bases (to form cations and anions containing tetrahedral and octahedral arrangements, respectively). On the other hand, parent molecules which are based on octahedral or tetrahedral arrangements are much less reactive towards Lewis acids and bases. The explanation for these observations was suggested to be that octahedral and tetrahedral geometries are energetically favourable, whereas a trigonal bipyramidal geometry is energetically unfavourable. The reasons for this

were, however, not explained. Regardless of the theoretical basis, the notion that the highly symmetric octahedral and tetrahedral arrangements are somehow more favourable than the much less symmetric trigonal bipyramidal can be used to rationalize a considerable number of acid-base reactions involving fluorides and oxyfluorides. For example, ClOF_3 (trigonal bipyramidal) is both a better fluoride acceptor and donor than ClO_2F (tetrahedral) or ClF_5 (octahedral). These observations are consistent with the



favourability of the highly symmetric arrangements of ligands and non-bonding electron pairs, and are difficult to rationalize on any other basis. The

fact that ClF_6^- has not yet been prepared, ClF_6^- can however be attributed to the steric difficulties involved with positioning six ligands around a Cl (V) central atom (to give an overall seven-coordinate structure if the lone pair is stereochemically active).

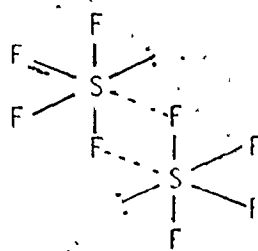
A considerable number of other acid-base reactions of various oxyfluorides can be rationalized on the basis of the structures of the parent molecule and the ion formed. Thus IOF_5 (octahedral) is inert towards reaction with F^- donors and forms oxygen bridged adducts with Lewis acids. The lack of reaction with F^- donors here cannot be attributed to steric factors since IF_7 (seven-coordinate) and IF_8^- (eight-coordinate) are both known. Similarly, SOF_2 (tetrahedral) and SO_2FCl (tetrahedral) form oxygen bridged adducts with Lewis acids and preserve the tetrahedral arrangement, whereas SOF_4 (trigonal bipyramidal) forms the SOF_3^+ ion (tetrahedral) when reacted with a Lewis acid.¹⁴⁷

The work reported in this thesis for the most part agrees with the suggestion of Christie et al. However, reliable estimates of the relative Lewis acidities or basicities of various molecules are sometimes not easily obtainable. For instance, it was shown in Chapter IV that the reaction of BrO_2F and KF proceeds to an extent of less than 12% in twenty-four hours at room temperature. One might therefore conclude that BrO_2F is a relatively poor F^- acceptor. However, it was shown in Chapter III that KBrO_2F_2 can be prepared as a pure compound and is stable indefinitely at room temperature, suggesting that BrO_2F is a reasonably good F^- acceptor. Such ambiguous results occur because many of the reactions investigated in this thesis

are probably kinetically controlled. The product mixtures observed do not necessarily represent the most thermodynamically favoured ones, since the reaction may not have reached equilibrium if the reaction is made particularly slow by a high activation energy or by the insolubility of one of the reagents. Despite these difficulties, the evidence presented in this thesis suggests that BrOF_3 is a better fluoride ion acceptor than BrO_2F . Under rather similar conditions, BrOF_3 rapidly abstracts a fluoride ion from KHF_2 whereas BrO_2F does not. Also, the reaction of a mixture of KBrO_2F_2 and KBrOF_4 with a molar deficit of AsF_5 leaves a residue containing only KBrOF_4 . Thus BrOF_3 appears to be a stronger Lewis acid than BrO_2F (and this conclusion was used when a reaction scheme for $\text{KBrO}_3/\text{BrF}_3$ was proposed in Chapter III).

Direct comparison of the Lewis basicity of BrO_2F and BrOF_3 is more difficult to make. Ideally, one should allow a mixture of the two to compete for a Lewis acid. This was however not done, so the comparison must be made on a more qualitative basis. All the reactions of BrOF_3 with excess Lewis acid produced mixtures which contained no BrOF_3 . With bromyl fluoride on the other hand, small amounts of BrO_2F were sometimes observed in the product even when excess Lewis acid was used. Also, the BrO_2^+ salts generally seemed to be more stable than the BrO_2^+ salts. Although this evidence is by no means conclusive, it does suggest that BrOF_3 is a better Lewis acid than BrO_2F . Thus the ease of the reactions of BrO_2F and BrOF_3 with Lewis acids and F^- donors support the suggestion of Christie et al. If the association present in liquid BrOF_3 is the same as that which has

been suggested to be present, in SF_4 , BrF_3 , ClF_3 ¹¹ and ClOF_3 ¹², then this also suggests that octahedral coordination is a more favourable arrangement than a trigonal bipyramidal one. Similar cases where octahedral coordination is achieved through the formation of bridges have been reported and include molecules such as



SeOF_4 , TeOF_4 ¹³ and IO_2F_3 ¹⁴ and in these cases the monomers would be "unfavourable" five-coordinate structures.

Other work presented in this thesis, however, shows that the symmetry argument is not always reliable and that other factors must be important. The facile reaction of SeO_2 with KF to produce KSeO_2F cannot be attributed to the change in the symmetry about Se since in both the SeO_2 polymer starting material and in the SeO_2F^- anion, the Se is tetrahedrally surrounded by three ligands and one lone pair. Furthermore, SeO_2F^- shows a significant tendency to accept a fluoride ion to give $\text{SeO}_2\text{F}_2^{2-}$. This is somewhat surprising since in this reaction both the decrease in the symmetry of the electron pair arrangement and the electrostatic repulsion between the SeO_2F^- and the incoming F^- ion must be overcome. Even more surprising then is the related tellurium system where the TeO_2F^- ion (which should have a stable electron pair arrangement) is not known whereas the "less favourable" $\text{TeO}_2\text{F}_2^{2-}$ ion is readily formed.¹⁶⁵ This points out one of the limitations of this approach to reactivity. Trends in acid-base behaviour for a number of analogous molecules within a group of the periodic table (e.g. ClOF_3 ,

BrOF_3 and IOF_3) cannot be predicted by this method since the molecules will all have the same electron pair arrangement in their primary coordination spheres.

It was concluded in Chapter IV that BrOF_3 fluorinates a number of iodine oxides and oxyfluorides more rapidly than BrF_5 , and that BrOF_3 must also hydrolyse considerably faster than BrF_5 . Although it would be tempting to assign this difference in the reaction rates to the less favourable electron pair arrangement around BrOF_3 (trigonal bipyramidal) compared to BrF_5 (octahedral), a steric argument can be successfully applied as well. The rate at which a group (for example, H_2O) adds to a BrF_5 molecule can be predicted to be considerably slower than the rate of addition to a BrOF_3 molecule. The five-coordinate BrOF_3 can readily become six-coordinate (if the lone pair is counted as occupying a position) whereas the six-coordinate BrF_5 would have to become either seven-coordinate or six-coordinate with a stereochemically inactive lone pair, both of which are unfavourable processes. For example, the reaction of BrF_5 with KF to give KBrF_6 proceeds rather slowly (more than one week to obtain complete reaction at room temperature in the presence of excess BrF_5) and vibrational and X-ray powder diffraction data suggest that the product is octahedral with the lone pair being stereochemically inactive (although this is not necessarily conclusive since the distortion from O_h symmetry could be very small). On the basis of the rate of addition of an incoming group, one can therefore rationalize the more rapid rate of reaction of BrOF_3 compared to BrF_5 . Furthermore, a similar argument can be used to explain why BrOF_4^-

hydrolyses more rapidly than BrF_6^- (Chapter III). Addition of H_2O to BrOF_4^- followed by loss of F^- is possible, but addition of H_2O to BrF_6^- is clearly unfavourable since an eight-coordinate (or seven-coordinate if the lone pair is inactive) is involved. Hence steric arguments can be applied to rationalize this reaction as well. Consideration of the symmetry about the central atom would lead us to predict that BrF_6^- should be less favourable than BrOF_4^- (or at best, equally favourable if the lone pair is inactive) and would fail to rationalize the observed rates of hydrolysis.

In summary therefore, the suggestion that a molecule's reactivity is dependent upon the symmetry of the arrangement of the ligands and lone pairs about the central atom does seem to rationalize a great deal of reaction chemistry and some of the results obtained in the present work. However, several exceptions to these trends do occur and there are clearly a number of factors involved, some of which evidently dominate over the symmetry considerations in certain cases.

Known and Unknown Oxyfluoro Compounds of the Halogens.

In Table 1.1 all the oxyfluorides of the halogens in the + (V) and + (VII) oxidation states along with the singly charged ions derived from them are listed. The square brackets show which ones have not yet been prepared.

All of the expected oxyfluoro compounds of Cl(V) , Br(V) and I(V) have now been reported. Although the properties and structures of the bromine (V) compounds do not differ radically from those that might be

be anticipated based on a comparison with the chlorine and iodine analogues, they are nevertheless in many cases less stable than the related oxyfluoro species of the other halogens.

Considerably fewer oxyfluoro compounds containing halogens in the + (VII) oxidation state have been reported. However, for several of these unknown compounds, apparently straightforward preparative routes have failed and some rationalization for this lack of success can be given. For instance, ClO_3F has been shown to be inert towards reaction with a variety of Lewis acids and fluoride ion donors.¹ The failure to obtain ClO_3^+ and ClO_3F_2^- has been attributed to the strength of the Cl-F bond and the lack of a molecular dipole moment which is a result of the pseudo-tetrahedral arrangement about the central atom. On the same basis, it might be anticipated that BrO_3F would be similarly inert towards Lewis acids and fluoride ion donors. The work presented in this thesis supports this but since these reactions have not yet been investigated in detail, definitive conclusions as to the possible existence of BrO_3^+ and BrO_3F_2^- cannot be made. The reaction of IOF_5 and IO_2F_3 with the strong Lewis acids SbF_5 and AsF_5 have failed to produce the cations IOF_4^+ and IO_2F_2^+ . In the former case, an oxygen bridged $\text{F}_5\text{M}-\text{O}-\text{IF}_5$ adduct is formed; whereas in the latter case oxygen bridged $(\text{MF}_4 \cdot \text{IO}_2\text{F}_4)_n$ polymers are produced (M = Sb, As). These results may be in large measure attributable to the tendency of iodine to favour a high coordination number, which is also reflected in the polymeric nature of the oxyfluorides IO_2F_3 , IO_2F and IOF_3 and by the facile hydration of IO_4^- to H_4IO_6^- in aqueous

solution. The fact that straightforward reactions have failed to produce species such as ClO_3^+ , ClO_3F_2^- , IOF_4^+ and IO_2F_2^+ make it unlikely that these will be observed as isolable entities, although they may eventually be shown to have marginal stability under extreme conditions (for example at low temperature in a matrix).

Although no efforts to prepare the anions ClOF_6^- and BrOF_6^- have been reported (since the parent oxyfluorides are not known), these may be expected to be of low stability for steric reasons. The failure to prepare the fluorides XF_7 ($\text{X} = \text{Cl}, \text{Br}$) by means of a reaction between the XF_6^+ cation and a fluoride ion donor at low temperature suggests that the central atom is incapable of accommodating seven groups in its primary coordination sphere. Moreover, the anomalously high chemical shift of the ^{19}F nmr resonance for ClF_6^+ has been attributed to considerable crowding in the valence shell of the chlorine, which also suggests that a seventh electron pair could not be accommodated. Finally, the "non-existence" of ClF_6^- and the apparent lack of stereochemical activity of the lone pair in BrF_6^- indicate that seven electron pairs cannot be disposed about a Br (V) or Cl (V) central atom and it can be anticipated that the crowding would be even more severe about a Br (VII) or Cl (VII) central atom. In view of this, it would be rather surprising if the anions ClOF_6^- and BrOF_6^- were found to be stable.

Although the apparent "non-existence" of a number of the entries in square brackets in Table 1.1 can be rationalized, no convincing reasons can be found why some of the other unknown halogen (VII) oxyfluorides should

not be stable. This is particularly true of the Br (VII) species BrOF_5 and BrO_2F_3 , and the ions derived from the latter, BrO_2F_2^+ and BrO_2F_4^- . Steric reasons cannot be the dominating factor here since bromine surrounded by six ligands is found in the stable ions BrF_6^- and BrF_6^+ . Similarly, the fact that ClOF_5 and ClO_2F_4^- have not yet been prepared is somewhat surprising in view of the stability of the isoelectronic ClF_6^+ cation.¹⁰ In this case it could be argued that the extra repulsions in the valence shell of the central atom introduced by replacing a fluorine ligand in ClF_6^+ by a doubly bonded oxygen might destabilize the molecule. In the case of the I (VII) oxyfluoro compounds, IO_3F has not been well characterized. Although a preparative route has been published,⁵¹ explicit experimental details were not provided and an attempt to repeat the preparation has failed.⁵¹ Attempts to prepare IO_3F by different methods have also been unsuccessful.^{51,68} Consequently, no information is available on the structure of IO_3F , or on the possibility of forming the ions IO_3^+ or IO_3F_2^- .

That there are several reasonable oxyfluoro compounds of the halogens which are as yet unknown demonstrates that there is still a considerable amount of work to be done on these systems.

REFERENCES

1. A. J. Downs and C. J. Adams, in "Comprehensive Inorganic Chemistry", J. C. Bailar, H. J. Emeléus, R. Nyholm and A. F. Trotman-Dickenson, Ed., Pergamon Press (1973), Vol. 2, p. 1107, and references therein.
2. L. Stein, in "Halogen Chemistry", V. Gutman, Ed., Academic Press (1967), Vol. 1, p. 133.
3. A. I. Popov, in "M.T.P. International Review of Science: Inorganic Chemistry Series One", V. Gutman, Ed., Butterworths and University Park Press, (1972), Vol. 3, p. 53.
4. T. A. O'Donnell, in "Comprehensive Inorganic Chemistry", J. C. Bailar, H. J. Emeléus, R. Nyholm and A. F. Trotman-Dickenson, Ed., Pergamon Press (1973), Vol. 2, p. 1009.
5. D. Martin and G. Tantot, J. Fluorine Chem., 6, 477 (1975).
6. C. E. Fogle and R. T. Rewick, U.S. Patent 3,615,206 (1971).
7. R. J. Gillespie and G. J. Schrobilgen, Inorg. Chem., 13, 1230 (1974).
8. M. Schmeisser and K. Brandle, Adv. Inorg. Chem. Radiochem., 5, 41 (1963).
9. B. J. Brisdon, in "M.T.P. International Review of Science: Inorganic Chemistry Series One", V. Gutman, Ed., Butterworths and University Park Press (1972), Vol. 3, p. 215.
10. R. Schwartz and M. Schmeisser, Ber., 70, 1163 (1967).
11. C. Campbell, J. P. M. Jones and J. J. Turner, Chem. Comm., 888 (1968).
12. J-L. Pascal and J. Potier, ibid., 446 (1973).
13. J-L. Pascal, A.C. Pavia, J. Potier and A. Potier, C. R. Acad. Sc., C, 279, 43 (1974).
14. J-L. Pascal, A.C. Pavia, J. Potier and A. Potier, ibid., 280, 661 (1975).

15. B. Lewis and W. Feitknecht, J. Amer. Chem. Soc., 53, 2910 (1931).
16. B. Lewis and H. J. Schumacher, Z. Anorg. Allg. Chem., 182, 182 (1929).
17. A. Pflugmacher, H. J. Rabben and H. Dahmen, *ibid.*, 279, 313 (1955).
18. A. J. Arvia, P. J. Aymonino and H. J. Schumacher, *ibid.*, 298, 1 (1959).
19. J. L. Pascal, A. C. Pavia, J. Potier and A. Potier, C.R. Acad. Sci. C, 282, 53 (1976).
20. K. Selte and A. Kjekshus, Acta Chem. Scand., 24, 1912 (1970).
21. K. O. Christe and C. J. Schack, Adv. Inorg. Chem. Radiochem., 18, 319 (1974).
22. M. Schmeisser and E. Pammer, Angew. Chem., 67, 156 (1955).
23. M. Schmeisser and E. Pammer, *ibid.*, 69, 781 (1957).
24. O. Ruff and W. Menzel, Z. Anorg. Allg. Chem., 202, 49 (1931).
25. A. Engelbrecht, G. Mayr, G. Ziller and E. Schandara, Monatsh. Chem., 105, 796 (1974).
26. R. J. Gillespie and J. P. Krasznai, Inorg. Chem., 16, 1384 (1977).
27. M. Brownstein, R. J. Gillespie and J. P. Krasznai, Can. J. Chem., submitted for publication.
28. N. Bartlett and F. O. Sladky, J. Amer. Chem. Soc., 90, 5316 (1968).
29. K. O. Christe, C. J. Schack, D. Pilipovich and W. Sawodny, Inorg. Chem., 8, 2439 (1969).
30. A. J. Edwards and R. J. C. Sills, J. C.S. Dalton, 1726 (1974).
31. D. F. Smith, G. M. Begun and W. H. Fletcher, Spectrochim. Acta, 20, 1763 (1964).
32. A. J. Arvia and P. J. Aymonino, *ibid.*, 19, 1449 (1963).
33. C. R. Parent and M. C. L. Gerry, J. Mol. Spectrosc., 49, 343 (1974).
34. D. K. Huggins and W. B. Fox, Inorg. Nucl. Chem. Lett., 6, 337 (1970).

35. K. O. Christe and E. C. Curtis, *Inorg. Chem.*, 11, 35 (1972).
36. R. Bougon, P. Plurien and J. Isabey, *C. R. Acad. Sci., C*, 273, 415 (1971).
37. K. O. Christe, E. C. Curtis and C. J. Schack, *Inorg. Chem.*, 11, 2212 (1972).
38. R. Bougon, T. Bui Huy, A. Cadet, P. Charpin and R. Rousson, *ibid.*, 13, 690 (1974).
39. R. Bougon, J. Isabey and P. Plurien, *C. R. Acad. Sci., C*, 271, 1366 (1971).
40. D. Pilipovich, C. B. Lindahl, C. J. Schack, R. D. Wilson and K. O. Christe, *Inorg. Chem.*, 11, 2189 (1972).
41. K. O. Christe and E. C. Curtis, *ibid.*, 11, 2196 (1972).
42. K. O. Christe and E. C. Curtis, *ibid.*, 11, 2209 (1972).
43. K. O. Christe, C. J. Schack and D. Pilipovich, *ibid.*, 11, 2205 (1972).
44. E. Jacob, *Angew. Chem. Int. Ed.*, 15, 158 (1976).
45. G. Tantot and R. Bougon, *C. R. Acad. Sci., C*, 281, 271 (1975).
46. R. Bougon, P. Joubert and G. Tantot, *J. Chem. Phys.*, 66, 1562 (1977).
47. R. Bougon, T. Bui Huy, P. Charpin, R. J. Gillespie and P. Spekken, *Inorg. Chem.*, submitted for publication.
48. R. Bougon and T. Bui Huy, *C. R. Acad. Sci., C*, 283, 461 (1976).
49. R. Bougon, T. Bui Huy, P. Charpin and G. Tantot, *ibid.*, 283, 71 (1976).
50. H. A. Carter and F. Aubke, *Inorg. Chem.*, 10, 2296 (1971).
51. J. P. Krasznai, Ph.D. Thesis, McMaster University, Hamilton, Canada (1975).
52. E. E. Aynsley, R. Nichols and P. L. Robinson, *J. Chem. Soc.*, 623 (1953).
53. L. Helmholtz and M. T. Rodgers, *J. Amer. Chem. Soc.*, 62, 1537 (1940).
54. A. Finch, P. N. Gates and M. A. Jenkinson, *J. Fluorine Chem.*, 3, 111 (1972/73).

55. J. B. Milne and D. Moffett, *Inorg. Chem.*, 14, 1077 (1975).
56. A. J. Edwards and P. Taylor, *J. Fluorine Chem.*, 4, 173 (1974).
57. R. R. Ryan and L. B. Asprey, *Acta. Cryst.*, B28, 979 (1972).
58. J. B. Milne and D. Moffett, *Inorg. Chem.*, 15, 2165 (1976).
59. A. Engelbrecht and H. Atzwanger, *Monatsh. Chem.*, 83, 1087 (1952).
60. A. H. Clark, B. Beagley and D. W. J. Cruickshank, *Chem. Comm.*, 14 (1968).
61. D. R. Lide and D. E. Mann, *J. Chem. Phys.*, 25, 1138 (1956).
62. H. H. Claassen and E. H. Appelman, *Inorg. Chem.*, 9, 622 (1970).
63. K. O. Christe, *Inorg. Nucl. Chem. Lett.*, 8, 453 (1972).
64. K. O. Christe, R. D. Wilson and E. C. Curtis, *Inorg. Chem.*, 12, 1356 (1973).
65. K. O. Christe, *Inorg. Nucl. Chem. Lett.*, 8, 457 (1972).
66. K. O. Christe and R. D. Wilson, *Inorg. Chem.*, 12, 1356 (1973).
67. K. O. Christe and E. C. Curtis, *ibid.*, 12, 2245 (1973).
68. E. H. Appelman and M. H. Studier, *J. Amer. Chem. Soc.*, 91, 4561 (1969).
69. M. Schmeisser and K. Lang, *Angew. Chem.*, 67, 156 (1955).
70. A. Engelbrecht and P. Peterfy, *Angew. Chem. Int. Ed.*, 8, 768 (1969).
71. I. R. Beattie and G. J. Van Schalkwyk, *Inorg. Nucl. Chem. Lett.*, 10, 343 (1974).
72. R. J. Gillespie and J. P. Krasznai, *Inorg. Chem.*, 15, 1251 (1976).
73. I. R. Beattie, R. Crocombe, A. German, P. Jones, C. Marsden, G. Van Schalkwyk and A. Bukovsky, *J. C. S. Dalton*, 14, 1380 (1976).
74. H. A. Carter, J. N. Ruddick, J. R. Sams and F. Aubke, *Inorg. Nucl. Chem. Lett.*, 11, 29 (1975).
75. D. F. Smith and G. M. Begun, *J. Chem. Phys.*, 42, 2236 (1965).

76. R. J. Gillespie and J. W. Quail, *Proc. Chem. Soc.*, 278 (1963).
77. J. H. Holloway, H. Selig and H. H. Claassen, *J. Chem. Phys.*, 54, 4305 (1971).
78. R. J. Gillespie, "Molecular Geometry", Van Nostrand Reinhold, London (1972).
79. F. von Stadion, *Gilbert's Ann.*, 52, 197, 339 (1816).
80. F. Ammermüller and G. Magnus, *Pogg. Ann.*, 28, 514 (1833).
81. E. H. Appelman, *Accts. of Chem. Res.*, 6, 113 (1973).
82. E. H. Appelman, *J. Amer. Chem. Soc.*, 90, 1900 (1968).
83. J. G. Malm and E. H. Appelman, *At. Energy Rev.*, 7, 21 (1969).
84. E. H. Appelman, *Inorg. Chem.*, 8, 223 (1969).
85. E. H. Appelman, *Inorg. Syn.*, 13, 1 (1972).
86. G. K. Johnson, P. N. Smith, E. H. Appelman and W. N. Hubbard, *Inorg. Chem.*, 9, 119 (1970).
87. W. F. De Coursey, Ph.D. Thesis, Iowa State College, Ames, Iowa (1953).
88. W. M. Latimer, "Oxidation Potentials", Prentice Hall, Inc., Englewood Cliffs, N.J. (1952).
89. G. J. Schrobilgen, Ph.D. Thesis, McMaster University, Hamilton, Canada (1973).
90. R. J. Gillespie and G. J. Schrobilgen, *Inorg. Chem.*, 15, 22 (1976).
91. R. J. Gillespie, P. Spekkens, J. B. Milne and D. Moffett, *J. Fluorine Chem.*, 7, 43 (1976).
92. P. A. W. Dean and R. J. Gillespie, *J. Amer. Chem. Soc.*, 91, 7264 (1969).
93. R. C. Thompson, Ph.D. Thesis, McMaster University, Hamilton, Canada (1962).
94. F. Schreiner, J. G. Malm and J. C. Hindman, *J. Amer. Chem. Soc.*, 87, 25 (1965).
95. J. Shamir and I. Yaroslavsky, *Israel J. Chem.*, 7, 495 (1969).

96. T. Surles, H. H. Hyman, L. A. Quarterman and A. I. Popov, *Inorg. Chem.*, 9, 2726 (1970).
97. F. Seel and J. Boudier, *Z. Anorg. Allg. Chem.*, 342, 173 (1966).
98. G. Mitra, *ibid.*, 340, 110 (1965).
99. G. Mitra, *ibid.*, 368, 336 (1969).
100. C. J. Adams, *Inorg. Nucl. Chem. Lett.*, 10, 831 (1974).
101. H. H. Claassen, E. L. Gasner, H. Kim and J. L. Huston, *J. Chem. Phys.*, 49, 253 (1968).
102. R. J. Gillespie and P. Spekkens, *J. C. S. Dalton*, 2391 (1976).
103. R. J. Gillespie, B. Landa and G. J. Schrobilgen, *Inorg. Chem.*, 15, 1256 (1976).
104. R. Rousson and M. Drifford, *J. Chem. Phys.*, 62, 1806 (1975).
105. G. M. Begun, W. H. Fletcher and D. F. Smith, *ibid.*, 42, 2236 (1965).
106. L. L. Alexander and I. R. Beattie, *J. Chem. Soc., A*, 3091 (1971).
107. H. S. Gutowsky and C. J. Hoffman, *J. Chem. Phys.*, 19, 1259 (1951).
108. A. P. Irsa and L. Friedman, *J. Inorg. Nucl. Chem.*, 6, 77 (1958).
109. E. N. Sloth, L. Stein and C. W. Williams, *J. Phys. Chem.*, 73, 276 (1969).
110. K. O. Christe, *Inorg. Chem.*, 11, 1215 (1972).
111. G. R. Jones, R. D. Burbank and N. Bartlett, *ibid.*, 9, 2264 (1970).
112. H. Selig, H. H. Claassen and J. H. Holloway, *J. Chem. Phys.*, 52, 351 (1970).
113. E. A. Robinson, D. S. Lavery and S. Weller, *Spectrochim. Acta*, 25A, 151 (1969).
114. K. Nakamoto, "Infrared Spectra of Inorganic and Coordination Compounds". Wiley, New York (1970).

115. R. A. Frey, R. L. Redington and A. L. K. Aljibury, J. Chem. Phys., 54, 344 (1971).
116. K. O. Christe and C. J. Schack, Inorg. Chem., 9, 1852 (1970).
117. E. J. Baran and P. J. Aymonino, Z. Naturforsch., 27B, 1568 (1972).
118. E. H. Appelman, B. Beagley, D. W. J. Cruickshank, A. Foord, S. Rutlad and V. Ulbrecht, J. Mol. Struct., 35, 139 (1976).
119. J. Shamir and J. Binenboym, Inorg. Chim. Acta, 2, 37 (1968).
120. H. Selig and H. Holzman, Israel J. Chem., 7, 417 (1969).
121. E. L. Muetterties and W. D. Phillips, J. Amer. Chem. Soc., 81, 1084 (1959).
122. G. Franz and F. Neumayr, Inorg. Chem., 3, 921 (1964).
123. G. J. Schrobilgen, Private Communication.
124. C. J. Schack and K. O. Christe, Inorg. Chem., 13, 2378 (1974).
125. H. A. Carter, S. P. L. Jones and F. Aubke, *ibid.*, 9, 2485 (1970).
126. T. Surles, L. A. Quarterman and H. H. Hyman, J. Fluorine Chem., 3, 21 (1973/74).
127. Handbook of Chemistry and Physics, 50th Ed., The Chemical Rubber Co., Cleveland, Ohio. (1969).
128. N. Bartlett and P. L. Robinson, J. Chem. Soc., 3417 (1961).
129. J. A. Evans and D. A. Long, J. Chem. Soc. A, 1688 (1968).
130. M. Azeem, M. Brownstein and R. J. Gillespie, Can. J. Chem., 47, 4159 (1969).
131. A. J. Edwards, J. C. S. Dalton, 2325 (1972).
132. R. Bougon, T. Bui Huy and P. Charpin, Private Communication, see Reference 47.
133. S. Nunziante Cesaro, M. Spoliti, A. J. Hinchcliffe and J. S. Ogden, J. Chem. Phys., 55, 5834 (1971).

134. J. Goubeau and W. Bues, *Z. Anorg. Allg. Chem.*, 268, 221 (1952).
135. N. N. Greenwood, *J. Chem. Soc.*, 3811 (1959).
136. J. J. Harris, *Inorg. Chem.*, 5, 1627 (1966).
137. K. O. Christe and W. Maya, *ibid*, 8, 1253 (1969).
138. G. M. Begun and A. C. Rutenberg, *ibid*, 6, 2212 (1967).
139. P. A. W. Dean, R. J. Gillespie, R. Hulme and D. A. Humphreys, *J. Chem. Soc. A*, 341 (1971).
140. H. Takeo, E. Hirota and Y. Morino, *J. Mol. Spect.*, 34, 370 (1970).
141. R. J. Gillespie and M. J. Morton, *Chem. Comm.*, 1565 (1968).
142. L. A. Woodward, *Trans. Farad. Soc.*, 54, 1271 (1958).
143. K. O. Christe, J. Guertin, A. Pavlath and W. Sawodny, *Inorg. Chem.*, 6, 533 (1967).
144. J. A. Rolfe and L. A. Woodward, *Trans. Farad. Soc.*, 51, 778 (1955).
145. J. D. McCullough, *J. Amer. Chem. Soc.*, 59, 789 (1937).
146. K. Kuhlmann and D. M. Grant, *J. Phys. Chem.*, 68, 3208 (1964).
147. M. Brownstein, P. A. W. Dean and R. J. Gillespie, *Chem. Comm.*, 9 (1970).
148. C. MacLean and E. L. Mackor, *Prox. XI, Colloque Ampere, Eindhoven*, North Holland Publishing Co., Amsterdam, (1962), p. 571.
149. E. L. Pace and H. V. Samuelson, *J. Chem. Phys.*, 44, 3682 (1966).
150. A. J. Edwards and G. R. Jones, *J. Chem. Soc. A*, 1891 (1970).
151. A. M. Qureshi and F. Aubke, *Can. J. Chem.*, 48, 3117 (1970).
152. R. J. Gillespie and B. Landa, *Inorg. Chem.*, 12, 1383 (1973).
153. T. Surles, A. Perkins, L. A. Quarterman, H. H. Hyman, and A. I. Popov, *J. Inorg. Nucl. Chem.*, 34, 3561 (1972).
154. K. O. Christe and W. Sawodny, *Inorg. Chem.*, 12, 2879 (1973).

155. K. O. Christe and C. J. Schack, *Inorg. Chem.*, 9, 2296 (1970).
156. K. O. Christe, J. Hon and D. Pilipovich, *ibid*, 12, 84 (1973).
157. R. J. Gillespie and G. J. Schrobilgen, *ibid*, 13, 2370 (1974).
158. R. J. Gillespie and G. J. Schrobilgen, *ibid*, 13, 765 (1974).
159. M. Brownstein and H. Selig, *ibid*, 11, 656 (1972).
160. J. W. Emsley, J. Feeney and L. H. Sutcliffe, "High Resolution Nuclear Magnetic Resonance Spectroscopy", Pergamon Press, (1965), Vol. 1 and 2.
161. J. A. Pople, *Mol. Phys.*, 7, 301 (1963).
162. R. Paetzold and K. Aurich, *Z. Anorg. Allg. Chem.*, 335, 281 (1965).
163. J. B. Milne and D. Moffett, Private Communication, see Reference 91 and 164.
164. D. Moffett, Ph.D. Thesis, University of Ottawa, Ottawa, Canada (1974).
165. J. B. Milne and D. Moffett, *Inorg. Chem.*, 12, 2240 (1973).
166. G. E. Walrafen, *J. Chem. Phys.*, 37, 1468 (1962).
167. R. Paetzold and K. Aurich, *Z. Anorg. Allg. Chem.*, 348, 94 (1966).
168. K. O. Christe, E. C. Curtis, C. J. Schack and D. Pilipovich, *Inorg. Chem.*, 11, 1679 (1972).
169. K. Seppelt, *Chem. Ber.*, 105, 2431 (1972).
170. T. Birchall and R. J. Gillespie, *Spectrochim. Acta*, 22, 681 (1966).
171. R. Paetzold and K. H. Ziegenbald, *Z. Chem.*, 4, 461 (1964).
172. A. W. Cordes, *Inorg. Chem.*, 6, 1204 (1967).
173. R. Paetzold, *Z. Chem.*, 4, 272 (1964).
174. F. Seel and D. Golitz, *Z. Anorg. Allg. Chem.*, 327, 28 (1964).
175. P. Spekkens, B.Sc. Thesis, University of Ottawa, Ottawa, Canada (1972).

176. L. Brown, G. M. Begun and G. E. Boyd, J. Amer. Chem. Soc., 91,
2250 (1969).
177. J. N. Keith and I. J. Solomon, Inorg. Chem., 9, 1560 (1970).
178. M. H. Studier, J. Amer. Chem. Soc., 90, 1901 (1968).
179. K. Baum, C. D. Beard and V. Grakaustas, J. Amer. Chem. Soc., 97,
267 (1975).
180. W. Adelhelm and E. Jacob, 6th European Symposium on Fluorine Chemistry,
Dortmund, Germany, March 1977.
181. D. Pilipovich, H. H. Rogers and R. D. Wilson, Inorg. Chem., 11, 200 (1972).
182. F. Powell and E. R. Lippincott, J. Chem. Phys., 32, 1883 (1960).
183. S. Sunder and R. E. D. McClung, Can. J. Phys., 52, 2299 (1974).
184. D. F. Evans, J. Chem. Soc., 877 (1960).
185. J. Bacon, R. J. Gillespie and J. W. Quail, Can. J. Chem., 41, 3060 (1963).
186. E. D. Becker, "High Resolution N.M.R.", Academic Press, (1969), p. 1.
187. S. Brownstein, Can. J. Chem., 38, 1597 (1960).
188. C. E. Crouthamel, A. M. Hayes and D. S. Martin, J. Amer. Chem. Soc.,
73, 82 (1951).
189. G. E. Walrafen, J. Chem. Phys., 39, 1479 (1963).
190. A. Simon and M. Weist, Z. Anorg. Allg. Chem., 268, 301 (1952).
191. J. Liang, Ph.D. Thesis, McMaster University, Hamilton, Canada (1976).
192. H. H. Hyman, M. Kilpatrick and J. J. Katz, J. Amer. Chem. Soc., 79,
3668 (1957).
193. G. Dallinga, J. Gaaf and E. L. Mackor, Rec. Tr. Chim., 89, 1068 (1970).
194. R. J. Gillespie, T. E. Peel and E. A. Robinson, J. Amer. Chem. Soc.,
93, 5083 (1971).

195. R. J. Gillespie, J. Chem. Soc., 2537 (1950).
196. L. Kolditz and U. Preiss, Z. Anorg. Allg. Chem., 325, 263 (1963).
197. K. Dehnicke and J. Weidlein, *ibid*, 342, 225 (1966).
198. K. O. Christe, C. J. Schack and R. D. Wilson, Inorg. Chem., 14, 2224 (1975).
199. J. Shamir, J. Binenboym and H. H. Claassen, J. Amer. Chem. Soc., 90, 6223 (1968).
200. H. S. Gutowsky, D. W. McCall and C. P. Slichter, J. Chem. Phys., 21, 279 (1953).
201. L. C. Hoskins and R. C. Lord, *ibid*, 46, 2402 (1967).
202. J. F. Liebman and B. B. Jarvis, J. Fluorine-Chem., 5, 41 (1975).
203. M. H. Studier and E. H. Appelman, J. Amer. Chem. Soc., 93, 2349 (1971).
204. H. A. Carter, A. M. Qureshi and F. Aubke, Chem. Comm., 1461 (1968).
205. R. Bougon, Private Communication.
206. K. O. Christe and D. Pilipovich, Inorg. Chem., 8, 391 (1969).
207. P. A. W. Dean and R. J. Gillespie, J. Amer. Chem. Soc., 91, 7260 (1969).
208. K. Seppelt, Angew. Chem. Int. Ed., 13, 92 (1974).
209. R. Bougon, P. Charpin and J. Soriano, C. R. Acad. Sc., C, 272, 565 (1971).
210. K. O. Christe, Inorg. Chem., 12, 1580 (1973).